Notes on Strings

R.J. Marks II Notes

(1969)

2/21/95

Hal,

Here is the math for your idea of making arbitrary FIR filters from Szasz series. Gotta do some computer work. We will need the values of impulse response, $h[n]$.

Any ideas?

-Bob-

- Szasz Series, K^{TH} order

$$s[n] = \sum_{k=1}^{K} a_k\, e^{\alpha_k n} \cos \omega_k n \qquad (1)$$

- Problem: For a given length, N, and $h[n]$ = desired impulse response, find parameters

$$\begin{aligned} &\{a_k \mid 1 \le k \le K\} \\ &\{\alpha_k \mid 1 \le k \le K\} \qquad (2) \\ &\{\omega_k \mid 1 \le k \le K\} \end{aligned}$$

that makes

$$s[n] \approx h[n] \quad \text{for } 0 \le n < N. \qquad (3)$$

- CASE 1 : K given (4)
- CASE 2 : K not given (best is K 'small') (5)

In both cases, the impulse response is $h[n]$.

- Some interpretations of "$\approx$" in (3).
  1. ℓ_2 (minimum mean square error) norm

$$E_2 = \sum_{n=0}^{N-1} \left(s[n] - h[n] \right)^2 \qquad (6)$$

Find parameters in (2) that minimize E_2.

  2. ℓ_∞ (minimize maximum deviation)

$$E_\infty = \max_{0 \le n < N} \left| s[n] - h[n] \right| \qquad (7)$$

Find parameters than minimize E_∞.

- Optimization Techniques
  1. Genetic Algorithm (Optimization for dummies)
     Note: can optimize either (6) or (7) for K specified or not (4) or (5).
  2. Steepest descent - for E_2 in (6).

$$\frac{\delta E_2}{\delta a_i} = 2\sum_{n=0}^{N-1} \frac{\delta s[n]}{\delta a_i}\left(s[n]-h[n]\right)$$

$$= 2\sum_{n=0}^{N-1} e^{\alpha_i n}\cos\omega_i n\left(s[n]-h[n]\right) \quad (8)$$

$$\frac{\delta E_2}{\delta \alpha_i} = 2a_i\sum_{n=0}^{N-1} n\, e^{\alpha_i n}\cos\omega_i n\left(s[n]-h[n]\right) \quad (9)$$

$$\frac{\delta E_2}{\delta \omega_i} = -2a_i\sum_{n=0}^{N-1} n\, e^{\alpha_i n}\sin\omega_i n\left(s[n]-h[n]\right) \quad (10)$$

Iterative steepest descent:

$$a_i \leftarrow a_i - \eta_a \frac{\delta E_2}{\delta a_i} \quad (11)$$

$$\alpha_i \leftarrow \alpha_i - \eta_\alpha \frac{\delta E_2}{\delta \alpha_i} \quad (12)$$

$$\omega_i \leftarrow \omega_i - \eta_\omega \frac{\delta E_2}{\delta \omega_i} \quad (13)$$

where η_a, η_α and η_ω are step sizes.

TO: Bob Marks

From Doc Phillips

I think I got it

3/4/96

1

STRING SPAWNING

Given an original string of length = N

Spawn new strings via combination of 2 methods –

1. String halving + addition
2. shortening of string – 'Donate' lost points to make up the next string.

EXAMPLE: Assume $N = 16$

(A) $16 \xrightarrow{\text{spawns}} 16-1 \rightarrow 16-2 \rightarrow 16-3 \rightarrow 16-4 \rightarrow 16-5 \rightarrow 16-6 \rightarrow 16-7$

$\downarrow$

(B) $\frac{16}{2} \xrightarrow{\text{spawns}} \frac{16}{2}-1 \rightarrow \frac{16}{2}-2 \rightarrow \frac{16}{2}-3$

$\downarrow$

(C) $\frac{16}{4} \xrightarrow{\text{spawns}} \frac{16}{4}-1 \rightarrow \frac{16}{4}-2$

We now have strings of length:

(A) $N, N-1, N-2, N-3, N-4, N-5, N-6, N-7,$

(B) $\frac{N}{2}, \frac{N}{2}-1, \frac{N}{2}-2, \frac{N}{2}-3,$

(C) $\frac{N}{4}, \frac{N}{4}-1, \frac{N}{4}-2$

=

(A) 16, 15, 14, 13, 12, 11, 10, 9,

(B) 8, 7, 6, 5,

(C) 4, 3, 2

Thus we can generate any length string from $N \rightarrow N-k$ in unary increments

3/4/96 HC

(2)

SPAWNING METHOD #2

$$\begin{tikzcd}
N \arrow[r] \arrow[d, "\text{Spawns}"'] & N-16 \arrow[r] \arrow[d, "\text{Spawns}"'] & N-32 \arrow[r] \arrow[d] & N-48 \arrow[r] \arrow[d] & N-64 \cdots \arrow[d] \\
\frac{N}{2} \arrow[d, "\text{Spawns}"'] & \frac{N-16}{2} \arrow[d] & \frac{N-32}{2} \arrow[d] & \frac{N-48}{2} \arrow[d] & \frac{N-64}{2} \arrow[d] \\
\frac{N}{4} \arrow[d, "\text{Spawns}"'] & \frac{N-16}{4} \arrow[d] & \frac{N-32}{4} \arrow[d] & \frac{N-48}{4} \arrow[d] & \frac{N-64}{4} \arrow[d] \\
\frac{N}{8} \arrow[d, "\text{Spawns}"'] & \frac{N-16}{8} \arrow[d] & \frac{N-32}{8} & \frac{N-48}{8} & \vdots \\
\frac{N}{16} & \frac{N-16}{16} & \vdots & \vdots & \\
\vdots & \vdots & & &
\end{tikzcd}$$

GIVES WINDOWS OF:

(A) $N, N-16, N-32, N-48, N-64 \ldots$

(B) $\frac{N}{2}, \frac{N-16}{2}, \frac{N-32}{2}, \frac{N-48}{2}, \frac{N-64}{2}$

(C) $\frac{N}{4}, \frac{N-16}{4}, \frac{N-32}{4} \ldots$ etc.

$\downarrow$

etc.

(3)

13-782 500 SHEETS, FILLER 5 SQUARE
42-381 50 SHEETS EYE-EASE® 5 SQUARE
42-382 100 SHEETS EYE-EASE® 5 SQUARE
42-389 200 SHEETS EYE-EASE® 5 SQUARE
42-392 100 RECYCLED WHITE 5 SQUARE
42-399 200 RECYCLED WHITE 5 SQUARE
Made in U.S.A.
National® Brand

3/4/96 AP

EXAMPLE OF METHOD #2

$N = 256$

Window A $\Rightarrow$ 256, 240, 224, 208, 192, 176, 160, 144

B $\Rightarrow$ 128, 120, 112, 104, 96, 88, 80, 72

C $\Rightarrow$ 64, 60, 56, 52, 48, 44, 40, 36

D $\Rightarrow$ 32, 30, 28, 26, 24, 22, 20, 18

E $\Rightarrow$ 16, 15, 14, 13, 12, 11, 10, 9, --- etc.

Note: ΔN for $A \Rightarrow 16$, $B \Rightarrow 8$, $C \Rightarrow 4$, $D \Rightarrow 2$, $E \Rightarrow 1$

Superficially, both methods lose data to Dedrift. However, adjacent windows can be made using discarded remainder points of a prior window. Worst case, $\frac{N}{2}-1$ points need to be 'mapped' to the next full string.

Hal's Neat February Idea

by Bob the FLOP Counter
February 28, 1996

Recall: One complex multiply = 4 real multiplies and 2 real adds.

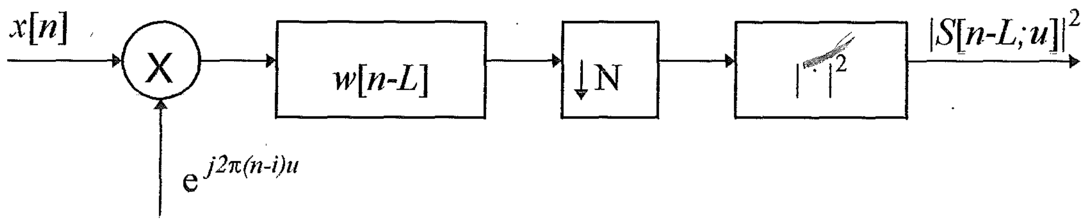

1. Let's count the FLOPS except for the window. Assume the input is real.
   - One real times complex multiply (for the e to the j) = two real multiplies per window each N values in the window = **$2N$ multiplies per window**
   - One $|\cdot|^2$operation = **two real multiplies per window** and **one add**
2. Figure 4 in the patent is still used as the FIR filter. There are
   - Three complex-times-a-real multiplication per clock cycle
     - $\Rightarrow$ = 6 real multiplies per clock cycle
     - $\Rightarrow$ **= $6N$ real multiples per window**
   - Three complex adds = six real adds per clock cycle
     - $\Rightarrow$ **= $6N$ (sequential) adds per window**
3. Instead of Figure 5 in the patent, we have

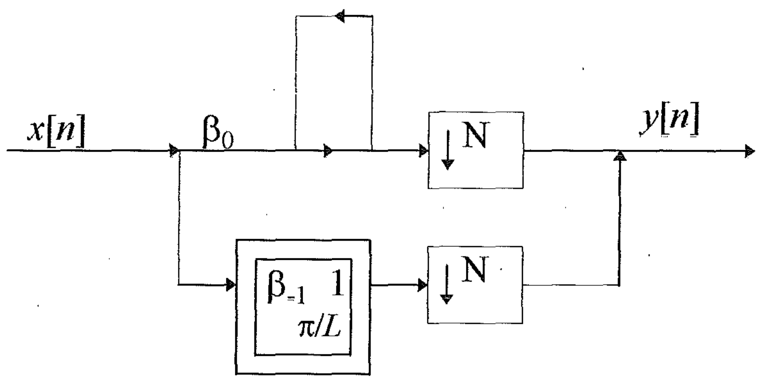

There are no shift registers or cancellations. The top loop is an accumulator. Counting the flops:

- One complex times real multiply for β_0
  - $\Rightarrow$ **= 2N real multiplies**
- **One add** at output

Note: the decimation by N here is the same as in the top figure.

Add 'em up:

real multiplies	=	$(2N+2) + (6N) + (2N+1)$	=	$10N+3$	real multiplies
real adds	=	$1 + (6N) + 1$	=	$\underline{6N+1}$	real adds
				$16N+4$	FLOPS

This is for one frequency line. The result is $O(N^2)$. On a linear frequency bin spacing, FFT's, of course, still win.

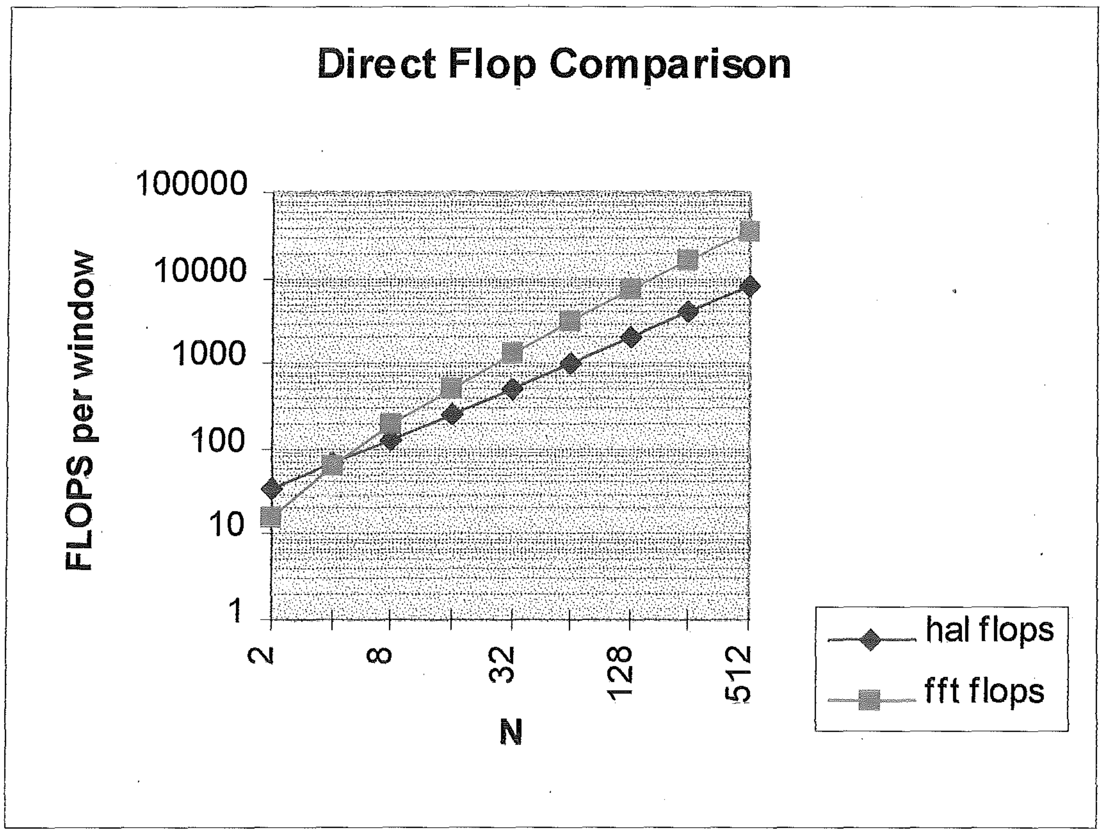
Direct Flop Comparison
FLOPS per window
100000
10000
1000
100
10
1
2
8
32
128
512
N
hal flops
fft flops

2/28/96

Hal,

Here is some analysis.

Figures assume all VFAST windows are as long as (longest) FFT window. I still need to look at effects of smaller windows. Will make better.

I need to talk to you about $\hat{B}$.

-Bob-

PS: I still need to digest this more. A reality check is needed.

Hal's Second Great Idea in Feb 1996

PARAMETERIZE VFAST & FFT

- FFT : M frequency bins
  Assume 3db (or other) crossing.

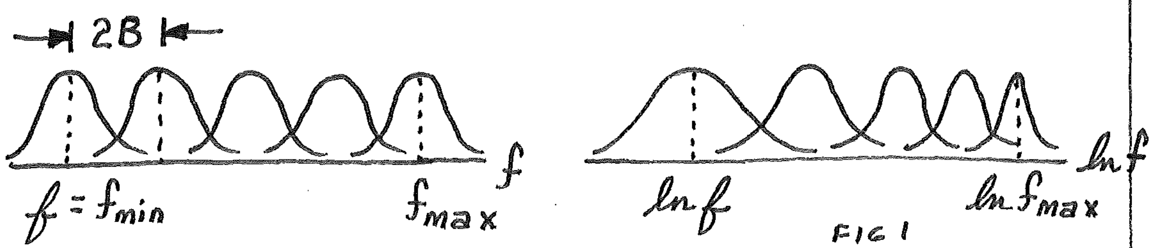

FIG 1

$$f_{max} = f + 2(M-1)B \tag{1}$$

- VFAST : N frequency bins
  Assume 3db (or other) crossing

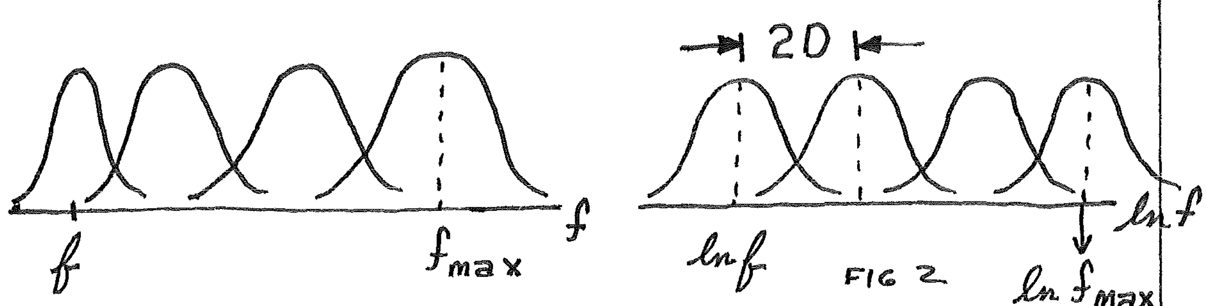

FIG 2

$$\ln f_{max} = (\ln f) + 2(N-1)D \tag{2}$$

Equating (1) and (2) $\Longrightarrow$

$$f + 2(M-1)B = f\,e^{2(N-1)D} \tag{3}$$

or

$$1 + 2(M-1)\hat{B} = e^{2(N-1)D} \tag{4}$$

where

$$\hat{B} = B/f \tag{5}$$

To match the FFT & VFAST, equate fatest bin in FFT to D

FFT:

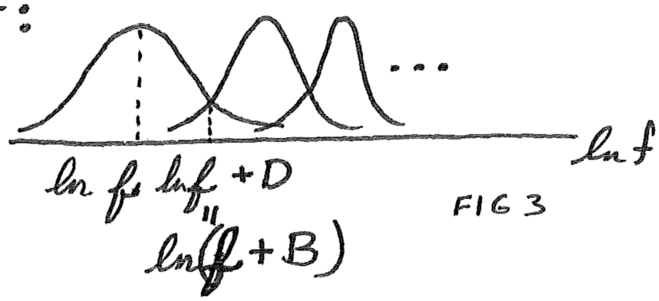

FIG 3

Thus

$$\ln f + D = \ln(f + B)$$

$$D = \ln 1 + \hat{B} \tag{6}$$

or

$$1 + \hat{B} = e^{D} \tag{7}$$

Plug into (4)

$$1 + 2(M-1)\hat{B} = (1 + \hat{B})^{2(N-1)} \tag{8}$$

Solve for M:

$$M = \frac{(1 + \hat{B})^{2(N+1)} - 1}{2\hat{B}} + 1 \tag{9}$$

FFT Bins

N = VFAST BINS

The relation depends on

$$\hat{B} = B/f = B/f_{min} \tag{10}$$

FFT:

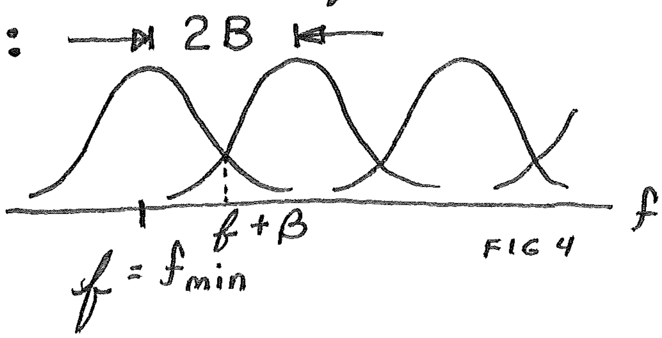

FIG 4

Hal: What are good values for $\hat{B}$?

M bins at $8M \log_2 M$ total FLOPS (FFT) (11)

Using Hal's Neat February Idea:

Longest window: M units

$$N(16M+4)$$
$$= 4N(4M+1) \text{ FLOPS} \tag{12}$$

This does not take into account shorter windows.

Note: We can solve for N in (9)

$$N = 1 + \frac{\ln(1 + 2(M-1)\hat{B})}{2\ln(1+\hat{B})} \tag{13}$$

FIG 5

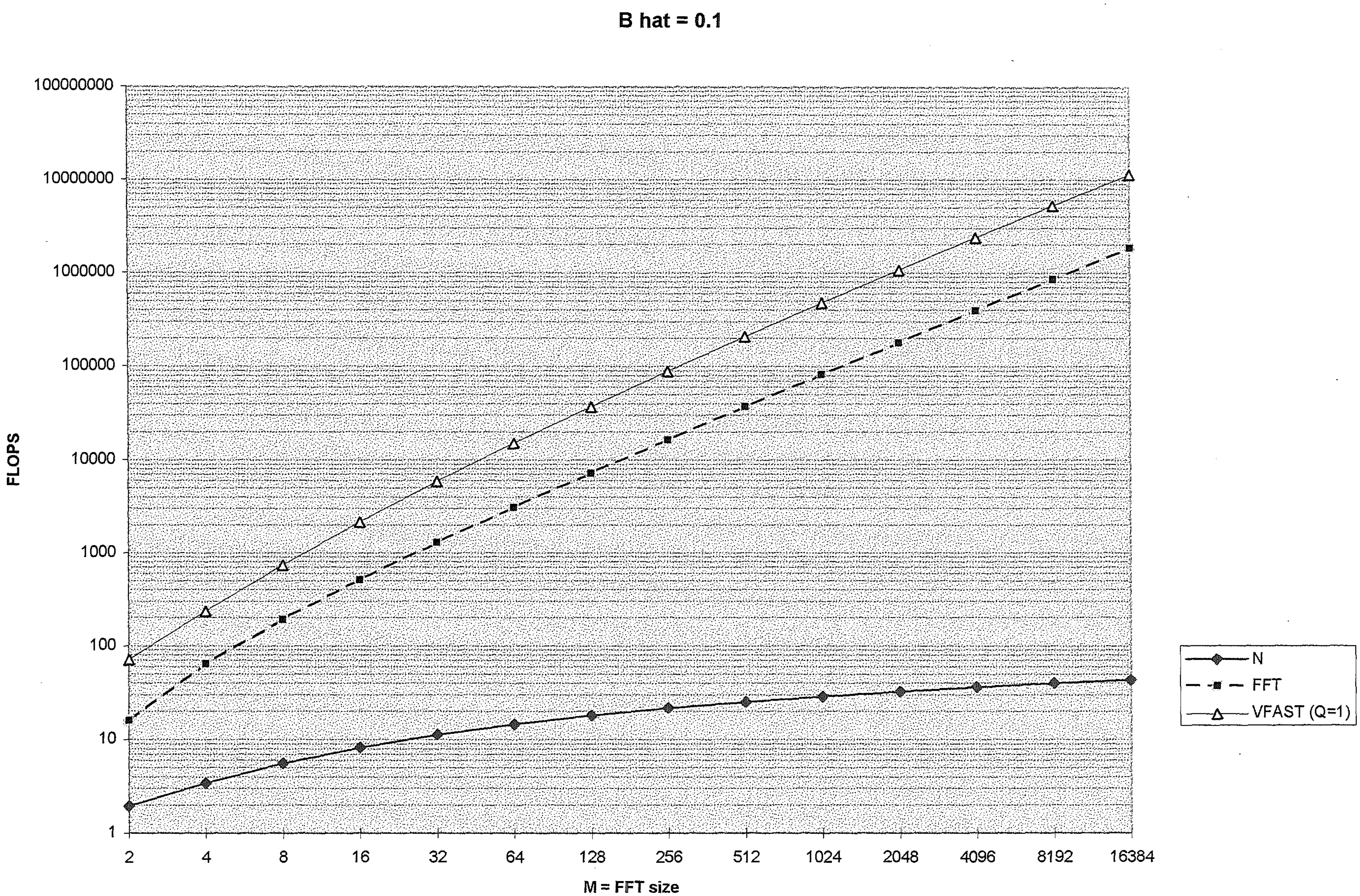

B hat = 0.1
FLOPS
100000000
10000000
1000000
100000
10000
1000
100
10
1
2
4
8
16
32
64
128
256
512
1024
2048
4096
8192
16384
M = FFT size
N
FFT
VFAST (Q=1)

4

FIG 2

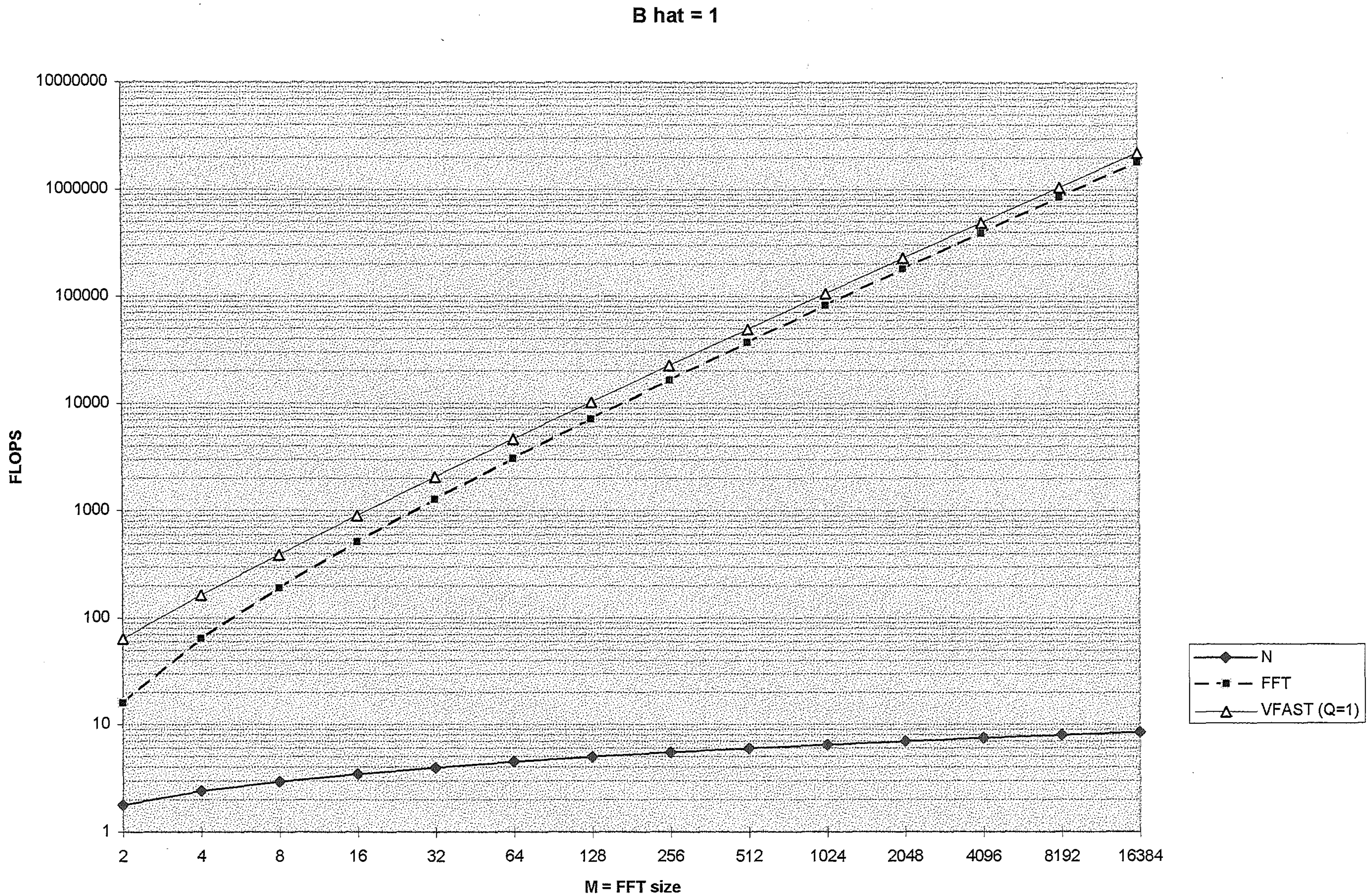
B hat = 1
10000000
1000000
100000
10000
1000
100
10
1
FLOPS
2
4
8
16
32
64
128
256
512
1024
2048
4096
8192
16384
M = FFT size
N
FFT
VFAST (Q=1)

5

FIG 7

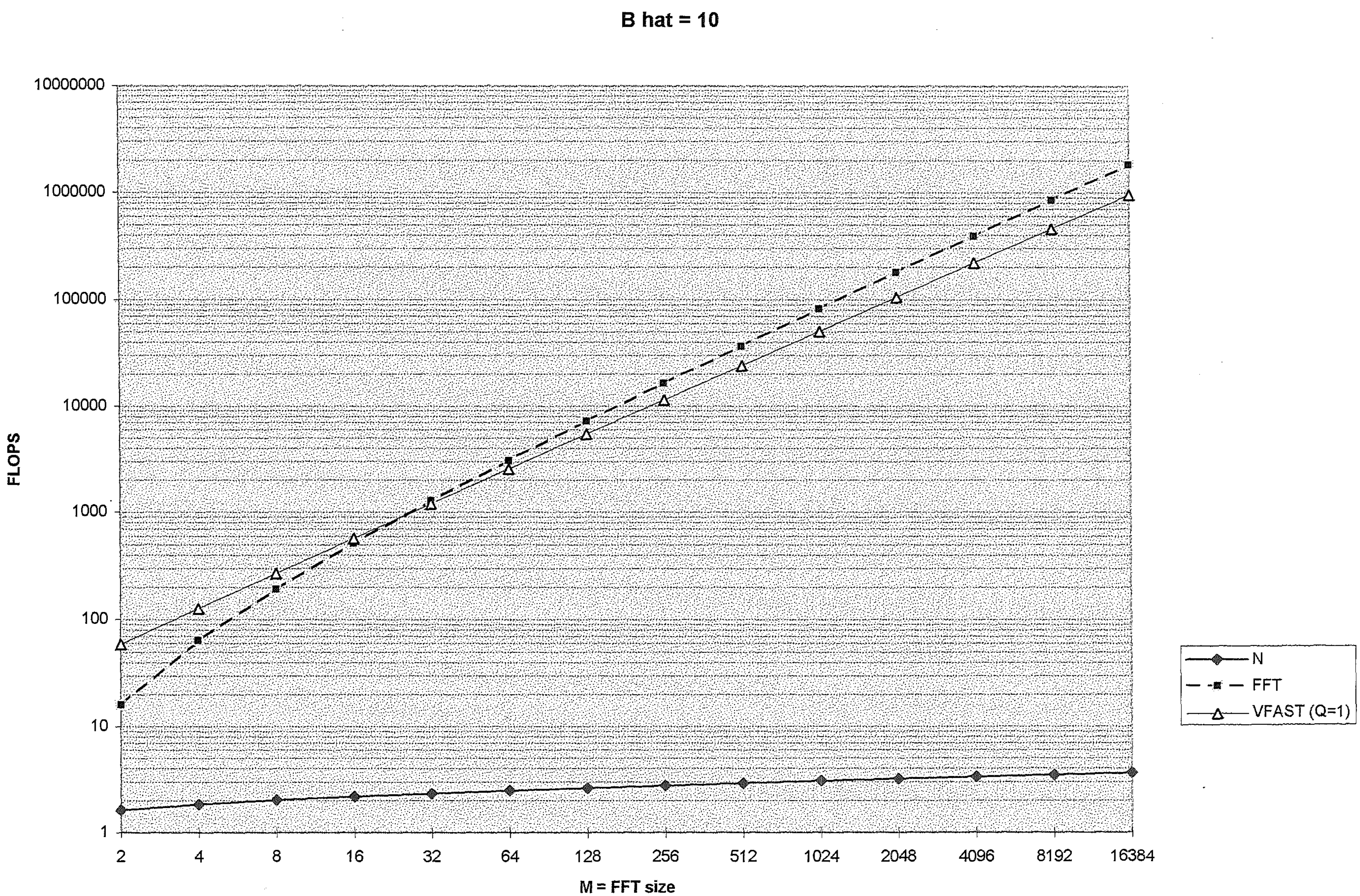
B hat = 10
FLOPS
10000000
1000000
100000
10000
1000
100
10
1
2
4
8
16
32
64
128
256
512
1024
2048
4096
8192
16384
M = FFT size
N
FFT
VFAST (Q=1)

6

FIG 8

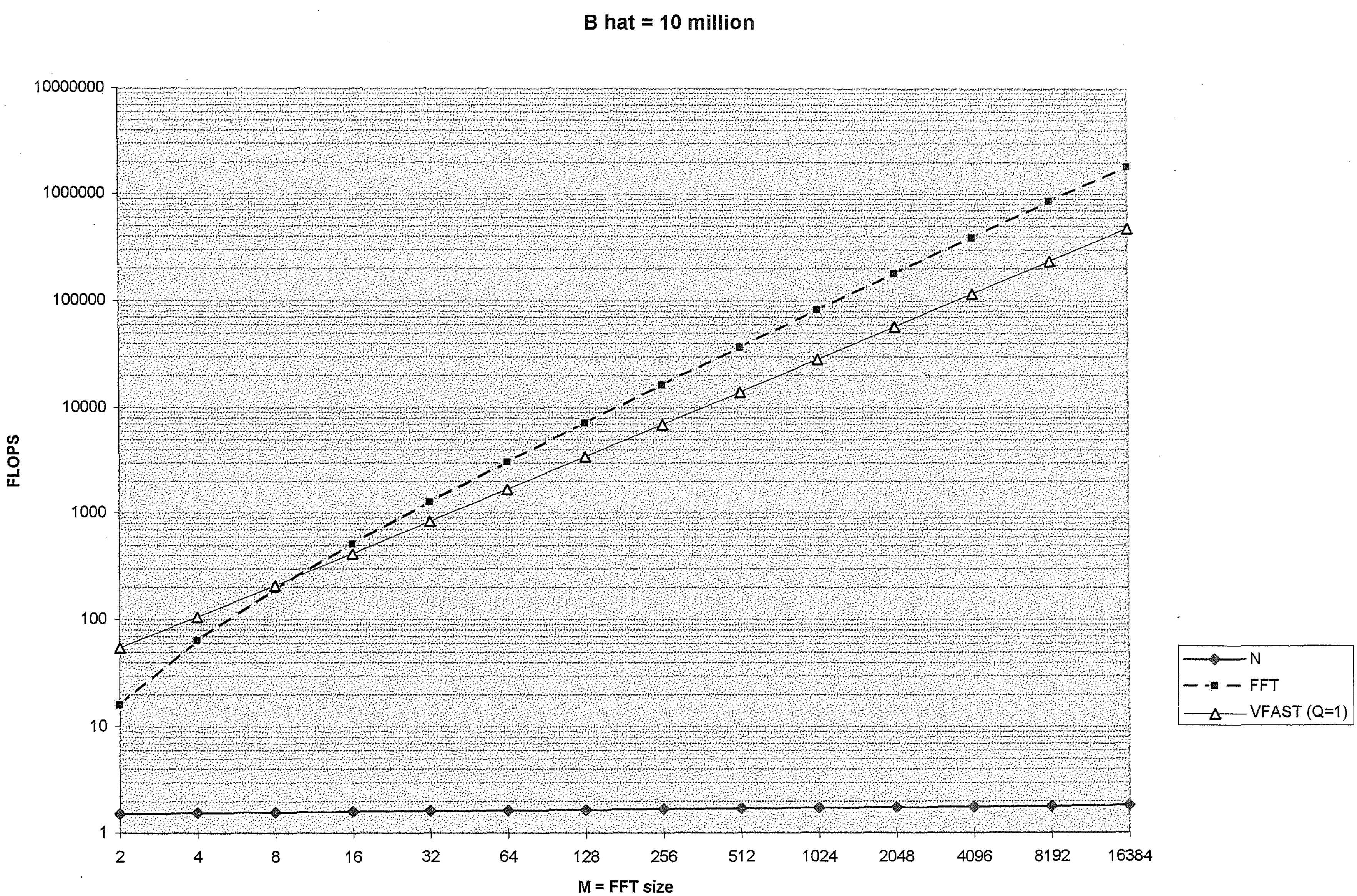
B hat = 10 million
10000000
1000000
100000
10000
1000
100
10
1
FLOPS
2
4
8
16
32
64
128
256
512
1024
2048
4096
8192
16384
M = FFT size
N
FFT
VFAST (Q=1)

7

2/28/96

Hal,

Here is Chapters 2 & 3.

Chapter 2, as we discussed last night is worthless. The Detroit problem.

Chapter 3 is the math for chopping up the string. It <u>does</u> work. We decided last night it doesn't work. It does. Not sure what it means.

-Bob-

Formulas: $\hat{B} = 1/Q$ (14)

$Q = Q$ of left most (fatest) bin

Eq 9: $$M = \frac{\left(1+\frac{1}{Q}\right)^{2(N+1)} - 1}{\frac{2}{Q}} + 1 \qquad (15)$$

Eq. 13: $$N = 1 + \frac{\ln\left(1 + 2(M-1)/Q\right)}{2\ln\left(1+\frac{1}{Q}\right)} \qquad (16)$$

FFT Flops: (M lines) $$F_{FFT} = 8\, M \log_2 M$$

VFAST Flops $Q = 1$, 1 line length L $$F_{VFAST} = 4\,(4L+1) \qquad (17)$$

VFAST:

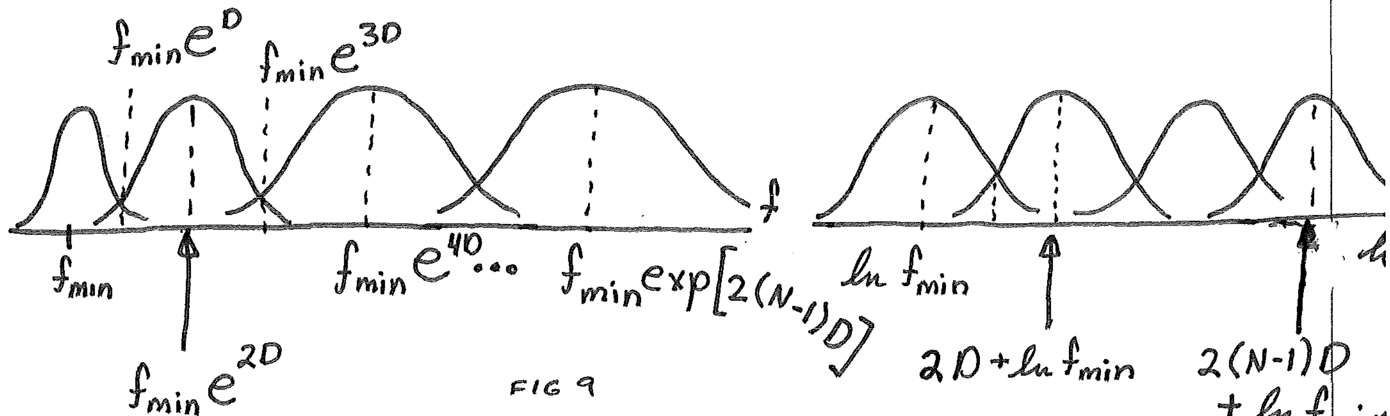

FIG 9

The longest window will be used to compute the f_{min} bin. To equate to FFT, assume this is of length M. Assume for all bins

window length × bandwidth = constant (18)

For f_{min} bin, bandwidth, measured on right side from f_{min} to $f_{min}e^{D}$ is

$$W_{min} = f_{min}\left(e^{D} - 1\right) \qquad (19)$$

Thus

$$C = \text{constant}$$
$$= M\bar{W}_{min} = M f_{min}(e^{D} - 1) \qquad (20)$$

Let next highest frequency bin have window of length M_1. Then

$$M_1 \times f_{min}(e^{3D} - e^{2D}) = M_1 \times f_{min}\, e^{2D}(e^{D} - 1)$$
$$= C = M f_{min}(e^{D} - 1) \qquad (21)$$

Thus

$$M_1 = M e^{-2D} \qquad (22)$$

The n^{th} bin, clearly, has a window of length

$$M_n = M e^{-2nD} \quad ; \quad 0 \le n < N \qquad (23)$$

The VFAST Flops, using Hal's neat idea, for the $n^{\underline{th}}$ window is

$$F_n = 4(4M_n + 1) \quad ; \quad 0 \le n < N \qquad (24)$$
$$= 4(4M e^{-2nD} + 1)$$

The total VFAST FLOPS are

$$F = \sum_{n=0}^{N-1} F_n$$
$$= 4\left(4M\left(\sum_{n=0}^{N-1} e^{-2nD}\right) + N\right)$$

Geometric Series (25)

$$= 4\left(4M\, \frac{1 - e^{-2ND}}{1 - e^{-2D}} + N\right)$$

or, using (7) and (14)

$$F = 4\left(4M \frac{1-\left(1+\frac{1}{Q}\right)^{-2N}}{1-\left(1+\frac{1}{Q}\right)^{-2}} + N\right) \qquad (26)$$

For the FFT, use (8). Use (13) to find N from M.

Note: In the example plot to follow, N, computed from (13), is not rounded.

First order Szasz

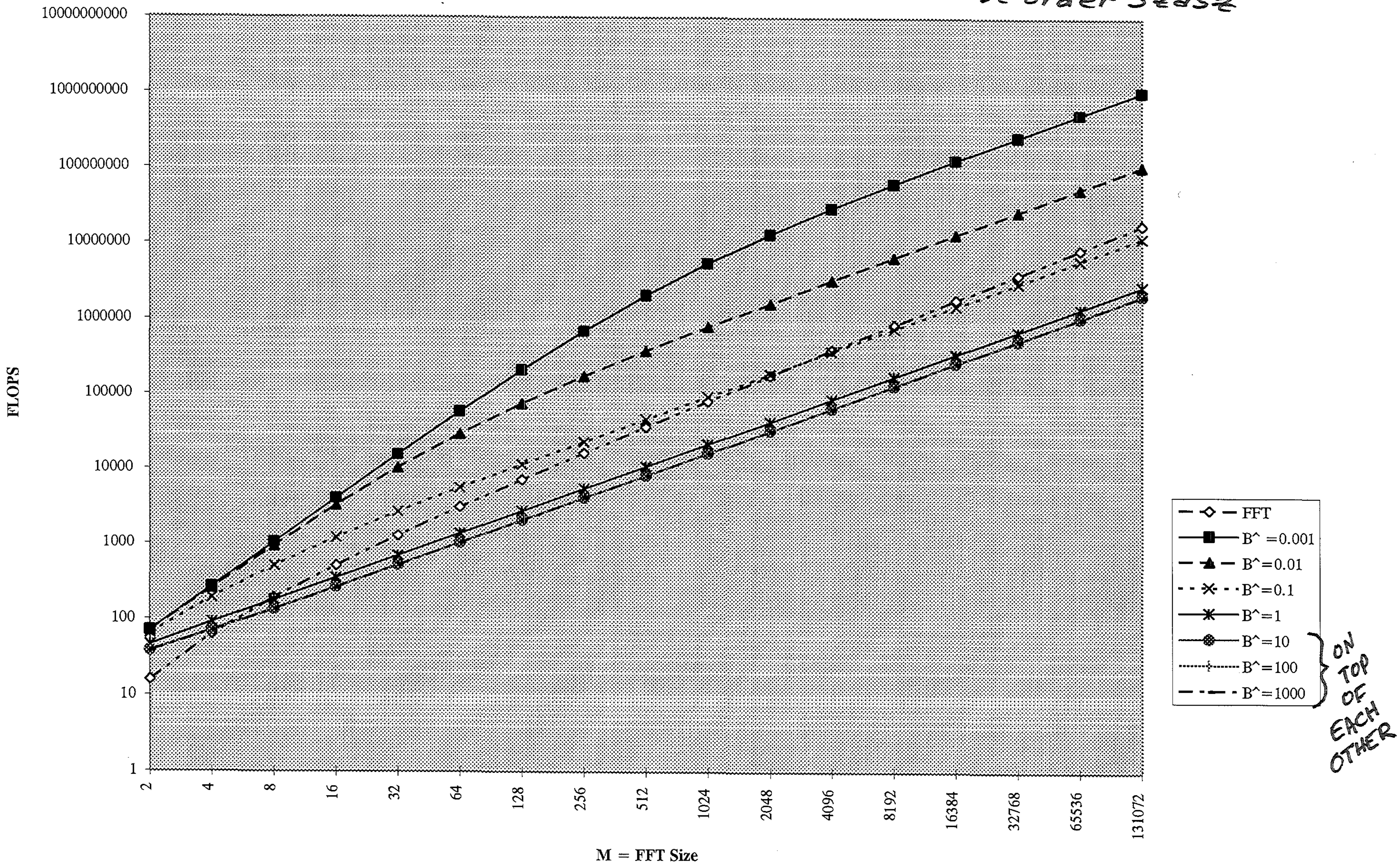

FIG 10

Chapt 3: Chopping up the string

$$\mathbb{X}(u) = \sum_{n=0}^{N-1} x[n]\, e^{-j2\pi nu} \quad (27)$$

$e^{-j2\pi nu} = \cos 2\pi nu - j \sin 2\pi nu$ is periodic with period $1/u$. In other words

$$e^{-j2\pi(n+\frac{1}{u})u} = e^{-j2\pi nu} \times e^{-j2\pi} = e^{-j2\pi nu} \quad (28)$$

Consider breaking the sequence on N points is broken into segments of length

$$k = 1/u$$

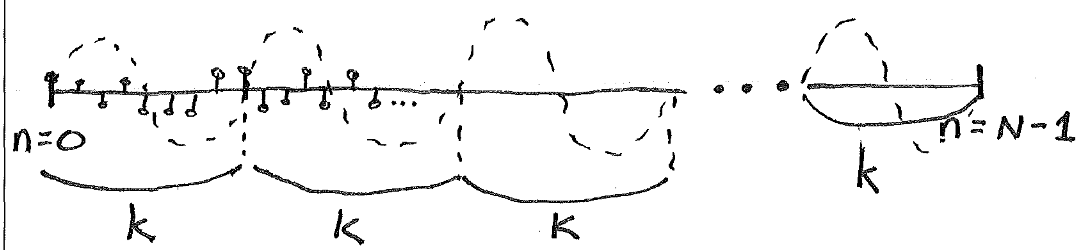

FIG 11

There are a total of

$$\mathbb{K} = \frac{N}{k} \quad (29)$$

groups. Now some math:

$$\mathbb{X}(u) = \sum_{n=0}^{N-1} x[n]\, e^{-j2\pi nu}$$

$$= \left[\sum_{n=0}^{k-1} + \sum_{n=k}^{2k-1} + \sum_{n=2k}^{3k-1} + \ldots + \sum_{n=(\mathbb{K}-1)k}^{\mathbb{K}k}\right] \times x[n]\, e^{-j2\pi nu} \quad (30)$$

$$= \sum_{p=0}^{\mathbb{K}-1} \sum_{n=pk}^{(p+1)k-1} x[n]\, e^{-j2\pi nu}$$

$m = n - pk$

$n = m + pk$

$$= \sum_{p=0}^{\mathbb{K}-1} \sum_{m=0}^{k-1} x[m+pk]\, e^{-j2\pi(m+pk)u} \quad (31)$$

But $e^{-j2\pi pku} = e^{-j2\pi pk\frac{1}{k}} = 1$. Thus (32)

$$\mathbb{X}(u) = \sum_{p=0}^{\mathbb{K}-1} \sum_{m=0}^{k-1} x[m+pk]\, e^{-j2\pi mu} \quad (33)$$

or

$$\mathbb{X}(u) = \sum_{m=0}^{k-1} \left(\sum_{p=0}^{\mathbb{K}-1} x[m+pk] \right) e^{-j2\pi m/k}$$

$$= \sum_{m=0}^{N/\mathbb{K}} \left(\sum_{p=0}^{\mathbb{K}-1} x[m + \frac{p\mathbb{K}}{N}] \right) e^{-j2\pi m/k} \qquad (34)$$

Thus, you can break up the sequence in Figure 11, add them, and run them through a Szasz series

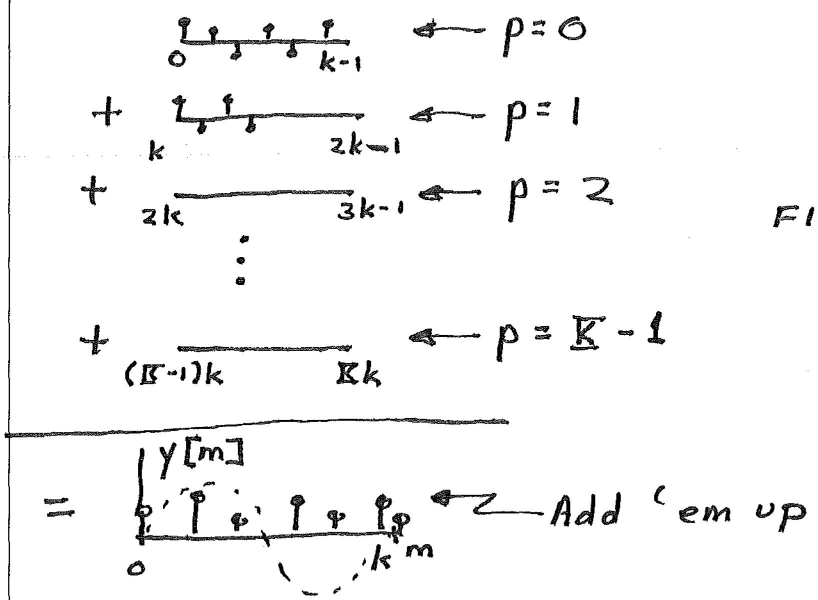

FIG 12

Define:

$$y[m] = \sum_{p=0}^{\mathbb{K}-1} x[m + \frac{p\mathbb{K}}{N}] \qquad (35)$$

Then

$$\mathbb{Y}(u) = \sum_{m=0}^{k-1} y[m] e^{-j2\pi nu}$$

$$= \mathbb{X}(u) \text{ in eq. } 27 \qquad (36)$$

ONLY FOR $u = 1/k$

3/2/96

Hal:

The string is $O(N)$. Better than FFT's $O(N \log_2 N)$.

-Bob-

Notes: Only get octaves

Chapter 4: String cutting

First, we consider computing the number

$$\sum_{n=1}^{J} x[n]\, e^{j2\pi n u} \qquad (37)$$

where u is a fixed number. One way is

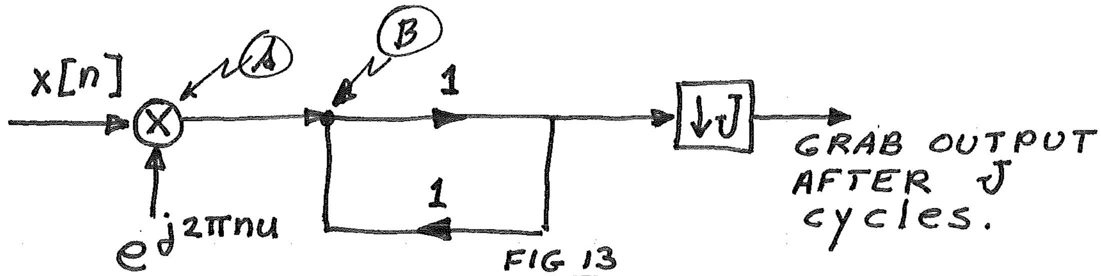

FIG 13

Total ops:

$$\text{OPS} = \Big(J\ \underbrace{\text{complex number}}_{e^{j2\pi nu}}\ \text{times}\ \underbrace{\text{real number}}_{x[n]}\ \text{mults}\Big)_{A} + \big(J\ \text{complex adds}\big)_{B}$$

$$= (2J\ \text{real multiplies}) + (2J\ \text{real adds})$$

$$= 4J\ \text{ops} \qquad (38)$$

Start with a string of length $N = 2^P$

CUT 0:

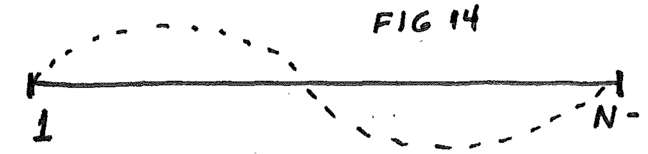

FIG 14

frequency $k = 1$

Cut in 2 pieces and add

CUT 1:

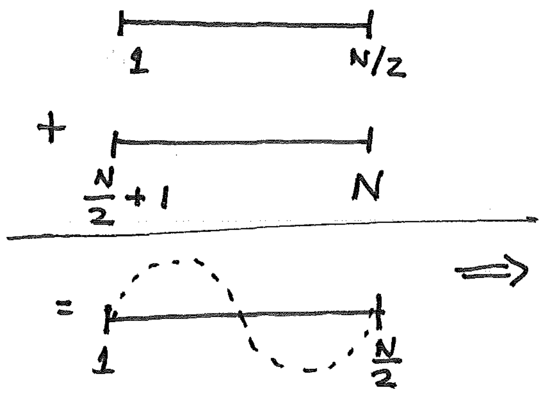

FIG 15

$\Rightarrow$ frequency $k = 2$

Do it again

CUT 2:

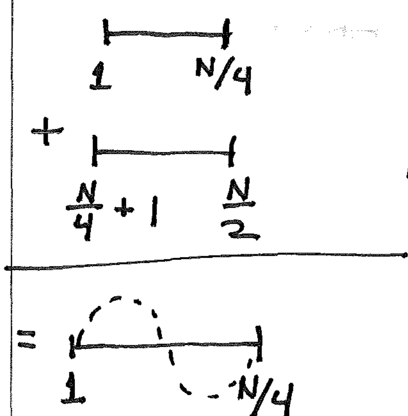

FIG 16

$\Rightarrow$ frequency $k = 4$

for the p^{th} cut, the frequency is 2^p.

Q: How many are there?

A: $1 + \log_2 N$ (39)

From (38)

For FIG 14, $J = N$ and we need $4N$ ops
" " 15, $J = \frac{N}{2}$ " " " $4\frac{N}{2}$ ops
" " 16, $J = \frac{N}{4}$ " " " $4\frac{N}{4}$ ops (40)

⋮

LAST TERM, $J = \frac{N}{2^P} = \frac{N}{N} = 1$, we need $4\frac{N}{N}$ ops

where we have assumed

$$N = 2^P \tag{41}$$

Adding up all ops in (40) gives

$$ops_1 = \sum_{p=0}^{P} 4\frac{N}{2^p} = 4N\sum_{p=0}^{P}\frac{1}{2^p} \tag{42}$$

Since (Geometric series)

$$\sum_{p=0}^{P} a^p = \frac{1 - a^{P+1}}{1 - a} \tag{43}$$

we have

$$ops_1 = 4N \times 2\left(1 - \frac{1}{2^{P+1}}\right)$$

$$\approx 8N\left(1 - \frac{1}{2}\cdot\frac{1}{N}\right)$$

$$= 8N - 4 \tag{44}$$

This is the total ops for computing line from each string cut.

Lets count the ops of adding strings.

$$\left.\begin{array}{ll} \text{To get FIG 15, we need} & \frac{N}{2} \text{ real adds} \\ \text{" " " 16, we need} & \frac{N}{4} \text{ " "} \\ \vdots & \\ \text{To get last string, we need} & \frac{N}{N} = \frac{N}{2^P} = 1 \text{ real add} \end{array}\right\} \quad (45)$$

Total adds

$$ops_2 = \sum_{p=1}^{P} \frac{N}{2^p} = N \sum_{p=1}^{P} \frac{1}{2^p} = N\left(-1 + \sum_{p=0}^{P} \frac{1}{2^p}\right) \quad (46)$$

$$= N\left(-1 + 2\left(1 - \frac{1}{2^{P+1}}\right)\right)$$

$$= N\left(1 - \frac{1}{N}\right) = N - 1 \quad .$$

Total ops are, from (44) and (46), are

$$ops = ops_1 + ops_2$$

$$= 9N - 5 \quad (47)$$

This is incredible!

This is <u>without</u> decimation at low frequencies.

For the FFT, we need

$$ops_{FFT} = 8 N \log_2 N \quad (48)$$

<u>if</u> we compute <u>all</u> frequency lines and keep the ones we want (log spacing).

Notes:

① Windows

Both FFT & String can be windowed. This adds N ops to each (This is not included in fig. 11. For a given $x[n]$, we multiply by window:

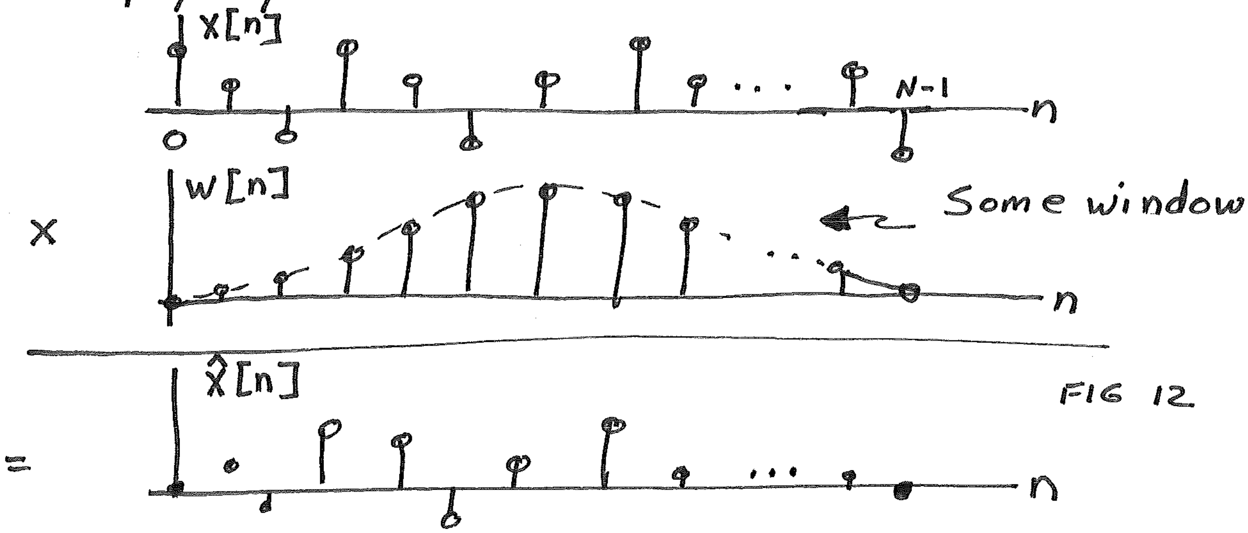

FIG 12

$$\hat{x}[n] = x[n]\, w[n] \tag{49}$$

We put $\hat{x}[n]$ into FFT <u>OR</u> STRING. The ops from then on are the same.

Ops in (49) are the same.

② In FIG 13, the ops are done sequentially. They can also be done in parallel by doing an 'inner product'

$$\begin{array}{ccccccc} x[1] & x[2] & \cdots & x[n] & \cdots & x[J] \\ \times e^{j2\pi u} & \times e^{j2\pi(2u)} & \cdots & \times e^{j2\pi(nu)} & \cdots & \times e^{j2\pi Ju} \\ \hline \end{array} \quad (50)$$

$$\underbrace{x[1]e^{j2\pi u} \quad x[2]e^{j2\pi(2u)} \cdots e^{j2\pi(nu)} \cdots x[J]e^{j2\pi Ju}}_{\text{add 'em up}}$$

The e^{j}'s here are stored in memory.

Maybe this is quicker in cycles. The ops are the same as in FIG 13.

Next steps: ① Decimation

② Szasz Cycles (?)

Addendum to Chapter 4

We also need to consider the DFT.

$$\mathbb{X}(u_p) = \sum_{n=1}^{N} x[n]\, e^{-j2\pi n u_p} \tag{51}$$

This is simply a matrix-vector multiply with $u_p = 2^p/N$; $1 \le p \le P = \log_2 N$

$$\overset{\uparrow}{\underset{\downarrow}{P}} \begin{bmatrix} \mathbb{X}(u_p) \end{bmatrix} = \downarrow P \begin{bmatrix} \xrightarrow{n} \\ e^{j2\pi n 2^p/N} \\ \end{bmatrix} \begin{bmatrix} \\ x[n] \\ \\ \end{bmatrix} \updownarrow N \tag{52}$$

Assume $x[n]$ is real. Count ops

$$\left.\begin{aligned} &P \text{ groups of } N \text{ real-times-complex multiplies} \\ &\qquad = 2PN \text{ real multiplies} \\ &P \text{ groups of } N-1 \text{ complex adds.} \\ &\qquad = 2P(N-1) \text{ real adds} \end{aligned}\right\} \tag{53}$$

Thus, including N multiplies for windowing

$$\begin{aligned} ops_{DFT} &= 4PN - 2P + N \\ &= 2\log_2 N\,(2N-1) + N \end{aligned} \tag{54}$$

This is better than FFT

$$ops_{FFT} = 8N\log_2 N + N \tag{55}$$

But not better than string cutting

$$ops_{STR} = 10N - 5 = 5(2N-1) \tag{56}$$

Sheet1 Chart 1

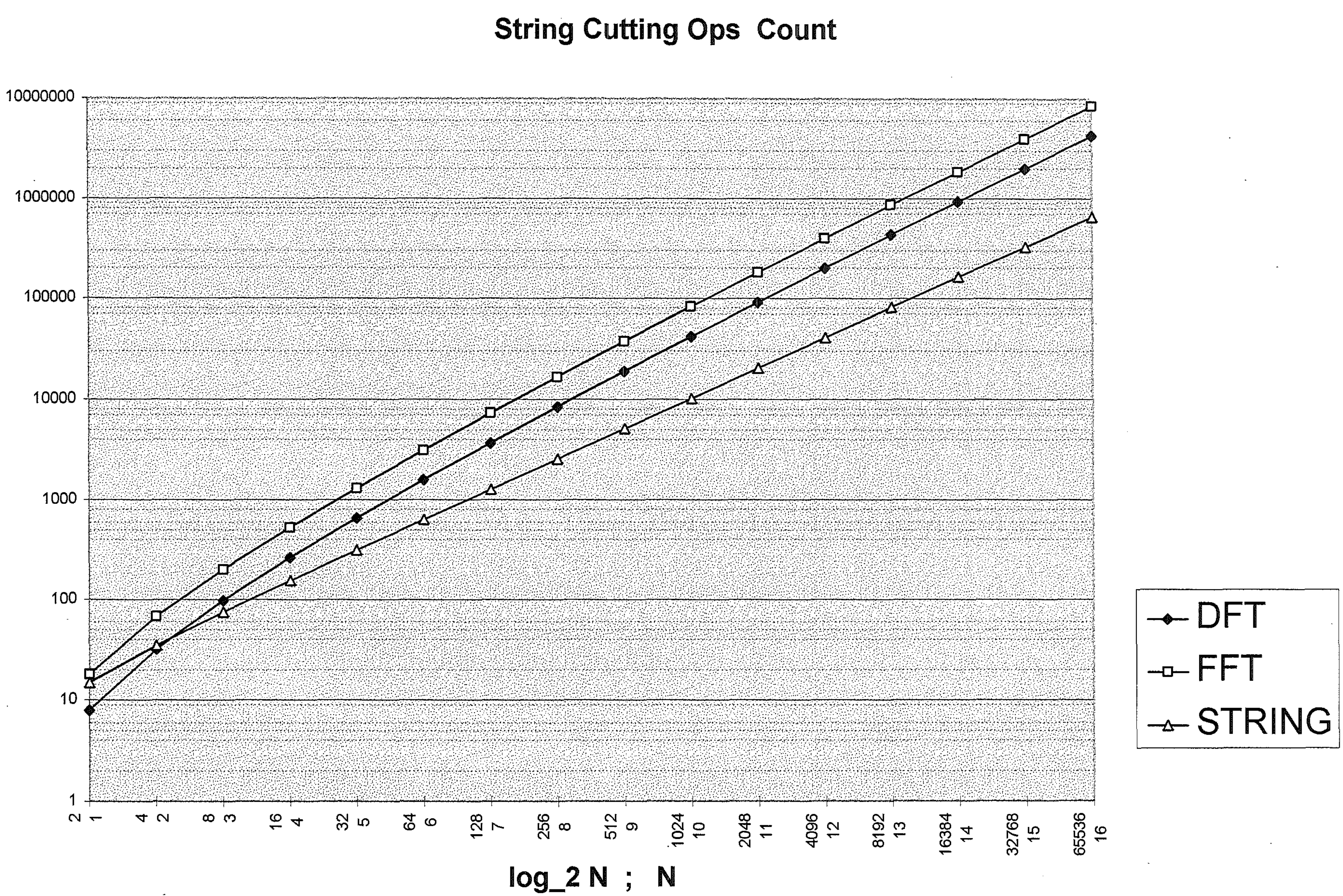

FIG 13

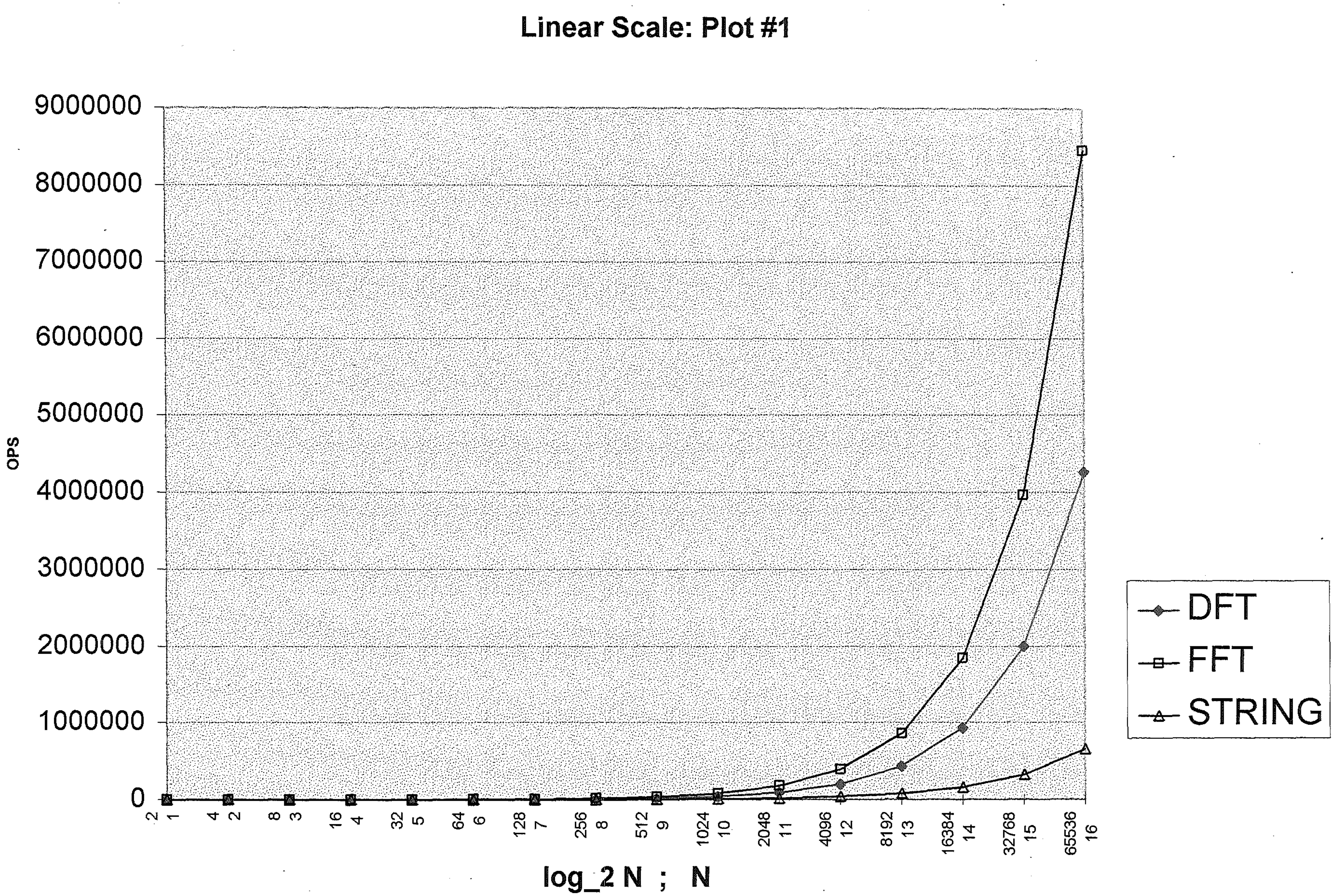

Linear Scale: Plot #1
9000000
8000000
7000000
6000000
5000000
4000000
3000000
2000000
1000000
0
OPS
2 1
4 2
8 3
16 4
32 5
64 6
128 7
256 8
512 9
1024 10
2048 11
4096 12
8192 13
16384 14
32768 15
65536 16
log_2 N ; N
DFT
FFT
STRING

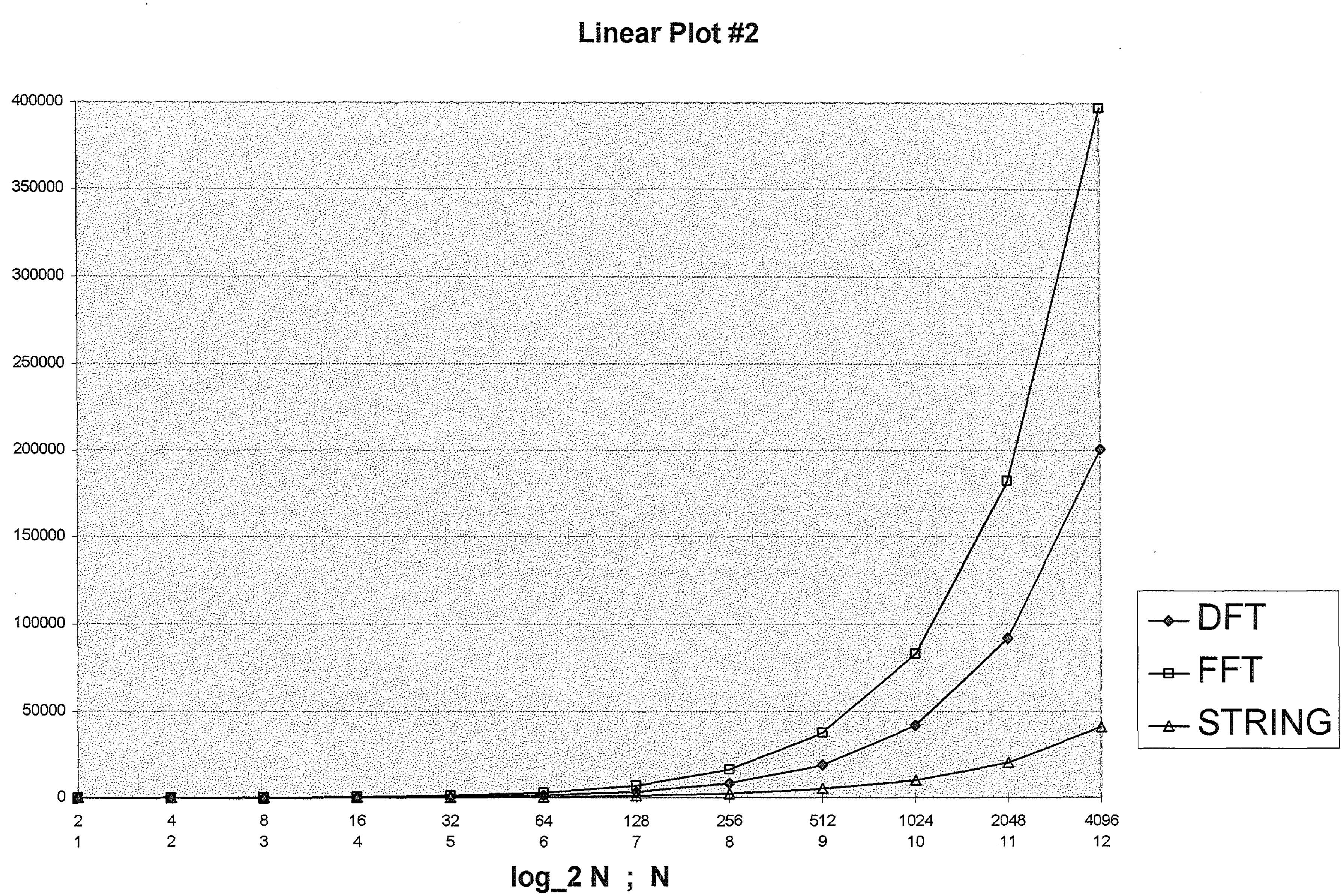

Linear Plot #2
400000
350000
300000
250000
200000
150000
100000
50000
0
2 4 8 16 32 64 128 256 512 1024 2048 4096
1 2 3 4 5 6 7 8 9 10 11 12
log_2 N ; N
DFT
FFT
STRING

24

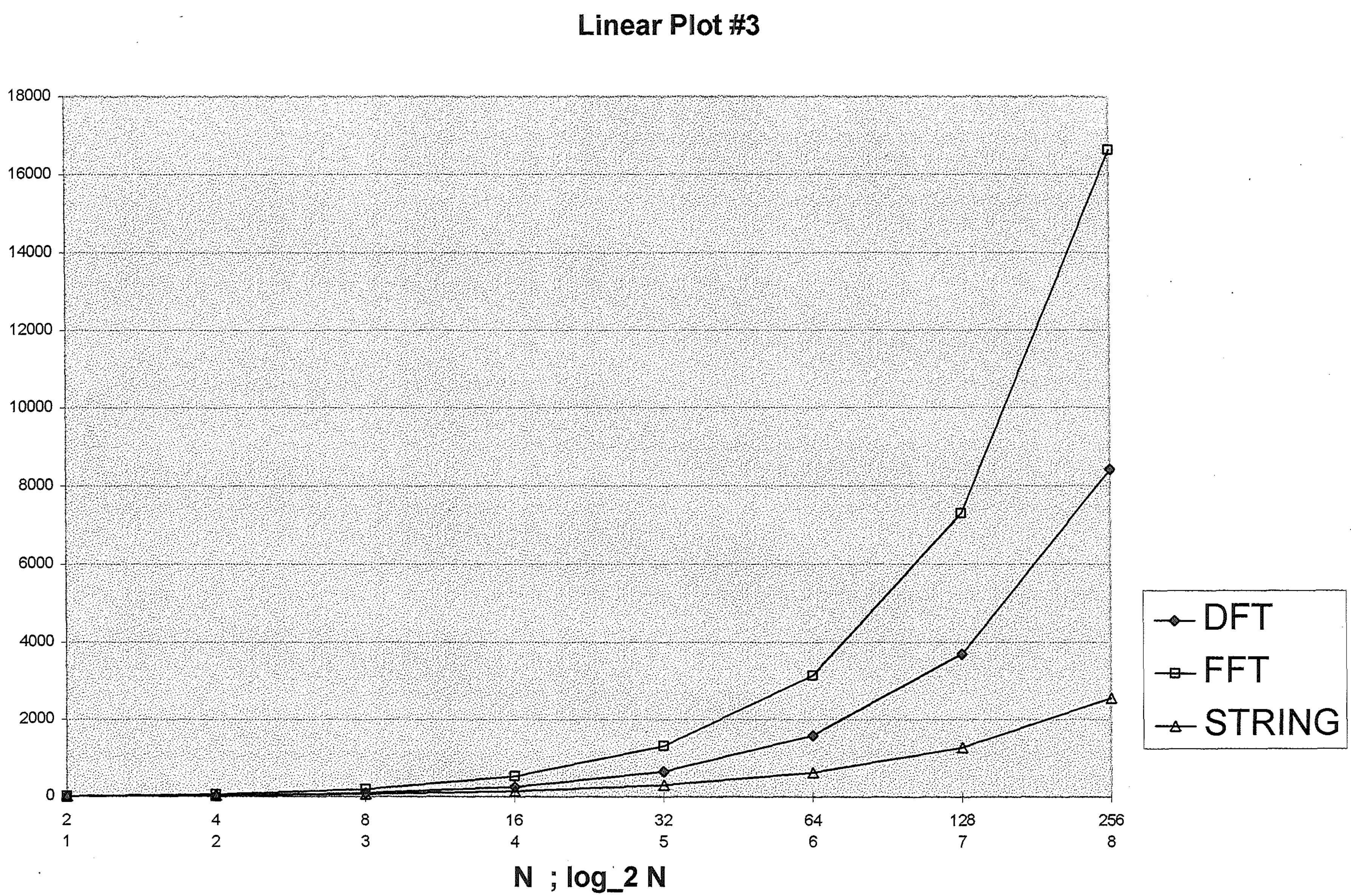
Linear Plot #3
18000
16000
14000
12000
10000
8000
6000
4000
2000
0
2
1
4
2
8
3
16
4
32
5
64
6
128
7
256
8
N ; log_2 N
DFT
FFT
STRING

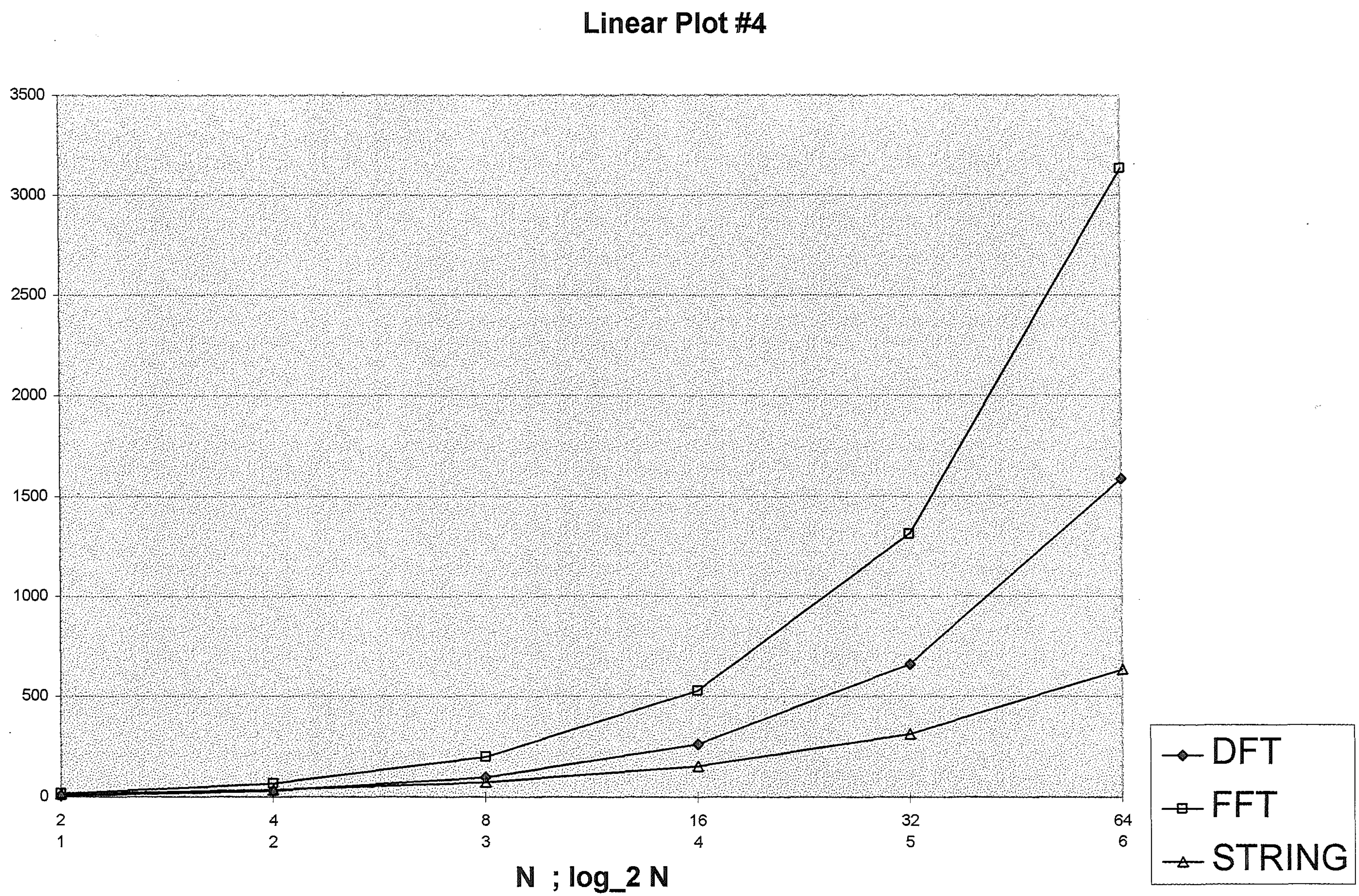
Linear Plot #4
3500
3000
2500
2000
1500
1000
500
0
2 4 8 16 32 64
1 2 3 4 5 6
N ; log_2 N
DFT
FFT
STRING

Chapt 5:

"Decimation and Interpolation using Strings and Zero padding"

Every sequence of N points has a continuous spectrum:

$$\mathbb{X}(u) = \sum_{n=0}^{N-1} x[n]\, e^{-j 2\pi n u} \qquad (57)$$

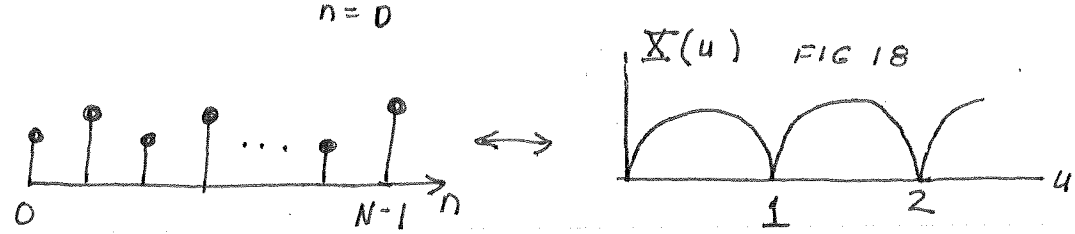

FIG 18

Since $\mathbb{X}(u)$ is a Fourier series, it is periodic with a period of one. The uniform DFT generates N samples of $\mathbb{X}(u)$:

$$\mathbb{X}_N[k] = \sum_{n=0}^{N-1} x[n]\, e^{-j 2\pi n \frac{k}{N}} \quad ; \; 0 \le k \le N-1 \qquad (58)$$

Compare this with (57). The sample points are at $u = k/N$.

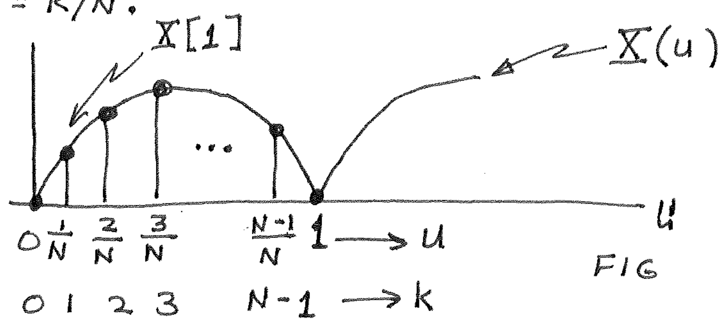

FIG 19

Frequency here can either be expressed as a function of u or discrete frequency, k.

Suppose, then, we wished to sample $X(u)$ at M other than N points?

- Case 1 : $M > N$, M an integer

To sample $X(u)$ at $M > N$ points, we simply zero pad $x[n]$ to $M-1$:

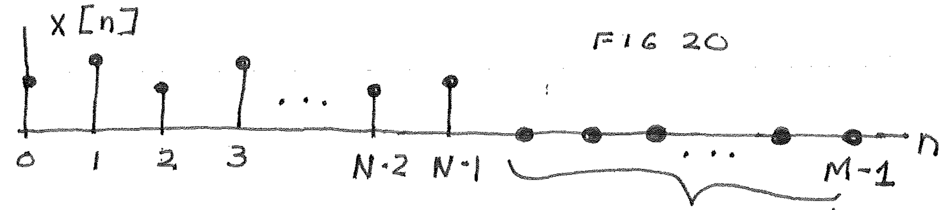

FIG 20

Do a DFT on the M points

$$X_M[k] = \sum_{n=0}^{M-1} x[n]\, e^{-j2\pi n \frac{k}{M}}$$

$$= \sum_{n=0}^{N-1} x[n]\, e^{-j2\pi n \frac{k}{M}} \qquad (59)$$

Compare with (57). Clearly

$$X_M[k] = X\left(\frac{k}{M}\right) \; ; \quad 0 \le k \le N-1 \qquad (60)$$

The DFT of Fig 20 is therefore

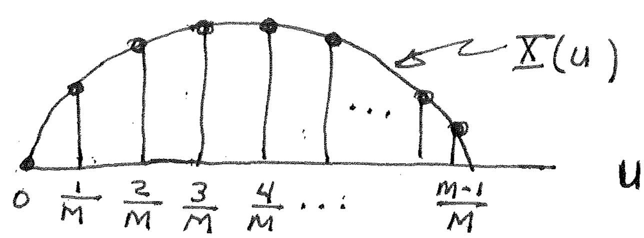

FIG 21

Szasz Interpretation:

For the sequence of length N, we have the lowest (non-zero) frequency over a cycle of length N:

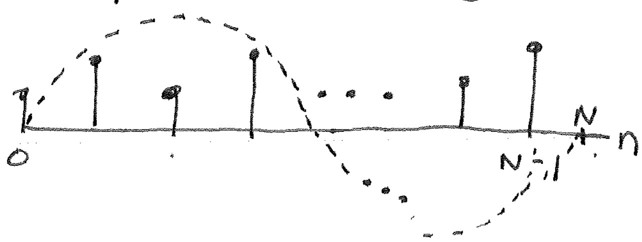

FIG 22

We get frequency

$$u = \frac{1}{N} \tag{61}$$

by applying the sequence in FIG ~~22~~ 13 to FIG 22. Chapter 4 (p. 14). Use parameters

$$u = 1/N \quad , \quad J = N \tag{62}$$

For the sequence of length M in FIGURE 20, we have the lowest non-zero frequency $u = 1/M$:

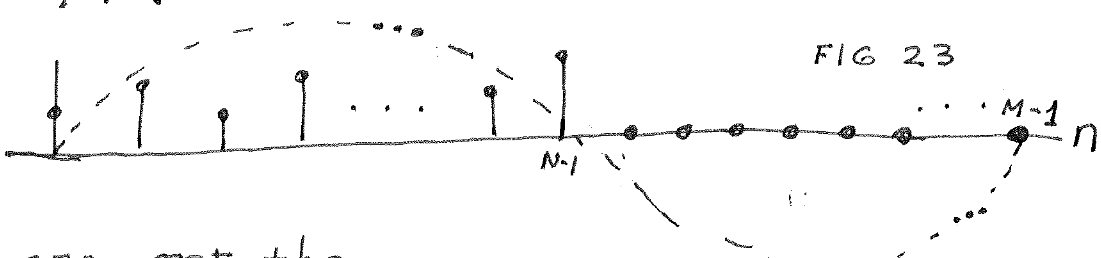

FIG 23

We can get the frequency $u = 1/M$ by using FIG 22 with

$$u = 1/M \quad , \quad J = M \tag{63}$$

BUT, since the final samples are zero, we can simply use $J = N$.

CASE 2 : $M < N$ or M rational

Assume

$$M = A/B \qquad (64)$$

where both A and B are integers. M is therefore a rational number.

We generate these samples by

1. Zero padding $x[n]$ to $AN-1$
2. Cut the string into B pieces.
   (Note assumption: NA/B is an integer) (65)
3. Do an FFT (or SZASZ) on the result.

Example: $M = 2/3$, $A = 2$, $B = 3$.
Assume $N = 6$. Note, $NA/B = 4 =$ Integer

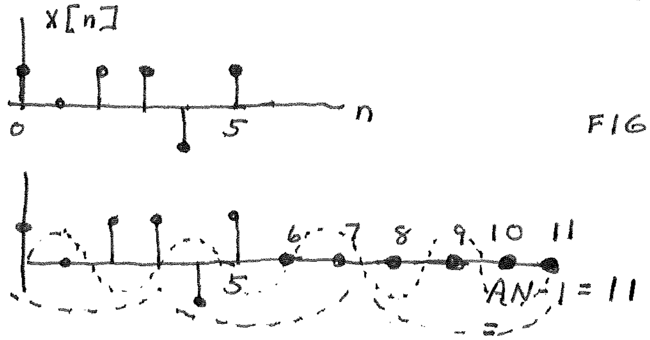

FIG 24

zero pad

Cut in to 3 strings:

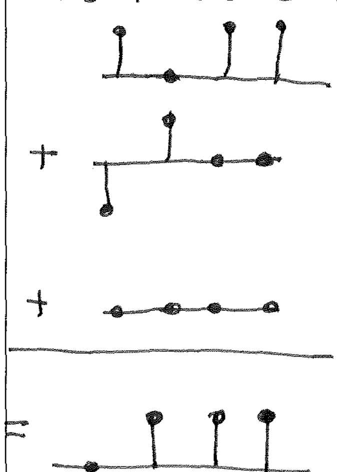

FIG 25

→ RUN THRU DFT FOR 4 POINTS

How it looks in the frequency domain:

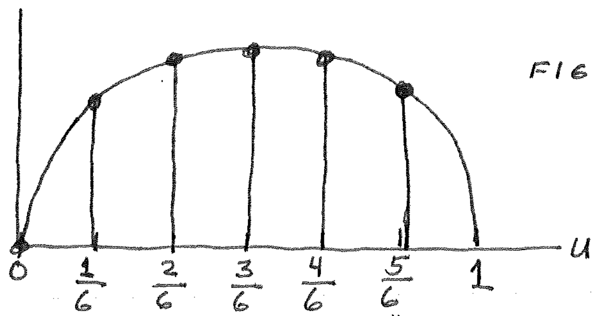

FIG 26

← N=6 spectrum for X[n] in FIG 24

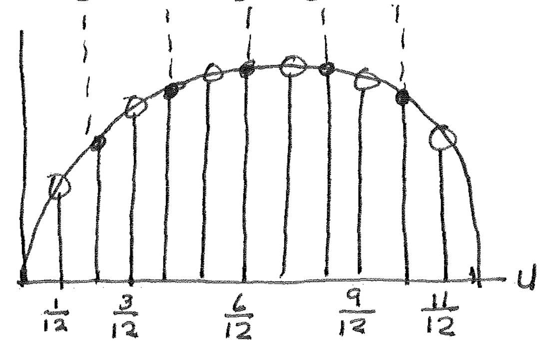

← FFT in x[n] in FIG 24 after zero padding

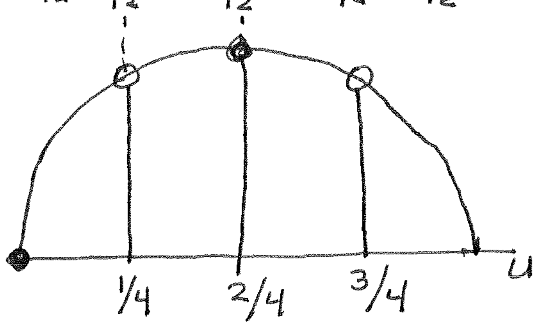

← STRING CUTTING in FIG 25 decimates all but every third sample!

Szasz look: Run the sequence after string cutting (bottom of p.30, FIG 25) into system below (from FIG 13)

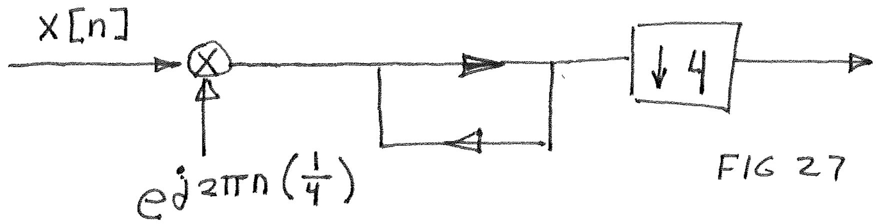

FIG 27

Output will be $u=\frac{1}{4}$ frequency line

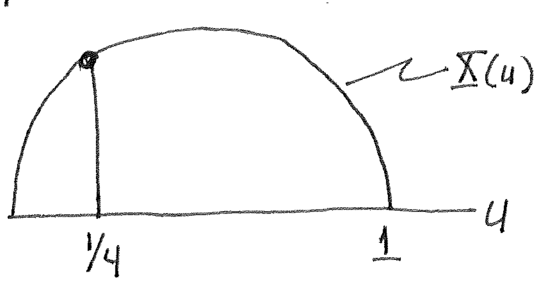

FIG 28

String cutting: What frequency set can we generate?

Consider a string of length N

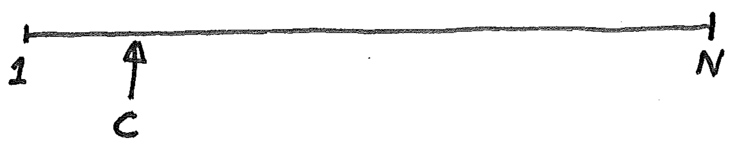

FIG. 29

A cut point, C, is chosen. The string is chopped into a number of pieces

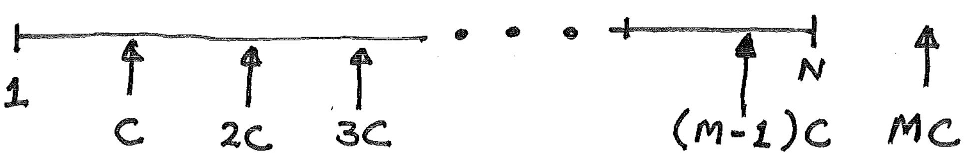

FIG 30

Clearly:

$$M = \left\langle \frac{N}{C} \right\rangle \qquad (66)$$

where

$$\langle ☺ \rangle = \text{'Round up' operation}$$
$$= \text{integer greater than } ☺ \qquad (66)$$

For example, $\langle 3.782987 \rangle = \langle \pi \rangle = 4$

The DTFT* of the original string is

$$X(u) = \sum_{n=1}^{N} x[n]\, e^{-j 2\pi n u} \qquad (67)$$

*DTFT = Discrete Time Fourier Transform

Break this into sub-strings:

$$\underline{X}(u) = \left[\sum_{n=1}^{c} + \sum_{n=c+1}^{2c} + \sum_{n=2c+1}^{3c} + \ldots + \sum_{n=(M-1)c+1}^{Mc} \right] x[n] e^{-j2\pi nu}$$

$$= \sum_{m=0}^{(M-1)} \sum_{n=mc+1}^{(m+1)c} x[n] e^{-j2\pi nu} \qquad (68)$$

Make variable substitution, $p = n - mc$ $\Rightarrow n = p + mc$. Thus

$$\underline{X}(u) = \sum_{m=0}^{M-1} \sum_{p=1}^{c} x[p+mc] e^{-j2\pi(p+mc)u}$$

$$= \sum_{p=1}^{c} e^{-j2\pi pu} \sum_{m=0}^{M-1} x[p+mc] e^{-j2\pi mcu} \qquad (69)$$

If we cut the strings and <u>then</u> transform, the result is

$$\underline{X}_c(u) = \sum_{p=1}^{c} e^{-j2\pi pu} \left[\sum_{m=0}^{M-1} x[p+mc] \right] \qquad (70)$$

sum of strings.

Compare with Eq. 69. $\underline{X} = \underline{X}_c$ in general, iff

$$e^{-j2\pi mcu} = 1 \qquad (71)$$

We want to define the set of integers that divide into c. Define the set

$$\mathcal{S}_c = \{ q \mid \frac{c}{q} = \text{integer} \} \qquad (72)$$

For example:

$$\mathcal{S}_{12} = \{1, 2, 3, 4, 6, 12\} \qquad (73)(247)$$

Equation (71) is true if for all $m \in [0, M)$

$$cu = \text{integer} \tag{74}$$

Let I = integer. Allowable frequencies are

$$u = \frac{I}{q} \quad ; q \in \mathcal{S}_c \tag{75}$$

For $c = 12$, for example, we have frequencies:

$I = 1$	$\frac{1}{1}$	$\frac{1}{2}$	$\frac{1}{3}$	$\frac{1}{4}$	$\frac{1}{6}$	$\frac{1}{12}$
2	$\cancel{\frac{2}{1}} \to 1$	$\cancel{\frac{2}{2}} \to 1$	$\frac{2}{3}$	$\cancel{\frac{2}{4}}$	$\cancel{\frac{2}{6}}$	$\cancel{\frac{2}{12}}$
3	$\cancel{\frac{3}{1}}$	$\cancel{\frac{3}{2}} \to \frac{1}{2}$	$\cancel{\frac{3}{3}}$	$\frac{3}{4}$	$\cancel{\frac{3}{6}}$	$\cancel{\frac{3}{12}}$
4	$\cancel{\frac{4}{1}}$	$\cancel{\frac{4}{2}}$	$\cancel{\frac{4}{3}}$	$\cancel{\frac{4}{4}}$	$\cancel{\frac{4}{6}}$	$\cancel{\frac{4}{12}}$
5	$\cancel{\frac{5}{1}}$	$\cancel{\frac{5}{2}}$	$\cancel{\frac{5}{3}}$	$\cancel{\frac{5}{4}}$	$\frac{5}{6}$	$\frac{5}{12}$
6	$\cancel{\frac{6}{1}}$	$\cancel{\frac{6}{2}}$	$\cancel{\frac{6}{3}}$	$\cancel{\frac{6}{4}}$	$\cancel{\frac{6}{6}}$	$\cancel{\frac{6}{12}}$
7	$\cancel{\frac{7}{1}}$	$\cancel{\frac{7}{2}}$	$\cancel{\frac{7}{3}}$	$\cancel{\frac{7}{4}}$	$\cancel{\frac{7}{6}}$	$\frac{7}{12}$
8	$\cancel{\frac{8}{1}}$	$\cancel{\frac{8}{2}}$	$\cancel{\frac{8}{3}}$	$\cancel{\frac{8}{4}}$	$\cancel{\frac{8}{6}}$	$\cancel{\frac{8}{12}}$
9	$\cancel{\frac{9}{1}}$	$\cancel{\frac{9}{2}}$	$\cancel{\frac{9}{3}}$	$\cancel{\frac{9}{4}}$	$\cancel{\frac{9}{6}}$	$\cancel{\frac{9}{12}}$
10	$\cancel{\frac{10}{1}}$	$\cancel{\frac{10}{2}}$	$\cancel{\frac{10}{3}}$	$\cancel{\frac{10}{4}}$	$\cancel{\frac{10}{6}}$	$\cancel{\frac{10}{12}}$
11	$\cancel{\frac{11}{1}}$	$\cancel{\frac{11}{2}}$	$\cancel{\frac{11}{3}}$	$\cancel{\frac{11}{4}}$	$\cancel{\frac{11}{6}}$	$\frac{11}{12}$
12	$\cancel{\frac{12}{1}}$	$\cancel{\frac{12}{2}}$	$\cancel{\frac{12}{3}}$	$\cancel{\frac{12}{4}}$	$\cancel{\frac{12}{6}}$	$\cancel{\frac{12}{12}}$
13	same as $1 = I$					
14	" " $2 = I$					

FIG 31

Note: $$\Sigma(u) = \Sigma(u + \text{integer}) \tag{76}$$

Thus: $\Sigma\left(\frac{5}{2}\right) = \Sigma\left(\frac{3}{2}\right) = \Sigma\left(\frac{1}{2}\right)$

Only circled numbers are allowable frequencies. Others are redundant.

Note that the circled frequencies in FIG. 31 are simply:

$$\left\{ u = \frac{q}{12} \;\middle|\; 0 \le q < 12 \right\}$$

In general, we can therefore generate the frequencies

$$\left\{ u = \frac{q}{C} \;\middle|\; 0 \le q < C \right\} \tag{77}$$

Conclusion

1. A sequence $x[n]$ has a DTFT given by (67).

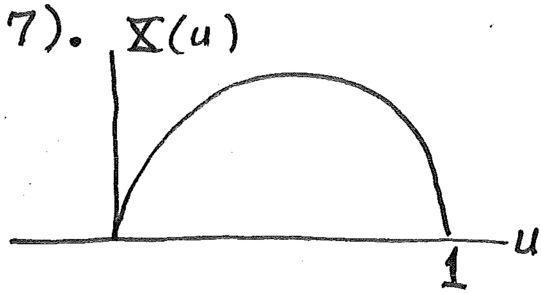

FIG. 32

2. Cut $x[n]$ into pieces of length C. Add them. Then a FFT on the sum gives C equally spaced points:

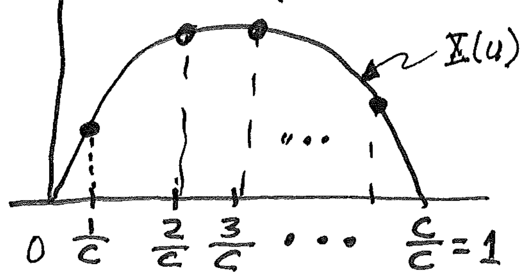

FIG 33

A Szasz can give any one of these points.

4/15/96

Chapter 8: Using flattened sinusoids

There is hope for estimating low frequencies using flattened sinusoids

Chapter 8

"Hal's flat sinusoid idea: What's the error?"

The original DFT is

$$\mathbb{X}(u) = \Sigma_{n=1}^{N} x[n]\, e^{-j2\pi n u} \tag{8-1}$$

Let's divide this into P intervals each of length p. Thus

$$N = p\,P \tag{8-2}$$

and

$$\begin{aligned} \mathbb{X}(u) = & \sum_{n=1}^{p} x[n]\, e^{-j2\pi n u} \\ & + \sum_{n=p+1}^{2p} x[n]\, e^{-j2\pi n u} \\ & + \dots + \sum_{n=(q-1)p+1}^{qp} x[n]\, e^{-j2\pi n u} \\ & + \dots + \sum_{n=(P-1)p+1}^{Pp} x[n]\, e^{-j2\pi n u} \end{aligned} \tag{8-3}$$

$$= \sum_{q=1}^{P} \sum_{n=(q-1)p+1}^{qp} x[n]\, e^{-j2\pi n u} \tag{8-4}$$

For the q^{th} interval, replace $e^{-j2\pi n u}$ by $e^{-j2\pi(pq)u}$. This makes the complex sinusoid constant (flat) over the q^{th} interval. The result is

$$\mathbb{X}_P(u) = \sum_{q=1}^{P} \sum_{n=(q-1)p+1}^{qp} x[n]\, e^{-j2\pi p q u}$$

$$= \sum_{q=1}^{P} e^{-j2\pi p q u} \sum_{n=(q-1)p+1}^{qp} x[n] \tag{8-5}$$

The sum over n is simply the sum of the signal samples over the q^{th} ~~p~~-interval. Define

$$x_p[q] = \sum_{n=(q-1)p+1}^{qp} x[n] \qquad (8\text{-}6)$$

Then (8-5) becomes

$$X_p(u) = \sum_{q=1}^{P} x_p[q]\, e^{-j2\pi q\,(pu)} \qquad (8\text{-}7)$$

This is simply a DTFT* of the summed intervals. For example, let $N = 12$, $P = 3$ and $p = 4$.

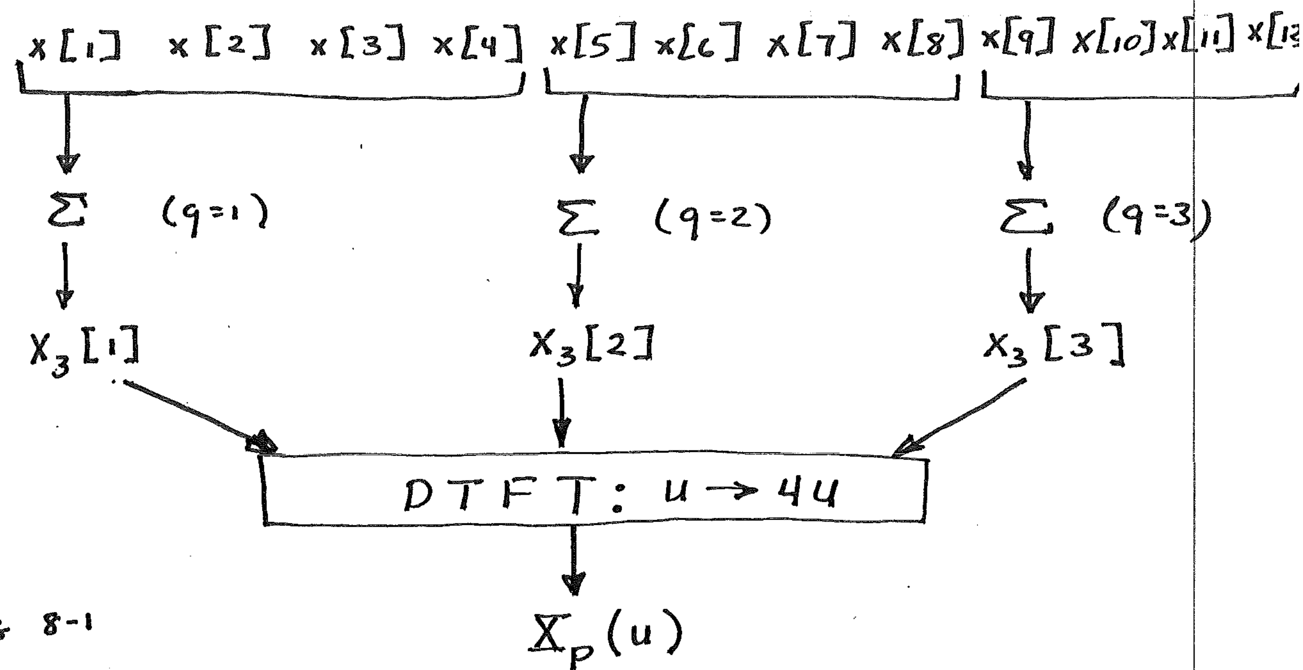

FIG 8-1

The big question:

What is the error between $X_p(u)$ and $X(u)$ in Eq. 8-2

*Discrete Time Fourier Transform

The error between $\underline{X}(u)$ and $\underline{X}_{\underline{P}}(u)$ at frequency u is

$$\mathcal{E}_{\underline{P}}(u) = \left| \underline{X}(u) - \underline{X}_{\underline{P}}(u) \right|^2 \tag{8-8}$$

$$= \left| \sum_{q=1}^{\underline{P}} \sum_{n=(q-1)P+1}^{qP} x[n] \left[e^{-j2\pi nu} - e^{-j2\pi qPu} \right] \right|^2$$

Use the inequality

$$\left| \sum_m a_m \right|^2 \leq \sum_m |a_m|^2 \tag{8-9}$$

gives

$$\mathcal{E}_{\underline{P}}(u) \leq \sum_{q=1}^{\underline{P}} \left| \sum_{n=(q-1)P+1}^{qP} x[n] \left[e^{-j2\pi nu} - e^{-j2\pi qPu} \right] \right|^2 \tag{8-10}$$

Schwarz's inequality is

$$\left| \sum_m a_m b_m \right|^2 \leq \sum_m |a_m|^2 \sum_m |b_m|^2 \tag{8-11}$$

Applying to (8-10) gives

$$\mathcal{E}_{\underline{P}}(u) \leq \sum_{q=1}^{\underline{P}} \left[\sum_{n=(q-1)P+1}^{qP} |x[n]|^2 \times \sum_{n=(q-1)P+1}^{qP} \left| e^{-j2\pi nu} - e^{-j2\pi qPu} \right|^2 \right] \tag{8-12}$$

The first sum over n is simply the energy of the signal over the $q^{\underline{th}}$ interval

$$E_q = \sum_{n=(q-1)P+1}^{qP} |x[n]|^2 \tag{8-13}$$

The second sum in (8-12) takes more work. Let

$$S_q = \sum_{n=(q-1)p+1}^{qp} \left| e^{-j2\pi nu} - e^{-j2\pi qpu} \right|^2 \tag{8-14}$$

so that (8-12) can be written

$$\mathcal{E}_p(u) \leq \sum_{q=1}^{p} E_q \, S_q \tag{8-15}$$

Clearly

$$S_q = \sum_{n=(q-1)p+1}^{qp} \left[2 - 2\cos 2\pi(n-pq)u \right]$$

$$= 2\left[p - \mathrm{Re} \sum_{n=(q-1)p+1}^{qp} e^{j2\pi(n-pq)u} \right]$$

$$= 2p - 2\,\mathrm{Re}\, e^{-j2\pi pqu} \sum_{n=(q-1)p+1}^{qp} e^{j2\pi nu} \tag{8-16}$$

Let

$$s = \sum_{n=(q-1)p+1}^{qp} \alpha^n = \alpha^{(q-1)p+1} + \alpha^{(q-1)p+2} + \ldots + \alpha^{qp}$$

$$\alpha s = \alpha^{(q-1)p+2} + \ldots + \alpha^{qp} + \alpha^{qp+1}$$

$$(1-\alpha)s = \alpha^{(q-1)p+1} - \alpha^{qp+1} \tag{8-17}$$

or

$$s = \frac{\alpha^{qp+1}\left[\alpha^{-p} - 1\right]}{1-\alpha} \tag{8-18}$$

$$s = \frac{\alpha^{qp+1}(1-\alpha^{-p})}{\alpha - 1} = \frac{\alpha^{qp+1-\frac{p}{2}}(\alpha^{\frac{p}{2}} - \alpha^{-\frac{p}{2}})}{\alpha^{\frac{1}{2}}(\alpha^{\frac{1}{2}} - \alpha^{-\frac{1}{2}})} \tag{8-19}$$

For $\alpha = e^{j2\pi u}$,

$$s = e^{j2\pi(qp - \frac{1}{2} - \frac{p}{2})} \frac{\sin \pi p u}{\sin \pi u} \tag{8-20}$$

Substituting into (8-16)

$$S_q = 2p - 2\,\mathrm{Re}\, e^{j2\pi(qp - \frac{1}{2} - \frac{p}{2} - qp)} \frac{\sin \pi p u}{\sin \pi u} \tag{8-21}$$

$$= 2\left[p - \cos \pi (p+1) u \frac{\sin \pi p u}{\sin \pi u}\right]$$

Substituting into (8-15)

$$\mathcal{E}_P(u) \le 2 \sum_{q=1}^{P} E_q \left[p - \cos \pi (p+1) u \frac{\sin \pi p u}{\sin \pi u}\right]$$

$$= 2E\left[p - \cos \pi (p+1) u \frac{\sin \pi p u}{\sin u \pi}\right] \tag{8-22}$$

where the energy of the entire signal is

$$E = \sum_{q=1}^{P} E_q = \sum_{n=1}^{N} |x[n]|^2 \tag{8-23}$$

In normalized form, the result is

$$\frac{\mathcal{E}_P(u)}{E} \le 2\left[p - \cos \pi (p+1) u \frac{\sin \pi p u}{\sin \pi u}\right] \tag{8-24}$$

$$s = \frac{\alpha^{qp+1}\,(1-\alpha^{-p})}{\alpha - 1} = \frac{\alpha^{qp+1-\frac{p}{2}}\,(\alpha^{\frac{p}{2}} - \alpha^{-\frac{p}{2}})}{\alpha^{\frac{1}{2}}\,(\alpha^{\frac{1}{2}} - \alpha^{-\frac{1}{2}})} \qquad (8\text{-}19)$$

For $\alpha = e^{j2\pi u}$,

$$s = e^{j2\pi(qp - \frac{1}{2} - \frac{p}{2})}\,\frac{\sin \pi p u}{\sin \pi u} \qquad (8\text{-}20)$$

Substituting into (8-16)

$$S_q = 2p - 2\,\mathrm{Re}\, e^{j2\pi(\cancel{qp} - \frac{1}{2} - \frac{p}{2} - \cancel{qp})}\,\frac{\sin \pi p u}{\sin \pi u} \qquad (8\text{-}21)$$

$$= 2\left[p - \cos \pi(p+1)u\,\frac{\sin \pi p u}{\sin \pi u}\right]$$

Substituting into (8-15)

$$\mathcal{E}_P(u) \le 2 \sum_{q=1}^{P} E_q \left[p - \cos \pi(p+1)u\,\frac{\sin \pi p u}{\sin \pi u}\right]$$

$$= 2E\left[p - \cos \pi(p+1)u\,\frac{\sin \pi p u}{\sin u\pi}\right] \qquad (8\text{-}22)$$

where the energy of the entire signal is

$$E = \sum_{q=1}^{P} E_q = \sum_{n=1}^{N} |x[n]|^2 \qquad (8\text{-}23)$$

In normalized form, the result is

$$\frac{\mathcal{E}_P(u)}{E} \le 2\left[p - \cos \pi(p+1)u\,\frac{\sin \pi p u}{\sin \pi u}\right] \qquad (8\text{-}24)$$

Comments:

(A)
$$\left.\frac{\sin \pi p u}{\sin \pi u}\right|_{u=0} = \left.\frac{\sin \pi p u}{\sin \pi u}\right|_{u=1} = p \qquad (8\cdot 25)$$

Thus, from (8·24)

$$\left.\frac{\mathcal{E}_p(u)}{E}\right|_{u=0} = 0 \qquad (8\cdot 26)$$

This makes sense since 'flattening' DC means nothing.

(B) For $u=\frac{1}{2}$, (8·24) becomes

$$\frac{\mathcal{E}_p(\frac{1}{2})}{E} \leq 2\left[p - \cos\left(\frac{\pi(p+1)}{2}\right)\frac{\sin\frac{\pi p}{2}}{\sin\frac{\pi}{2}}\right] \qquad (8\cdot 27)$$

- If p is even, $\sin\frac{\pi p}{2} = 0$
- If p is odd, $\cos\frac{\pi(p+1)}{2} = 0$

Thus

$$\mathcal{E}_p(\tfrac{1}{2})/E \leq 2p \qquad (8\cdot 28)$$

Where $2p$ is twice the length of an interval.

(c) For $P = N$ intervals, $p = 1$ and (8-24) becomes

$$\left.\frac{\mathcal{E}_P(u)}{E}\right|_{P=N} \leq 2\left[1 - \cos 2\pi u \; \frac{\sin \pi u}{\sin \pi u}\right]$$

$$= 2\,(1 - \cos 2\pi u)$$

$$= 4 \sin^2 \pi u \qquad (8\text{-}29)$$

This *should* be zero and suggests the bound is bad in the middle.

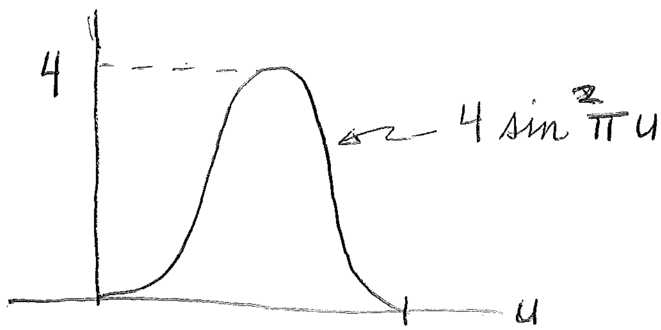

But it is good for $u \to 0, 1$

FIG 8-2

(d) Some plots follow.

Note: The bounds for $1/N$ are pretty small! This is *good*! Why? Cause we're interested in $X\left(\frac{1}{N}\right)$.

$p=2$

$N=128,\ P=64$

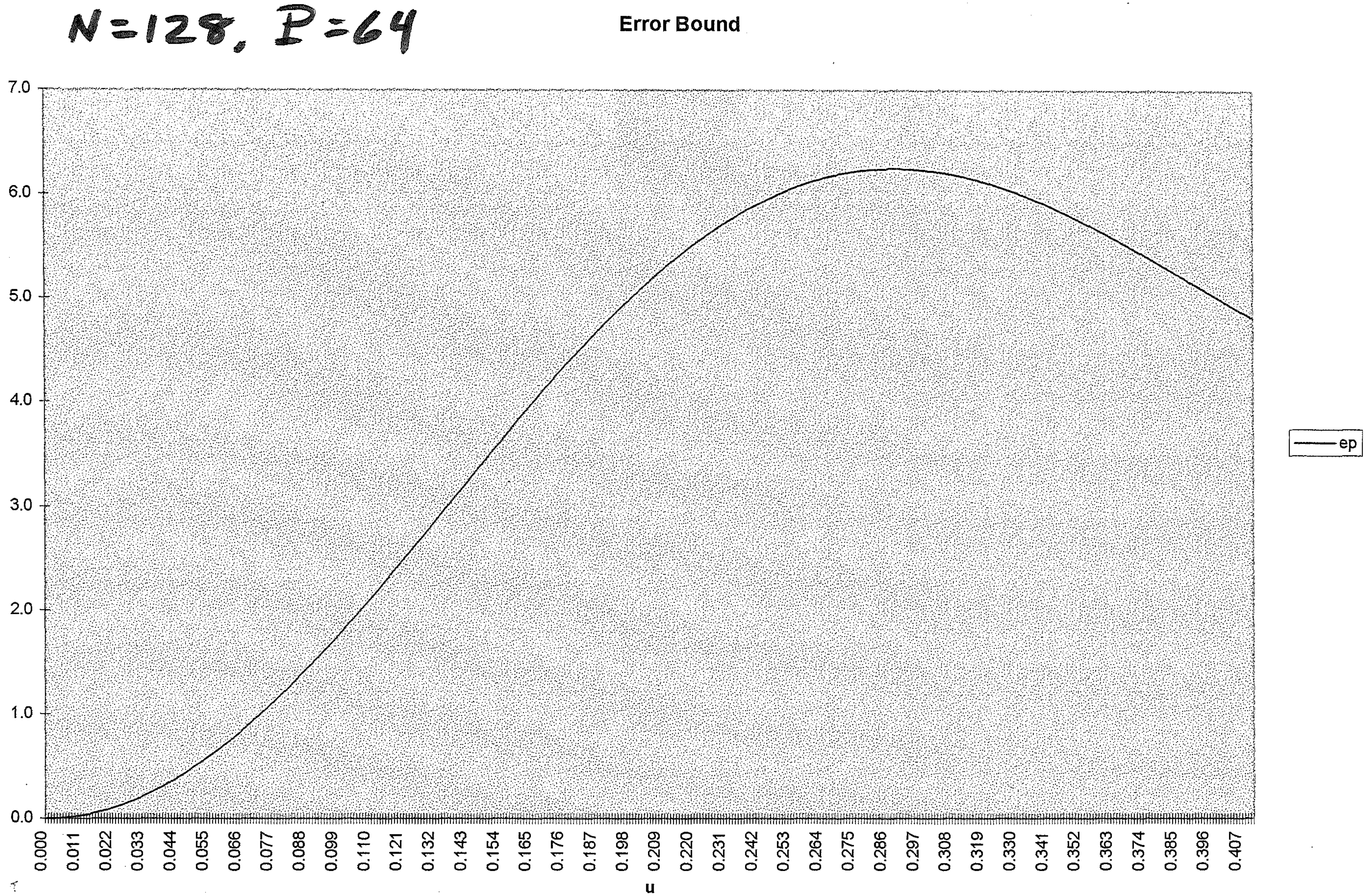

99-8

$p = 2$

$N = 128, P = 64$

Error Bound

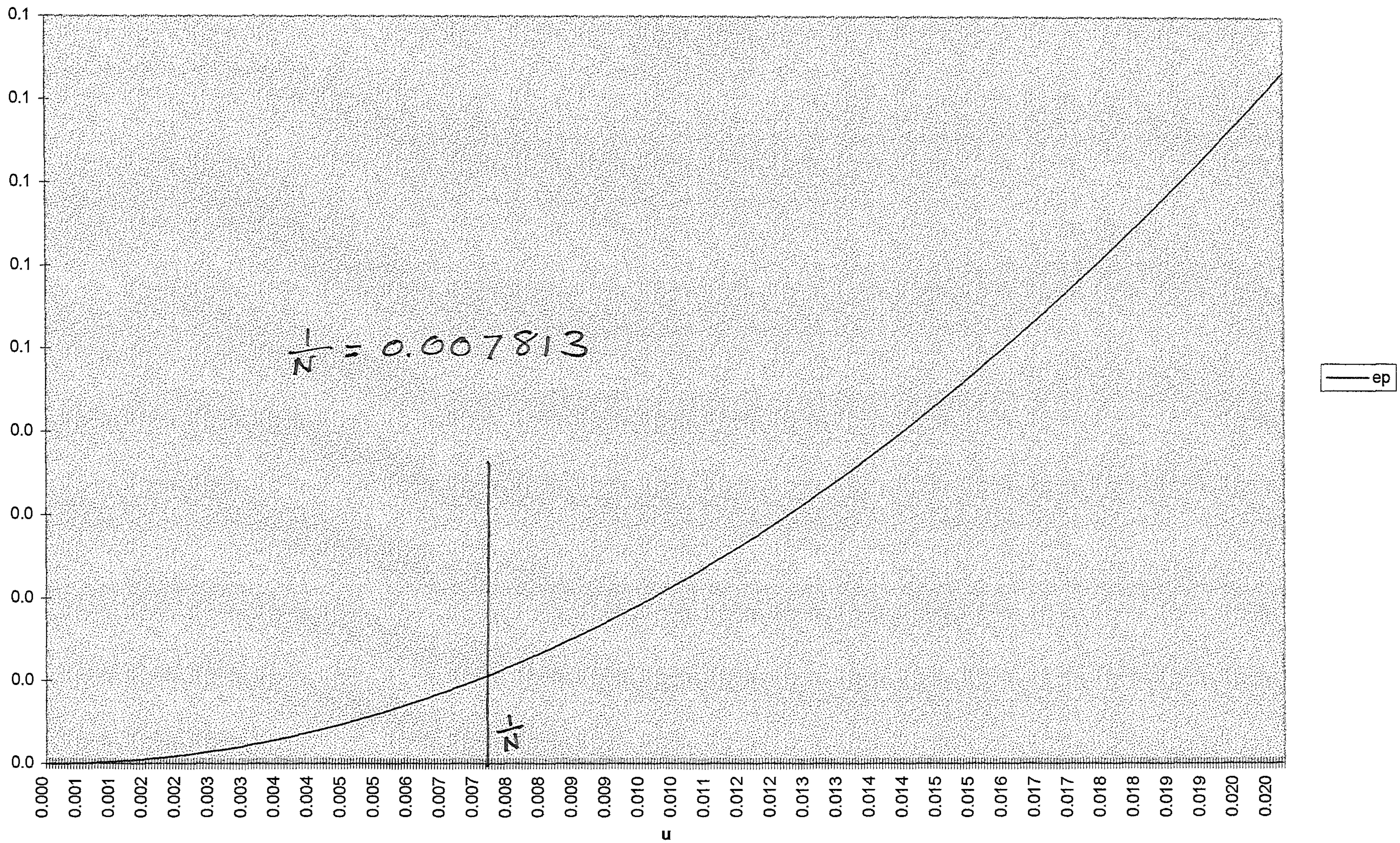

8-6c

p = 8

N = 128, P = 16

Error Bound

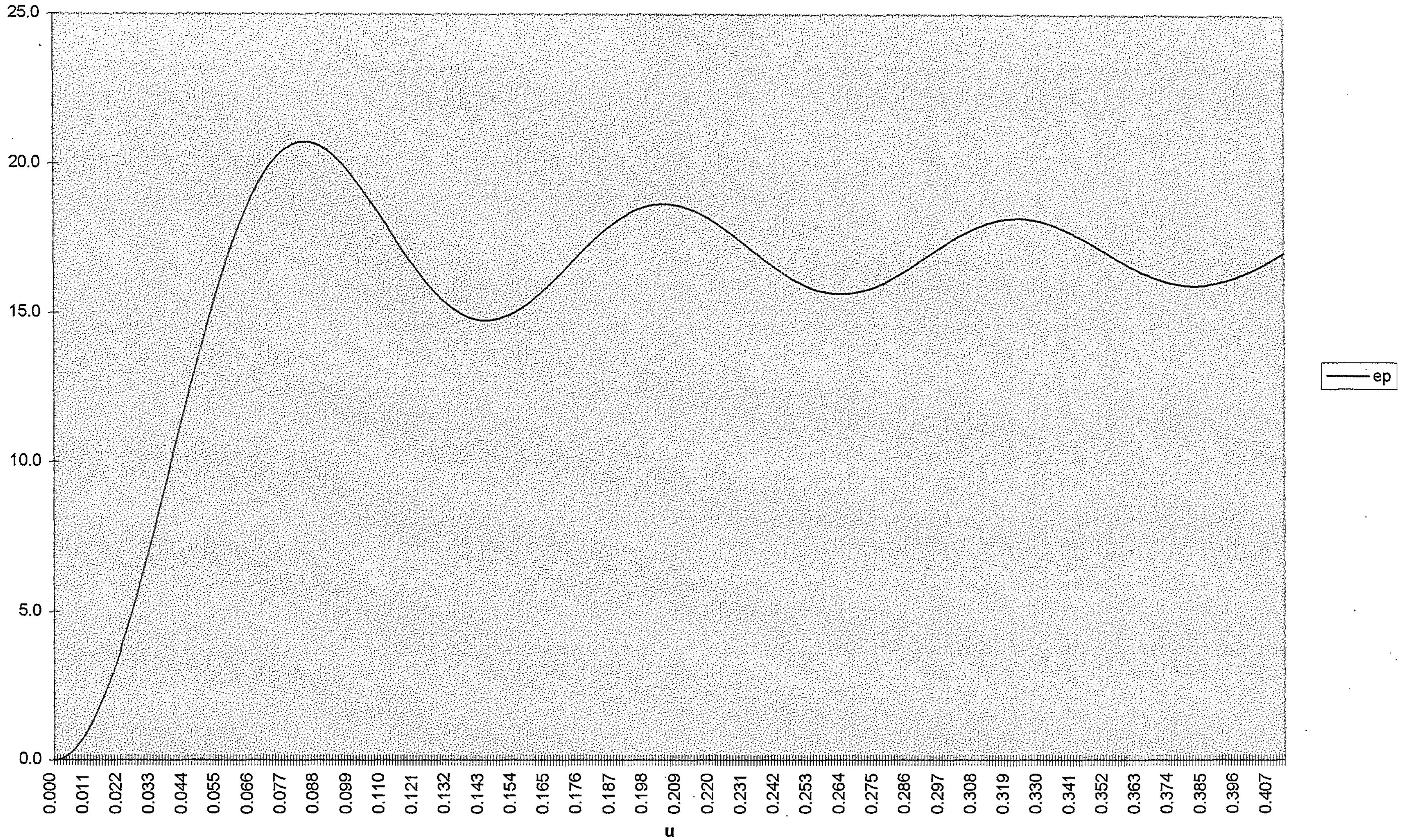

p9-8

$p = 8$

$N = 128,\ P = 16$

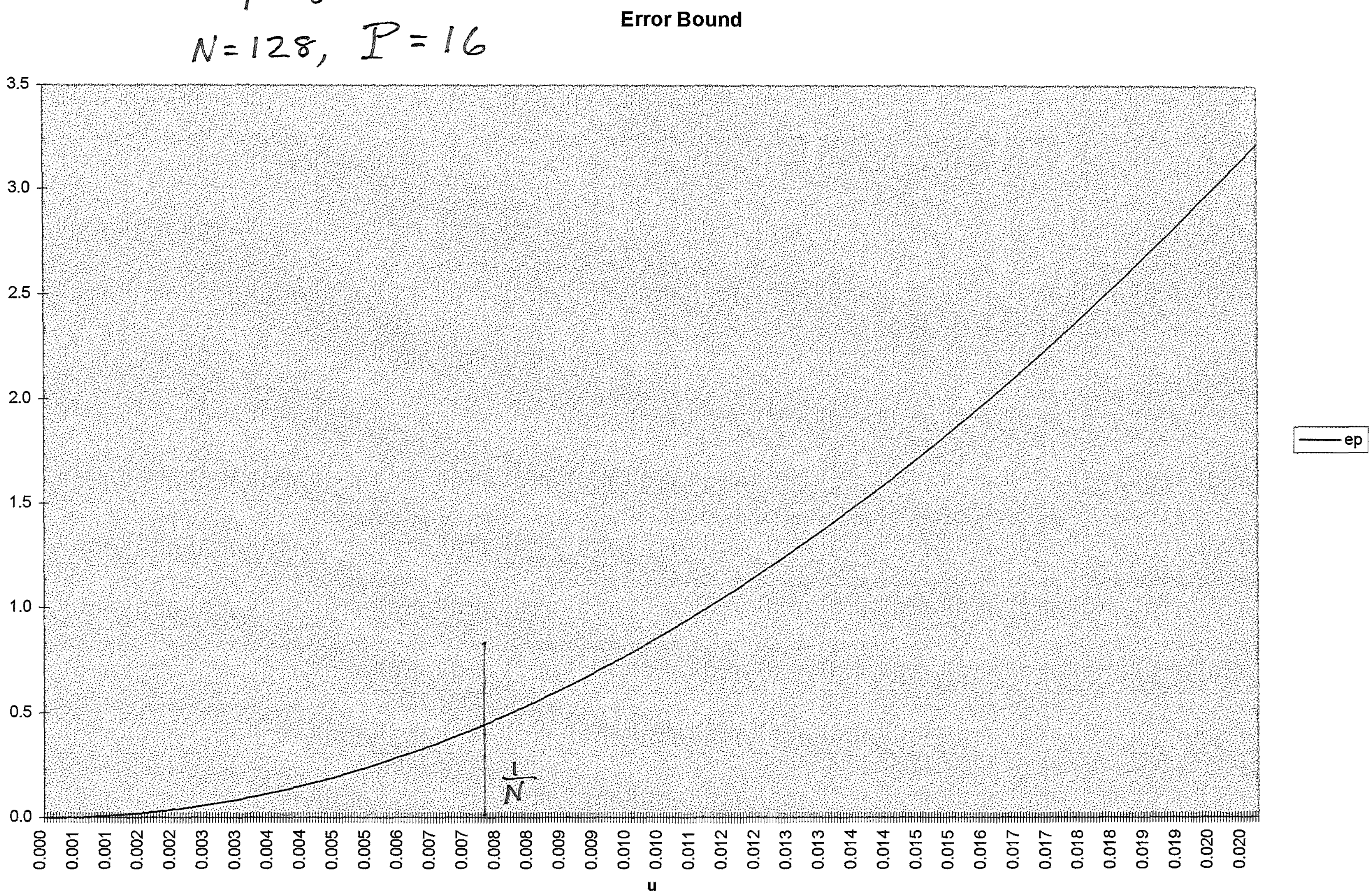

a 7-8

p = 32

N = 128, P = 4,

Error Bound

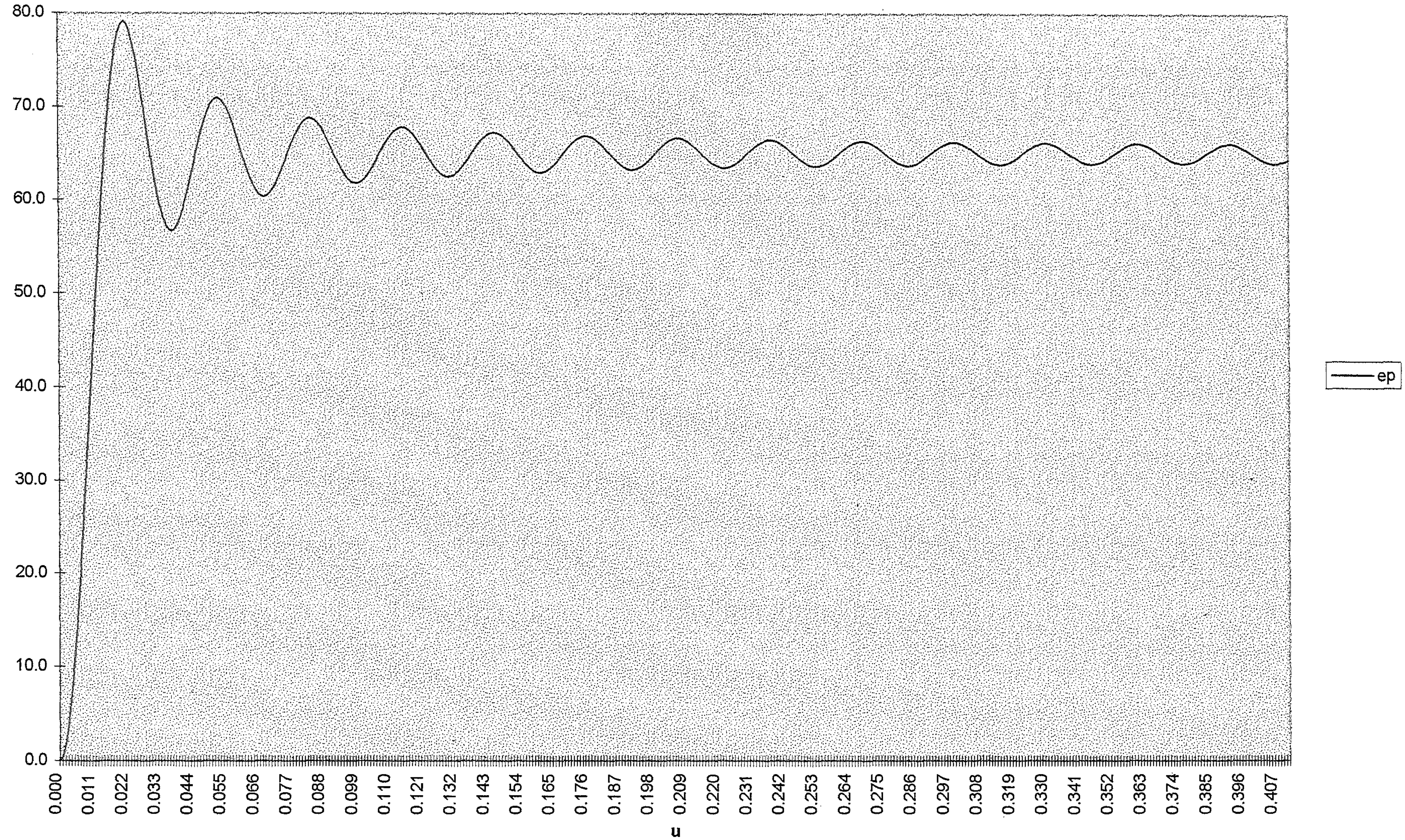

f 9-8

$\rho = 32$

Error Bound

$N = 128, \quad P = 4$

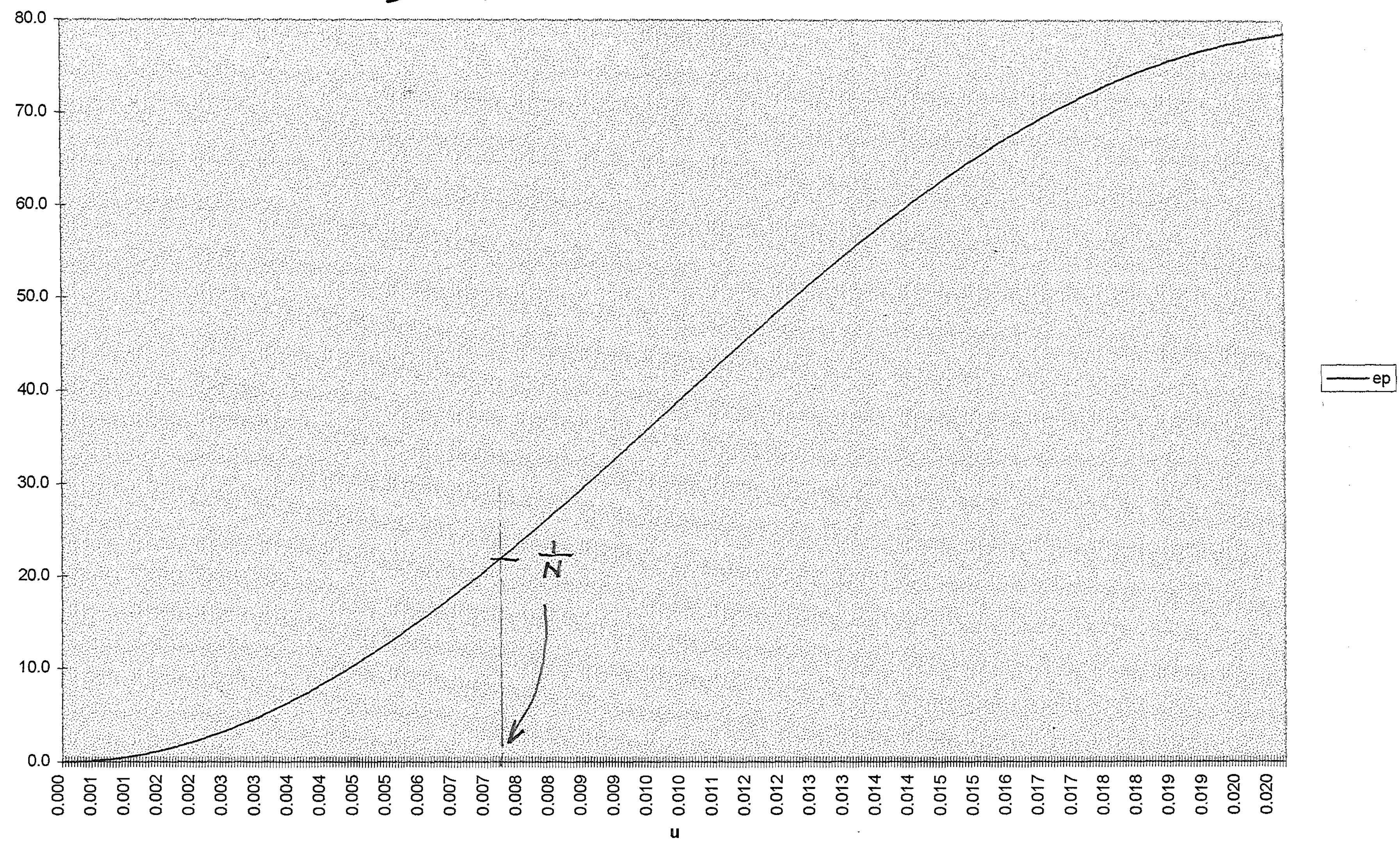

$N = 2046$
$p = 36, P = 64$

Error Bound

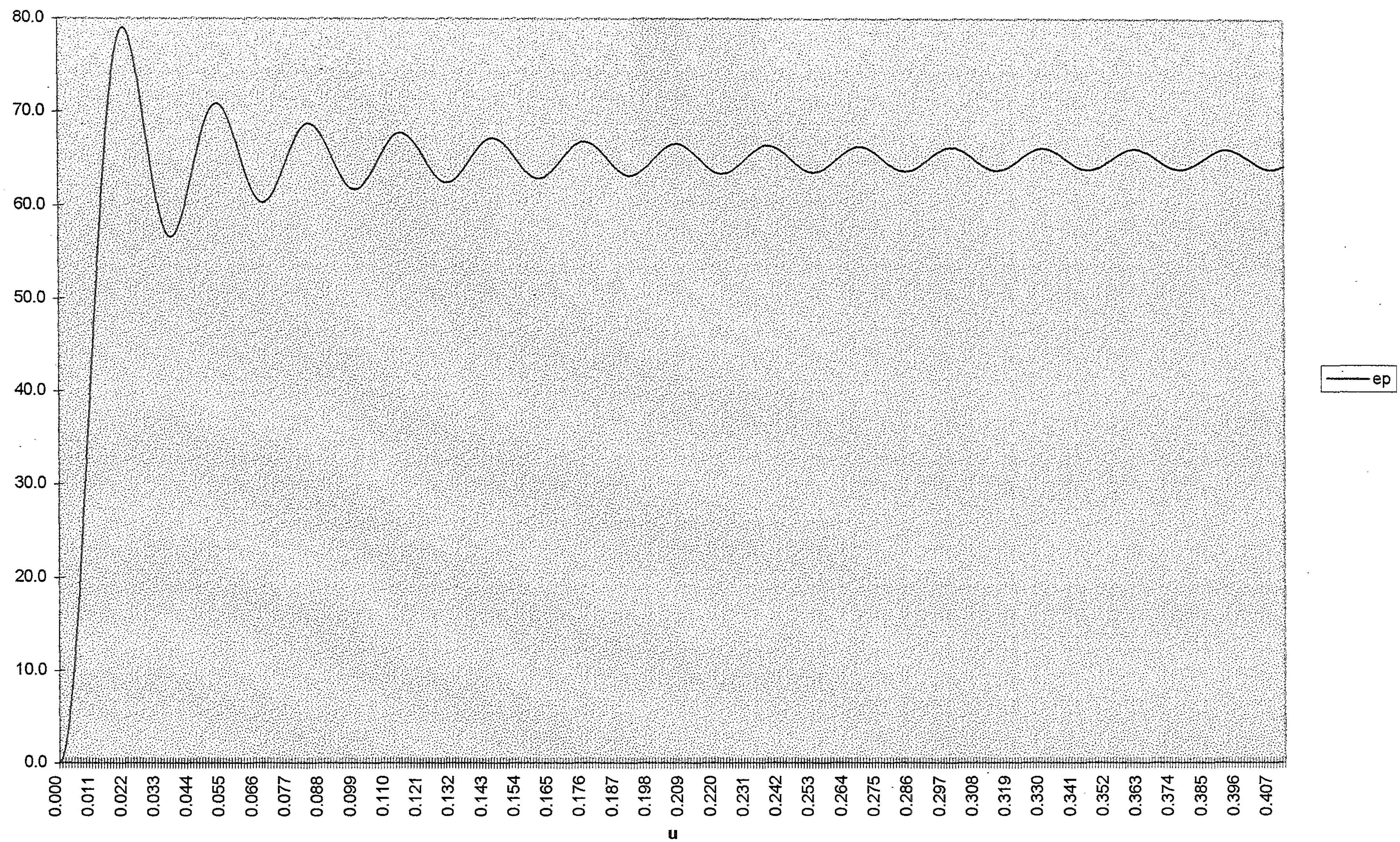

8-64

$N = 2046$

$p = 36, \underline{P} = 64$

Error Bound

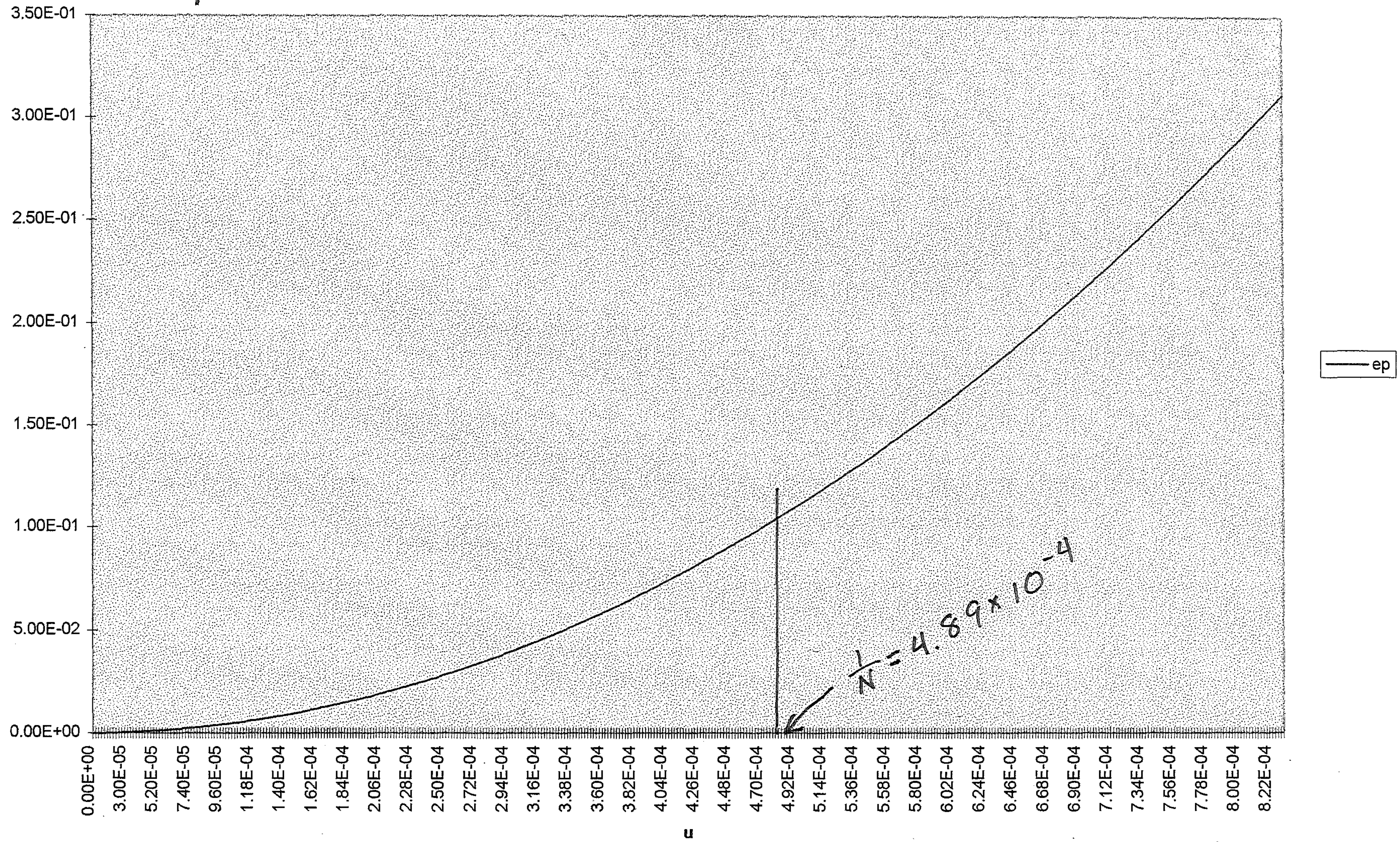

8-6r

$N = 2046$

$\underline{P} = 16, \; p = 128$

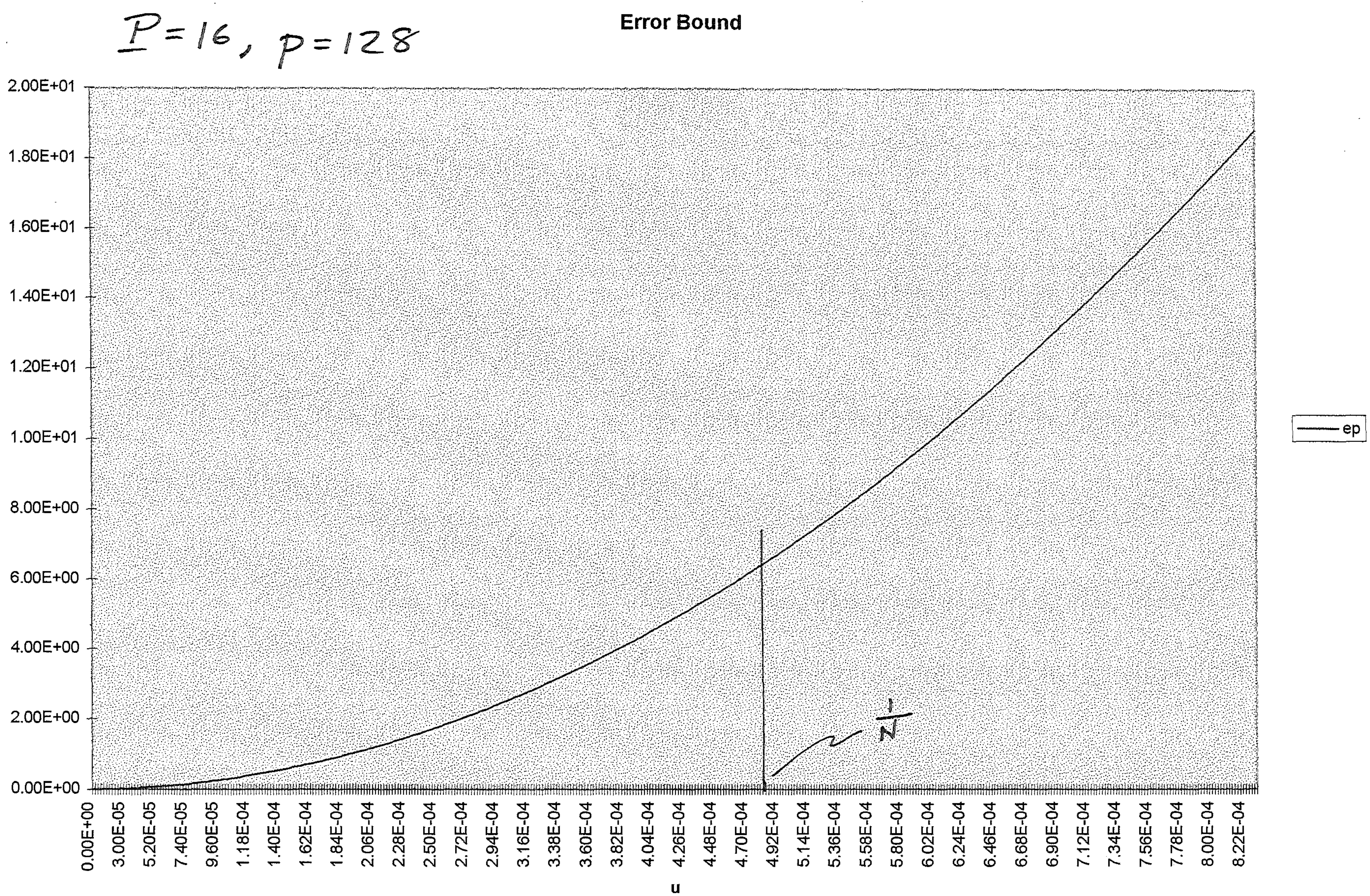

p9-8

"The Bound for $\mathcal{E}_P(1/N)/E$"

If we use the flat sinusoid to generate $\bar{X}_P(\frac{1}{N}) \approx \bar{X}(\frac{1}{N})$, what is the error bound?

From (8-24);

$$\frac{\mathcal{E}_P(1/N)}{E} \leq 2\left[p - \cos\frac{\pi(p+1)}{N} \quad \frac{\sin\frac{\pi p}{N}}{\sin\frac{\pi}{N}}\right] \tag{8-29a}$$

or

$$\frac{\mathcal{E}_P(1/N)}{E} \leq 2\left[\frac{N}{P} - \cos\frac{\pi\left(\frac{N}{P}+1\right)}{N} \quad \frac{\sin\frac{\pi}{P}}{\sin\frac{\pi}{N}}\right] \tag{8-29b}$$

or

$$\frac{\mathcal{E}_p(\frac{1}{N})}{E} \leq 2\left[p - \cos\frac{\pi(p+1)}{Pp} \quad \frac{\sin\frac{\pi}{P}}{\sin\frac{\pi}{pP}}\right] \tag{8-29c}$$

The next three figures are (8-29a) vs p. for various N.

Then, two Figures are (8-29b) vs. P for various N.

error bound versus p=flat interval length

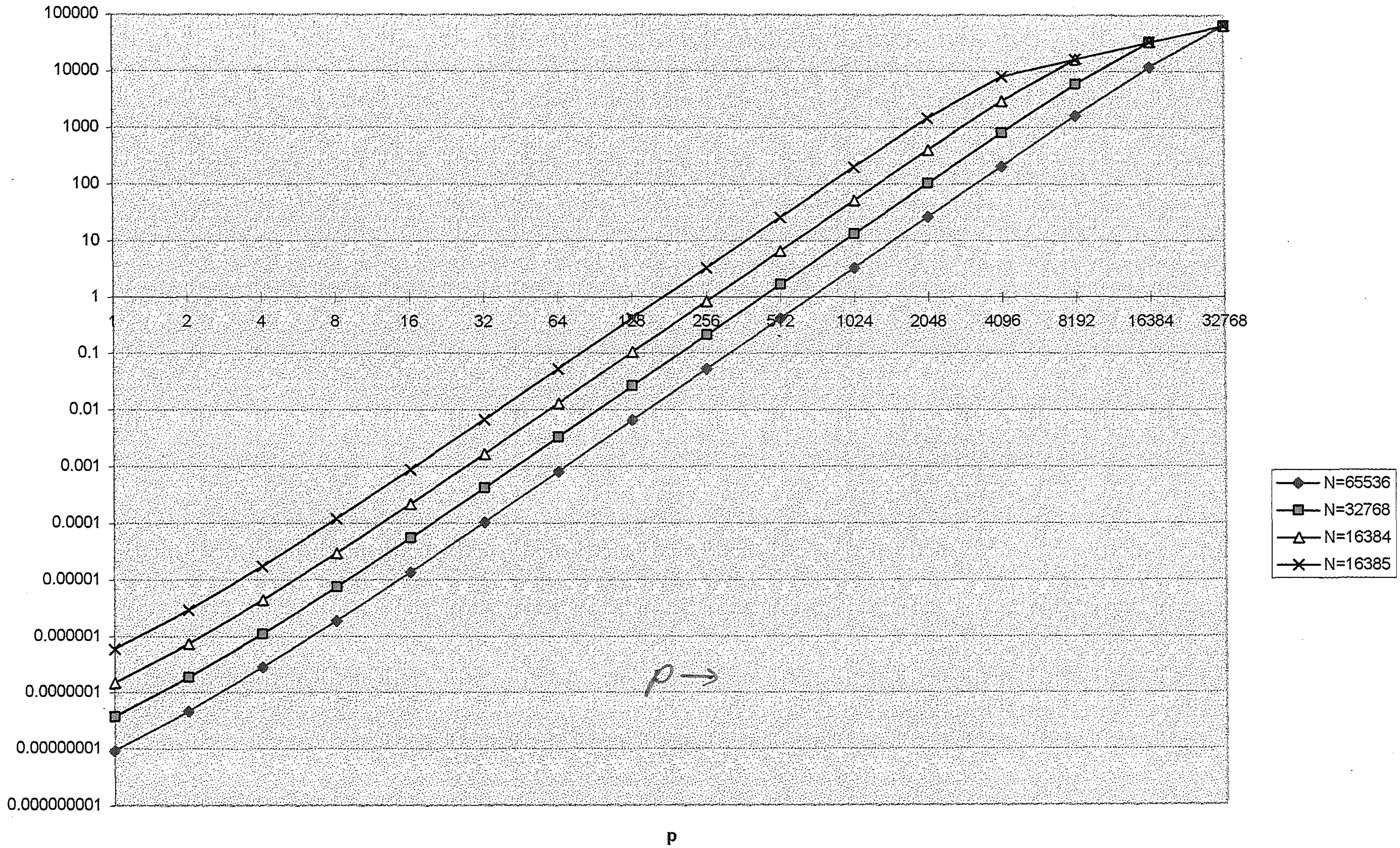

8.72

error bound versus p=flat interval length

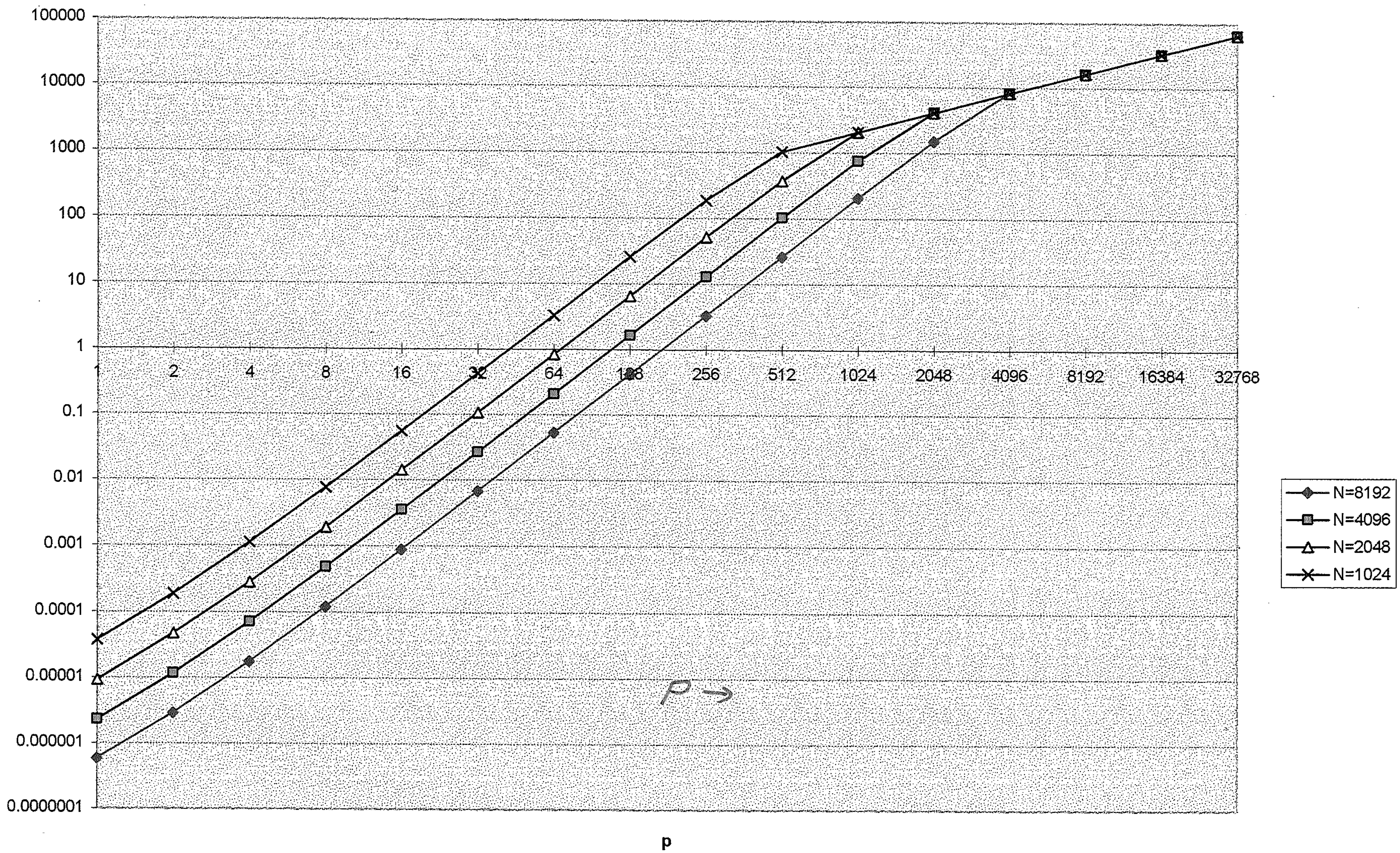

8-7b

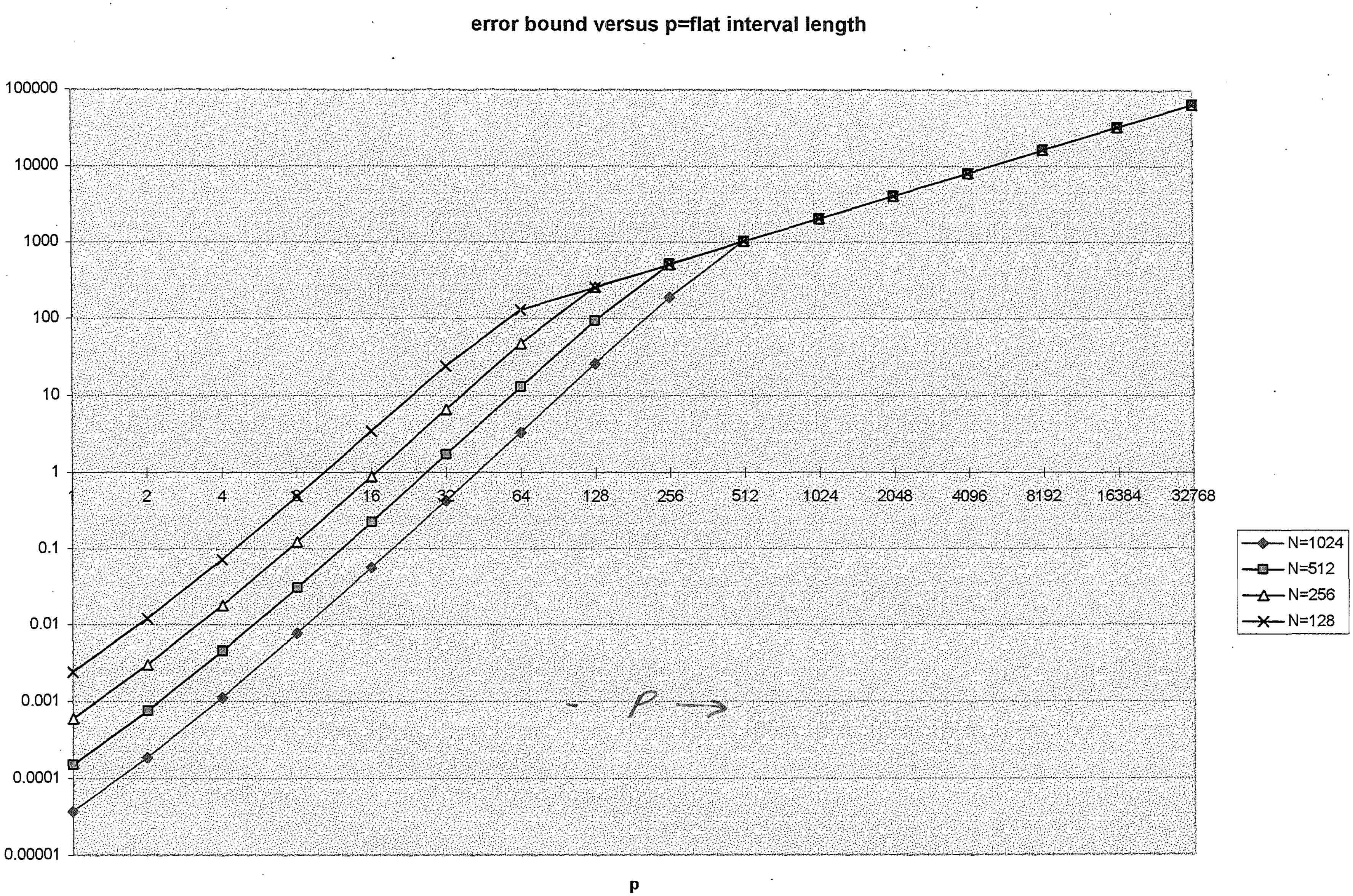
error bound versus p=flat interval length
100000
10000
1000
100
10
1
0.1
0.01
0.001
0.0001
0.00001
1
2
4
8
16
32
64
128
256
512
1024
2048
4096
8192
16384
32768
N=1024
N=512
N=256
N=128
p
p

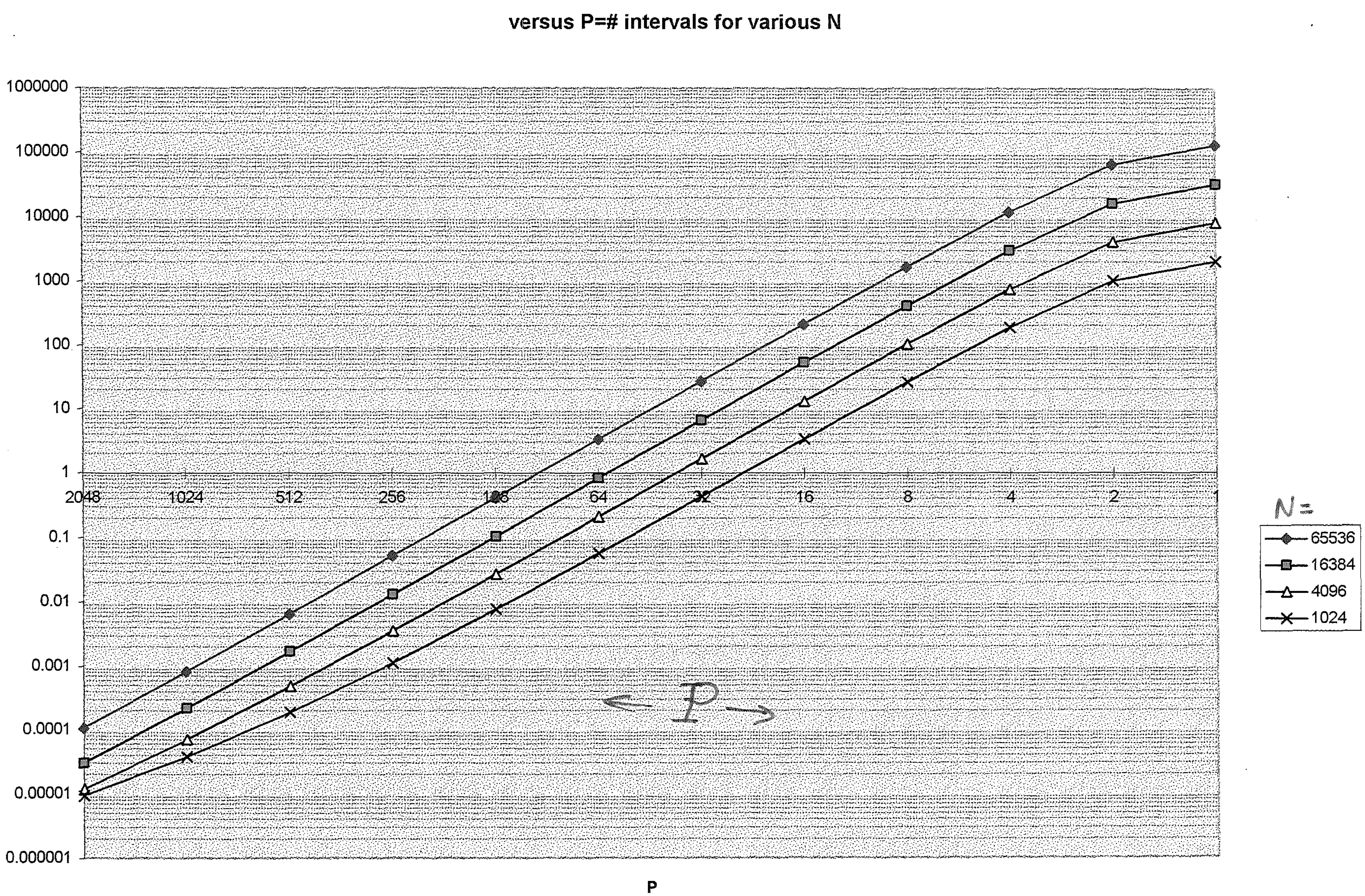
versus P=# intervals for various N
1000000
100000
10000
1000
100
10
1
0.1
0.01
0.001
0.0001
0.00001
0.000001
2048
1024
512
256
128
64
32
16
8
4
2
1
P
<- P ->
N=
65536
16384
4096
1024

8-7d

versus P=# intervals for various N

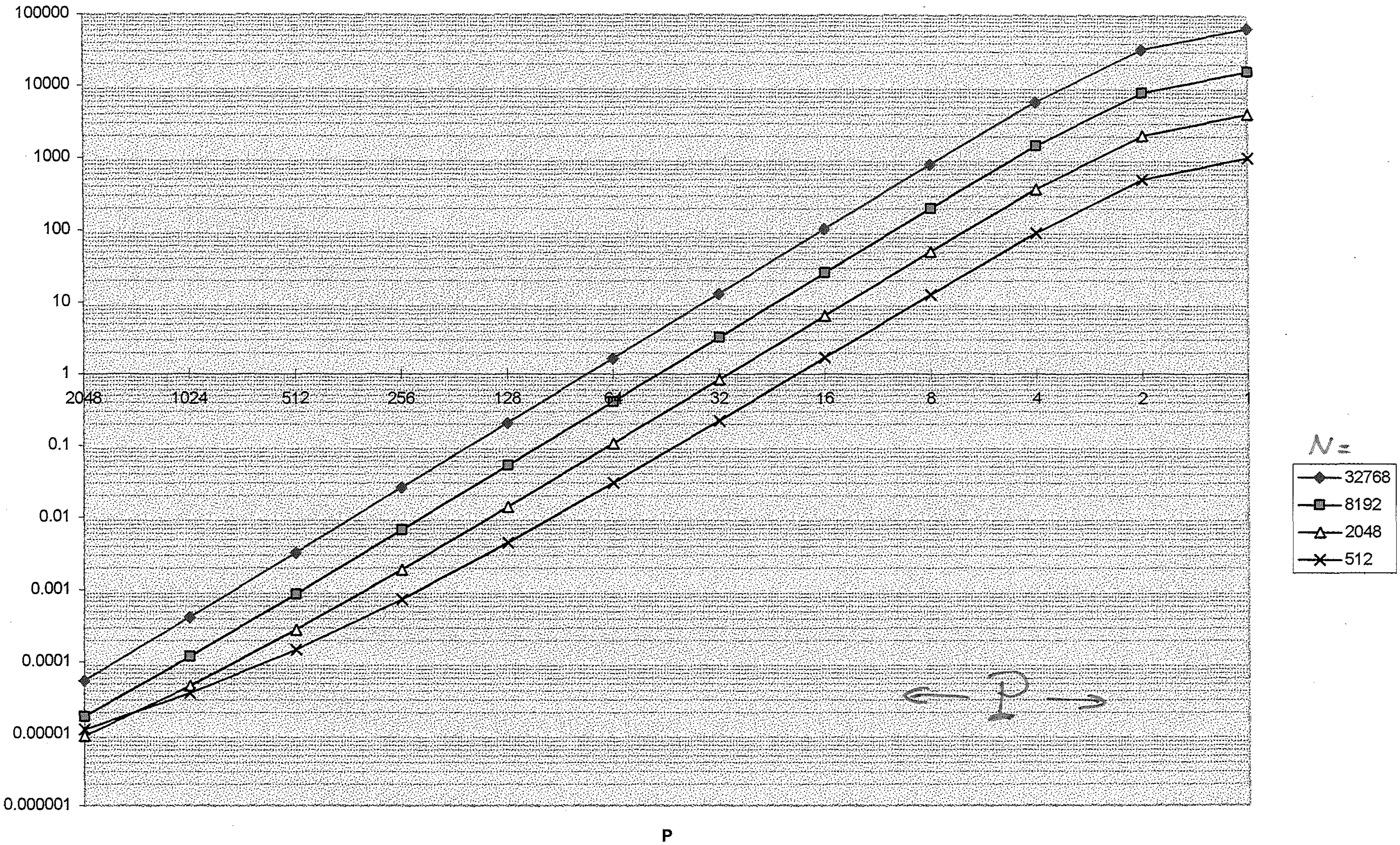

8-3

The <u>overall</u> mean square error is

$$\epsilon_P = \int_0^1 \mathcal{E}_P(u)\,du \qquad (8\cdot 30)$$

From (8-12) and (8-13),

$$\epsilon_P \le \sum_{q=1}^{P} E_q \sum_{n=(q-1)p+1}^{qp} \int_0^1 \left| e^{-j2\pi nu} - e^{-j2\pi qpu} \right|^2 du$$

$$= 2\sum_{q=1}^{P} E_q \sum_{n=(q-1)p+1}^{qp} \int_0^1 \left[1 - \cos 2\pi(n-pq)u\right] du$$

$$= 2\sum_{q=1}^{P} E_q \sum_{n=(q-1)p+1}^{qp} \left[1 - \int_0^1 \cos 2\pi(n-pq)u\, du\right]$$

$$= 2\sum_{q=1}^{P} E_q \sum_{n=(q-1)p+1}^{qp} \left[1 - \delta[n-pq]\right] \qquad (8\cdot 30)$$

Of course! There is no error at $n = pq$ since the e^j's are the same here.

Thus

$$\epsilon_P \le 2(p-1)E \Rightarrow \frac{\epsilon_P}{E} \le 2(p-1) \qquad (8\cdot 31)$$

Notes:

- For $P = N$, $p = 1$ and

$$\epsilon_N = 0 \qquad (8\cdot 32)$$

  This is as it should be

- The bound grows linearly wrt invariant interval.

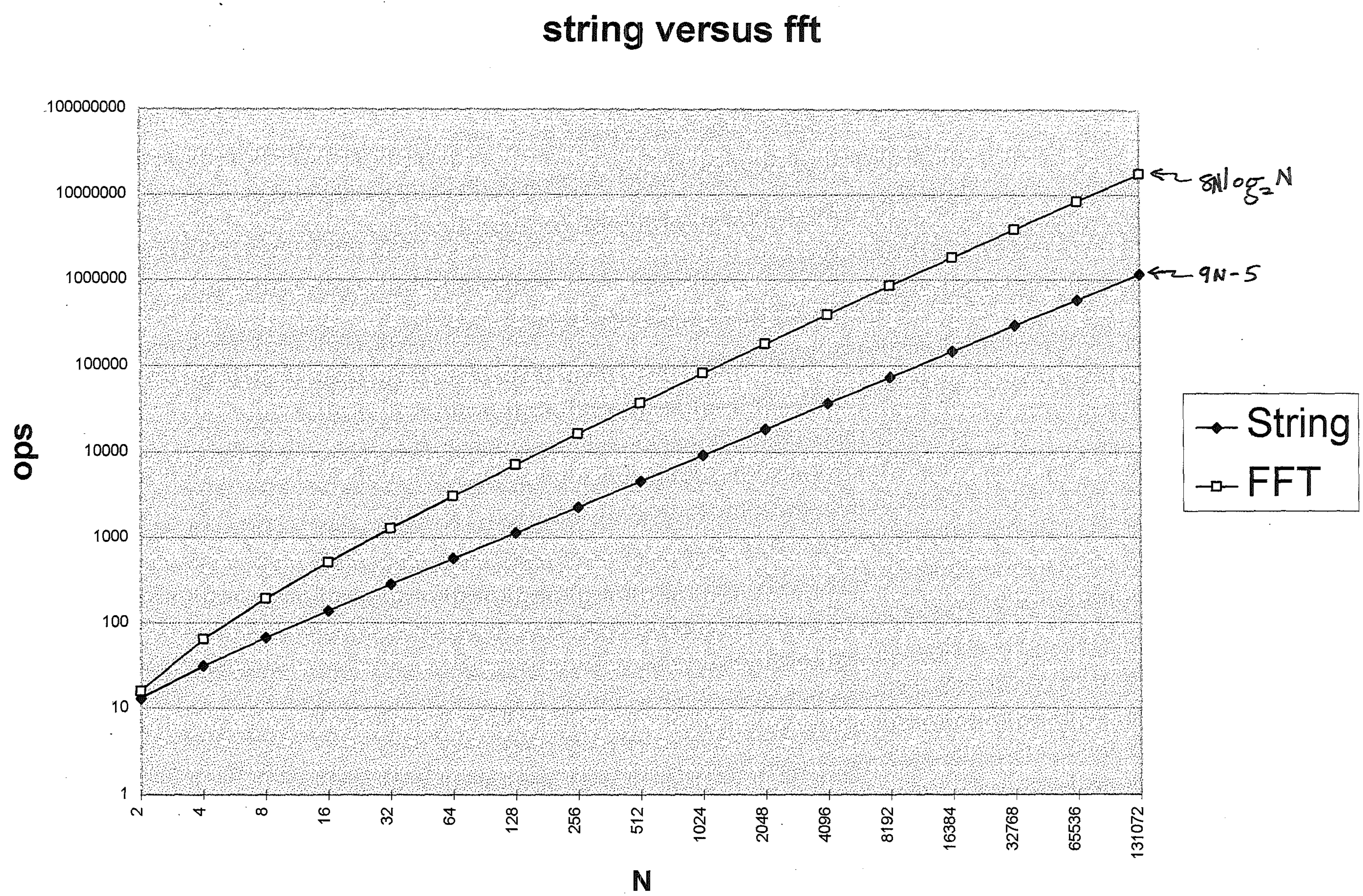

string versus fft
100000000
10000000
1000000
100000
10000
1000
100
10
1
ops
2
4
8
16
32
64
128
256
512
1024
2048
4096
8192
16384
32768
65536
131072
N
String
FFT
8Nlog2N
9N-5

FIG 17

PIA Example

Just because the bound for all u is bad does not mean the PIA (piecewise invariant approximation) does not work. Let's work a specific example. We are specifically interested in $u \to 0$ behavior.

The true spectrum is (from 8-1):

$$X(u) = \sum_{n=1}^{N} x[n]\, e^{-j2\pi n u} \tag{8-33}$$

The PIA, from (8-5), is

$$X_P(u) = \sum_{q=1}^{P} e^{-j2\pi p q u} \sum_{n=(q-1)p+1}^{pq} x[n] \tag{8-34}$$

- Example: Let

$$x[n] = \begin{cases} 1 & ; \quad 1 \le n \le N/2 \\ 0 & ; \quad N/2 < n \le N \end{cases} \tag{8-35}$$

From (8-33), the true output is

$$X(u) = \sum_{n=1}^{N/2} e^{-j2\pi n u}$$

$$= a + a^2 + a^3 + \dots + a^{N/2} \quad ; \quad a = e^{-j2\pi u}$$

$$a\, X(u) = a^2 + a^3 + \dots + a^{\frac{N}{2}} + a^{\frac{N}{2}+1} \tag{8-36}$$

Subtracting:

$$X(u) = \frac{a\left(a^{N/2} - 1\right)}{a - 1} = \frac{a \cdot a^{\frac{N}{4}} \left(a^{N/4} - a^{-N/4}\right)}{a^{1/2}\left(a^{1/2} - a^{-1/2}\right)}$$

$$= e^{-j2\pi\left(\frac{1}{2} + \frac{N}{4}\right)u} \times \frac{\sin \frac{\pi N u}{2}}{\sin \pi u}$$

$$= e^{-j\frac{\pi}{2}(1+2N)u}\, \frac{\sin \frac{\pi N u}{2}}{\sin \pi u} \tag{8-37}$$

Now for the PIA. We sum only over the first $\underline{P}/2$ intervals.

$$\underline{X}_{\underline{P}}(u) = p \sum_{q=1}^{P/2} (e^{-j2\pi pu})^q$$

$$= p\,\alpha^{\frac{P}{4}+\frac{1}{2}} \frac{\alpha^{P/4} - \alpha^{-P/4}}{\alpha^{1/2} - \alpha^{-1/2}} \;;\; \alpha = e^{-j2\pi pu}$$

$$= p\,e^{-j\frac{\pi}{2}(2\underline{P}+1)pu} \frac{\sin \frac{\pi}{2} p \underline{P} u}{\sin \pi p u}$$

$$= p\,e^{-j\frac{\pi}{2}(2\underline{P}+1)pu} \frac{\sin \frac{\pi N}{2} u}{\sin \pi p u} \qquad (8\text{-}38)$$

Thus

$$|\underline{X}_{\underline{P}}(u)| = p \left| \frac{\sin \frac{\pi N u}{2}}{\sin \pi p u} \right| \qquad (8\text{-}39)$$

and

$$|\underline{X}(u)| = \left| \frac{\sin \frac{\pi N u}{2}}{\sin \pi u} \right| \qquad (8\text{-}40)$$

Figures follow.

Note, particurly, at behavior for small u and $u = 1/N$ particularly.

B-9a

N = 128, p=16
P = 8

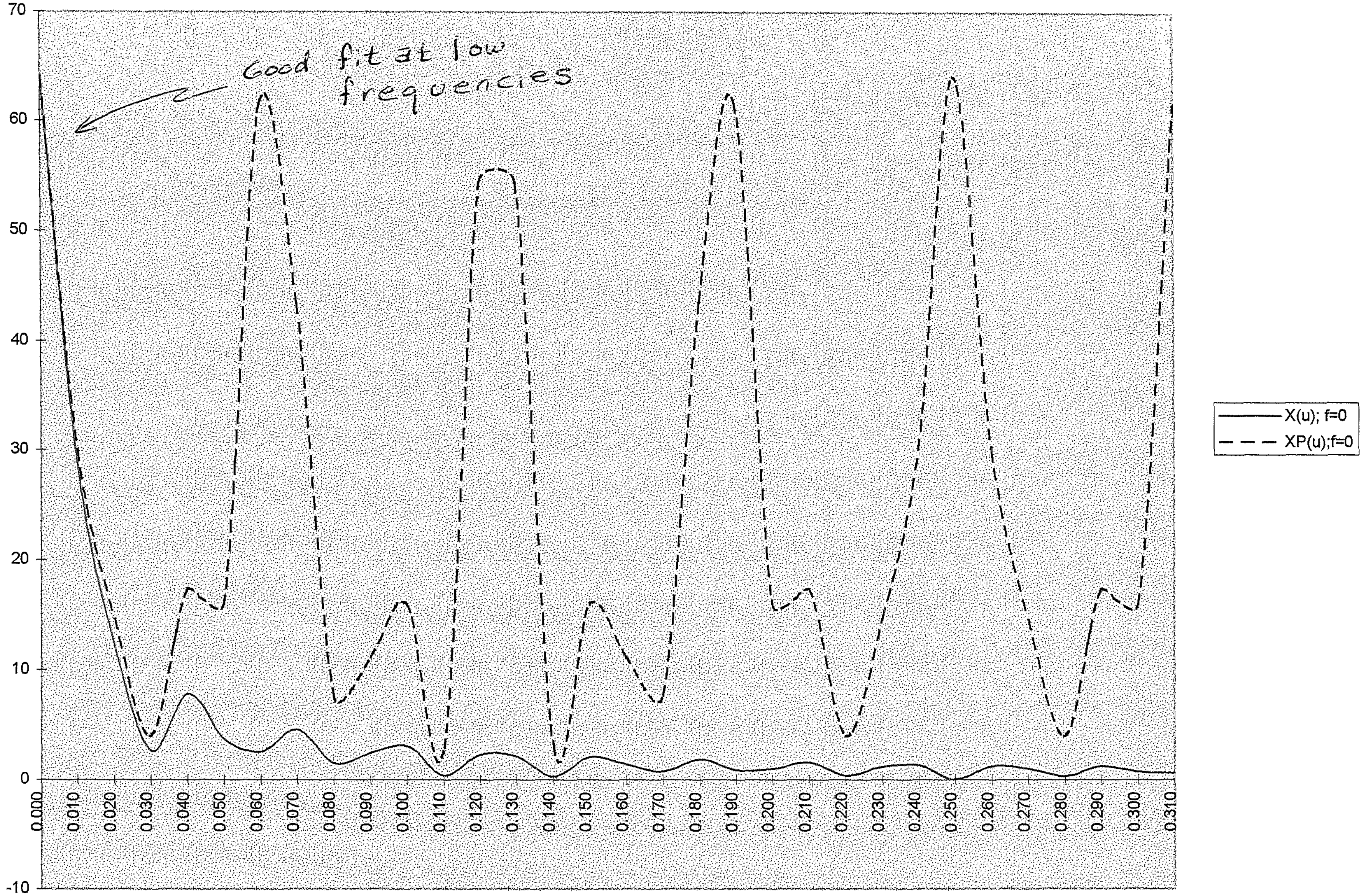

N=128, p=8, P=16

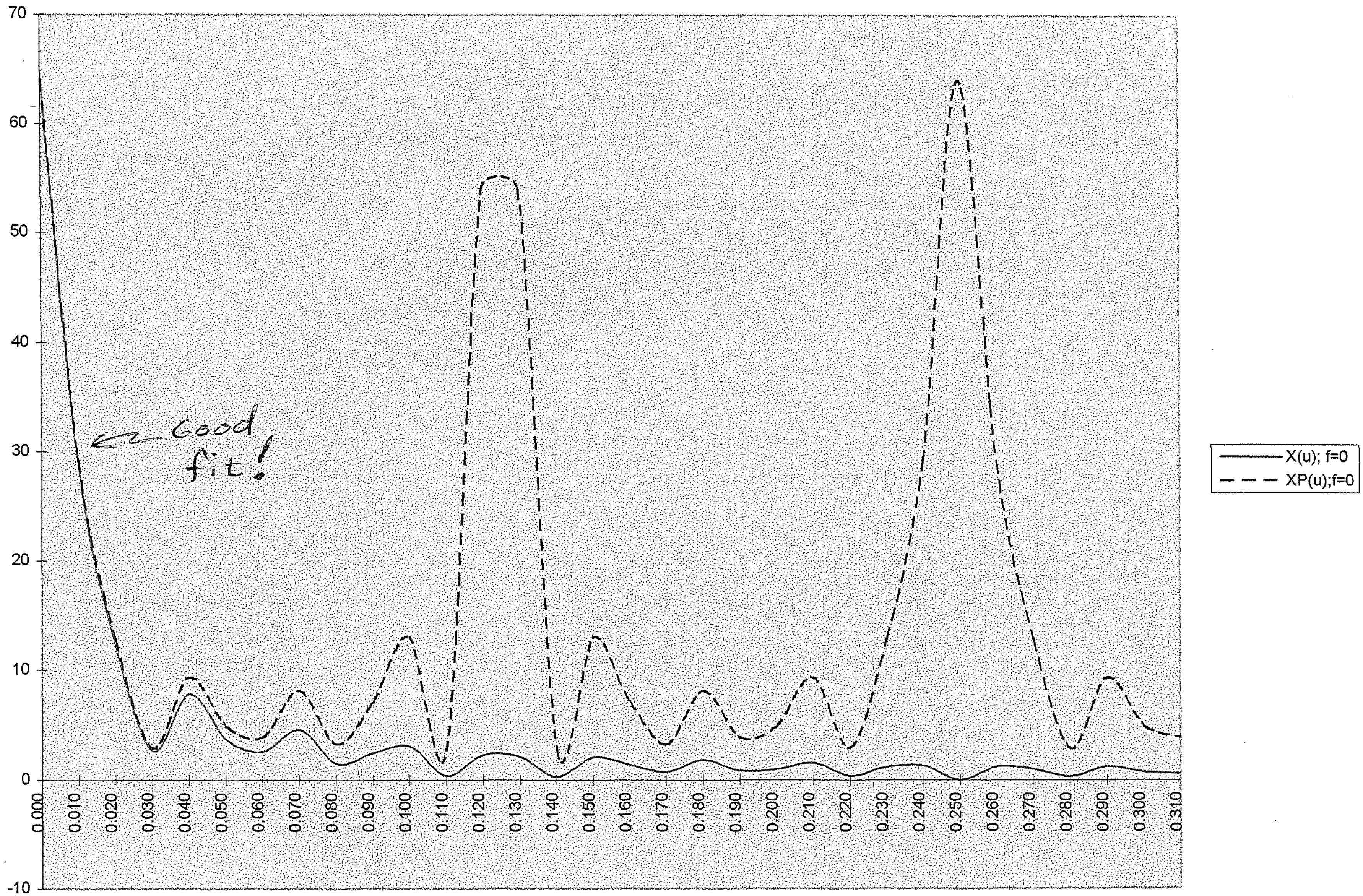

8-9b

N = 128, p = 4, P = 32

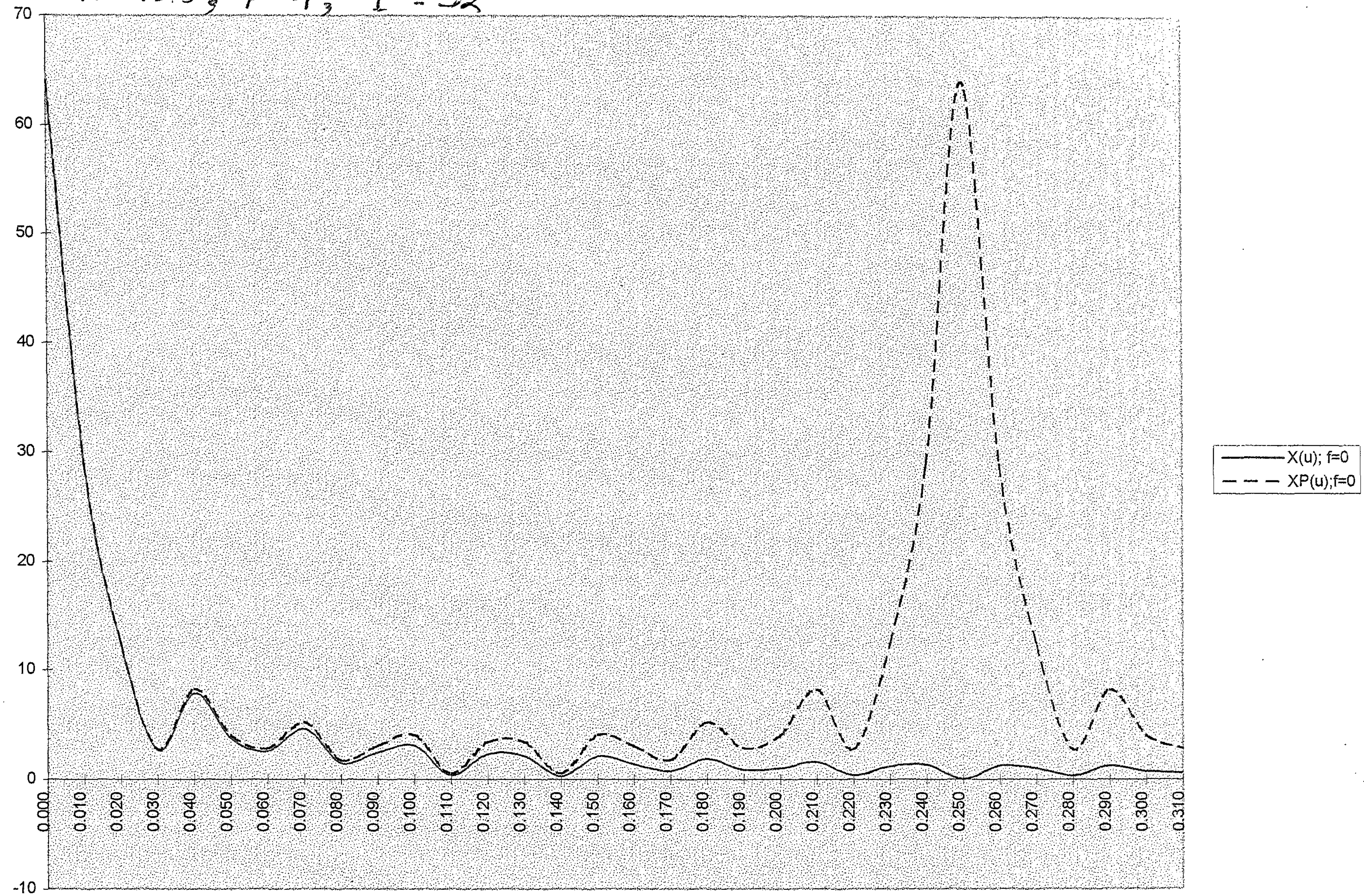

B-9c

$N=128,\ p=2,\ P=64$

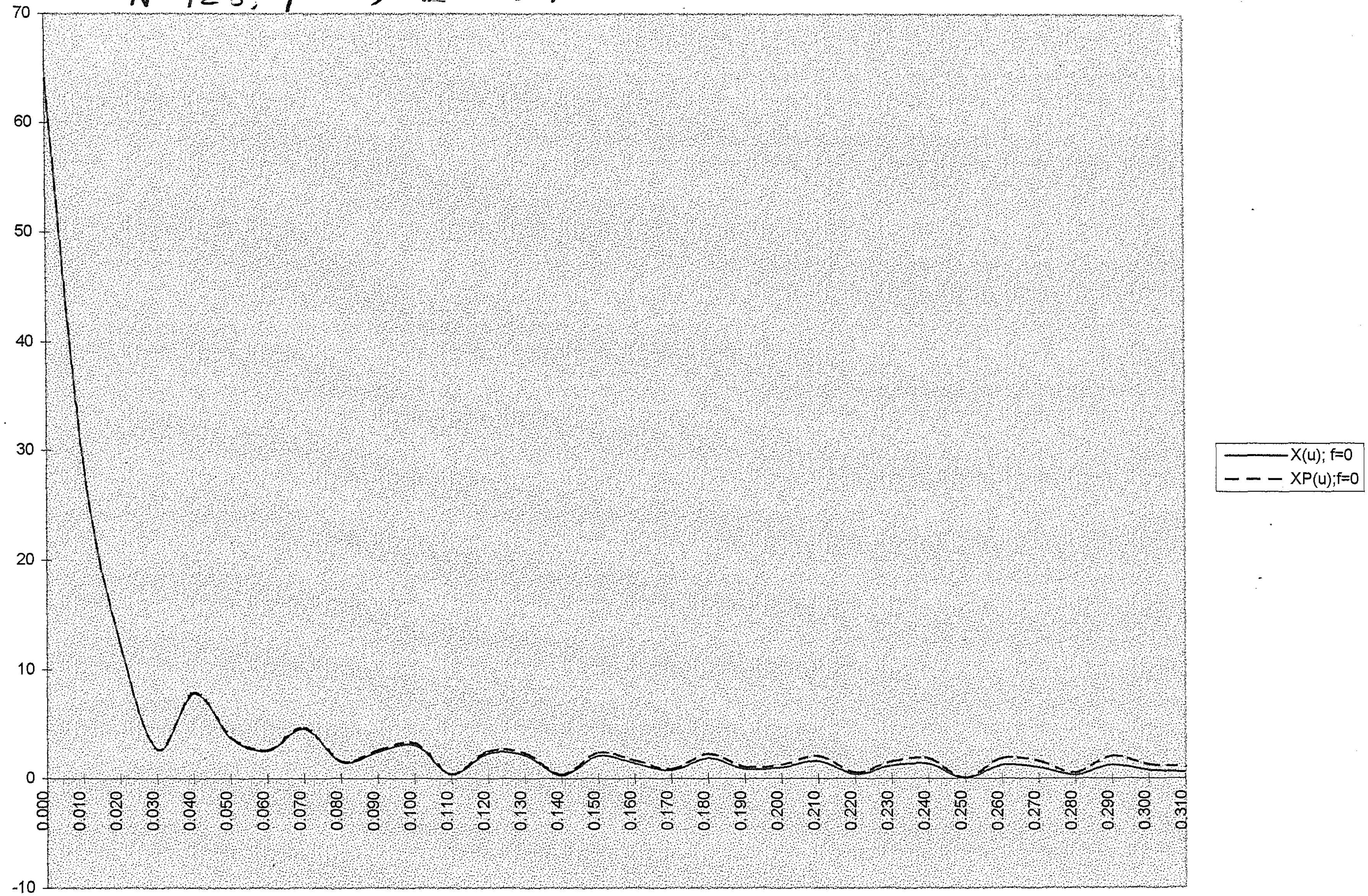

Pb-9

N=128, p=32, P=4

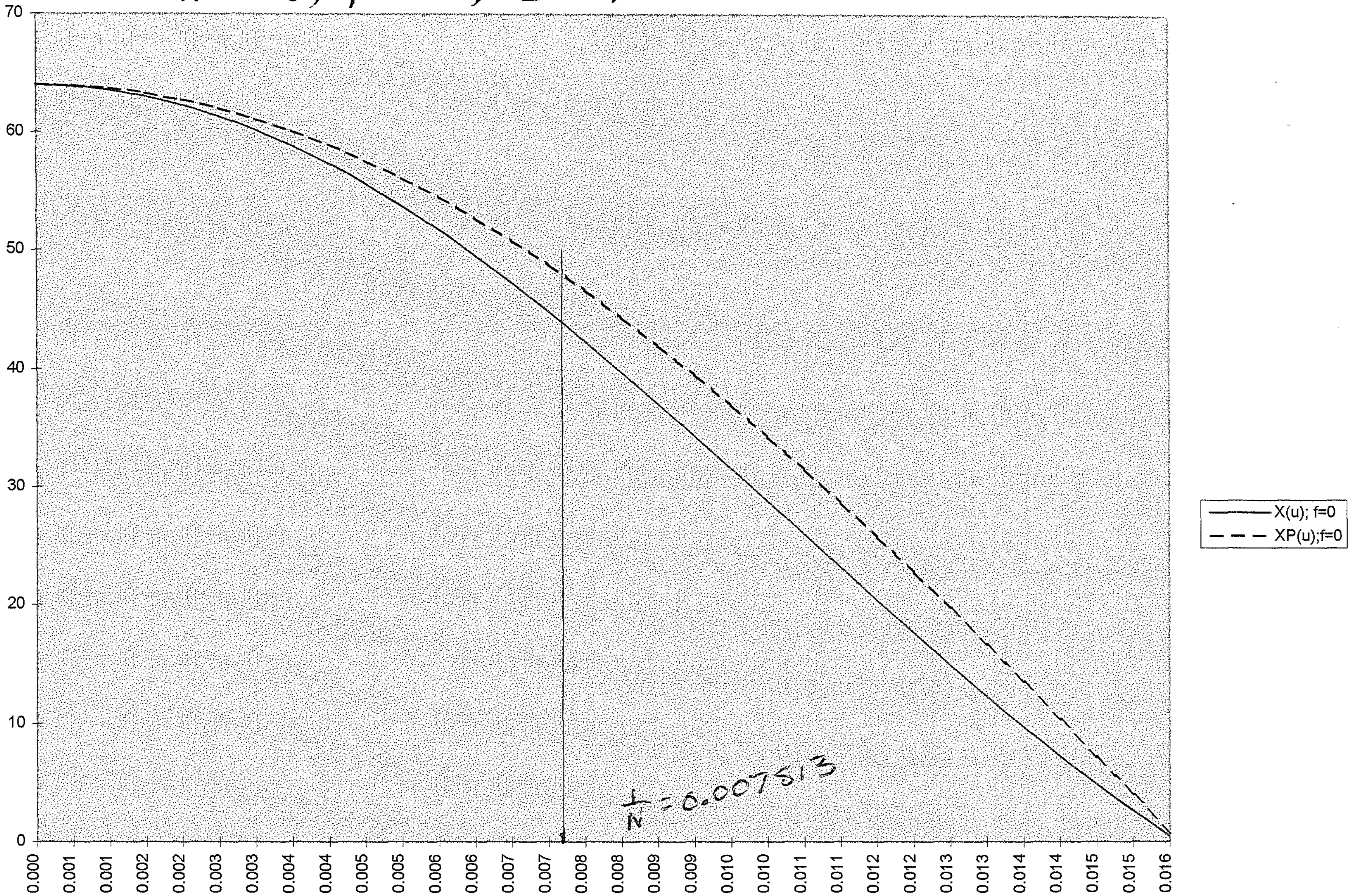

8-9e

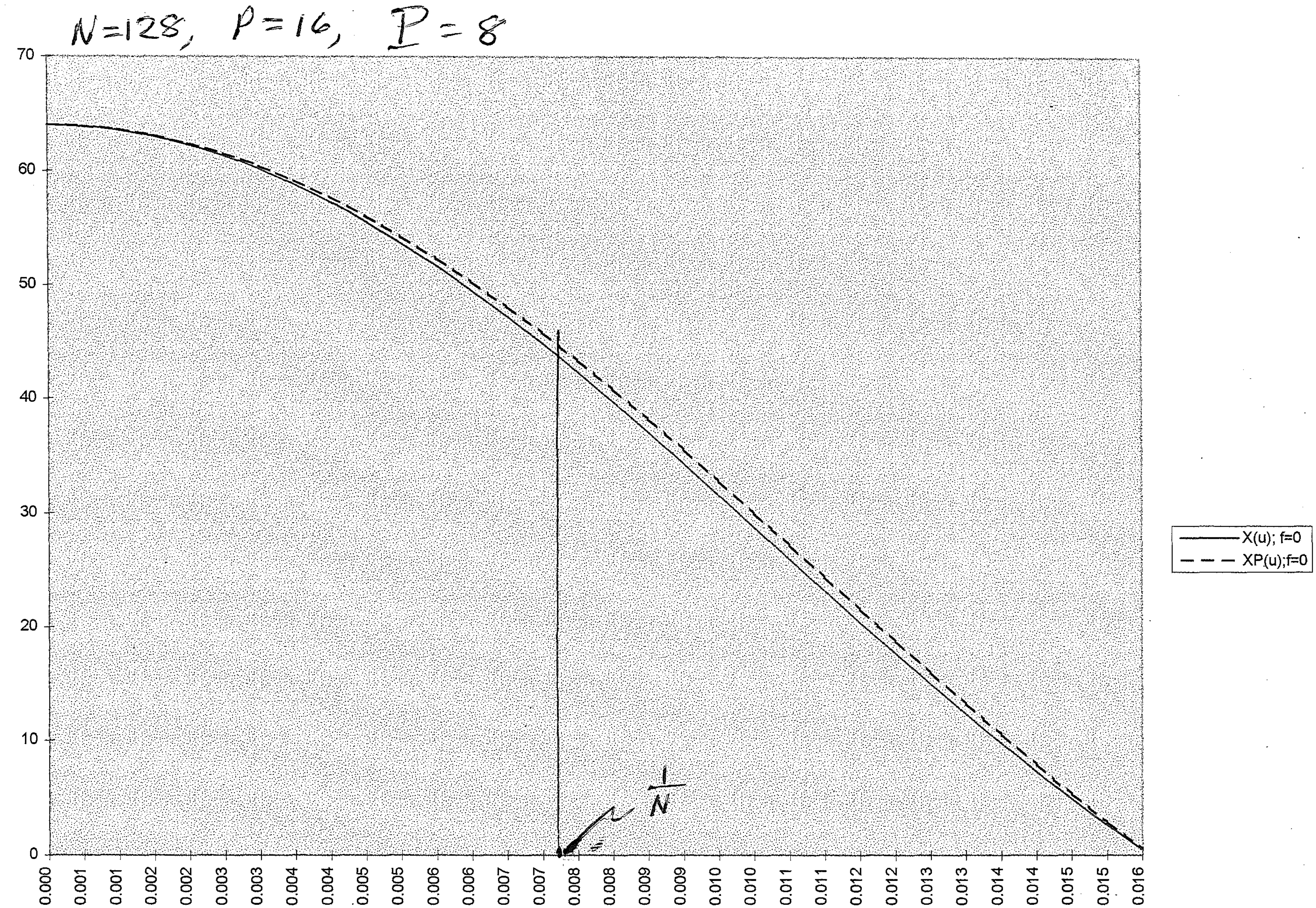
N=128, P=16, P = 8
70
60
50
40
30
20
10
0
0.000
0.001
0.001
0.002
0.002
0.003
0.003
0.004
0.004
0.005
0.005
0.006
0.006
0.007
0.007
0.008
0.008
0.009
0.009
0.010
0.010
0.011
0.011
0.012
0.012
0.013
0.013
0.014
0.014
0.015
0.015
0.016
$\frac{1}{N}$
X(u); f=0
XP(u);f=0

J 6-8

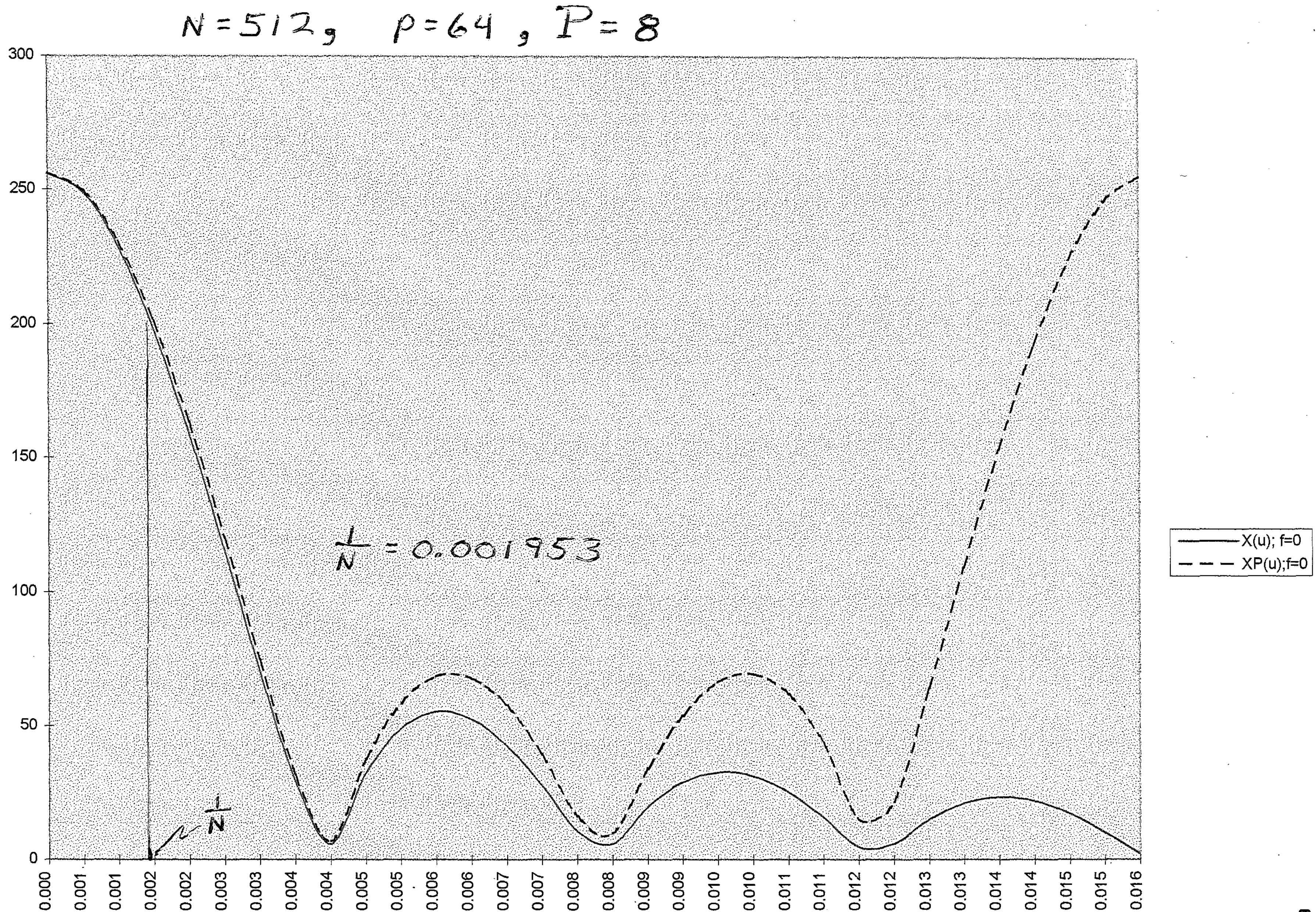
N = 512, p = 64, P = 8
1/N = 0.001953
1/N
300
250
200
150
100
50
0
0.000
0.001
0.001
0.002
0.002
0.003
0.003
0.004
0.004
0.005
0.005
0.006
0.006
0.007
0.007
0.008
0.008
0.009
0.009
0.010
0.010
0.011
0.011
0.012
0.012
0.013
0.013
0.014
0.014
0.015
0.015
0.016
X(u); f=0
XP(u);f=0

8-9 8

N=512, P=128 P=4

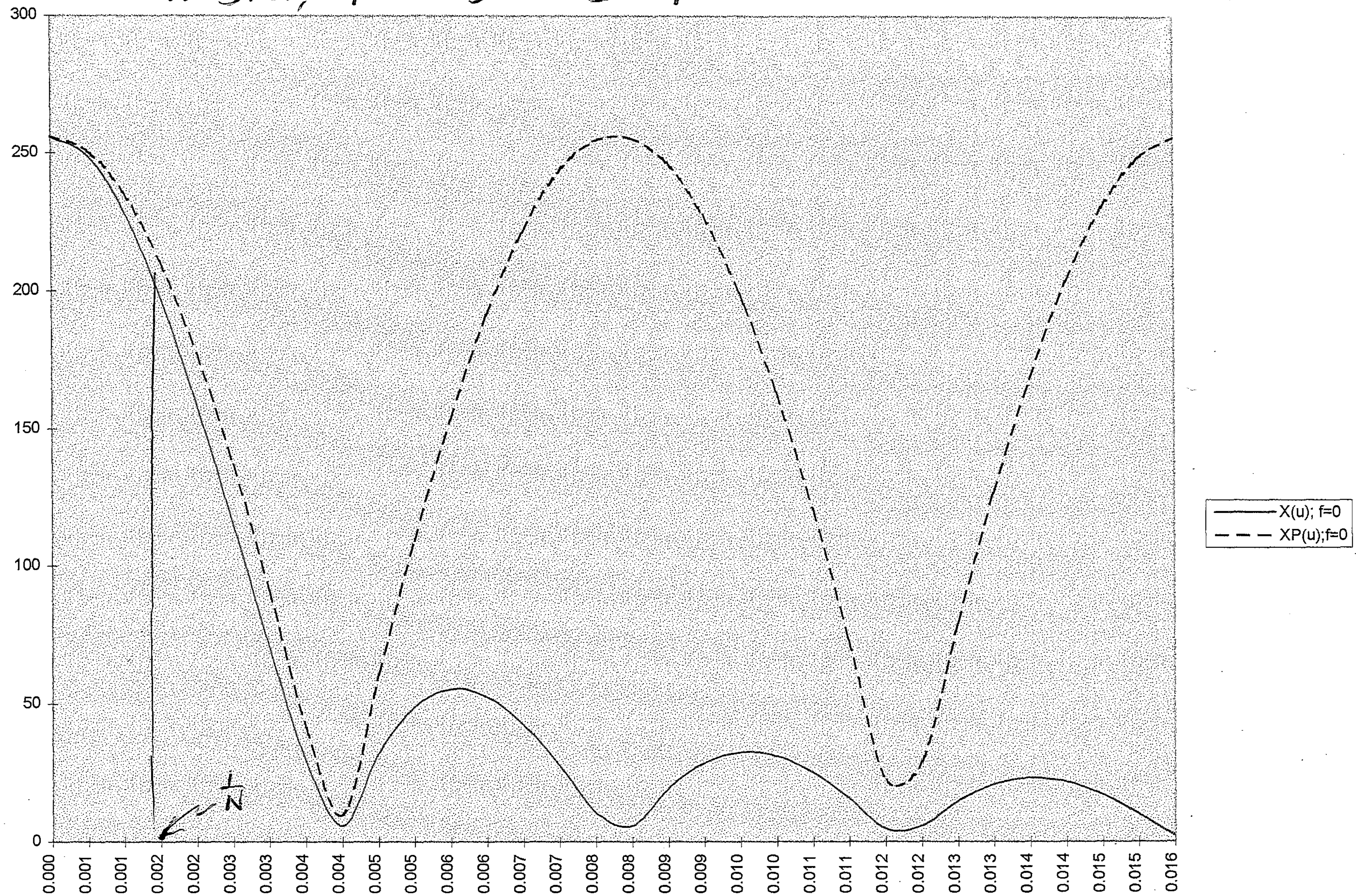

8-9-4

★ Let's see if we can approximate $\mathcal{E}_P(u)$ for small u. Let's repeat (8-8):

$$\mathcal{E}_P(u) = \left| \sum_{q=1}^{P} \sum_{n=(q-1)p+1}^{pq} x[n] \left(e^{-j2\pi nu} - e^{-j2\pi pqu} \right) \right|^2 \tag{8-41}$$

For small θ

$$e^{-j\theta} \approx 1 - j\theta \tag{8-42}$$

Thus

$$\mathcal{E}_P(u) \xrightarrow[u\to 0]{} \left| \sum_{q=1}^{P} \sum_{n=(q-1)p+1}^{pq} x[n] \left(-j2\pi u \, (n-pq) \right) \right|^2$$

$$= (2\pi u)^2 \left| \sum_{q=1}^{P} \sum_{n=(q-1)p+1}^{pq} x[n] \, (n-pq) \right|^2 \tag{8-43}$$

The 'worst' the n sum can get is for $n = (q-1)p+1$. This worst case condition gives

$$\frac{\mathcal{E}_P(u)}{(2\pi u)^2} \xrightarrow[u\to 0]{} \left| \sum_{q=1}^{P} \sum_{n=(q-1)p+1}^{pq} x[n] * p \right|^2 \tag{8-44}$$

or

$$\mathcal{E}_P(u) \rightarrow (2\pi p u)^2 \left| X(0) \right|^2 \tag{8-45}$$

where

$$X(0) = \sum_{n=1}^{N} x[n] \tag{8-46}$$

The error at $u = 1/N$ is thus approximately

$$\mathcal{E}_P\left(\tfrac{1}{N}\right) \approx \left(\frac{2\pi P}{N}\right)^2 X^2(0)$$

$$= \left| (2\pi/P) \, X(0) \right|^2 \tag{8-47}$$

Another approximation of the error comes from the measure

$$\epsilon_p(u) = X(u) - X_p(u) \qquad (8\text{-}48)$$

Since $\epsilon_P(0) = 0$, a first order approximation for $\epsilon_p(u)$ is

$$\epsilon_p(u) \xrightarrow[u \to 0]{} \left[X'(0) - X_P(0) \right] u \qquad (8\text{-}49)$$

Comparing (8-48) to (8-8) reveals

$$\mathcal{E}_P(u) = \left| \epsilon_P(u) \right|^2 \qquad (8\text{-}50)$$

Thus

$$\mathcal{E}_P(u) \xrightarrow[u \to 0]{} u^2 \left| X'(0) - X'_P(0) \right| \qquad (8\text{-}51)$$

Differentiating (8-1) gives

$$X'(u) = -j2\pi \sum_{n=1}^{N} n\, x[n]\, e^{-j2\pi n u} \qquad (8\text{-}52)$$

and

$$X'(0) = -j2\pi \sum_{n=1}^{N} n\, x[n] \qquad (8\text{-}53)$$

Similarly, from (8-5)

$$X'_P(u) = -j2\pi p \sum_{q=1}^{P} q\, e^{-j2\pi p q u} \sum_{n=(q-1)p-1}^{qp} x[n] \qquad (8\text{-}54)$$

and

$$X'_P(0) = -j2\pi p \sum_{q=1}^{P} q \sum_{n=(q-1)p-1}^{qp} x[n] \qquad (8\text{-}55)$$

Plug (8-53) and (8-55) into (8-51):

$$\mathcal{E}_P(u) \xrightarrow[u\to 0]{} u^2 \left| -j2\pi \sum_{q=1}^{P} \sum_{n=(q-1)p-1}^{qP} x[n]\,(n-pq) \right|^2$$

Note: This is the same result as (8-43) and will give the same result.

Chapt. 7

Hal,

Here is the 'music chapter'

12 notes per octave

$\times$ 3.32 octaves per decade

$\approx$ 40 divisions per decade.

Music and
Log Frequency Calibration:

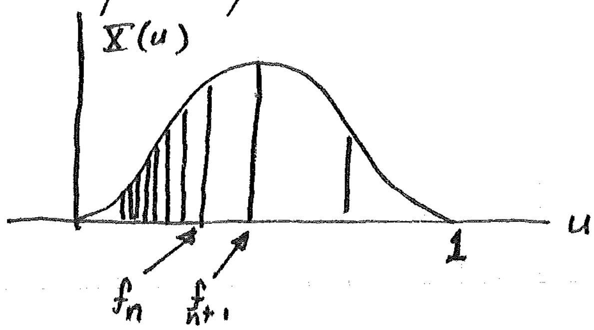

FIG 34

For log calibration, the ratio of adjacent frequencies is a constant

$$\frac{f_{n+1}}{f_n} = \text{Constant} \tag{78}$$

Suppose, for example, we wish to divide an octave into 12 log-spaced intervals. Then

$$\text{Constant} = 2^{\frac{1}{12}} = 1.059463094 \tag{79}$$

This is the case for musical calibration (12 chromatic steps per octave). When this is done, the musical scale is said to be 'tempered' as in Bach's 'The Well Tempered Clavicord'. The choice of 12 notes is motivated by harmonics.

An example is given in Fig. 35 for a sequence of length $2^{19} = 524288$. For $n=1$, the sequence is zero padded to

$$3 \times 2^{19}$$

and then chopped into $2^m = 2^2 = 4$ pieces. This string is tripled and chopped into some power of 2. For $n=1$, the string is of length:

$$2^{19} \times 3 \div 2^2 = 393219 \tag{80}$$

This string is tripled and divided

$$393219 \times 3 \div 2^2 = 294912 \tag{81}$$

The next entry is

$$294913 \times 3 \div 2^{1} = 442368 \tag{82}$$

The power of 2 in (80), (81) and (82) is chosen to get the result between 2^{19} and 2^{18}.

Repetition gives the numbers in column Ⓐ in FIG. 35. Note that the result for $n=12$ is appoximately an octave below 2^{19}.

The numbers in column Ⓐ are rearranged in ascending order in column Ⓑ. The next ratio is between two adjacent frequencies. The result, in each case, should be $2^{1/12}$. The ratios are close.

'Cents' are the intervals resulting $ in music by dividing a note into 100 pieces. The cent error column in FIG. 35 is computed from the formula

$$\text{cent error} = \frac{\log\left(\frac{\text{ratio}}{2^{1/12}}\right)}{\log\left(2^{\frac{1}{1200}}\right)}$$

$$= \log_{2^{\frac{1}{1200}}}\left(\frac{\text{ratio}}{2^{1/12}}\right) \tag{83}$$

A B

N	2^N	n	(3^n)*(2^N)	m	(3^n)*2^(N-m)	*	ordered	ratio	cent error		
19	524288	0	524288	0	524288		265720.5	1.053497942	-9.78		
19	524288	1	1572864	2	393216		279936	1.053497942	-9.78		
19	524288	2	4718592	4	294912		294912	1.067871094	13.69		
19	524288	3	14155776	5	442368		314928	1.053497942	-9.78		
19	524288	4	42467328	7	331776		331776	1.067871094	13.69		
19	524288	5	127401984	8	497664		354294	1.053497942	-9.78		
19	524288	6	382205952	10	373248		373248	1.053497942	-9.78		
19	524288	7	1146617856	12	279936		393216	1.067871094	13.69		
19	524288	8	3439853568	13	419904		419904	1.053497942	-9.78		
19	524288	9	10319560704	15	314928		442368	1.067871094	13.69		
19	524288	10	30958682112	16	472392		472392	1.053497942	-9.78		
19	524288	11	92876046336	18	354294		497664	1.053497942	-9.78		
19	524288	12	2.78628E+11	20	265720.5		524288	1.067871094	13.69		
							559872				
							2^(1/12) =	1.059463094			

FIGURE 35

Q: What is the shortest string that can be used for such a division

A: $2^{18} = 262144$. This is shown in Fig. 36. All of the entries in column (A) are integers (except for $n=12$ which is an octave of $n=0$ and won't be used).

Q: Can't we generate the 12 frequencies and then use octave string cutting (in Chapt 4) to compute the 12 frequencies an octave higher?

A: Yes, but we have to increase N (and 2^N). For one octave, we need $N=19$ or

$$2^{19} = 524{,}288 \qquad (84)$$

This is shown is FIG. 37 where column (C) is half of column. (B) and still all integers.

- For two octaves, $N=20$ is needed. See Figure 38. Column (D) is half of (C).

(E) is half of (D). For $N=20$, all entries in column (D) are integers. Column (E) is not.

- For 3 octaves, we need $N=21$. See Figure 39.

N	2^N	n	(3^n)*(2^N)	m	(A) (3^n)*2^(N-m)	*	(B) ordered	ratio	cent error		
18	262144	0	262144	0	262144		132860.25	1.053497942	-9.78		
18	262144	1	786432	2	196608		139968	1.053497942	-9.78		
18	262144	2	2359296	4	147456		147456	1.067871094	13.69		
18	262144	3	7077888	5	221184		157464	1.053497942	-9.78		
18	262144	4	21233664	7	165888		165888	1.067871094	13.69		
18	262144	5	63700992	8	248832		177147	1.053497942	-9.78		
18	262144	6	191102976	10	186624		186624	1.053497942	-9.78		
18	262144	7	573308928	12	139968		196608	1.067871094	13.69		
18	262144	8	1719926784	13	209952		209952	1.053497942	-9.78		
18	262144	9	5159780352	15	157464		221184	1.067871094	13.69		
18	262144	10	15479341056	16	236196		236196	1.053497942	-9.78		
18	262144	11	46438023168	18	177147		248832	1.053497942	-9.78		
18	262144	12	1.39314E+11	20	132860.25		262144	1.067871094	13.69		
							279936				
							2^(1/12) =	1.059463094			

FIG 36

Sheet2

N	2^N	n	(3^n)*(2^N)	m	A (3^n)*2^(N-m)	*	B ordered	ratio	cent error	C 1 octave.		
19	524288	0	524288	0	524288		~~265720.5~~	1.053497942	-9.78	~~132860.3~~		
19	524288	1	1572864	2	393216		279936	1.053497942	-9.78	139968		
19	524288	2	4718592	4	294912		294912	1.067871094	13.69	147456		
19	524288	3	14155776	5	442368		314928	1.053497942	-9.78	157464		
19	524288	4	42467328	7	331776		331776	1.067871094	13.69	165888		
19	524288	5	127401984	8	497664		354294	1.053497942	-9.78	177147		
19	524288	6	382205952	10	373248		373248	1.053497942	-9.78	186624		
19	524288	7	1146617856	12	279936		393216	1.067871094	13.69	196608		
19	524288	8	3439853568	13	419904		419904	1.053497942	-9.78	209952		
19	524288	9	10319560704	15	314928		442368	1.067871094	13.69	221184		
19	524288	10	30958682112	16	472392		472392	1.053497942	-9.78	236196		
19	524288	11	92876046336	18	354294		497664	1.053497942	-9.78	248832		
19	524288	12	2.78628E+11	20	~~265720.5~~		524288	1.067871094	13.69	262144		
							559872					
							2^(1/12) =	1.059463094				

FIG 37

					A		B			C	D	E
N	2^N	n	(3^n)*(2^N)	m	(3^n)*2^(N-m)	*	ordered	ratio	cent error	1 octave.	2 octave	3 octave
20	1048576	0	1048576	0	1048576		531441	1.053497942	-9.78	265720.5	132860.3	66430.125
20	1048576	1	3145728	2	786432		559872	1.053497942	-9.78	279936	139968.0	69984
20	1048576	2	9437184	4	589824		589824	1.067871094	13.69	294912	147456.0	73728
20	1048576	3	28311552	5	884736		629856	1.053497942	-9.78	314928	157464.0	78732
20	1048576	4	84934656	7	663552		663552	1.067871094	13.69	331776	165888.0	82944
20	1048576	5	254803968	8	995328		708588	1.053497942	-9.78	354294	177147.0	88573.5
20	1048576	6	764411904	10	746496		746496	1.053497942	-9.78	373248	186624.0	93312
20	1048576	7	2293235712	12	559872		786432	1.067871094	13.69	393216	196608.0	98304
20	1048576	8	6879707136	13	839808		839808	1.053497942	-9.78	419904	209952.0	104976
20	1048576	9	20639121408	15	629856		884736	1.067871094	13.69	442368	221184.0	110592
20	1048576	10	61917364224	16	944784		944784	1.053497942	-9.78	472392	236196.0	118098
20	1048576	11	1.85752E+11	18	708588		995328	1.053497942	-9.78	497664	248832.0	124416
20	1048576	12	5.57256E+11	20	531441		1048576	1.067871094	13.69	524288	262144.0	131072
							1119744					
							2^(1/12) =	1.059463094				

FIG 38

N	2^N	n	(3^n)*(2^N)	m	(3^n)*2^(N-m)	*	ordered	ratio	cent error	1 octave.	2 octave	3 octave
21	2097152	0	2097152	0	2097152		1062882	1.053497942	-9.78	531441	265720.5	132860.25
21	2097152	1	6291456	2	1572864		1119744	1.053497942	-9.78	559872	279936.0	139968
21	2097152	2	18874368	4	1179648		1179648	1.067871094	13.69	589824	294912.0	147456
21	2097152	3	56623104	5	1769472		1259712	1.053497942	-9.78	629856	314928.0	157464
21	2097152	4	169869312	7	1327104		1327104	1.067871094	13.69	663552	331776.0	165888
21	2097152	5	509607936	8	1990656		1417176	1.053497942	-9.78	708588	354294.0	177147
21	2097152	6	1528823808	10	1492992		1492992	1.053497942	-9.78	746496	373248.0	186624
21	2097152	7	4586471424	12	1119744		1572864	1.067871094	13.69	786432	393216.0	196608
21	2097152	8	13759414272	13	1679616		1679616	1.053497942	-9.78	839808	419904.0	209952
21	2097152	9	41278242816	15	1259712		1769472	1.067871094	13.69	884736	442368.0	221184
21	2097152	10	1.23835E+11	16	1889568		1889568	1.053497942	-9.78	944784	472392.0	236196
21	2097152	11	3.71504E+11	18	1417176		1990656	1.053497942	-9.78	995328	497664.0	248832
21	2097152	12	1.11451E+12	20	1062882		2097152	1.067871094	13.69	1048576	524288.0	262144
							2239488					
							2^(1/12) =	1.059463094				

FIG 39

PREVIOUS METHOD:

Weight 3^n by 2^{N-m}

NEW METHOD:

Weight 3^{M-N} by 2^n.

Results shown in FIG. 40.

Minimum string length = $3^{11} = 177{,}147$ (85)

- Note: Musically, old method based on circle of 5TH's. New Method is circle of 4TH's.

- Note: Both methods work because

$$3^{12} = 531{,}441 \approx 2^{19} = 524\,288 \tag{86}$$

This is an error of

$$\frac{\log \frac{3^{12}}{2^{19}}}{\log 2} = \log_2 \frac{3^{12}}{2^{19}} = 0.019 \text{ octaves} \tag{87}$$

Q: Can we combine new & old method?

A: Sure

Q: Can we extend this to something other than 3?

A: Sure.

Hybrid also. $\Longrightarrow$ Research needed

N	3^(-N)	n	(2^n)/(3^N)	*	ordered	ratio	cent error	M	3^M	(3^M)*ordered	1 octave
0	1.00E+00	0	1		0.493270184	1.067871094	13.7	11	177147	87381.3	43690.6667
1	3.33E-01	1	0.666666667		0.526748971	1.053497942	-9.8	11	177147	93312.0	46656
2	1.11E-01	3	0.888888889		0.554928957	1.067871094	13.7	11	177147	98304.0	49152
3	3.70E-02	4	0.592592593		0.592592593	1.053497942	-9.8	11	177147	104976.0	52488
4	1.23E-02	6	0.790123457		0.624295077	1.067871094	13.7	11	177147	110592.0	55296
5	4.12E-03	7	0.526748971		0.666666667	1.053497942	-9.8	11	177147	118098.0	59049
6	1.37E-03	9	0.702331962		0.702331962	1.053497942	-9.8	11	177147	124416.0	62208
7	4.57E-04	11	0.936442615		0.739905276	1.067871094	13.7	11	177147	131072.0	65536
8	1.52E-04	12	0.624295077		0.790123457	1.053497942	-9.8	11	177147	139968.0	69984
9	5.08E-05	14	0.832393436		0.832393436	1.067871094	13.7	11	177147	147456.0	73728
10	1.69E-05	15	0.554928957		0.888888889	1.053497942	-9.8	11	177147	157464.0	78732
11	5.65E-06	17	0.739905276		0.936442615	1.067871094	13.7	11	177147	165888.0	82944
12	1.88E-06	18	0.493270184		1	1.053497942	-9.8	11	177147	177147.0	88573.5
					1.053497942						
					2^(1/12) =	1.059463094					

FIG 40

4/15/95

Chapter 9: Goertzel

Bad news, I thing.

Goertzel k'o's Szasz in the 9th

- even windows.

Chapter 9: "The Goertzel Algorithm" 4/14/96

The transfer function for the Goertzel Algorithm is

$$H_k(z) = \frac{1 - W_N^k z^{-1}}{1 - 2\cos\left(\frac{2\pi k}{N}\right) z^{-1} + z^{-2}} \qquad (9\text{-}1)$$

$$= \frac{1 - z^{-1} e^{-j2\pi k/N}}{\left(1 - z^{-1} e^{-j2\pi k/N}\right)\left(1 - z^{-1} e^{+j2\pi k/N}\right)}$$

$$= \frac{1}{1 - z^{-1} e^{j2\pi k/N}} \qquad (9\text{-}2)$$

The inverse z transform gives the impulse response

$$h_k[n] = e^{j2\pi nk/N} \; \underbrace{U[n]}_{\text{UNIT STEP}} \qquad (9\text{-}3)$$

Note

$$H_k(z) = \sum_{n=0}^{\infty} h_k[n] z^{-n} \qquad (9\text{-}4)$$

For an input of $x[n]$, the output is

$$y_k[n] = x[n] * h_k[n] \qquad (9\text{-}5)$$

Assume $x[n] = 0$ for $n < 0$ (ie causal). Then

$$y_k[n] = \sum_{m=0}^{n} x[m] h_k[n-m]$$

$$= \sum_{m=0}^{n} x[m] e^{j2\pi(n-m)k/N}$$

$$= e^{j2\pi nk/N} \sum_{m=0}^{n} x[m] e^{-j2\pi mk/N} \qquad (9\text{-}6)$$

Thus

$$y_k[N] = \sum_{m=0}^{N} x[m] e^{-j2\pi mk/N}$$

$$= \underline{X}\left(\frac{k}{N}\right) \qquad (9\text{-}7)$$

Question: How many ops?

Equation (9.2) can be implemented by the IIR filter

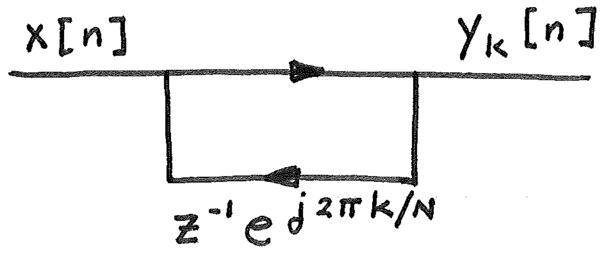

FIG 9-1

Since $X(N/k) = y_k[N]$, a total number of operations is

$$\begin{aligned} N \text{ complex multiplies} &= 6N \text{ ops} \\ N \text{ complex adds} &= \underline{2N \text{ ops}} \\ \text{total:} &\quad 8N \text{ ops} \end{aligned} \tag{9.8}$$

Suppose we window $x[n]$ prior to its input into the filter

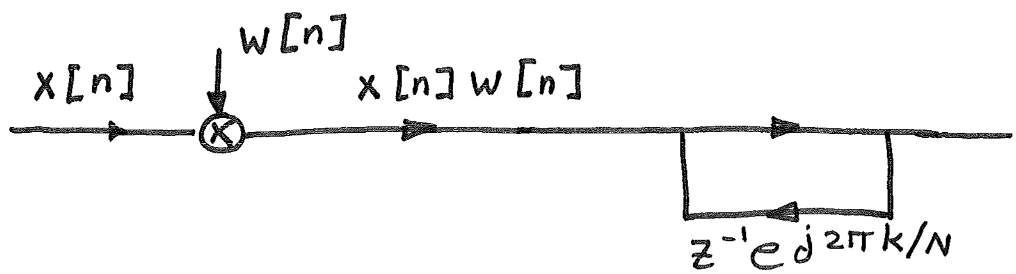

FIG 9.2

This adds about N ops. Thus, with windows, we have

$$9N \text{ ops (with window)} \tag{9.9}$$

How does this compare to Szasz series?

Here, the impulse response is

$$h_k[n] = e^{j2\pi k n/N} \sum_{q=-Q}^{Q} \alpha_q \, e^{j2\pi q n/N} \, U[n] \quad (9\text{-}10)$$

where Q is the order of the Szasz series. Thus

$$h_k[n] = \sum_{q=-Q}^{Q} \alpha_q \, e^{j2\pi(k+q)n/N} \, U[n] \quad (9\text{-}11)$$

For Hanning and Hamming windows, $Q = 1$ and we can use the following:

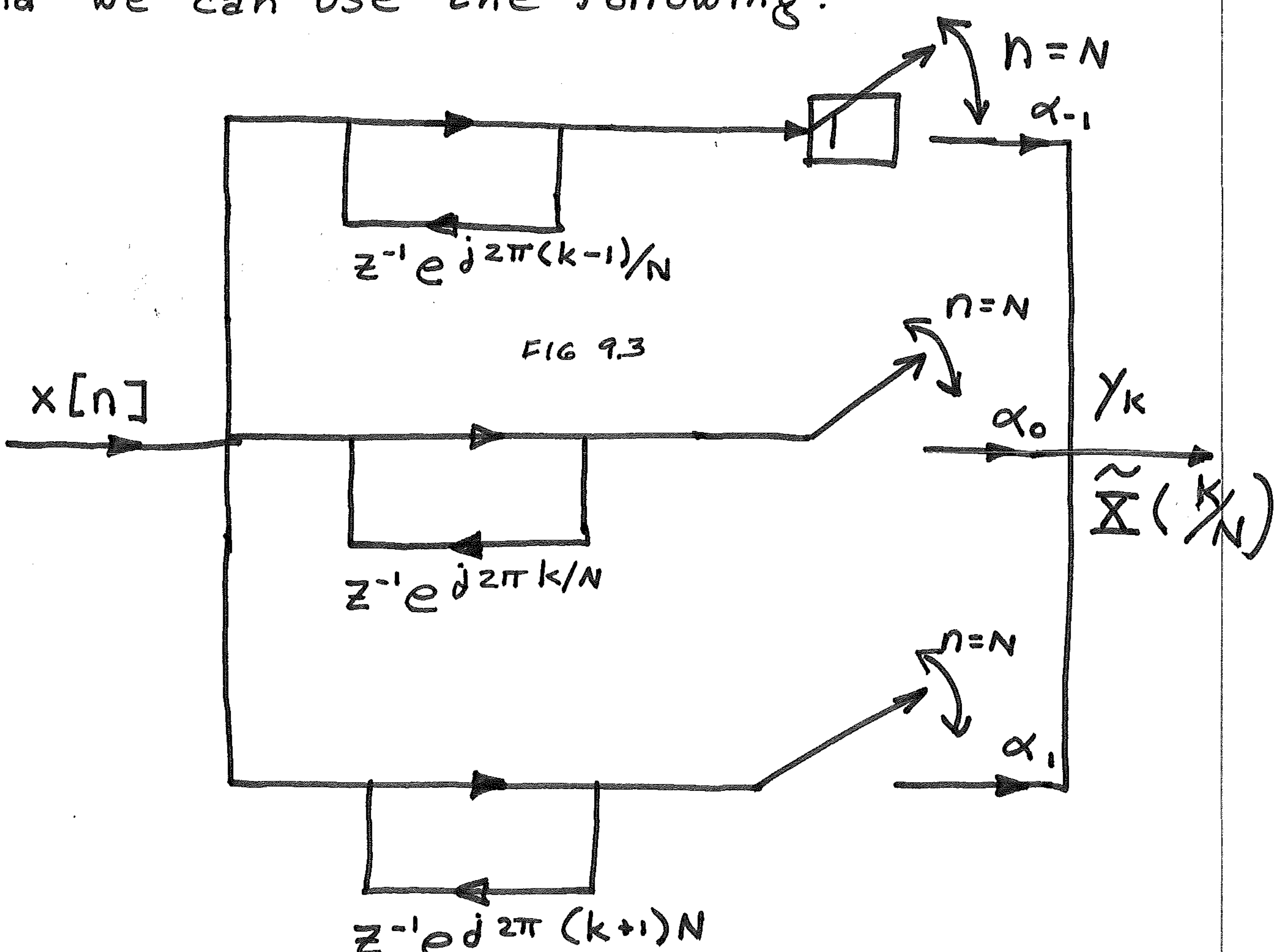

FIG 9.3

This is bad. The number of ops is

$$32N \text{ ops} \quad (Q=1) \quad (9\text{-}12)$$

In general $8(2Q+1)$ ops (9-13)

Addendum 8/1/96

Goertzel for $u \neq \frac{k}{N}$ when x is of

$$h_u[n] = e^{j2\pi nu}\, U[n] \tag{9-14}$$

$$y_k[n] = \sum_{m=0}^{n} x[m]\, e^{j2\pi(n-m)u} \tag{9-15}$$

$$= e^{j2\pi nu} \sum_{m=0}^{n} x[m]\, e^{-j2\pi mu} \tag{9-16}$$

$$y_k[N] = e^{j2\pi Nu} \sum_{m=0}^{N} x[m]\, e^{-j2\pi mu} \tag{9-17}$$

Algorithm for $u \neq k/M$

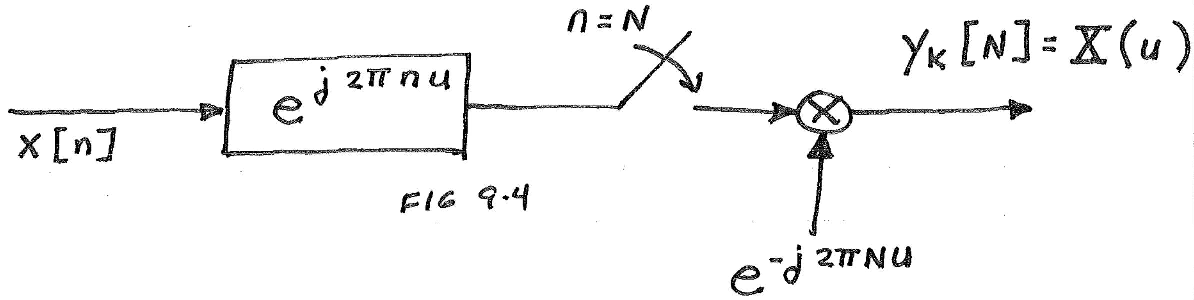

FIG 9-4

Alternately:

$$h_u[n] = e^{j2\pi(n-N)u}\, u[n] \tag{9-18}$$

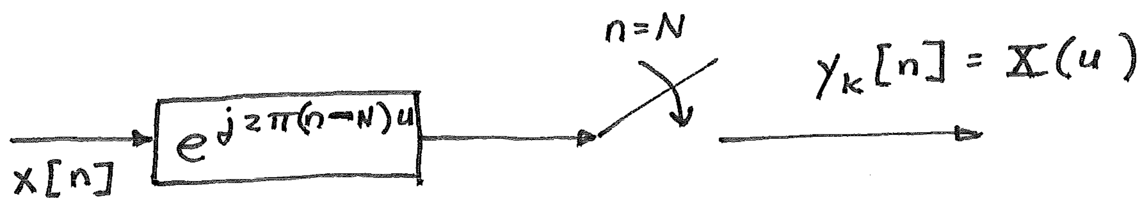

FIG 9-5

If windows are desired:

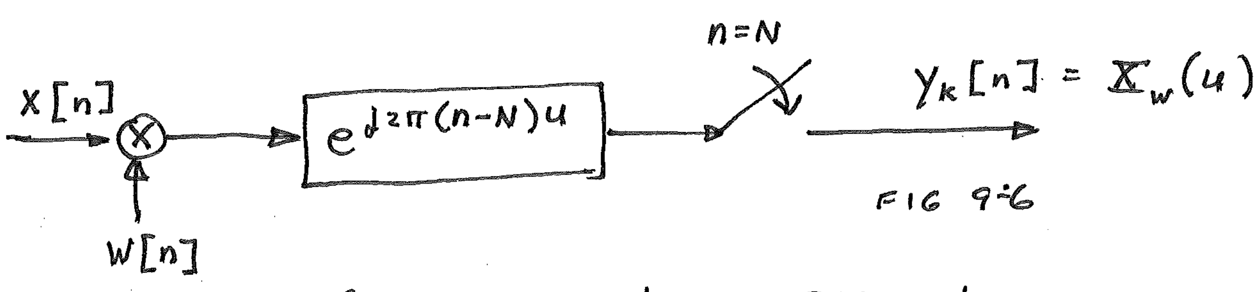

FIG 9-6

The number of ops is about 9N, the same as Fig 9-2.

A filter to do this is:

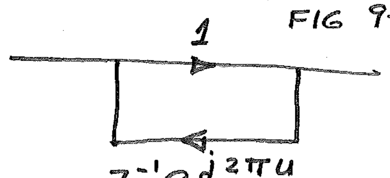

FIG 9-7

$$H_u(z) = \frac{1}{1 - z^{-1}e^{j2\pi u}} \qquad (9\text{-}19)$$

$$h_u[n] = e^{j2\pi n u}\, U[n] \qquad (9\text{-}20)$$

Then the figure in 9-4 can be implemented, with window, as

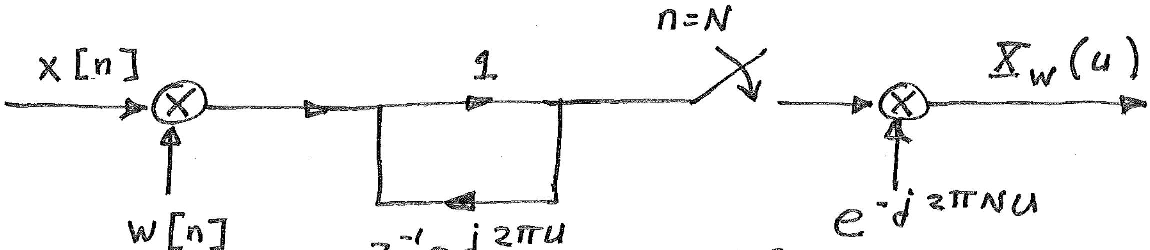

~~(9-21)~~

FIG 9-8

where

$$X_w(u) = \sum_{n=0}^{N} x[n]\, w[n]\, e^{-j2\pi n u} \qquad (9\text{-}21)$$

For log-spaced ~~algor~~ frequency bins with non-overlapping windows, THIS is the algorithm to beat.

4/15/96

Chapter 10: String cutting in Continuous Time

Interesting; but useful?

Chapter 10

"String Cutting in Continuous Time"

The CTFT (continuous time Fourier transform) is

$$X(u) = \int_{-\infty}^{\infty} x(t)\, e^{-j2\pi ut}\, dt \qquad (10\text{-}1)$$

Note:

$$\int_{-\infty}^{\infty} = \ldots \int_{-\frac{2}{u}}^{-\frac{1}{u}} + \int_{-\frac{1}{u}}^{0} + \int_{0}^{\frac{1}{u}} + \int_{\frac{1}{u}}^{\frac{2}{u}} + \ldots$$

$$= \sum_{n=-\infty}^{\infty} \int_{\frac{n}{u}}^{\frac{n+1}{u}} \qquad (10\text{-}2)$$

Thus

$$X(u) = \sum_{n=-\infty}^{\infty} \int_{n/u}^{\frac{n+1}{u}} x(t)\, e^{-j2\pi ut}\, dt \qquad (10\text{-}3)$$

Variable substitution:

$$\xi = t - \frac{n}{u}$$

gives

$$X(u) = \sum_{n=-\infty}^{\infty} \int_{0}^{\frac{1}{u}} x\left(\xi + \frac{n}{u}\right) e^{-j2\pi u\left(\xi + \frac{n}{u}\right)}\, d\xi$$

$$= \int_{0}^{\frac{1}{u}} \sum_{n=-\infty}^{\infty} x\left(\xi + \frac{n}{u}\right) e^{-j2\pi \xi u}\, d\xi$$

or

$$X(u) = \sum_{n=-\infty}^{\infty} \int_{0}^{\frac{1}{u}} x\left(t + \frac{n}{u}\right) e^{-j2\pi ut}\, dt \qquad (10\text{-}4)$$

$$= \int_{0}^{\frac{1}{u}} \tilde{x}_u(t)\, e^{-j2\pi ut}\, dt$$

$$x_u(t) = \sum_{n=-\infty}^{\infty} x\left(t \pm \frac{n}{u}\right)$$

Alternately:

$$\bar{X}(u) = \int_0^{\frac{1}{u}} \tilde{x}_u(t)\, e^{-j2\pi ut}\, dt \tag{10-4}$$

where

$$\tilde{x}_u(t) = \sum_{n=-\infty}^{\infty} x\left(t+\frac{n}{u}\right) = \sum_{n=-\infty}^{\infty} x\left(t-\frac{n}{u}\right) \tag{10-5}$$

$$= x(t) * \sum_{n=-\infty}^{\infty} \delta\left(t-\frac{n}{u}\right)$$

$$= x(t) * |u| \sum_{n=-\infty}^{\infty} \delta(ut-n)$$

$$= x(t) * |u|\, comb(ut) \tag{10-6}$$

Let

$$\tilde{x}_u(t) \longleftrightarrow \tilde{\bar{X}}_u(v) \tag{10-7}$$

Then

$$\tilde{\bar{X}}_u(v) = \bar{X}(v) \times comb\left(\frac{v}{u}\right) \tag{10-8}$$

$$= \bar{X}(v) \times \sum_{n=-\infty}^{\infty} \delta\left(\frac{v}{u}-n\right)$$

$$= \bar{X}(v) \times |u| \sum_{n=-\infty}^{\infty} \delta(v-nu)$$

$$= |u| \sum_{n=-\infty}^{\infty} \bar{X}(nu)\, \delta(v-nu) \tag{10-9}$$

Inverse transforming

$$\tilde{x}_u(t) = |u| \sum_{n=-\infty}^{\infty} \bar{X}(nu)\, e^{-j2\pi nut} \tag{10-10}$$

Substituting into (10-4):

$$\underline{X}(u) = \int_0^{1/u} \left[|u| \sum_{n=-\infty}^{\infty} \underline{X}(nu) e^{-j2\pi nut} \right] e^{-j2\pi ut} dt$$

$$= |u| \sum_{n=-\infty}^{\infty} \underline{X}(nu) \int_0^{\frac{1}{u}} e^{-j2\pi u(n-1)t} dt$$

$$= \sum_{n=-\infty}^{\infty} \underline{X}(nu) \ \delta[n-1]$$

$$= \underline{X}(u) \qquad (10\text{-}11)$$

We have gone around in a circle! Neat!

<u>But</u>, there <u>is</u> useful information in (10-10). $\tilde{x}_u(t)$ has, as Fourier coefficients, the harmonics of $\underline{X}(u)$. Thus, stacking $x(t)$ into $\tilde{x}_u(t)$ allows generation of not only $\underline{X}(u)$, but of $\underline{X}(nu)$.

Neat!

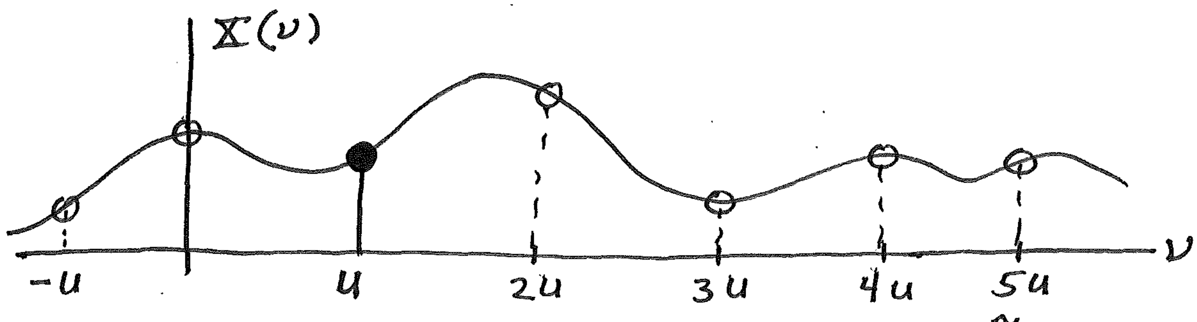

FIG. 10·1: Given $\underline{X}(u)$, computed from $\tilde{x}_u(t)$, the harmonics above can also be computed

Chapter 11 : Tempered Scale $\rightarrow \sqrt[12]{2}$

The assumption, as in Chapter 7, is that $\times 2^N$, for any n, raises or lowers by octaves and thus has no effect on the "note".
We start with $C = 1$

$A = \frac{5}{3}$	$E = 5$	$B = 15$
$C = \frac{3}{3}$	$G = 3$	$D = 9$
$F = \frac{1}{3}$	$\xleftarrow{\text{SECOND SUBHARMONIC}}$ $C = 1$ $\xrightarrow{\text{SECOND HARMONIC}}$	$G = 3$
$B^b = \frac{1}{9}$	$F = \frac{1}{3}$	$C = \frac{3}{3}$
$D^b = 1/15$	$A^b = \frac{1}{5}$	$E^b = \frac{3}{5}$

2nd Subharmonic
4th Subharmonic
2nd Harmonic
4th Harmonic

Table 1

[The n^{th} harmonic of frequency f_0 is $(n+1)f_0$. The n^{th} subharmonic $\frac{f_0}{n+1}$.
The 1^{ST} & 3^{rd} harmonics & subharmonics are octaves of the fundamental.]

Each of these numbers is multiplied by 2^N to place this number in the interval:
$[\frac{1}{2}, 1]$

$A = \frac{5}{6}$	$E = 5/8$	$B = \frac{15}{16}$
$C = 1$	$G = 3/4$	$D = \frac{9}{16}$
$F = \frac{2}{3}$	$C = 1$	$G = \frac{3}{4}$
$B^b = \frac{8}{9}$	$F = 2/3$	$C = 1$
$D^b = 8/15$	$A^b = 4/5$	$E^b = \frac{3}{5}$

Table 2

OR

$A = 0.833$	$E = 0.625$	$B = 0.9375$
$C = 1.000$	$G = 0.750$	$D = 0.5625$
$F = 0.667$	$C = 1.000$	$G = 0.75$
$B^b = 0.889$	$F = 0.667$	$C = 1$
$D^b = 0.533$	$A^b = 0.800$	$E^b = 0.600$

Table 3

We have an F# missing. We can obtain this in two ways:

1. F# = second harmonic of $B \Rightarrow \frac{15}{3} \times 3 = \frac{45}{16}$.
Lower 2 octaves: F# = 45/64 = 0.703125

2. F# = 2nd subharmonic of $D^b \Rightarrow \frac{8}{15} \times \frac{1}{3} = \frac{8}{45}$
Raise 2 octaves: F# = 32/45 = 0.7111111

Using this, we can arrange the notes in frequency order:

		RATIO
C	0.5	1.0667
D^b	0.53333	1.0547
D	0.56250	1.0667
E^b	0.60000	1.0417
E	0.62500	1.0667
F	0.66667	1.05467 or 1.0667
F#	0.703125 or 0.711111	1.02564 or 1.05469
G	0.750000	1.06667
A^b	0.800000	1.04167
A	0.833333	1.06667
B^b	0.888889	1.0547
B	0.937500	1.066667
C	1.000000	

Table 4

The 'RATIO' is the ratio of two adjacent numbers. The ratios are remarkably similar, ranging from 1.0416 to 1.0667. A compromise is to require the ratio to be

$$2^{\frac{1}{12}} = 1.05946$$

This comes from dividing an octave (2) into 12 geometic pieces. This is the ratio used in modern music since the time of Bach.

We can use this to establish number spacings that are approximately spaced log (12 notes per octave).

Augment table 2 with $F\# = 32/45$. (This gave the closest ratio to $\sqrt[12]{2}$ in table 4). The common denominator to all of these fractions is:

$$5 \times 3^2 \times 2^4 = 720 \tag{11-1}$$

Rewrite Table 2 using this common denominator

$A = \frac{600}{720}$	$E = \frac{450}{720}$	$B = \frac{675}{720}$
$C = \frac{720}{720}$	$G = \frac{540}{720}$	$D = \frac{405}{720}$
$F = \frac{480}{720}$	$C = \frac{720}{720}$	$G = \frac{540}{720}$
$B^b = \frac{640}{720}$	$F = \frac{480}{720}$	$C = \frac{720}{720}$
$Db = \frac{384}{720}$	$Ab = \frac{576}{720}$	$Eb = \frac{432}{720}$
		$F\# = \frac{512}{720}$

Table 5

Arrange numerators top down

720
675
640
600
576
540
512
480
450
432
405
384
360

Table 6

These are integers spaced rougly 12 notes per octave (The same ratios as in Table 4).

Note: If we wish two octaves, we begin with 2×720:

$2 \times 720 = 1440$
$2 \times 675 = 1350$
$2 \times 640 = 1280$
⋮
$2 \times 384 = 768$
$2 \times 360 = 720$
675
640
⋮
360

Table 7

This problem can be formulated as a genetic algorithm search.

Parameters to specify:

α = ratio of adjacent integers (11-2)

n_{min} and n_{max} ; N_{Max} (11-3)

The error of the n^{th} note is

$$e_n = |N\alpha^n - m_n| \quad ; n_{min} \le n \le n_{max}$$

where N is the string's length. ($N \le N_{Max}$).
The total error is

$$E = \max_{n_{min} \le n \le n_{max}} e_n \qquad (11\text{-}4)$$

The search is over N and the m_n's. All must be integers. An appropriate fitness function, for some positive number, β, is

$$F = e^{-\beta E} \qquad (11\text{-}5)$$

Note: The search is over a discrete set. E and F are not differentiable. The genome could be binary and be

$$[\underbrace{0110}_{N} \vdots \underbrace{0111}_{n_{min}} \vdots \underbrace{1101}_{n_{min}+1} \vdots 0010 \vdots \ldots \vdots \underbrace{1101}_{n_{max}}]$$

Note: The number of bits for N, defacto, determines N_{Max}.

Q: Where might this be useful?

A: At an FFT output where frequencies are limited to k/N.

Lets compare ops $\Rightarrow$ compute 12 frequency

① For Goertzel ($N = 720$)

$$12 \text{ lines} \times 9N \text{ ops per line} = 77{,}760 \text{ Goertzel ops} \quad (11\text{-}6)$$

② For FFT. For radix 2, must use $N = 1024 = 2^{10}$.

$$8N\log_2 N = 81{,}920 \text{ FFT ops} \quad (11\text{-}7)$$

The actual number will be less.

Goertzel does not do well here! It will do better for larger N. In general:

$$Ops_{Goertzel} = \#\text{lines} \times 9N \frac{ops}{line} \quad (11\text{-}8)$$

$$Ops_{FFT} = 8N\log_2 N \quad (11\text{-}9)$$

Let's examine efficiency. When does Goertzel beat the FFT in OPS?

Define

$$\mathrm{eff}_{G/F} = \frac{\mathrm{OPS}_{\mathrm{Goertzel}}}{\mathrm{OPS}_{\mathrm{FFT}}}$$

$$= \frac{8 \log_2 N}{9 L} \qquad (11\text{-}10)$$

where L is the number of lines. Roughly, when L exceeds $\log_2 N$, it is best to use the FFT.

Constant Q from long signals (Chapter 12)

8/8/96

The Fourier transform is

$$\mathbb{X}(u) = \sum_n x[n] e^{j2\pi nu} \quad (12\text{-}1)$$

We break this into wavelength of integer length λ:

$$\mathbb{X}(u) = \ldots \sum_{n=-\lambda}^{-1} + \sum_{n=0}^{\lambda-1} + \sum_{n=\lambda}^{2\lambda-1} \ldots \; x[n] e^{-j2\pi nu} \quad (12\text{-}2)$$

$$= \sum_p \sum_{m=p\lambda}^{(p+1)\lambda-1} x[m] e^{j2\pi mu}$$

Let $n = m - p\lambda$. Then

$$\mathbb{X}(u) = \sum_p \sum_{n=0}^{\lambda-1} x[n+p\lambda] e^{-j2\pi(n+p\lambda)u} \quad (12\text{-}3)$$

This is useful only when $\lambda u = k =$ integer, or

$$u = k/\lambda \quad (12\text{-}4)$$

In such a case

$$\mathbb{X}\left(\frac{k}{\lambda}\right) \equiv \mathbb{X}[k] = \sum_p \sum_{n=0}^{\lambda-1} x[n+p\lambda] e^{-j2\pi kn/\lambda} \quad (12\text{-}5)$$

We look at this two ways. First, the conventional magnitude

$$|\mathbb{X}[k]| = \left| \sum_p \sum_{n=0}^{\lambda-1} x[n+p\lambda] e^{-j2\pi kn/\lambda} \right| \quad (12\text{-}6)$$

and Hal's constant Q conjecture

$$|\mathbb{X}_{HAL}[k]| = \sum_p \left| \sum_{n=0}^{\lambda-1} x[n+p\lambda] e^{-j2\pi nk/\lambda} \right| \quad (12\text{-}7)$$

Note

$$|\mathbb{X}_{HAL}[k]| \geq |\mathbb{X}[k]|$$

Notes:

1. For on-frequency tones,

$$x_{ON\text{-}F}[n] = e^{j2\pi nk/\lambda} \qquad (12\text{-}8)$$

both (12-6) and (12-7) give the same result.

2. For off-frequency tones, $|X_{HAL}[k]|$ gives a lower Q - as conjectured. Here

$$x_{OFF}[n] = a e^{j2\pi n\nu} \quad ; \; \nu \neq \frac{k}{\lambda} \qquad (12\text{-}9)$$

Then (12-6) becomes

$$|X[k]| = |a| \left| \sum_p \sum_{n=0}^{\lambda-1} e^{j2\pi(n+p\lambda)\nu} e^{-j2\pi nk/\lambda} \right|$$

$$= |a| \left| \sum_{p=0}^{P-1} e^{j2\pi p\lambda\nu} \sum_{n=0}^{\lambda-1} e^{j2\pi n(\nu-\frac{k}{\lambda})} \right|$$

$$= |a| \left| \frac{\sin \pi P\lambda\nu}{\sin \pi\lambda\nu} \right| \left| \frac{\sin \pi\lambda(\nu-\frac{k}{\lambda})}{\sin \pi(\nu-\frac{k}{\lambda})} \right| \qquad (12\text{-}10)$$

where we have used the Appendix. For (12-7)

$$|X_{HAL}[k]| = |a| \sum_p \left| \sum_{n=0}^{\lambda-1} e^{j2\pi(n+p\lambda)\nu} e^{-j2\pi nk/\lambda} \right|$$

$$= |a| \sum_p \left| \sum_{n=0}^{\lambda-1} e^{j2\pi n(\nu-\frac{k}{\lambda})} \right|$$

$$= |a| \sum_{p=0}^{P-1} \left| \frac{\sin \pi\lambda(\nu-\frac{k}{\lambda})}{\sin \pi(\nu-\frac{k}{\lambda})} \right|$$

$$= |a| P \left| \frac{\sin \pi\lambda(\nu-\frac{k}{\lambda})}{\sin \pi(\nu-\frac{k}{\lambda})} \right| \qquad (12\text{-}11)$$

Note

$$|X[k]| \Big|_{\nu=\frac{k}{\lambda}} = |X_{HAL}[k]| \Big|_{\nu=\frac{k}{\lambda}} = |a| P \lambda \qquad (12\text{-}12)$$

A problem, however, is linearity. Consider, for example, the following signal

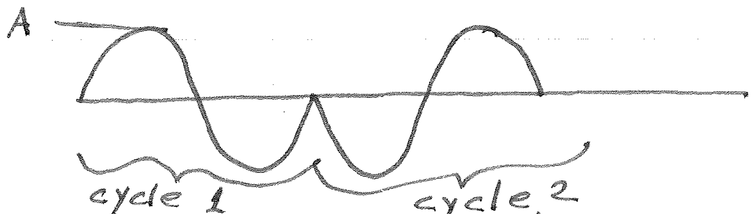

We wish to compute the output over two wavelengths. For one wavelength, we obtain the product

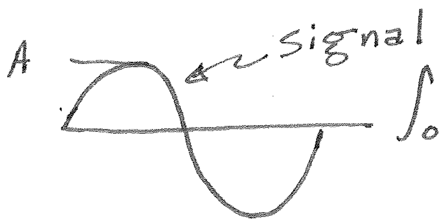

$$\int_0^{\lambda} A \sin \frac{2\pi t}{\lambda}\, e^{-j 2\pi t/\lambda}\, dt = \frac{A}{2}$$

For cycle 1, we get $\frac{A}{2}$. For cycle 2, we get $-A/2$.

The result from (12-6) is

$$| X[k] | = 0$$

And, from (12-7)

$$| X_{HAL}[k] | = A$$

This is not the result we want.

Appendix to Chapt 12

$$S = \sum_{m=0}^{N-1} e^{jm\theta} = \sum_{m=0}^{N-1} a^n = 1 + a + \ldots + a^{N-1}$$

$$aS = a + \ldots + a^{N-1} + a^N$$

$$\Rightarrow S = \frac{1 - a^N}{1 - a} = \frac{a^{N/2}}{a^{1/2}} \frac{a^{N/2} - a^{-N/2}}{a^{1/2} - a^{-1/2}}$$

$$S = a^{\frac{1}{2}(N-1)} \frac{a^{N/2} - a^{-N/2}}{a^{1/2} - a^{-1/2}}$$

$$= e^{\frac{j}{2}(N-1)\theta} \frac{\sin \frac{N\theta}{2}}{\sin \theta/2}$$

Note:

$$S\Big|_{\theta=0} = N$$

Discrete Time $\boxed{\text{Constant Q}}$ log spacings at less than octave spacing
incoherent addition, integer stuff

Tones → Perfect

Q_{Tones} → ~~Larger~~ Smaller

$X_{HAL} \geq X$

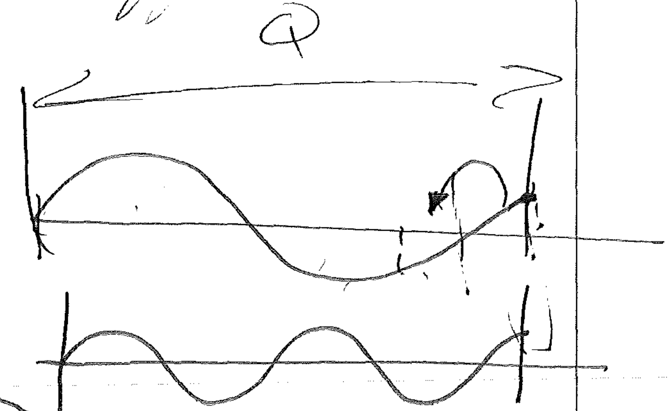

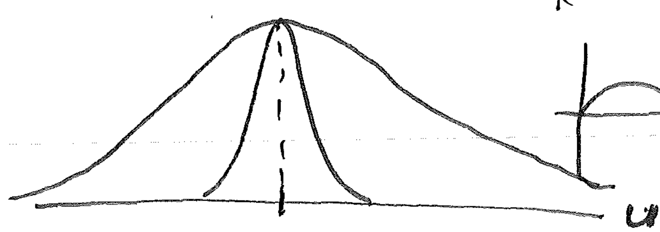

$\sqrt[12]{2}$

log. sp.

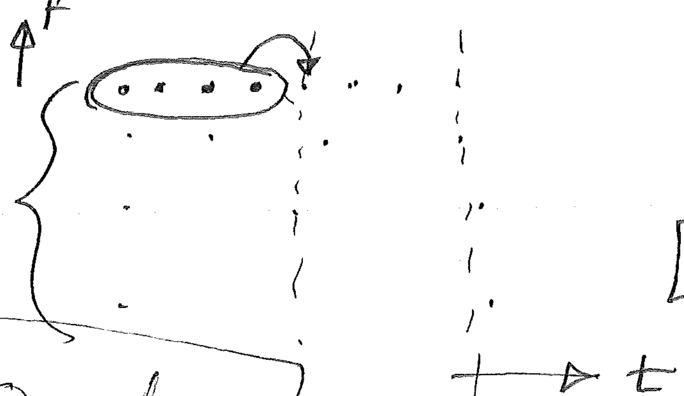

Q

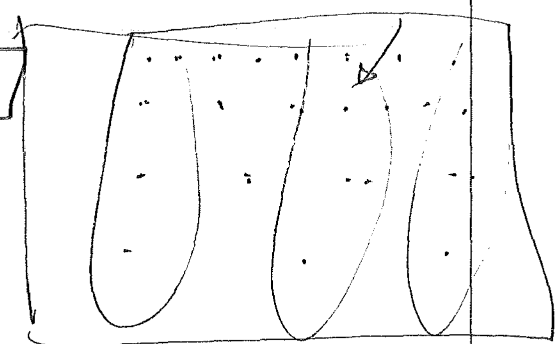

IS Quadra.

folding with

Grand Scheme

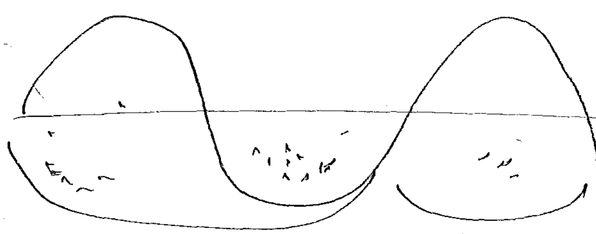

HI FREQ

Log Spacings

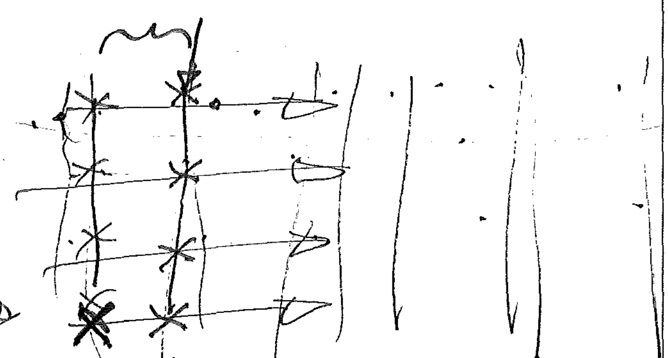

Q dictated by low frequency

Loose Info

★ Literature Search

Uniform samples. constant Q.

Strings → Phase in window is there

Flat Spots

Chapt 13

Fourier Transform Magnitude:

$$|X(u)| = \left| \sum_{n=0}^{N-1} x[n]\, e^{-j2\pi nu} \right| \qquad (1)$$

Hi Q transform:

$$X_P(u) = \sum_{p=0}^{P-1} \left| \sum_{n=pd}^{(p+1)d-1} x[n]\, e^{-j2\pi nu} \right| \qquad (2)$$

where there are P intervals of duration d and

$$N = Pd \qquad (3)$$

FIG 1

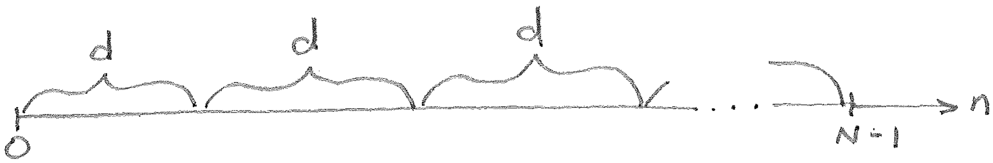

Theorem: $X_P(u) \geq |X(u)|$ (4)

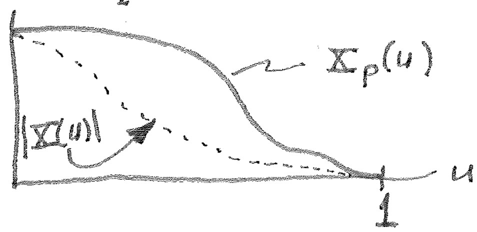

FIG 2

Proof: From (1):

$$|X(u)| = \left| \sum_{p=0}^{P-1} \sum_{n=pd}^{(p+1)d-1} x[n]\, e^{-j2\pi nu} \right|$$

$$\leq \sum_{p=0}^{P-1} \left| \sum_{n=pd}^{(p+1)d-1} x[n]\, e^{-j2\pi nu} \right|$$

$$= X_P(u) \qquad (5)$$

Theorem: When

$$x[n] = e^{j2\pi n v}, \tag{6}$$

$$|X(u)| = \left| \frac{\sin \pi N(u-v)}{\sin \pi(u-v)} \right| \tag{7}$$

and

$$X_p(u) = P \left| \frac{\sin \pi N(u-v)/P}{\sin \pi (u-v)} \right| \tag{8}$$

Corr: When (6) is true,

$$|X(v)| = X_p(v) = N \tag{9}$$

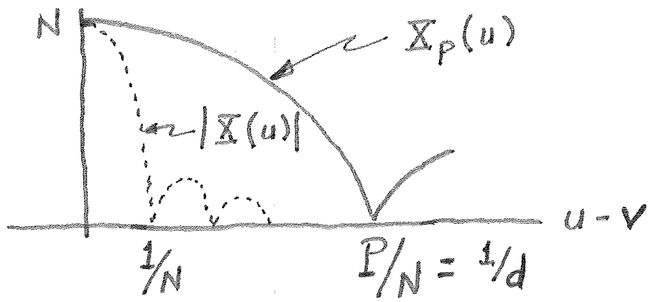

FIG 3

Proof: $\cancel{S(u)} = |X(u)| = \left| \sum_{n=0}^{N-1} e^{j2\pi n(u-v)} \right|$

$$= \left| \frac{\sin \pi N(u-v)}{\sin \pi(u-v)} \right| \tag{10}$$; from geometric series

$$X_p(u) = \sum_{p=0}^{P-1} \left| \sum_{n=pd}^{(p+1)d-1} e^{j2\pi n(u-v)} \right| \tag{11}$$

$$= \sum_{p=0}^{P-1} \left| \frac{\sin \pi d(u-v)}{\sin \pi(u-v)} \right| \tag{12}$$; from geometric series

One more step gives (8)

Observation: The Q is increased by a factor of P.

Chapter 14 8/15/97

Summary:

1. FFT's of combined strings give the same result as decimating the FFT of the unfolded string. The Q's are also the same - and thus pretty high.

2. Hal's Low-Q transform can't gereate all of these points in a computionally efficient method.

3. Hal's Low-Q transform can generate individual low-Q points. The number of operations per freq pt is $O(N)$ compared to $O(\lg N)$ for an FFT approach.

THEOREM:

Consider $\{ x[n] \mid 0 \le n < N \}$ and its DTFT:

$$\mathbb{X}(u) = \sum_{n=0}^{N-1} x[n] e^{-j2\pi n u} \tag{1}$$

We divide $x[n]$ into P wavelengths of length λ:

$$P\lambda = N \tag{2}$$

Fold $x[n]$ into strings of duration k & define

$$x_k[n] = \sum_{p=0}^{P-1} x[n+\lambda p] \tag{3}$$

The FFT of $x_k[n]$ gives $\{ \mathbb{X}(\frac{m}{\lambda}) \mid 0 \le m < \lambda \}$ (4)

PICTURE OF THEOREM:

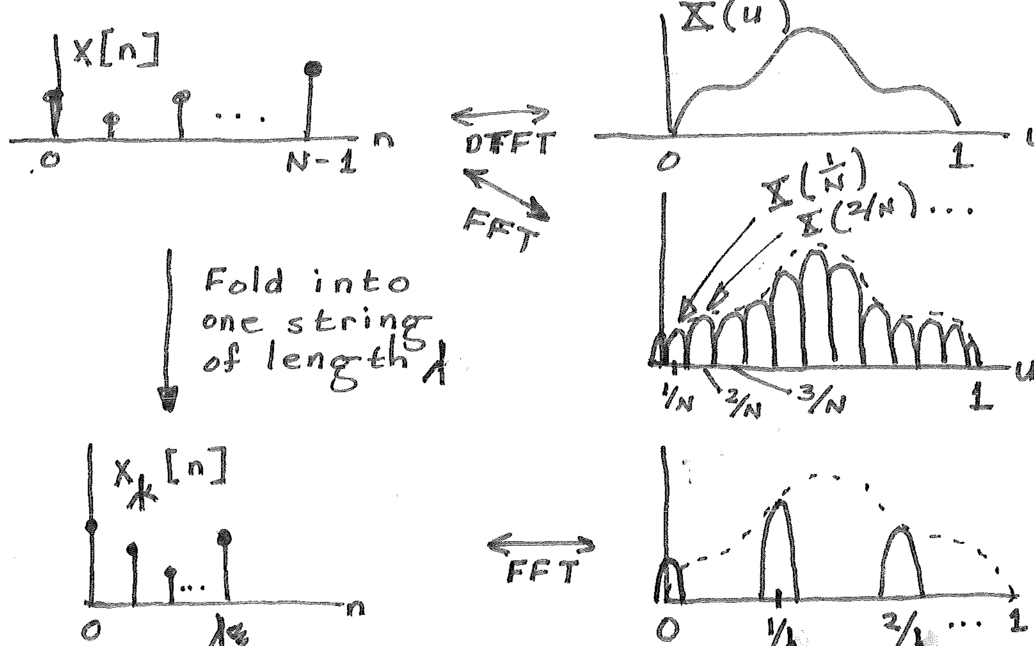

FIG 1

We Get Every P^{th} Frequency line exactly as we would by decimating FFT of $x[n]$.

Proof:

$$X(u) = \sum_{n=0}^{N-1} x[n] e^{-j2\pi nu} \quad ; \text{Let } N = P\lambda \tag{5}$$

$$= \sum_{p=0}^{P-1} \sum_{n=0}^{\lambda-1} x[n+p\lambda] e^{-j2\pi(n+p\lambda)u} \tag{6}$$

Thus

$$X(k/\lambda) = \sum_{p=0}^{P-1} \sum_{n=0}^{\lambda-1} x[n+p\lambda] e^{-j2\pi nk/\lambda} \tag{7}$$

$$= \sum_{n=0}^{\lambda-1} \left[\sum_{p=0}^{P-1} x[n+p\lambda] \right] e^{-j2\pi nk/\lambda} \tag{8}$$

$$= \sum_{n=0}^{\lambda-1} x_{\lambda}[n] e^{-j2\pi nk/\lambda} \tag{9}$$

For Hal's low-Q transform, define

$$X_p(u) = \sum_{p=0}^{P-1} \left| \sum_{n=0}^{\lambda-1} x[n+p\lambda] e^{-j2\pi(n+p\lambda)u} \right| \quad (10)$$

$$= \sum_{p=0}^{P-1} \left| \sum_{n=0}^{\lambda-1} x[n+p\lambda] e^{-j2\pi nu} \right| \quad (11)$$

We wish to evaluate this at the points

$$u = k/\lambda \quad (12)$$

This gives:

$$X_p(k/\lambda) = \sum_{p=0}^{P-1} \left| \sum_{n=0}^{\lambda-1} x[n+p\lambda] e^{-j2\pi nk/\lambda} \right| \quad (13)$$

Note: We can not use strings to evaluate the DFT in (13) to obtain all the points

$$u = \frac{k}{\lambda} \quad ; \quad 0 \le k < \lambda \quad (14)$$

If we use L strings of length ℓ such that

$$\lambda = L\ell \quad (15)$$

then we could obtain frequencies

$$\frac{k}{\ell} \quad ; \quad 0 \le k < \ell \quad (16)$$

Thus, if $\lambda = 24$, we would desire frequencies

$$u = 0, \frac{1}{24}, \frac{2}{24}, \frac{3}{24}, \frac{4}{24}, \ldots, \frac{22}{24}, \frac{23}{24} \quad (17)$$

If we used $L=4$, $\ell=6$, we could generate the frequencies at:

$$u = \frac{1}{6}, \frac{2}{6}, \frac{3}{6}, \ldots, \frac{5}{6} \quad (18)$$

$$= \frac{4}{24}, \frac{8}{24}, \frac{12}{24}, \ldots, \frac{20}{24} \quad (19)$$

or every $L^{TH} = 4^{TH}$ frequency sample

Finding One frequency bin centered at $u = kL/\lambda$ with a Q of P/N.

PARAMETER DEFINITION:

k = integer between 0 and $\ell = \lambda/L$

N = number of points in $x[n]$

λ = division of N points (incoherent)

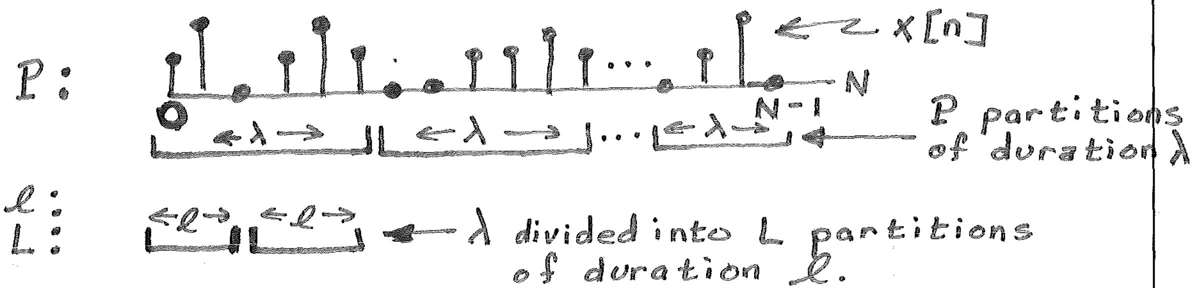

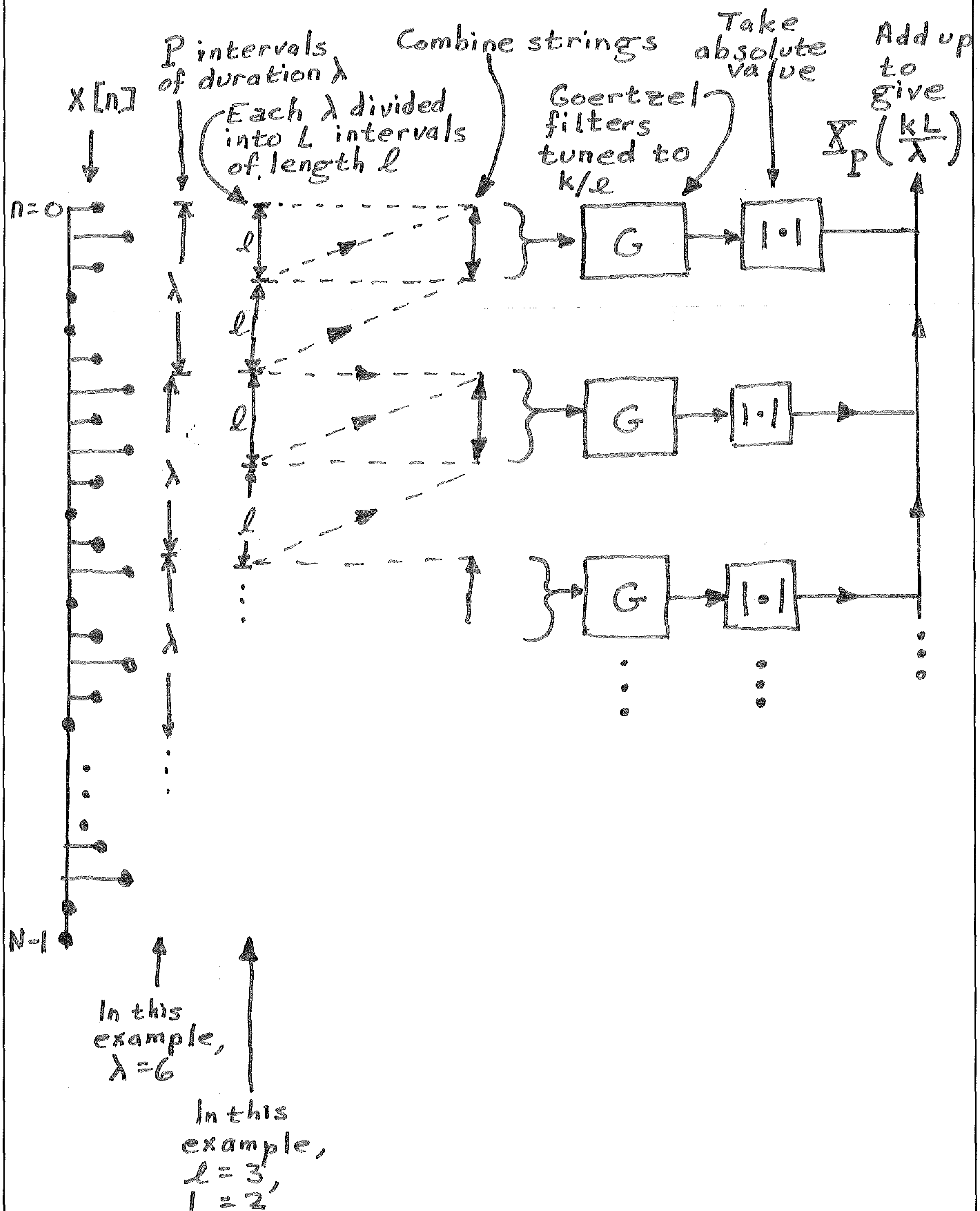

x[n]
P intervals of duration λ
Each λ divided into L intervals of length ℓ
Combine strings
Goertzel filters tuned to k/ℓ
Take absolute value
Add up to give $X_P\left(\frac{kL}{\lambda}\right)$
n=0
N-1
ℓ
λ
G
|·|
In this example, λ=6
In this example, ℓ=3, L=2

IEEE

TRANSACTIONS ON NEURAL NETWORKS

NEURAL NETWORKS COUNCIL

Robert J. Marks II
Editor-in-Chief

PLEASE REPLY TO:
University of Washington
Department of Electrical Engineering
c/o 1131 199th Street S.W., Suite N
Lynnwood, WA 98036-7138 USA

Hal,

These are Technical Write-Ups. There's one more coming on Chapt. 14.

– Bob –

A Piecewise Isoplanantic Approximation for the DFT

[redacted]

The discrete time Fourier transform (DTFT), $X(u)$, of a sequence $x[n]$ of length N can be written as

$$X(u) = \sum_{n=1}^{N} x[n] \mathrm{e}^{-j2\pi nu} \tag{1}$$

The *discrete Fourier transform* (DFT) follows as

$$X[k] = X\left(\frac{k}{N}\right) = \sum_{n=1}^{N} x[n] \mathrm{e}^{-j2\pi nk/N} \ ; \ 1 \le k \le N \tag{2}$$

For a given frequency, u, the DTFT can be evaluated by the inner product of two vectors of length N. One of the vectors contain the N values of $x[n]$ and the other the corresponding values of $\exp(-j2\pi nu)$.

How can the operation in Equation 1 be simplified? One approach is the FFT. Another approach, *the piecewise isoplanatic approximation* (PIA) can be used without significantly altering accuracy when the value of u is small. To apply the PIA, the vector containing the $x[n]$'s are broken into P intervals each of length λ. Thus

$$N = P\lambda$$

The idea is this. Each of the components of the P intervals are added. Call the sum of the q^{th} interval, $\{1 \le q \le P\}$,

$$x_P[q] = \sum_{n=(q-1)\lambda+1}^{q\lambda} x[n]$$

These values can be placed in a shorter vector of length P. We form the PIA DTFT

$$X_P(u) = \sum_{q=1}^{P} x_P[q] \mathrm{e}^{-j2\pi q\lambda u} \tag{3}$$

$N \to \lambda$
$\lambda \to Q$

This operation, illustrated in Figure 1, requires the inner product two much smaller dimensioned vectors. The save in operations, not counting the adding of the numbers in the intervals, is on the order of $\lambda = N/P$.

For small u,[1]

$$X_P(u) \approx X(u). \tag{4}$$

Indeed, for zero frequency ($u = 0$), Equation 4 is a strict equality. For small u, we can show

$$\begin{aligned} \epsilon_P(u) &= |X(u) - X_P(u)|^2 \\ &\leq 2E\left[\lambda - \cos\left(\pi(\lambda+1)u\right)\frac{\sin(\pi\lambda u)}{\sin(\pi u)}\right] \end{aligned} \tag{5}$$

where the total energy of the signal is

$$E = \sum_{n=1}^{N} |x[n]|^2. \tag{6}$$

Plots of

$$\frac{\epsilon_P\left(\frac{1}{N}\right)}{E}$$

versus P are shown in Figures 2 and 3 for various values of N. Note that, for $P = N$, the value of $\epsilon_P(u)$ is identically zero. Thus, the bounds in Figures 2 and 3 for $P = N$ are pessimistic. The bounds for $P > N$ are, of course, without meaning.

Proof

The DTFT in Equation 1 can be written as

$$X(u) = \sum_{q=1}^{P} \sum_{n=(q-1)\lambda+1}^{\lambda q} x[n] e^{-j2\pi nu}$$

and the PIA in Equation 3 can be written as

$$X_P(u) = \sum_{q=1}^{P} \sum_{n=(q-1)\lambda+1}^{\lambda q} x[n] e^{-j2\pi\lambda qu}$$

Substituting into Equation 5 gives

$$\epsilon_P(u) = \left|\sum_{q=1}^{P} \sum_{n=(q-1)\lambda+1}^{\lambda q} x[n]\left(e^{-j2\pi nu} - e^{-j2\pi\lambda qu}\right)\right|^2.$$

[1]Due to the periodicity of $X(u)$, this approximation is equally valid when u is *close* to any integer.

Using the inequality

$$\left|\sum_m a_m\right|^2 \leq \sum_m |a_m|^2$$

gives

$$\epsilon_P(u) \leq \sum_{q=1}^{P} \left| \sum_{n=(q-1)\lambda+1}^{\lambda q} x[n] \left(\mathrm{e}^{-j2\pi nu} - \mathrm{e}^{-j2\pi\lambda qu}\right) \right|^2 .$$

Schwarz's inequality,

$$\left|\sum_m a_m b_m\right|^2 \leq \sum_m |a_m|^2 \sum_m |b_m|^2$$

applied to this equation gives

$$\epsilon_P(u) \leq \sum_{q=1}^{P} \left[\sum_{n=(q-1)\lambda+1}^{\lambda q} |x[n]|^2 \sum_{n=(q-1)\lambda+1}^{\lambda q} \left|\mathrm{e}^{-j2\pi nu} - \mathrm{e}^{-j2\pi\lambda qu}\right|^2 \right] . \tag{7}$$

The first term in Equation 7 is simply the energy of the signal in the q^{th} interval.

$$E_q = \sum_{n=(q-1)\lambda+1}^{\lambda q} |x[n]|^2 . \tag{8}$$

Using the geometric series, the second term can be written in closed form as

$$\sum_{n=(q-1)\lambda+1}^{\lambda q} \left|\mathrm{e}^{-j2\pi nu} - \mathrm{e}^{-j2\pi\lambda qu}\right|^2 = 2\left[\lambda - \cos\left(\pi(\lambda+1)u\right) \frac{\sin(\pi\lambda u)}{\sin(\pi u)}\right]$$

Further recognizing from Equations 6 and 8, that

$$E = \sum_{q=1}^{P} E_q$$

reduces Equation 7 to Equation 5.

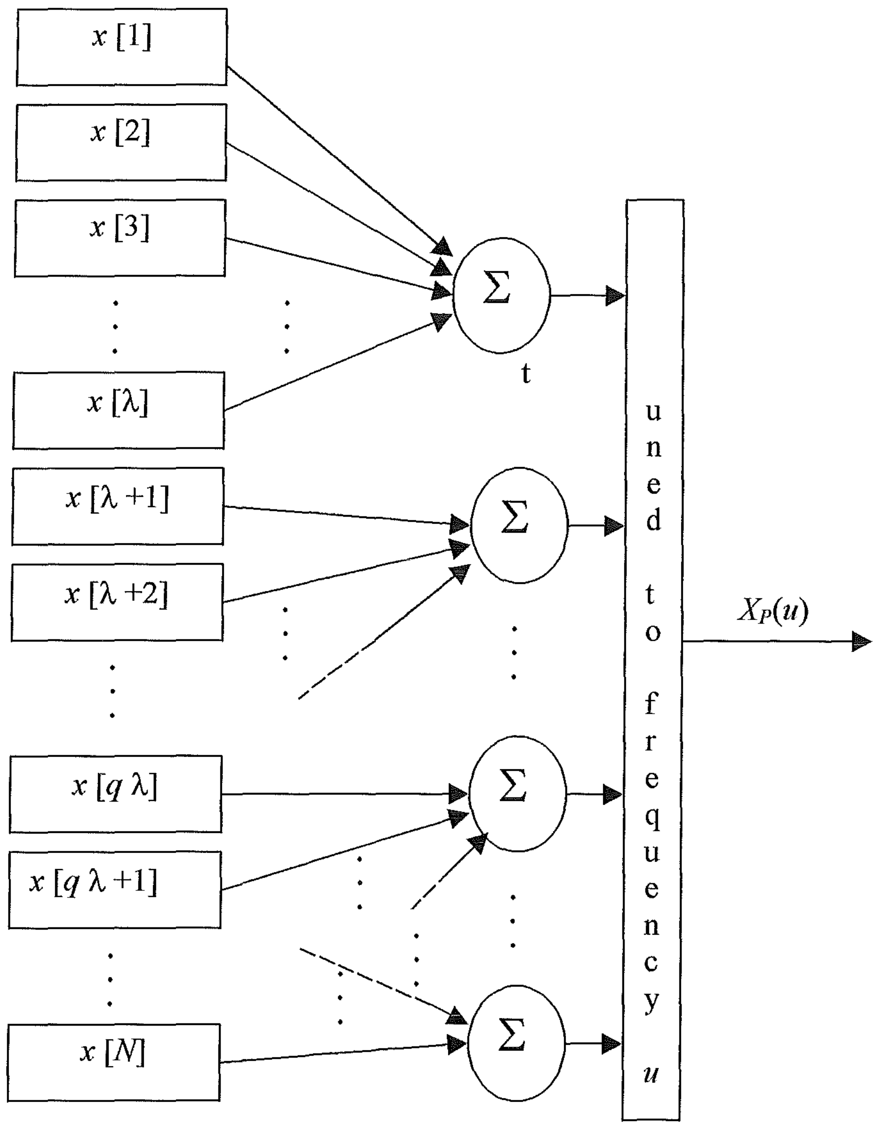

Figure 1: Illustration of the PIA of the DFT for a single frequency, u. There are a total of P input intervals that are summed.

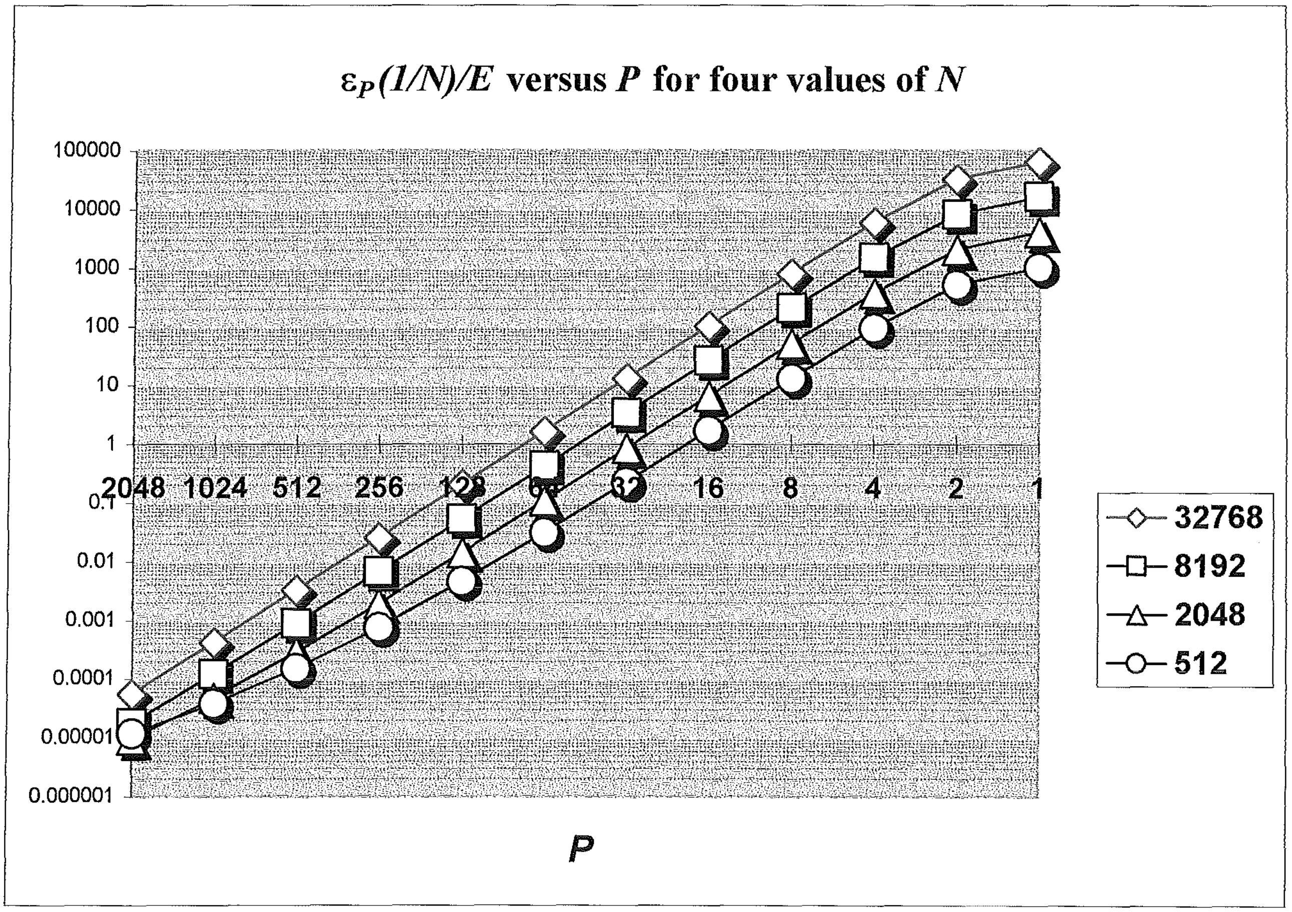

$\varepsilon_P(1/N)/E$ versus P for four values of N
100000
10000
1000
100
10
1
0.1
0.01
0.001
0.0001
0.00001
0.000001
2048
1024
512
256
128
64
32
16
8
4
2
1
32768
8192
2048
512
P

Figure 2

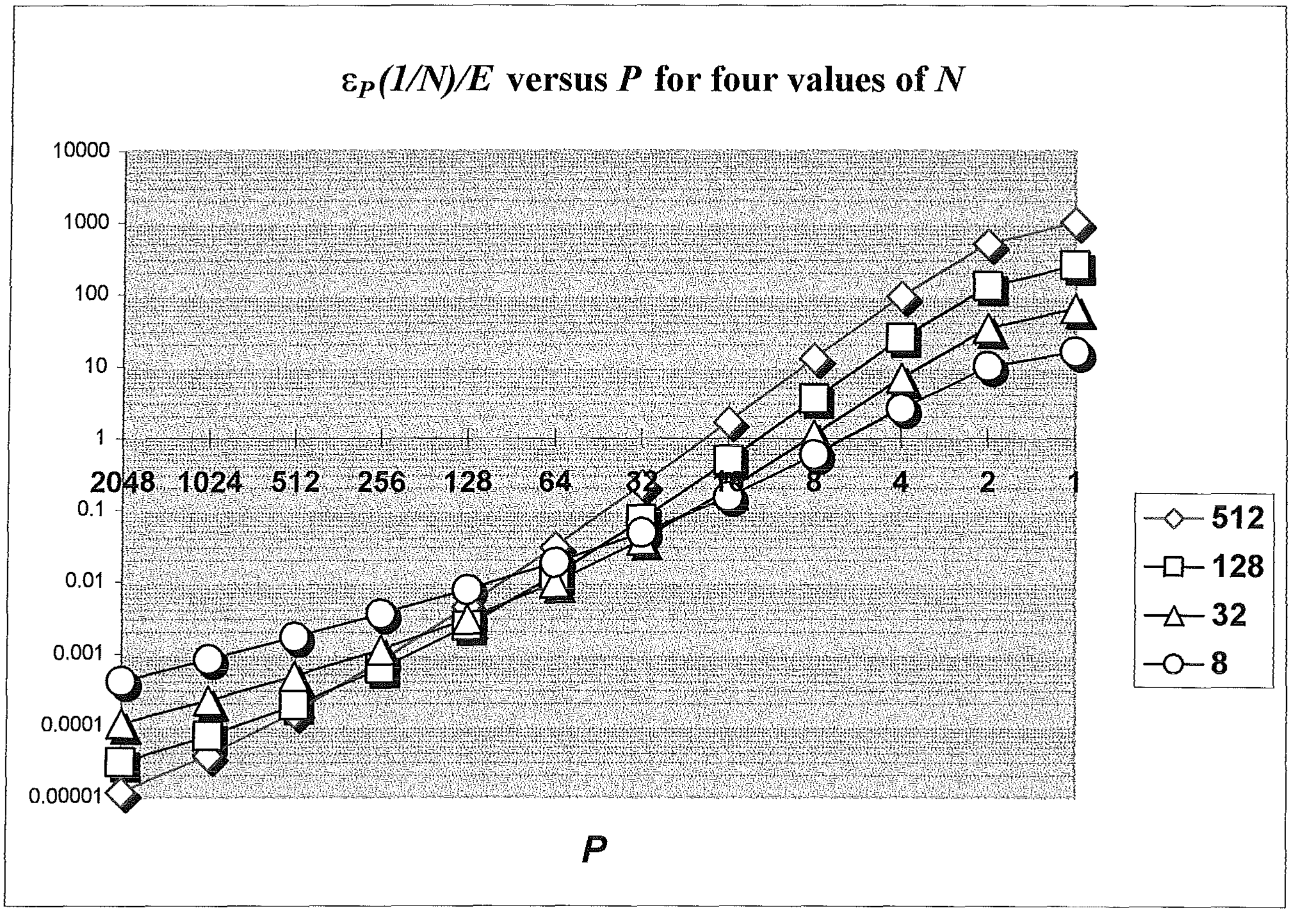

$\varepsilon_P(1/N)/E$ versus P for four values of N
10000
1000
100
10
1
0.1
0.01
0.001
0.0001
0.00001
2048
1024
512
256
128
64
32
16
8
4
2
1
P
512
128
32
8

Figure 3

Low Q Spectra From Long Signals

[redacted]

The discrete time Fourier transform (DTFT), $X(u)$, of a sequence $x[n]$ can be written as

$$X(u) = \sum_{n=-\infty}^{\infty} x[n]\mathrm{e}^{-j2\pi nu} \tag{1}$$

The *discrete Fourier transform* (DFT) follows as

$$X[k] = X\left(\frac{k}{N}\right) = \sum_{n=-\infty}^{\infty} x[n]\mathrm{e}^{-j2\pi nk/N} \;;\; 1 \leq k \leq N \tag{2}$$

The summation in the DTFT in Equation 1 can be broken into intervals of length λ and written as

$$X(u) = \sum_{p=-\infty}^{\infty} \sum_{m=p\lambda}^{(p+1)\lambda-1} x[m]\mathrm{e}^{-j2\pi mu}$$

Substituting $n = m - p\lambda$ gives

$$X(u) = \sum_{p=-\infty}^{\infty} \sum_{n=0}^{\lambda-1} x[n+p\lambda]\mathrm{e}^{-j2\pi(n+p\lambda)u}.$$

When $\lambda u = k =$ an integer,

$$X\left(\frac{k}{\lambda}\right) = X[k] = \sum_{p=-\infty}^{\infty} \sum_{n=0}^{\lambda-1} x[n+p\lambda]\mathrm{e}^{-j2\pi kn/\lambda} \tag{3}$$

From this expression follows two spectral representations.

1. The conventional spectral magnitude follows from Equation 3 as

$$|X[k]| = \left| \sum_{p=-\infty}^{\infty} \sum_{n=0}^{\lambda-1} x[n+p\lambda]\mathrm{e}^{-j2\pi kn/\lambda} \right|. \tag{4}$$

2. The *low Q* spectral magnitude is defined as

$$XQ[k] = \sum_{p=-\infty}^{\infty} \left| \sum_{n=0}^{\lambda-1} x[n+p\lambda]\mathrm{e}^{-j2\pi kn/\lambda} \right|. \tag{5}$$

1 Properties

- From the triangle inequality,

$$XQ[k] \geq |X[k]|$$

As a consequence, $XQ[k]$ can be shown to have a lower Q than $|X[k]|$.

- Let

$$x[n] = \begin{cases} ae^{j2\pi nv} & ; \quad 0 \leq n < N \\ 0 & ; \quad \text{otherwise} \end{cases}$$

  - For a frequency identically equal to $v = q/\lambda$ when q is an integer,

$$XQ[k] = |X[k]| \text{ when } v = \frac{q}{\lambda}.$$

  - Otherwise

$$|X[k]| = |a| \left| \frac{\sin(\pi N \lambda v)}{\sin(\pi \lambda v)} \right| \cdot \left| \frac{\sin\left(\pi\lambda(v - \frac{k}{\lambda})\right)}{\sin\left(\pi(v - \frac{k}{\lambda})\right)} \right| \tag{6}$$

and

$$XQ[k] = |a|N \left| \frac{\sin\left(\pi\lambda(v - \frac{k}{\lambda})\right)}{\sin\left(\pi(v - \frac{k}{\lambda})\right)} \right|. \tag{7}$$

Note that Equations 6 and 7 are both equal to $|a|N\lambda$ when $v = k/\lambda$.

2 Examples

In all of the figures, the spectrum magnitude is shown along with XQ for four and eight subdivisions of N points. The more subdivisions, the smaller the value of Q.

1. The spectrum magnitude of a single sinusoid of frequency $v = 0.5$ for $N = 32$ is shown.
2. The same as Figure 1, except $N = 128$.
3. The spectra of the sum of two sinusoids of length N with frequencies v_1 and v_2.

$$x[n] = e^{j2\pi v_1 n} + \beta e^{j2\pi v_2 n}$$

   In this figure, $v_1 = 0.2$, $v_2 = 0.8$, $\beta = 1$ and $N = 32$.
4. The same as Figure 3, except $\beta = 2$.
5. The same as Figure 3, except $\beta = 2$ and $N = 128$.
6. The same as Figure 3 with $N = 64$, $\beta = 1$, $v_1 = 0.4$, and $v_2 = 0.6$.
7. The same as Figure 6, except $N = 32$.

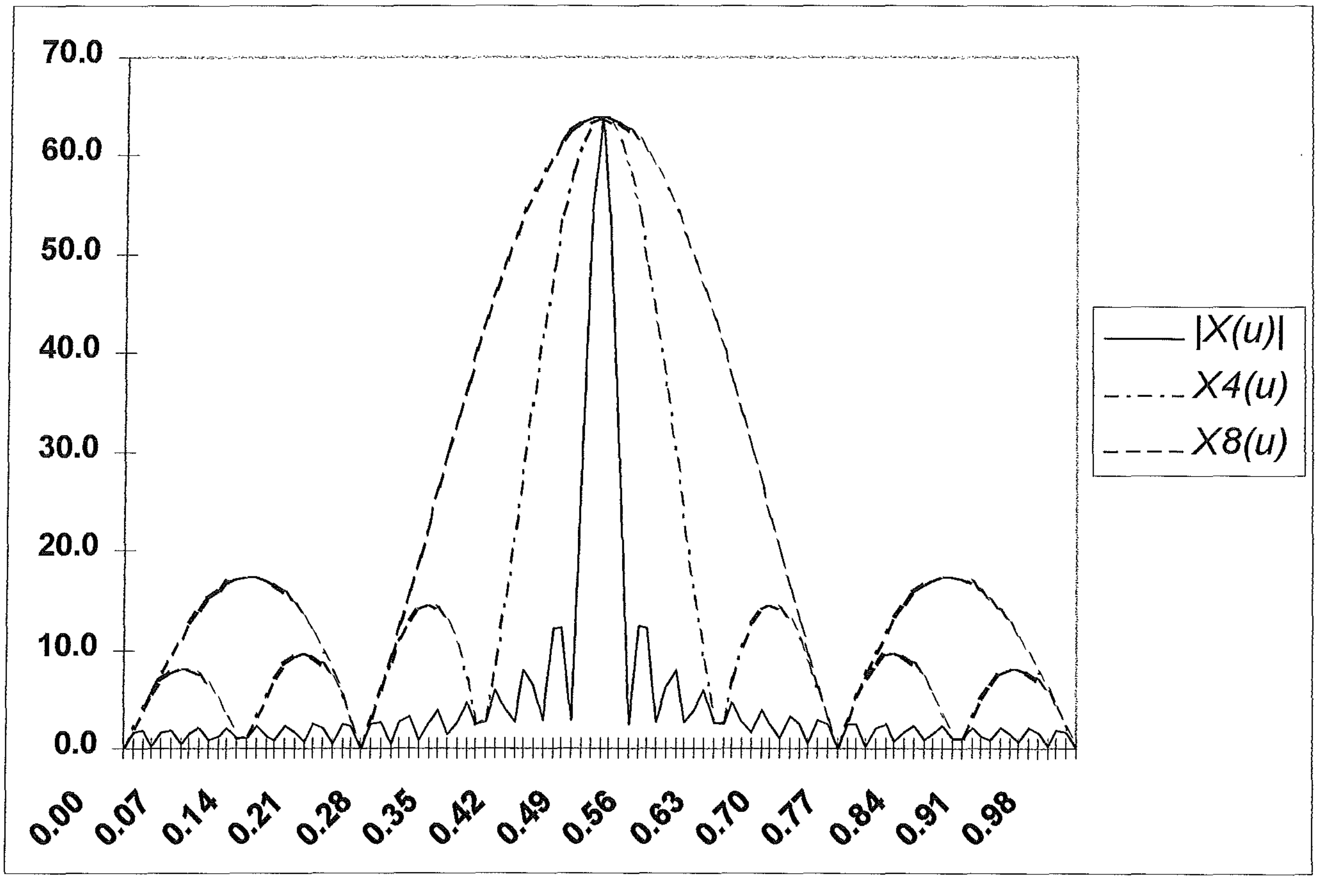
70.0
60.0
50.0
40.0
30.0
20.0
10.0
0.0
0.00
0.07
0.14
0.21
0.28
0.35
0.42
0.49
0.56
0.63
0.70
0.77
0.84
0.91
0.98
|X(u)|
X4(u)
X8(u)

Figure 1

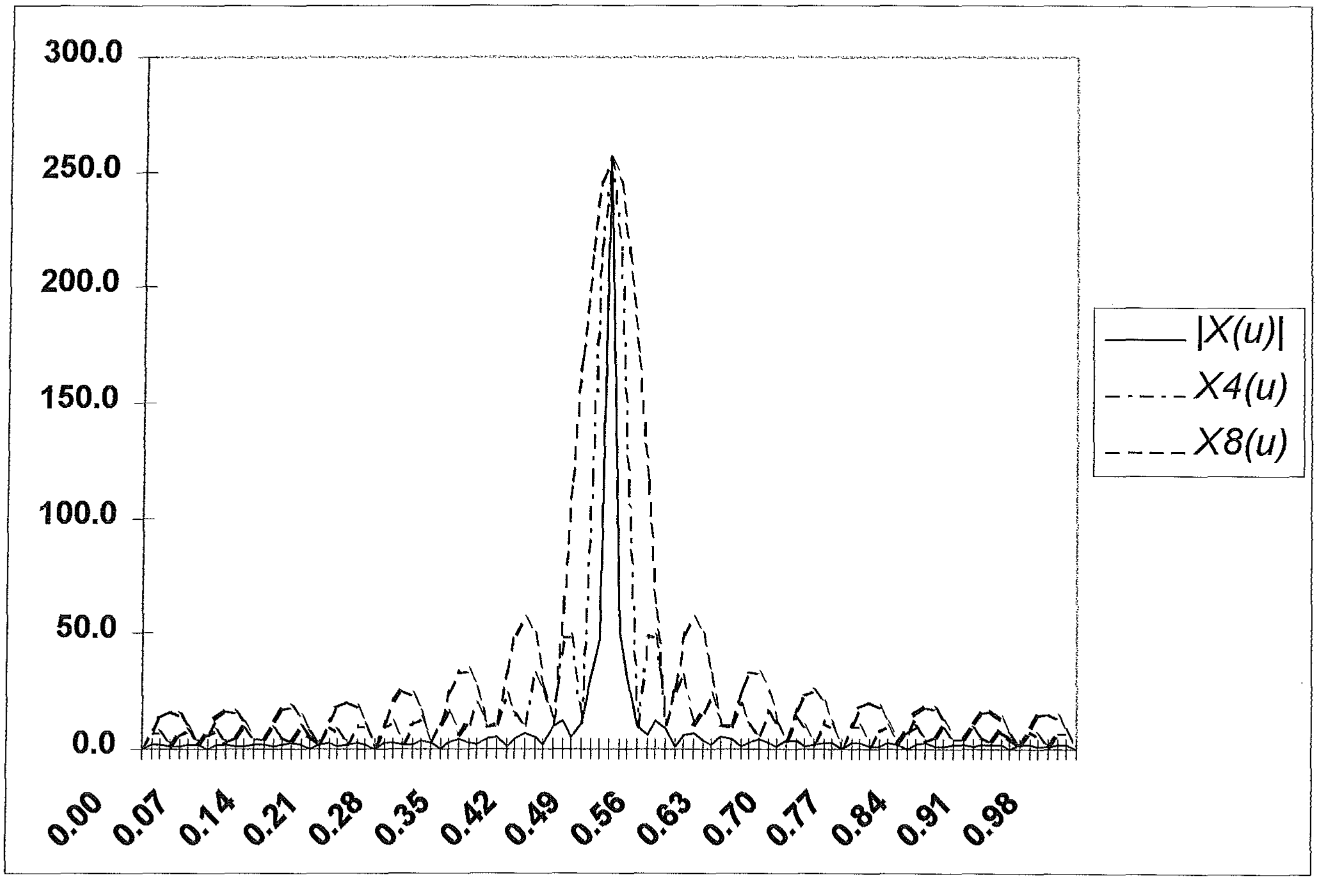

300.0
250.0
200.0
150.0
100.0
50.0
0.0
0.00
0.07
0.14
0.21
0.28
0.35
0.42
0.49
0.56
0.63
0.70
0.77
0.84
0.91
0.98
|X(u)|
X4(u)
X8(u)

Figure 2

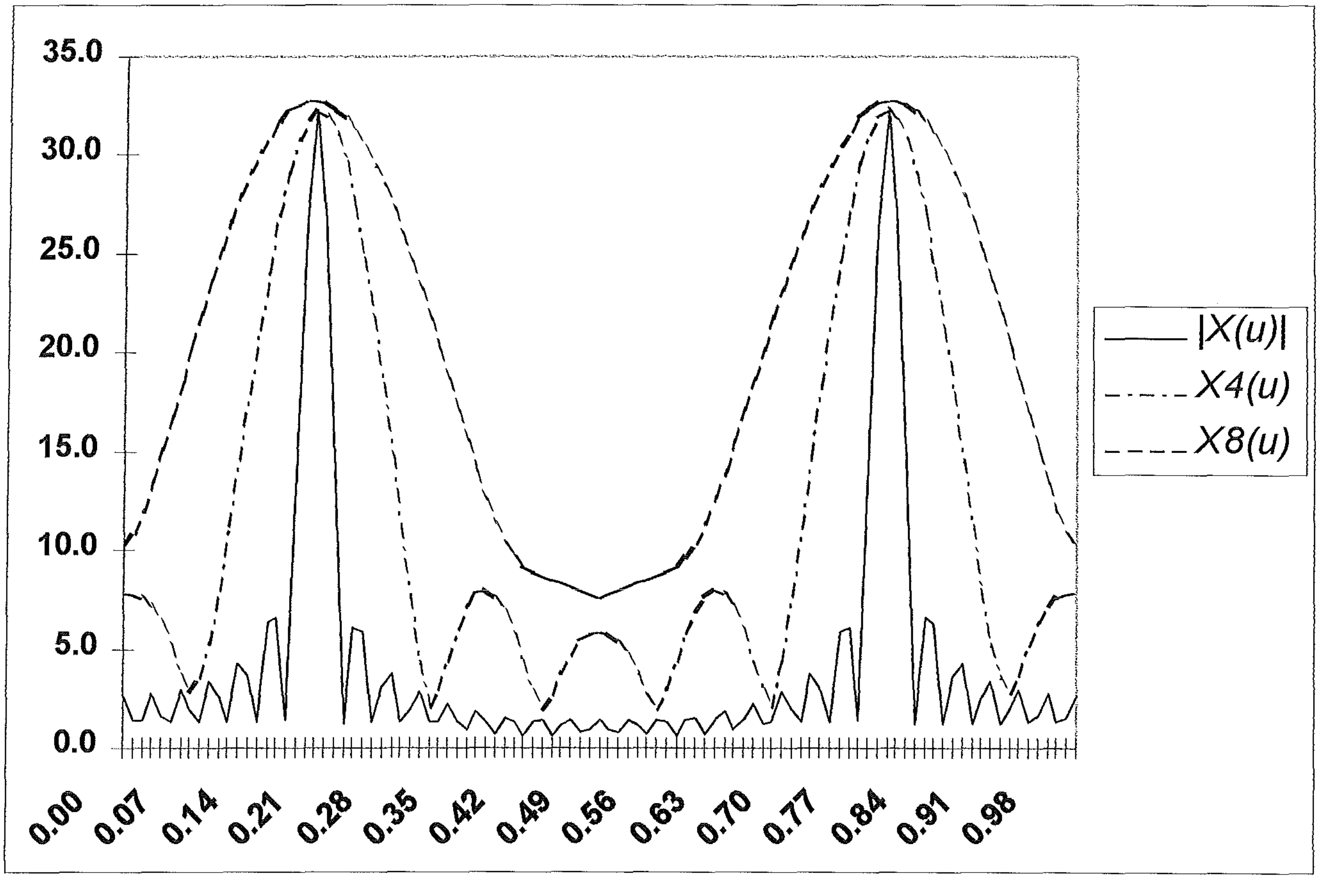

35.0
30.0
25.0
20.0
15.0
10.0
5.0
0.0
0.00
0.07
0.14
0.21
0.28
0.35
0.42
0.49
0.56
0.63
0.70
0.77
0.84
0.91
0.98
|X(u)|
X4(u)
X8(u)

Figure 3

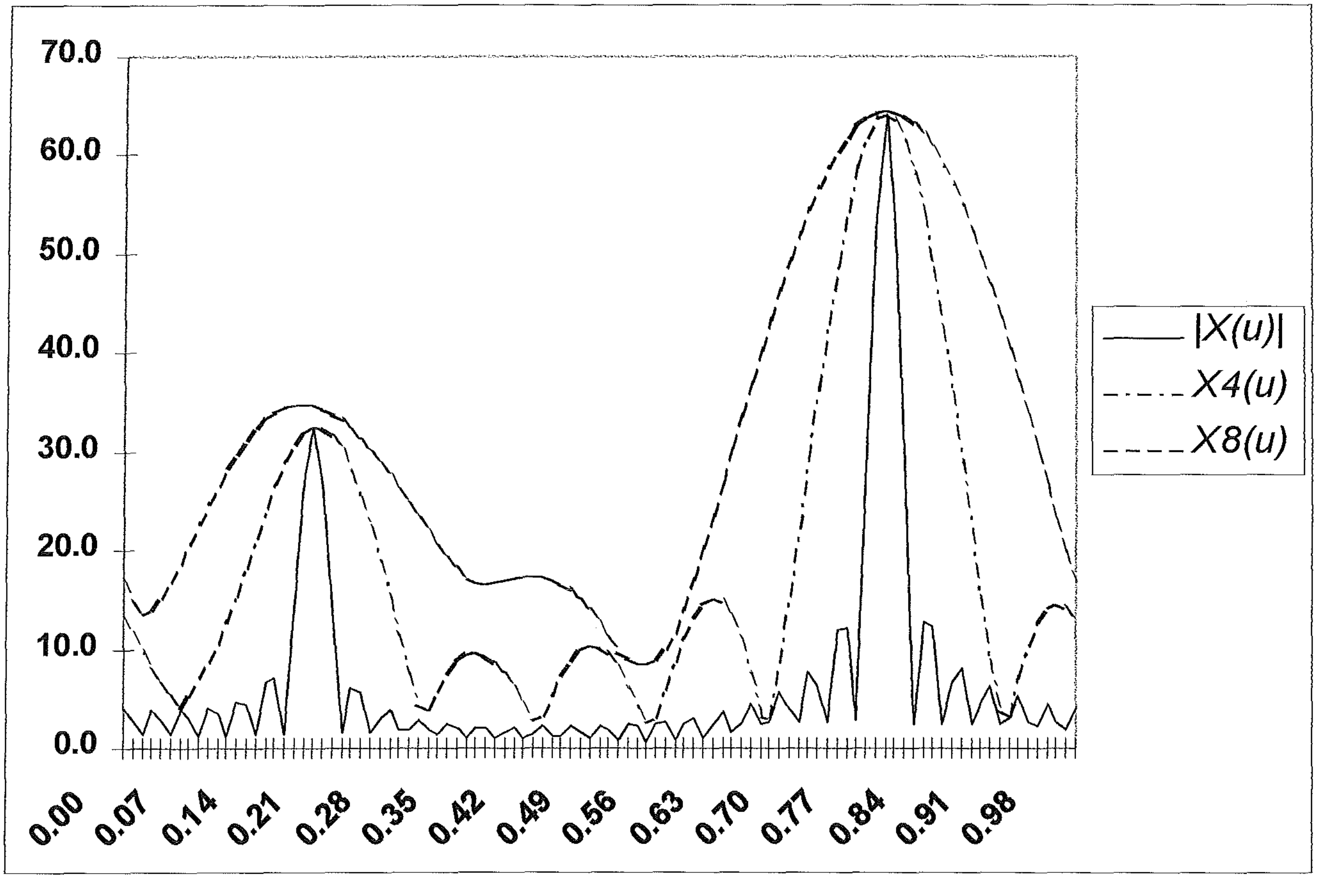

70.0
60.0
50.0
40.0
30.0
20.0
10.0
0.0
0.00
0.07
0.14
0.21
0.28
0.35
0.42
0.49
0.56
0.63
0.70
0.77
0.84
0.91
0.98
|X(u)|
X4(u)
X8(u)

Figure 4

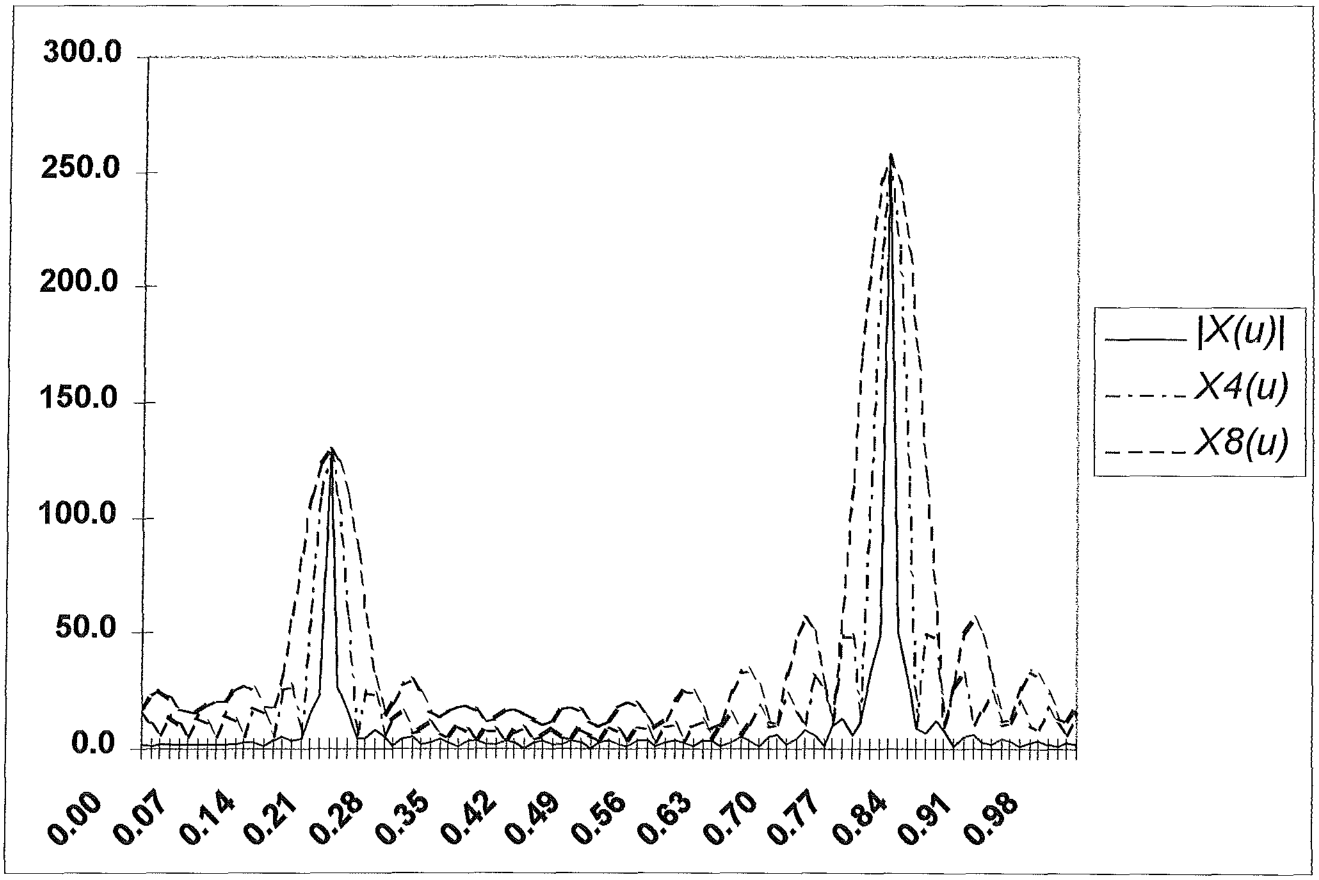
300.0
250.0
200.0
150.0
100.0
50.0
0.0
0.00
0.07
0.14
0.21
0.28
0.35
0.42
0.49
0.56
0.63
0.70
0.77
0.84
0.91
0.98
|X(u)|
X4(u)
X8(u)

Figure 5

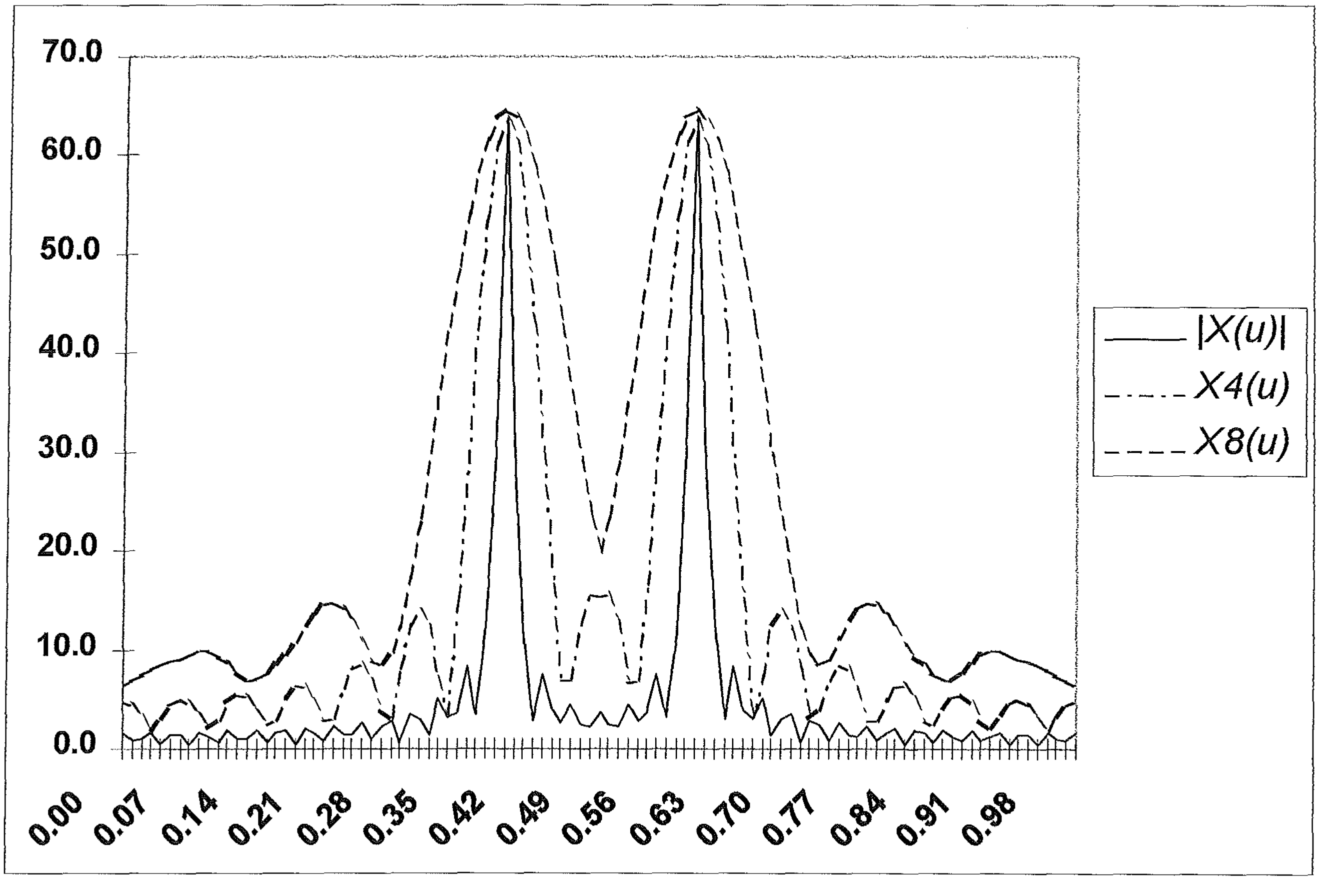

70.0
60.0
50.0
40.0
30.0
20.0
10.0
0.0
0.00
0.07
0.14
0.21
0.28
0.35
0.42
0.49
0.56
0.63
0.70
0.77
0.84
0.91
0.98
|X(u)|
X4(u)
X8(u)

Figure 6

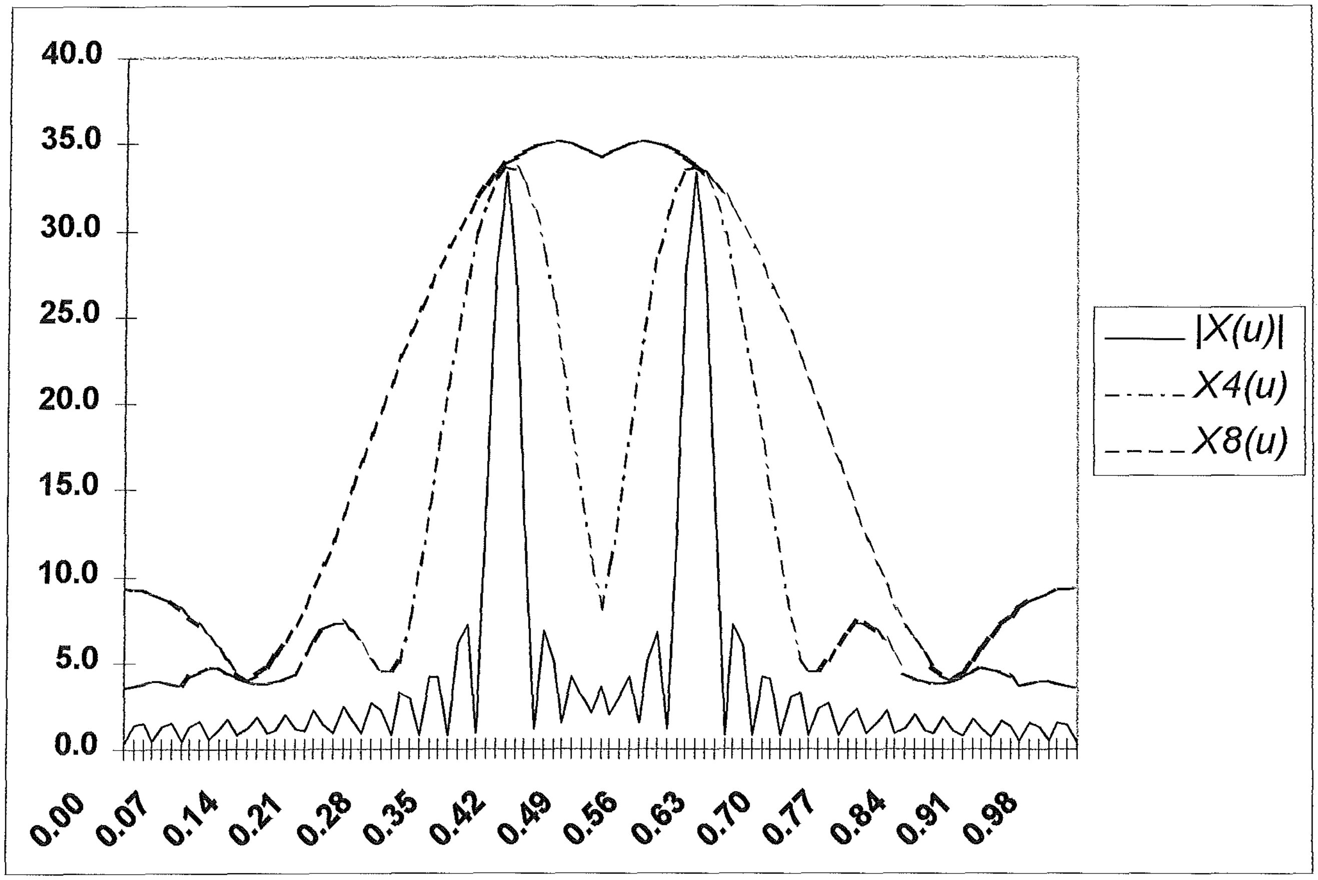

40.0
35.0
30.0
25.0
20.0
15.0
10.0
5.0
0.0
0.00
0.07
0.14
0.21
0.28
0.35
0.42
0.49
0.56
0.63
0.70
0.77
0.84
0.91
0.98
|X(u)|
X4(u)
X8(u)

Figure 7

MAGLOC™ a ring activated gun lock

Safety Conversion for Colt 1911A1 pistol

Once the gun is off your hand, it locks itself <u>automatically</u>

- Drop in safety device
- No batteries or keys required
- Installs in less than 10 minutes
- No time delay to fire
- Manufacturer guaranteed

Gun can only be fired by wearing a special ring

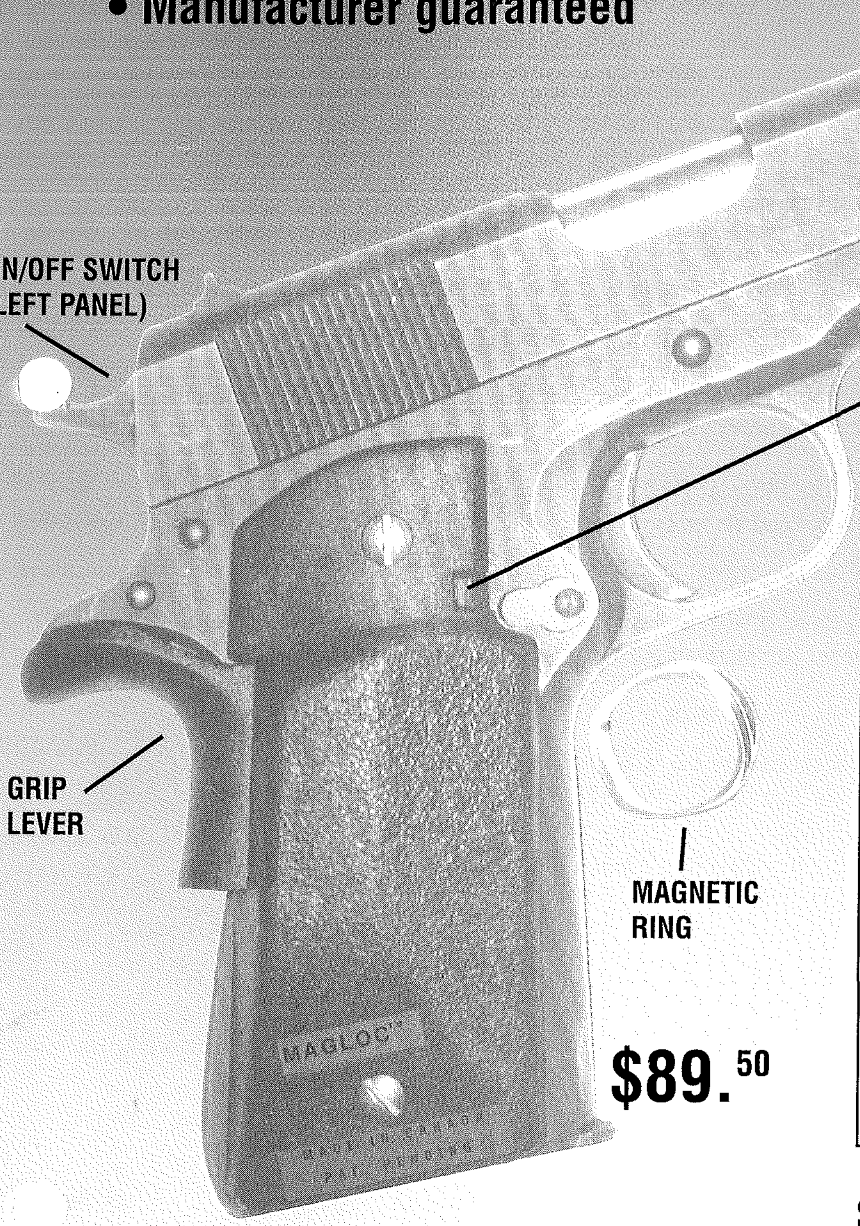

$89.^{50}

Coming soon:

Magloc™ for Smith & Wesson, Lady smith
Magloc™ for Shot Guns
Magloc™ for Beretta 92/96 pistol

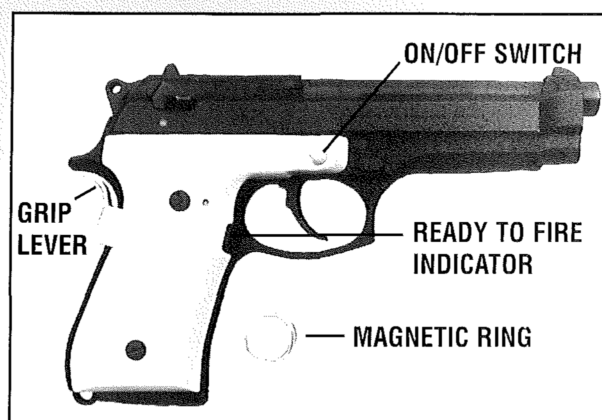

MAGLOC™ for BERETA 92/96 PISTOL

SMART LOCK TECHNOLOGY INC.
1160 Yew Ave.
Blaine, WA 98231 U.S.A.
Web Site: WWW.SMARTLOCK.COM

US Patent 5394717 & Patent Pending

MAGLOC™ Safety Conversion for Colt 1911A1 pistol

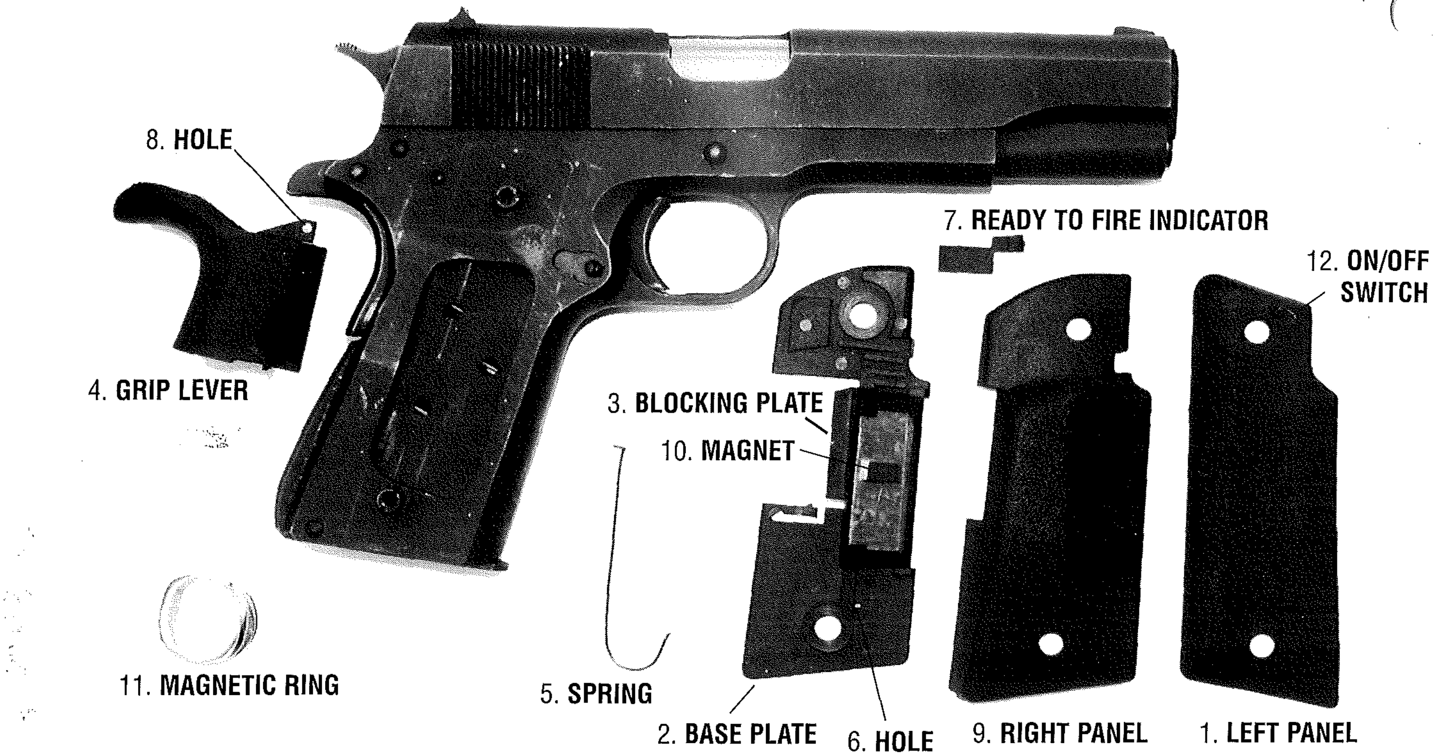

- Smart Lock Technology Inc. has spent over 6 years simplifying the MAGLOC™ safety device for conversion of firearms. Simply follow the numbering sequences shown above and you can have a Smart Firearm in less than 10 minutes.
- MAGLOC™ can be customized by adjusting the magnet (10) location according to the ring position of the user.
- The magnetic ring (has magnet on the underside) can be worn on either the middle or ring finger. It is an open ring design that can be adjusted up or down 1 size.

Order a MAGLOC™ now and receive a special introduction discount of $20 off the suggested retail price (add $5.50 for shipping & handling). Note: Limited one order per household. Introduction discount ends by May 31, 1998.

-- cut here --

To order, please complete the following and mail it to: Smart Lock Technology Inc.
1160 Yew Ave., Blaine, Washington 98231 USA or fax: (604) 448-1879

Name: ______________________ Daytime Phone Number:( ) ______________________
Mailing Address: ______________________ Fax:( ) ______________________
____
City ______________ State ______________ Zip ______________
Payment: Visa O Master O Money Order O
Card No.: ______________________ Expiry Date: ______________

Cardholder's Name: ______________________ Signature: ______________________
Ring Size: ______________ please measure the circumference of your right hand middle finger.

MAGLOC™ for ______________ at $ ________ less $20 discount + $5.50 S&H = Total: US$ __________

Note: If you are not satisfy with our product, just send it back in its original package within 14 days from the invoice date and we will remit your fund less S&H. Any merchandise returned after 14 days will be subjected to a 20% surcharge. (Refund can only be made at point of purchase with proof of receipt)

Biometric Scanning Safes

BIO SCANN

BIO SCANN

A Breakthrough in Safe Technology

If you needed your gun right now, how long would it take to get it? How about in the dark? If it would take more than one second, it may have been one second too long.

Introducing the *GUARDIAN* the world's only instant access safe.

It allows you to keep your gun safely locked from children and intruders, but allows you access to it in less than one second . . . even in the dark.

The *GUARDIAN* requires no keys or combinations. It has a newly developed access system utilizing a pattern recognition array which electronically scans your fingers when you try to open it.

The *GUARDIAN* is the only intelligent safe on the market. It not only decides if you are the proper user and unlocks itself in a fraction of a second, but it also counts how many times unauthorized persons attempt to open it and will stop them after a preset number of unsuccessful attempts.

How long does it take you to access your pistol? Remember, there may not be a second chance.

3 Models available with prices starting at $198. Wall safes available with Bio Scann.

For information call or write today: 1-800-467-SAFE or (918) 542-1304. Bedford Technologies, Inc., P.O. Box 328, Miami, OK 74355. Five years parts and labor warranty. Your satisfaction is guaranteed or your money back.

U.S. Patent Number 5,070,714

BTI

BEDFORD TECHNOLOGIES, INC.

MADE IN THE U.S.A.

SHOOTER'S EMPORIUM EXPANDED

QT9701
CHARGE-TRANSFER CAPACITANCE SENSOR IC

- Autocalibration on demand
- Auto-adaptive algorithms built in
- Multistage internal digital filtering
- 200µs response time
- 200ns to 1µs selectable pulse widths
- Direct MOSFET switch drive
- Simple external circuitry
- External threshold control option
- Analog sample gate control line
- Supports 2 kinds of drive circuitry
- Uses cloned e²prom setups from E2 board
- 4.5 to 5.5 volt single supply operation
- Inexpensive ceramic resonator
- Embeddable into most any product
- 28 pin SOIC or 28 pin plastic SDIP

PLASTIC SHRINK DIP OR SOIC
TOP VIEW

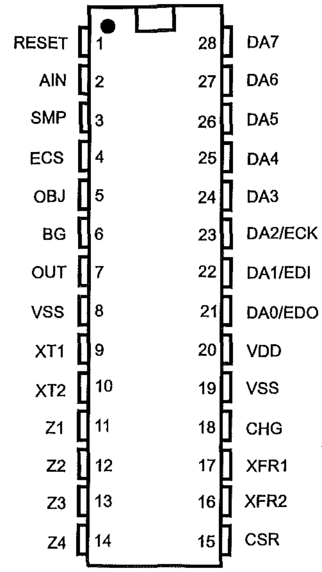

DESCRIPTION

The QT9701 is a charge-transfer (QT) processing IC. With a few external parts it becomes a complete sensor capable of detecting femtofarad capacitance changes while suppressing large amounts of stray 'C'. Sophisticated signal processing functions internal to the IC permit robust detection and allow a wide range of processing options. By using the charge transfer principle, the IC delivers performance superior to older technologies.

The device features an on-board ADC for signal acquisition and a high speed digital processing architecture which delivers up to 200µs response times. It features unparalleled flexibility in acquisition and processing of capacitance measurements. Virtually every internal processing function can be enabled, disabled, or altered to suit a specific application by the simple addition of a common inexpensive 8-pin e²prom which can be duplicated in production, and whose code source can be the QProx-E2 eval board. Without the e²prom, the IC operates in a default mode suitable for many sensing applications.

QT technology allows almost any metal-bearing surface or object to made inherently prox sensitive; a nonmetallic object can be sensitized by simply attaching something metallic to it. The effect readily penetrates through solid surfaces, allowing plastics and other nonconductors to become prox sensitive without modification. The sensor is highly tolerant of large capacitances, and will supress background 'C' automatically during a self-calibration procedure. When used with an e²prom, this calibration point can be locked in place so that the sensor will immediately begin to function after powerup without the need for a recalibration. The sensor is also capable of auto-threshold setting via a pushbutton or an external logic level. Auto-threshold uses a 'learn by example' method where the desired target object is presented and 'learned' to create the proper trip point.

The IC is designed for use in creating high performance capacitance detection systems for industrial and commercial use, and may be embedded on the circuit board of another product. Because the unit employs digital pulse technology, it is more immune to radiated RFI than other sensor types, and for many applications does not require shielding. The external circuitry and electrode drive are controlled by a low duty-cycle pulse sequence, so radiated RFI is kept to a minimum. The IC and external circuitry require a single +5 volt regulated power supply.

AVAILABLE OPTIONS

T_A	SOIC (S)	SHRINK DIP (D)
0°C to +70°C	QT9701-S	QT9701-D
-40°C to +85°C	QT9701-IS	QT9701-ID
-40°C to +125°C	QT9701-ES	QT9701-ED

TRAVEL

Hotel-Room 'Key' Cards Foil Prowlers—and Guests

By Jon Bigness
Staff Reporter of The Wall Street Journal

Hotels' electronic-lock systems are designed to foil would-be intruders. They do that—and often they do more: They stymie guests trying to get in their own rooms and can even imprison those already inside.

Blame the problems on mechanical breakdown, faulty installation, failed batteries or desk-clerk error. But whatever the cause, the thousands of travelers forced to fiddle with malfunctioning locks are often vocal on the subject.

"It's the most irritating thing in the world," says Nola Murphy, an aerobics instructor from Washington who was locked out of her room at the Sheraton Manhattan Hotel in New York because the "key" card didn't work. (A spokeswoman for the Sheraton Manhattan says key-card malfunctioning "doesn't seem to be a big problem for us," adding: "It's got to be one of those rare situations.")

Caryn Leschen

Marc Pazienza, a Washington lawyer, had a lockout experience at the Omni Waterside Hotel in Norfolk, Va., because of a defective key card; he says he was kept from entering his room for more than half an hour. "You have so much more to be concerned about other than something with the hotel going wrong," he laments. (The hotel hasn't received any complaints about key cards, says Michelle Cheffer, assistant to the general manager.)

The precise failure rate isn't known. But Chicago-based EMG Associates Inc., which sells and services electronic locks, can attest that it is high. Last year, EMG sold about 5,000 electronic locks—and repaired about 5,500. "Defects are prevalent," says Joshua Alper, president of EMG.

Manufacturers don't deny it. "All lock companies have problems," says Phil Wilder, director of marketing for Computerized Security Systems Inc. in Costa Mesa, Calif., one of the largest makers of electronic-lock systems.

One problem: Quality is getting lost in the rush to meet demand. In only a few years, electronic locks have been installed in a third of the nation's 3.2 million hotel rooms, and the pace is quickening because hotels feel the security advantages outweigh inconveniences.

The Holiday Inn, Howard Johnson's and Comfort Inn chains, among others, recently ordered their franchisees to ditch key-in-knob locks in favor of electronic systems, which cost about $250 a room. To fill orders, "companies are pushing locks out the doors and doing repairs regularly," says Mr. Alper.

Even functioning electronic locks can be confusing, because there are 30 different varieties coming from a dozen or so manufacturers. Arriving at the door, the traveler must determine whether to swipe or insert the card, have the arrow facing up or down or whether the card should be left in the lock while turning the handle. Then, if nothing happens, the problem is often a dead battery in the door lock.

Although most systems feature signals such as blinking lights that warn of low voltage, hotels routinely fail to replace batteries until they die, leaving guests locked in or out of rooms. Hotel executives such as Tom Daly, director of safety and security for Hilton Hotels Corp., play down that inconvenience to guests. "It's really only a matter of minutes" to get a battery changed, says Mr. Daly, whose company required all its hotels to upgrade to electronic locks three years ago.

Neglect isn't the only problem. Lock batteries can be knocked out by freezing temperatures. Indeed, most electronic locks are vulnerable to the elements. Saltwater corrodes them, humidity can short-circuit them

Please Turn to Page B6, Column 3

'Key' Cards Lock Out Hotel Guests

Continued From Page B1

and static electricity can wipe out their memory. "Anytime you expose a lock to weather, you're going to have a problem," says Mr. Wilder. Even indoor locks can be affected because key cards tend to pick up salt and sand, which can gum up a lock.

Human error also accounts for many problems with electronic locks. For example, a guest might not be able to get into a room because the front-desk clerk didn't correctly program the card.

Most alarming is when guests become prisoners in their rooms—raising the worst-case specters of heart attacks or fires. At best, lock-ins are a nuisance, as was the case recently for five teenage boys on a Bible retreat convened in a room at the Dallas/Fort Worth Airport Hilton. When they tried to leave the room, the door wouldn't open.

The door's electronic lock had malfunctioned but the teenagers "thought someone was playing a trick on them," says Wayne MacAffee, minister of students for the First Baptist Church of Oak Cliff, Texas. Mr. MacAffee waited outside the door for more than half an hour before hotel engineers pried it open with a crowbar.

The company that made the malfunctioning lock, Yale Security Inc. of Charlotte, N.C., has gotten out of the electronic-lock business altogether. It says that problems managing that part of its business prompted it to refocus on its core mechanical-lock lines.

The largest maker of hotel-door electronic locks is VingCard Inc. of Dallas, a unit of TrioVing in Norway. One of VingCard's systems had a glitch that in rare cases made doors impossible to open. Complaints about guests locked in their rooms were sent to the company from the Days Inn in Fargo, N.D., a Best Western in Gulf Shores, Ala., and a Hyatt Regency in Vancouver, British Columbia.

To date, there have been more than 50 guests locked in their rooms by the defective VingCard system—and any number of guests locked out—according to Paul Head, formerly VingCard's manager of quality control. With the product installed at more than 100,000 hotel rooms, Mr. Head says he was worried that many more lock-ins would take place and proposed to his superiors that the company fix the glitch. But he says he got nowhere. Next, he says, he wrote to executives of the parent company in Norway.

Mr. Head was fired not long after. In January, he sued the company for wrongful termination in Dallas County District Court.

VingCard declines to discuss the suit, which is pending. It calls the number of lock-ins "statistically insignificant" and says it responds aggressively whenever a problem occurs. It declines to discuss the matter further.

THE WALL STREET JOURNAL.

* * * FRIDAY, APRIL 12, 1996 **B1**

MARKETPLACE

Sports: *Hook, line and sinker—fishing bait that will lure you in* ***Page B7.***

The Home Front: *Finding the nation's most affordable housing market* ***Page B8.***

gets more difficult as the digital complexity increases for effects such as 3-D audio, yet the analog performance must still be "high fidelity."

AC '97 resolves this problem by splitting the codec function into two ICs with a standardized interface between them. This approach not only optimizes analog design, but also lets designers choose a digital IC from one vendor and an analog IC from another with assured connectivity.

AC '97 specifies a baseline function for the analog I/O, in a 7×7-mm, 48-pin device; it also lets you combine a 64-pin component with other functions. The digital controller can provide just basic functions or expand to 3-D sound, accelerators, multiplayer gaming, and synthesizers or digitally driven sound enhancements.

AC '97 allows the digital controller to be compatible with PCI, Universal Serial Bus, ISA, IEEE 1394, or other buses. Alternatively, you can incorporate the controller into a larger multifunction controller.

The two ICs communicate via a five-wire path, with clock, sync, input, output, and ground links. The baseline specification defines all interface and control registers and provides four line-level stereo inputs and two line-level mono inputs. It also defines support for 18- and 20-bit audio, four- or six-channel output, loudness and tone control, and other basic audio functions.

The five AC '97 specifiers expect to unveil the first devices to support the spec by this fall. Other IC vendors, such as Aztech Labs (Fremont, CA), Crystal Semiconductor (Austin, TX), ESS Technology Inc (Fremont, CA), and Oak Technology Inc (Sunnyvale, CA), also support the specification. The companies are offering the specification under a royalty-free reciprocal license basis through Intel.—by Bill Schweber

Intel Corp, Santa Clara, CA. (503) 264-0930; bill_piwonka@ccm. jf.intel.com; www.intel.com/pcsupp/platform/ac97/.

Circle No. 493

Software audio synthesizer supports four algorithms

Yet another vendor has developed a software-based audio synthesizer scheme that relies on the host to perform signal processing in lieu of a dedicated sound IC. The Cybersound software from Invision Interactive Inc, however, offers enhanced capabilities and reduces costs compared with competing products. Cybersound includes not only the FM- and wave-table-synthesis algorithms common on PC sound cards, but also the analog and physical-modeling synthesis algorithms usually found on synthesizers for professional musicians.

The choice of algorithms allows software developers and end users to choose the technique that best reproduces specific sound sources. For example, Invision claims that wave-table techniques deliver superior percussion sounds and that physical-modeling techniques more accurately reproduce wind instru-

Encryption lockout device provides security for less than $1

A new device from Exel Microelectronics provides a "challenge-and-response" protocol for authentication. In an electronic-key application (**Figure 1**), the XL107 SureLok die in the key receives power when you insert the key into the correct lock. The XL107 then alerts the lock host controller that the XL107 is present. The host, which has a corresponding XL107 programmed with an identical, secret 64-bit key, sends a 32-bit random number to the key device. The key-device XL107 then encrypts the 32-bit challenge using the 64-bit key, and the resulting 32-bit response returns to the host, which performs the same encryption. The host controller then compares the results for authentication.

The device needs no other components, because the host provides power. You can also use the XL107 to prevent unauthorized users from adding peripherals to any system, such as knockoff batteries to cellular phones or incompatible multiprocessor and video cards to workstations. The XL107 can hold as many as four 64-bit keys, providing access to four locks. The 64-bit keys are unreadable, thus guarding security. The XL107 is in production now and available in eight-pin plastic DIP and SOIC packages and as dice. The DIP costs $0.94 (1000).

—by Stephen Kempainen

Exel Microelectronics, San Jose, CA. (408) 432-0500, fax (408) 432-810, http://wwwexel.com. **Circle No. 494**

FIGURE 1

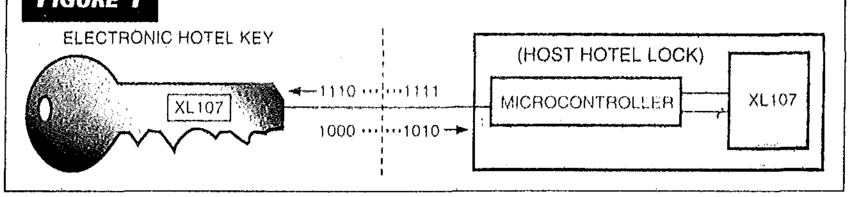

The XL107 SureLok die in the key receives power when you insert the key into the correct lock.

Editorial

Different game

BASED ON THE SIGNALS coming out of Washington and Tokyo over the past few weeks, it seems almost certain that the bilateral semiconductor trade agreement will be renewed in one form or another. A political consensus has already emerged supporting renewal, leaving Japanese and U.S. trade negotiators to the implementation details.

Since the 1991 U.S.-Japan Semiconductor Trade Arrangement is generally credited with quelling semiconductor-trade frictions between Japan and the United States, there may be a tendency this time around to assume that a renewed agreement will address the burning issues of the day. There's no doubt that great progress has been made on the semiconductor-trade front. But is the industry being lulled into a false sense of security?

Five years ago, the U.S. semiconductor industry was considered an industry "at risk," as the widely circulated "National Advisory Committee on Semiconductors" report put it at the time. Japan seemed invincible. The South Korean semiconductor dynamo had not yet begun to hum, and the semiconductor business was largely a high-volume-manufacturing game, in which the DRAM figured as king.

Five years later, Japan seems as concerned about the looming Korean presence in the world market as with guarding its home turf. Today, the industry's moves are dictated less by the commodity DRAM than by the commoditization of the personal computer and the rise of the multimedia/consumer-electronics market.

A new U.S.-Japan semiconductor trade pact is likely to be jockeyed into place by month's end, returning semiconductor-trade issues to the back burner. That will be a shame, since the current chip-trade debate virtually ignores the sea change in global electronics trade since the first pact was signed.

Yes, bilateral trade issues are important. But electronics trade has become a trillion-dollar global business increasingly threatened by multilateral disputes. Global economics and technology advances are conspiring to bring such issues as market access, dumping, pricing, silicon and software intellectual-property protection, and national and regional subsidies to the flash point.

Absent a global forum to discuss those issues, we're headed back to square one.

Richard Wallace

CROSSTALK

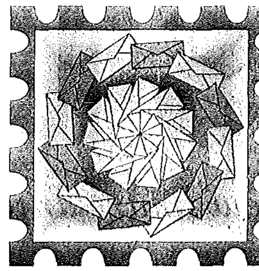

Smart card: who will seize the opportunity?

The editorial by Carol Fancher is right for the wrong reason (see "Executive Viewpoint," June 17, page 24). The reason that the United States lacks a realistic smart-card credit-card action plan is simple: the two bank credit-card associations (Visa and Mastercard) are service companies. They derive their revenues from their investment in networks and online authorization services. Each online authorization is paid for by the merchant. The fee is a 1.5- to 2- percent discount based on transaction value. Last year, that was $10 billion.

In 1987, Booz Allen performed an intensive study for Visa and Mastercard on the impact of smart-card credit cards. I have a copy of the report. It was never released to the association members, but they paid over $400,000 for the results, which stated that 86 percent of the online authorizations would be eliminated by smart-card credit-card activity. The result would also have *less* losses than the current magnetic-striped-card authorization system. The installed experience in France is a 90-percent reduction in the need for online authorizations to a central-site database.

What will motivate the associations to migrate? A catastrophic failure in the magnetic-striped-card solution would get attention. As the father of the magnetic-striped card, I don't believe that is likely. The other motivation would be a smart card-based solution that avoids the need for a dedicated network or online authorizations. That solution now exists. It is called Mondex. It has been accepted by major banks in the United Kingdom, Canada, Hong Kong, Australia, New Zealand and India.

The bottom line is that the smart-card credit card seems to offer 10 times the revenue of a conventional credit card. The real question is: Will bankers be smart enough to be the smart-card credit-card leaders? Last year, more than half of bank credit cards were not issued by banks. Will bankers give away the smart-card credit-card opportunity?

Jerome Svigals
Electronic Banking Consultant
Redwood City, Calif.

It's time we stopped ruminating on ATSC

There are not enough theatrical fog machines in existence to obfuscate the "interlaced" vs. "absolutely non-interlaced" issue as thoroughly as chairman Hundt and Bill Gates have (see June 17, page 128). So what if the highest-resolution mode (1,920 x 1,080) is interlaced. Not one month ago, the FCC allegedly gave the "green light" to the Grand Alliance ATSC standard platform; but since it stopped short of mandating it, we now must ruminate the issue anew.

Mr. Gates and Congress are butting in, and we have a serious problem. What good is a panel of experts to specify, design, construct, test, field-test and manufacture when non-technical personnel are going to shoot the entire project in the heart?

I will concede a preference for non-interlaced 60-frame/s television at the 484-line level, contrasted with NTSC, assuming *arguendo* images of similar signal-to-noise ratio and saturated color spatial resolution. However, at the exalted resolution of ATSC (1,920 x 1,080), the critical fusion frequency for a single pixel is much higher than 30 cps.

Why can't Microsoft, developer of the world's most bloated operating system, and Intel, developer of the world's strangest addressing architecture, hang with ATSC? This weekend, I purchased a Pentium 100 in a no-name main board with 16 Mbytes and all the toys (PCI slots, EDO DRAM, etc.) for $310. Silicon is free, folks. It doesn't take a few hundred thousand gates to make an embedded converter mapping engine for "interlaced to progressive." Sixteen Mbytes is large enough to hold one 2,048 x 2,048 x 8-bit RGB image with 4 Mbytes to spare.

One can only hope that the decision makers haven't been exposed to the various VGA-to-NTSC converters. Some are truly wretched, but home-video experience should not bear on an ATSC decision. The public deserves ATSC, and they're going to get warmed-over MPEG-1 and an eight-hour VHS at the rate we're going. ATSC in my lifetime . . . please?

York David Anthony
Field Manager
Concord, N.C.

Electronic Engineering
TIMES
A CMP Publication
(516) 562-5000. Fax: (516) 562-5326
eetimes@cmp.com
EET Interactive: http://techweb.cmp.com/eet

Publisher
Steve Weitzner sweitzner@cmp.com

Editor in Chief
Richard Wallace rwallace@cmp.com

Executive Editor, Special Reports
Nicolas Mokhoff nmokhoff@cmp.com
Executive Editor, EE Times
Tim Moran tmoran@cmp.com
Managing Editor, News
Alexander Wolfe awolfe@cmp.com

SECTION EDITORS
Robert Bellinger, The Profession
bbelling@cmp.com
Richard Goering, Design Feature
Brian Santo, EET-I, bsanto@cmp.com
Larry Lange, Associate Editor
llange@cmp.com
Chappell Brown, Technology
(508) 653-7826, chappellb@aol.com
Martin Gold, Product File
mgold@cmp.com
Brian Fuller, Business

DEPARTMENTS
Ron Wilson, Solid State
Ashok Bindra, Components
abindra@cmp.com
Rick Boyd-Merritt, Computers
rbmerrit@cmp.com
Stan Runyon, Test
6090658@mcimail.com

BUREAUS
San Mateo
Ron Wilson, Chief
(415) 525-4498, rwilson@cmp.com
Brian Fuller, News
(415) 525-4324, bfuller@cmp.com
Richard Goering, CAE, Design
(408) 335-3390, rgoering@cmp.com
Junko Yoshida, Consumer
(415) 525-4321, jyoshida@cmp.com
Craig Matsumoto, Business
cmatsumo@cmp.com
Washington, D.C.
George Leopold, (202) 383-4790
Fax: (202) 737-0980, gleopold@cmp.com
Margaret Ryan, Research
(516) 562-5629, mryan@cmp.com
Northeast
David Lieberman, Boards, Displays
(508) 597-2561, dlieberm@cmp.com
Chicago
Terry Costlow, Mass Storage, Components
(847) 657-3861, tcostlow@cmp.com
Colorado Springs
Loring Wirbel, Communications
(719) 481-3793, lwirbel@cmp.com
Flagstaff, Ariz.
Bernard C. Cole, Embedded Systems
(602) 773-7673, bccole@infomagic.com
Tokyo
David Lammers, Chief
8133-316-3666
Fax: 8133-316-0061, lambo@twics.com
Europe
Peter Clarke, London
44-171-254-7360
Fax: 44-171-254-7360, pclarke@lfields.demon.co.uk

COPY, ART & PRODUCTION
Managing Editor/Operations
Greg Lupion
Assistant Managing Editor/Operations
David Roman
Assistant Managing Editor/Copy
Tom Bartley
Senior Copy Editor
Diana Scheben
Copy Editor
Marilou Marciano
Art Director
Mira Ramji-Stein
Graphics Artist
Lynda Stratton
Senior Production Editor
Beverly Allen
Production Editors
Dale Anderson, Grace Waterhouse
Editorial Secretary
Joanna Raniori, eetimes@cmp.com

CONTRIBUTORS
R. Colin Johnson, Advanced Technologies
cognizer@teleport.com
Roland C. Wittenborg, Test & Measurement
Stan Baker, Programmable Logic

SUBSCRIPTION SERVICES
(847) 291-5215; Fax: (847)-291-4816,
Internet: EETOMEDA@aol.com

CMP OEM GROUP
Electronic Buyers' News
Electronic Engineering Times
OEM Magazine
Vice President/Group Publisher **Girish Mhatre**
Business Manager
Joanne Sulmonte

Printed in the USA
CMP Media, Inc.
600 Community Drive
Manhasset, N.Y. 11030
The full text of Electronic Engineering Times and all CMP Media Inc. is available via a variety of electronic services. For more information, call (516) 562-7405.

President/CEO **Michael S. Leeds**
President/Publishing **Kenneth D. Cron**
President/International **Daniel H. Leeds**
Executive Vice President/CIO **Grace Monahan**
Vice President/Chief Financial Officer **Joseph E. Sichler**
Vice President/Treasurer **Pearl Turner**
Vice President/General Counsel **Robert D. Marafioti**
Senior Vice President **Jeffrey L. Strief**
(Enterprise Computing, National Accounts)
Vice President/Group Publishers,
E. Drake Lundell (Personal Computing Group)
Girish Mhatre (OEM Group)
John Russell (Channel Group)
Vice President/Corporate Communications **Barbara Kerbel**
Vice President/Manufacturing **Stephen J. Grande**
Vice President/Customer Services **Georgette Ross**
Publishing Design Director **Joe McNeill**
Co-Chairpersons, Board of Directors
Gerard G. Leeds, Lilo J. Leeds

WALLET-SIZE READERS COULD BE THE NEXT GENERATION OF CREDIT CARDS

Smart cards lure component makers

BY TERRY COSTLOW

Atlanta — The expected boom in smart cards, which has attracted attention from many major semiconductor providers, is also prompting component and module makers to ratchet up their engineering and production operations. Several vendors at the CardTech/SecurTech conference here earlier this month have developed readers and other mechanisms for what's seen as the next generation of credit-card technology.

Smart cards pack a chip loaded with a specific amount of money, and the amount of a sale is deducted from memory during a transaction. Used as a cash replacement, smart cards reduce the potential for theft and shorten transaction time by eliminating change-making, proponents say.

The nascent nature of the smart-card market provides time for companies to develop advanced products before there's really any revenue to be made. Only a few trials are set for this year, and bankers and merchants won't make major decisions on deploying smart-card technology until they analyze the results. That means that even in 1997, the market for smart-card readers will be fairly small.

But not for long. Most of the cards that will be used in the United States—a number that some predict will be as high as 2.5 billion by the year 2000—will be read by machines that make contact with leads on the surface of the card. That represents a huge opening for those who make components for those machines. To get to that number of cards, smart-card readers will have to be common in retail outlets and transportation centers.

Each of those systems will need a connector, and many will need a mechanism for grabbing the card and positioning it. Connectors will come in many different styles, since there will be several types of readers.

Wallet-size readers

In banks, the readers are likely to be complex, heavy-duty mechanisms. Conversely, some companies are already making wallet-size readers that will tell users how much money is left in a card. Their contacts will be extremely simple, with size and weight more important than even reliability, since these are expected to be throwaway devices.

But the mainstay of the industry will be readers linked to point-of-sale terminals or housed inside vending machines. There, reliability and long lifetimes will be central features. Minimizing wear on the contacts will be critical, some designers say.

"We put the contacts on a carrier, and when the card is inserted [and] it comes into contact with the carrier, the carrier comes down a small ramp," said Paul Jacey, business development manager at Amphenol's Cardsystems and Components Operation (Noank, Conn.). "Moving the contacts onto the surface in that fashion minimizes friction, reducing wear on both the smart card and the contacts in the reader."

Smart-card readers are expected to crop up in stores and transportation centers.

Using such a mechanism has a dramatic impact on the lifetime of the contacts, Jacey explained. These landing-type contacts typically have lifetimes of about 500,000 cycles, while some of the edge-type contacts used in inexpensive readers have lifetimes as short as 10,000 insertion/removals, he said.

Unique problems

The systems with landing contacts, which are considered highly reliable, are relatively simple compared with the card-handling and reading equipment used in some banking applications. Many of those units are motorized, pulling the card completely inside the machine while it is in use.

"They always want to completely capture the card, for several reasons," said Rudy Cosler, new-business development marketing manager at Omron Electronics Inc. (Schaumburg, Ill.). "If you forget to take it out, they want to store it inside the bank so no one else can take it. If it's stolen, they don't want a thief to be able to pull it out and try using it again. Many banks also want to have strong rollers that flatten out bent cards. These machines have to work all the time, so everything in them has to be very durable."

Holding the card completely in place might work at an ATM, but it won't necessarily work in a vending machine on a freeway rest stop. A customer who stops at night in the middle of nowhere wants to be able to remove the card if the machine isn't operating, since the card might carry several dollars of unused value. That poses a dilemma for mechanism designers.

"We have to come up with techniques that keep the card available, but we have to make the system reliable," Jacey said. "If the card sticks out too far, users might flick it with their finger while they're thinking about what they buy. That type of vibration could impact the transaction, and it could damage the contacts over time. We have to be sure we consider that type of issue."

Another factor that has to be taken into account is what's called an "abnormal transaction termination." That happens when users remove the card in a hurry in order to void a transaction or so they can do something like catch a train.

"Our mechanism has to respond when they move the card at speeds up to 1 meter per second, which is very fast," Jacey said. "We want to shut off the switch that activates the contacts, and we have to do that in a

Continued on page 116

HP puts AlInGaP LEDs in flip-chip form

BY LORING WIRBEL

Palo Alto, Calif. — Hewlett-Packard Co.'s optoelectronics group has moved its aluminum-indium-gallium-phosphide (GaP) LED process to full production, providing what it says are much brighter yellow, amber and orange colors than were possible in earlier GaP materials.

This fall, the new SunPower llnGaP LED series will also ove from a standard surface-unt package to flip-chip pack-'s. Elimination of traditional ttach and wire bonding will 'de higher reliability for au-'ive and industrial applica-ccording to HP.

duct manager Dan said the path to flip-chip n far from straightfor-ing required four ma-d equipment break-First, metallization to be placed on both sides of the AlInGaP wafer to allow soldering on both sides of the die. Second, HP had to develop a proprietary pick-and-place SMT machine to move the die to its carrier, because equipment manufacturers could not offer systems with tight enough placement parameters.

HP also had to develop its own high-temperature soldering process to work with the new metallization on the die. Finally, the company had to develop a batch encapsulation process capable of whole-board encapsulation. The new encapsulation method carries the bonus of allowing lenses to be created through epoxy alone; that will reportedly allow HP to develop SunPower LEDs with high-focused-light patterns.

Was it worth all the effort? Kolody said that as manufacturers shift from through-hole to SMT packages, it makes sense to abandon wire bonding as soon as feasible. Wire-bond processes are more expensive and, because of breakage problems, less reliable. Direct-attach flip-chip methods can also offer lower package profiles, down to 0.6 mm. Kolody acknowledged that wire-bond SMT will survive in some sectors despite the emergence of flip-chip, but he predicted that the latter will dominate in automotive and telecommunication applications.

> The company expects flip-chip, which offers lower package profiles, to take off in automotive and telecom sectors.

In either package type, SunPower LEDs can offer luminosities of 65 mcd at 20 mA for amber and orange and 50 mcd for reddish orange. Luminous efficiency is 480 lumens/W for amber, 370 l/W for orange, and 197 l/W for reddish orange. Kolody said that in applications with arrays of LEDs or side-directed light pipes, such as in cellular-phone keypads, four AlInGaP LEDs will do the job of 12 GaP LEDs.

HP chose to start with its GaP process for its first move into flip-chip. HP is augmenting its initial test products in that process with the H670 family, measuring 2.0 x 1.25 x 1.1 mm and offered in orange, yellow, green and red, and the H690 family, measuring 1.6 x 0.8 x 0.6 mm and offered in the same colors.

The first SunPower devices are packaged in wire-bonded SMTs. The family includes the S670 series, measuring 2.0 x 1.25 x 0.8 mm; the S690 series, measuring 1.1 x 0.8 x 0.7 mm; and the right-angle-mounted S660 series, measuring 3.0 x 2.0 x 1.0 mm.

Unit prices in sample quantities are 10 cents each for flip-chip GaP LEDs and 20 cents each for SunPower AlInGaP LEDs.

The first SunPower flip-chip LEDs will debut this fall. Kolody said family members will include right-angle devices.

HP also is researching gallium-nitride devices and hopes to have high-reliability green and blue GaN LED prototypes ready by late 1997 or early 1998.

Call (800) 537-7715, ext. 1777

Reader Service No. 410

GRAHAM TROTT

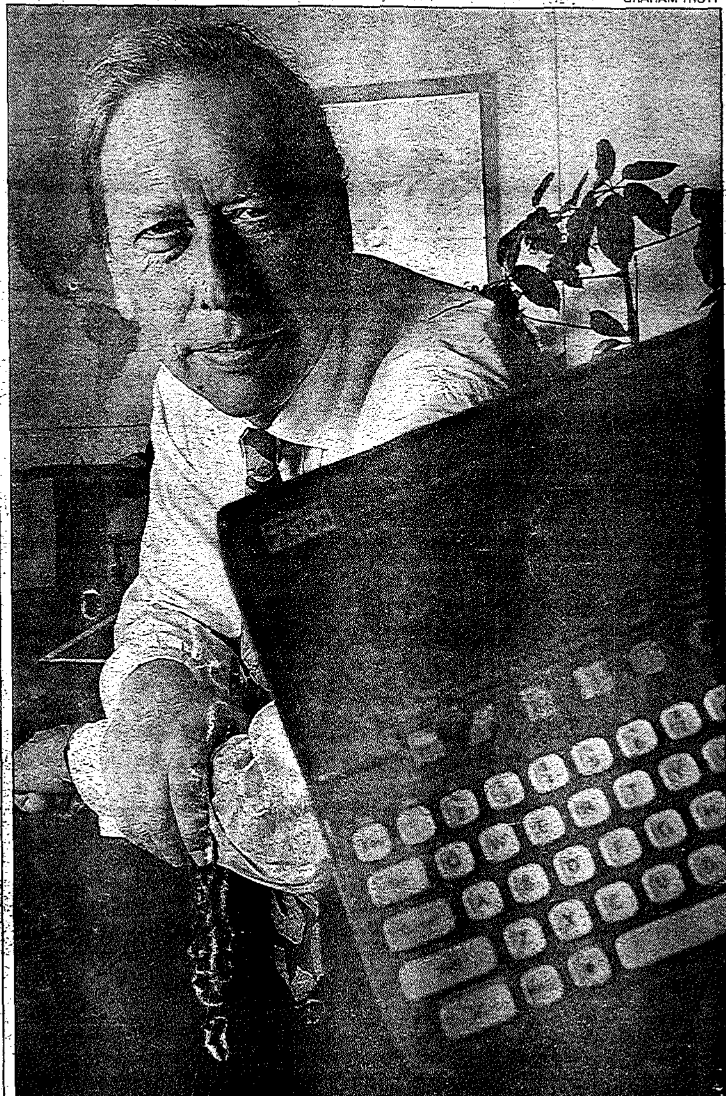

Potter: for Psion product development — not just sales — is the name of the game

Psion's mega-byte

It seems an unlikely match, so why is Psion bidding £234m for Alan Sugar's empire? Amanda Hall explains the technological potential

When news broke last week that Psion might bid for Amstrad, the market wondered whether David Potter, Psion's chairman, had lost his marbles.

Potter is an intellectual visionary in the fast-moving world of hand-held electronic gadgets, sitting on a share price that had climbed from 15p in 1991 to a high of 465p earlier this year. Why would he want to own Alan Sugar's Amstrad, where trading in the past two years has verged on the tragic and whose most memorable recent product launch was an electronic face-lifter? The group was described by one analyst last week as an "unresearchable company waiting to fall apart".

Not only was there little sign of product synergy but Potter and Sugar getting together? The flute playing former university lecturer who launched Psion in 1980 and the angry middle-aged man from Hackney who rose from selling car aerials in the late 1960s to make Amstrad a household name and transform the UK's personal computer market?

There had not been a more unlikely match since the Lords Hollick and Stevens merged MAI and United News and Media.

The idea was Sugar's. Two months ago he phoned Potter and called at Psion's north London headquarters to explain his proposal. Potter says his initial reaction was "sceptical", which, judging by the way he beamed and shifted in his seat when pressed on exactly what he meant by that, is a diplomatic way of saying he was gobsmacked at the suggestion.

"My first response was that this was off the wall. But when I examined it and brought in a non-executive to discuss it further, it seemed worth pursuing. We have a principle not to close off any idea automatically; if we only accepted the banal, the mundane, we'd be worse off for it."

Banal and mundane Sugar is certainly not.

At the heart of Sugar's pitch to Potter lies Dancall Telecom, a Danish mobile phone manufacturer which Amstrad bought from the receivers in 1993 for just £6·4m. Sugar wanted the business then for the same reason Potter wants it now: its GSM (Global Standard for Mobile Communications) know-how. Within 18 months of its sale to Amstrad, Dancall had launched a range of advanced cellular phones that thrust it on to the global GSM stage dominated by Motorola of the US, Nokia of Finland and Ericsson of Sweden.

But Potter does not want to sell phones. While sales of Psion's main product, the Series 3 palm-top personal computers, rose by 48 per cent last year and industry forecasts suggest the market will grow from the 1·5m in circulation now to 12m by 2002, product development — not just sales — is the name of the game.

Dancall's technology would take Psion into a brave new world of communications. It would allow it to bridge the gap between hand-held computers and cellular phones to produce a family of wireless devices that would allow you to sit on a beach, decide you want to make *Pride and Prejudice* your holiday reading and download it within seconds to your hand-held PC. He calls these devices "communicators".

"We're in a business that is changing fast because of the advances that are being made in semiconductors. Companies like ours can turn those advances to peoples' use but the barriers to entry into these new fields are substantial."

Sugar: monastic silence

The other part of Amstrad that lights up Potter's techno-commercial brain is DECT, Digital European Cordless Telephones, a technology that will allow every function performed by a mobile phone to be performed by a device no bigger than a credit card. "DECT phones have already started being manufactured in the past few months," he says. "We won't need clumsy phones with wires but will be able to walk around with a tiny device in our top pockets."

Unfortunately for Potter, getting his hands on this technology means having to buy other bits of Amstrad he could do without. One is ACE, the loss-making remains of Amstrad's consumer electronics business which this week is expected to be merged with Betacom in an effort to rationalise it and return it to profit.

The other is Viglen, which sells £100m of personal computers direct to consumers. The good news about Viglen is that it makes money: it is growing at about 20 per cent a year, has profit margins of 10 per cent and a "huge return on capital," Potter says. "We think we'd like to hold on to it at the present."

Potter's 200p a share offer values Amstrad at £234m, bang in line with a recent sum-of-the-parts valuation by its broker, James Capel. This sounds a lot for Psion, which is itself only capitalised at £241m, but the price is substantially lower once you take into account Amstrad's net cash, which Capel estimates at £55m.

For Sugar, who maintained a monastic silence all week, the deal will mean an extra £80m for his 36 per cent stake in the company he started in 1968 and took public in 1980. Over the past 16 years he has seen its share price rise from a few pence, to a mid-1980s high of over 1050p. Today it is 191p.

For Amstrad and its flamboyant founder, it is hard to see Psion as anything other than a way out.

One electronics analyst said: "Sugar is a man in need of an exit. For some time he's been saying all he wants is an office and a budget of about £2m to £5m a year to be able to come up with ideas. He's nearly 50, he's got more than enough money in the bank, he's in football at a time when it offers considerable commercial potential and Amstrad has come to the end of the road."

Sugar is unlikely to get a £2m-a-year ideas budget from Potter. They have agreed he will stay on as a consultant to the enlarged group provided the deal goes ahead, although it is hard to see even this arrangement lasting much longer than the bedding-down period.

Due diligence is under way and likely to take at least a further three weeks. Observers point out that this is by no means a done deal and say Potter may have to up his price depending on the outcome of two legal actions by Amstrad against computer disk-drive makers.

If the deal goes through, the Amstrad name will disappear and with it one of the most remarkable entrepreneurial success stories of 1980s corporate Britain. Potter has the task of leaving his mark on the present decade, without suffering the ignominious fall from grace that has soured Sugar.

Augustus bows to the | Rock cuts the Libyan knot

YOU. THE FIRST LOCK OF THE NEXT CENTURY... AND YOU ARE THE KEY

U.S. AND FOREIGN PATENTS ISSUED AND PENDING

770 971 4344

INNERKEY BY INTELOCK

77 GIBRALTAR DR., P.O. BOX 9018, PLEASANTON, CA 94566 USA 510.225.0300

PART NUMBER 15-085 REV 2

IS THE KEY TO THE FUTURE

NO KEY AT ALL

INNERKEY BRINGS YOU THE KEY YOU CAN'T LOSE – A SIMPLE PERSONAL DIGITAL CODE LOCKED SAFELY IN YOUR HEAD

If you've ever had the frustrating feeling that the traditional key was designed to be lost (and who hasn't?), InteLock's revolutionary electronic lock and deadbolt offer dependable, tamper-proof, digital technology to free you of the losable key – forever!

With a unique personal digital code allowing easy access to you and your family – but an impenetrable barrier to others – you can stop hiding keys outside, fumbling for keys in the dark, or worrying that your kids may be locked out while you're still miles away.

WHERE TO USE INNERKEY DIGITAL LOCKS, DIGITAL DEADBOLTS & RESPONSE DEADBOLTS

	interior doors	exterior back, side & garage doors	exterior front doors	office and commercial
Digital Lock	•	•		•
Digital Deadbolt		•	•	•
Digital Lock with Response Deadbolt		•	•	•

WHAT INNERKEY OWNERS SAY:

"It's the best purchase we've made all year! Now the children can't lock themselves out."
— Warminster, PA

"I'm doing backflips down my hallway."
— Knoxville, TN

"It's the answer to my prayers. What this product does – it gives me peace of mind. No more lost keys or lock outs! Yea! (And I installed it all by myself!)"
— Tulsa, OK

InnerKey: At Last, an Elegant Solution to a 4,000 Year Old Problem... The Lost Key

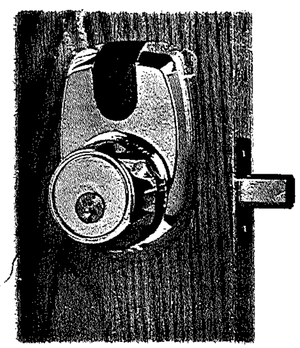

EXTERIOR

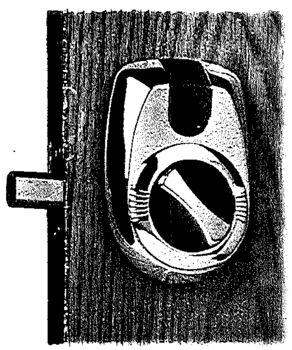

INTERIOR

With InnerKey, the anxiety of missing keys is ancient history. Interactive electronics and a personal entry code mean all you have to remember is a 3 or 4 digit code – not where you left the key.

CODE ENTRY
Simply turn code ring for deadbolt or knob for lock, to the right and left (as you would a combination lock), and then open door. 10,000 possible personal and alternate combinations using any 3 or 4 digits.

ULTRA BRIGHT LED READOUT
is visible day or night. Displays status of alternate code.

BUILT-IN PATENTED LOCK ALERT® TAMPER ALARM
sounds inside and outside. Activates for 10 seconds if lock is tampered with.

WIRELESS INFRA RED
eliminates wiring between lock and deadbolt (up to 18").

BATTERIES ARE INCLUDED WITH EACH INNERKEY PRODUCT

InnerKey Digital Deadbolt

Replaces any conventional deadbolt and can be used with your existing door hardware.

deadbolt 129

Only - 59.25 + deadbolt 149

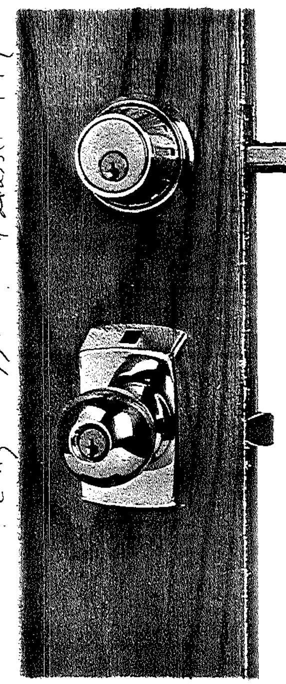

EXTERIOR

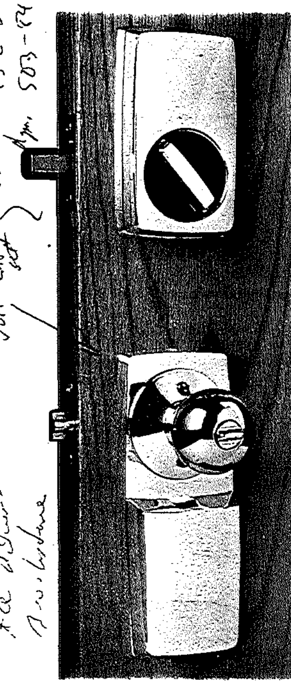

INTERIOR

Factory

Home Depot - Upper (st. pete)

Just entry set

452-589

503-744

Brass - w deadbolt 503-780

452-619

classic style

InnerKey Digital Lock & Response Deadbolt

Replaces any lock or lock and deadbolt set. Available in six knob and finish combinations.

2 years
3 years
"L" 3 month low battery alert
Normal Battery Life: 3 Years +

WILL I KNOW WHEN TO CHANGE THE BATTERIES?
YES. *InnerKey continuously checks battery power & alerts you 3 months in advance to replace batteries*

WILL INNERKEY WORK IN ALL WEATHER CONDITIONS?
RAIN HEAT FREEZING (-25°F)
YES. *InnerKey is designed to withstand the elements.*

IS INNERKEY EASY TO INSTALL?
YES. *InnerKey installs like any conventional lock. Usually in minutes. You don't need an engineering degree – just a screwdriver.*

IS INNERKEY RUGGED AND RELIABLE?
YES. *InnerKey is designed and manufactured to the highest ANSI standards for heavy-duty residential and medium-duty commercial locks. InnerKey comes with a one-year limited warranty.*

CAN I USE A KEY?
SURE. *InnerKey includes a mechanical key option. But if you're like most people, you will never use it.*

HOW CAN I FIND OUT MORE?
SIMPLE. *InteLock has a toll-free number to assist you with product or installation questions. Just call 1-800-562-5875 to reach one of our helpful customer representatives.*

Inventor thinks his gun lock is on target

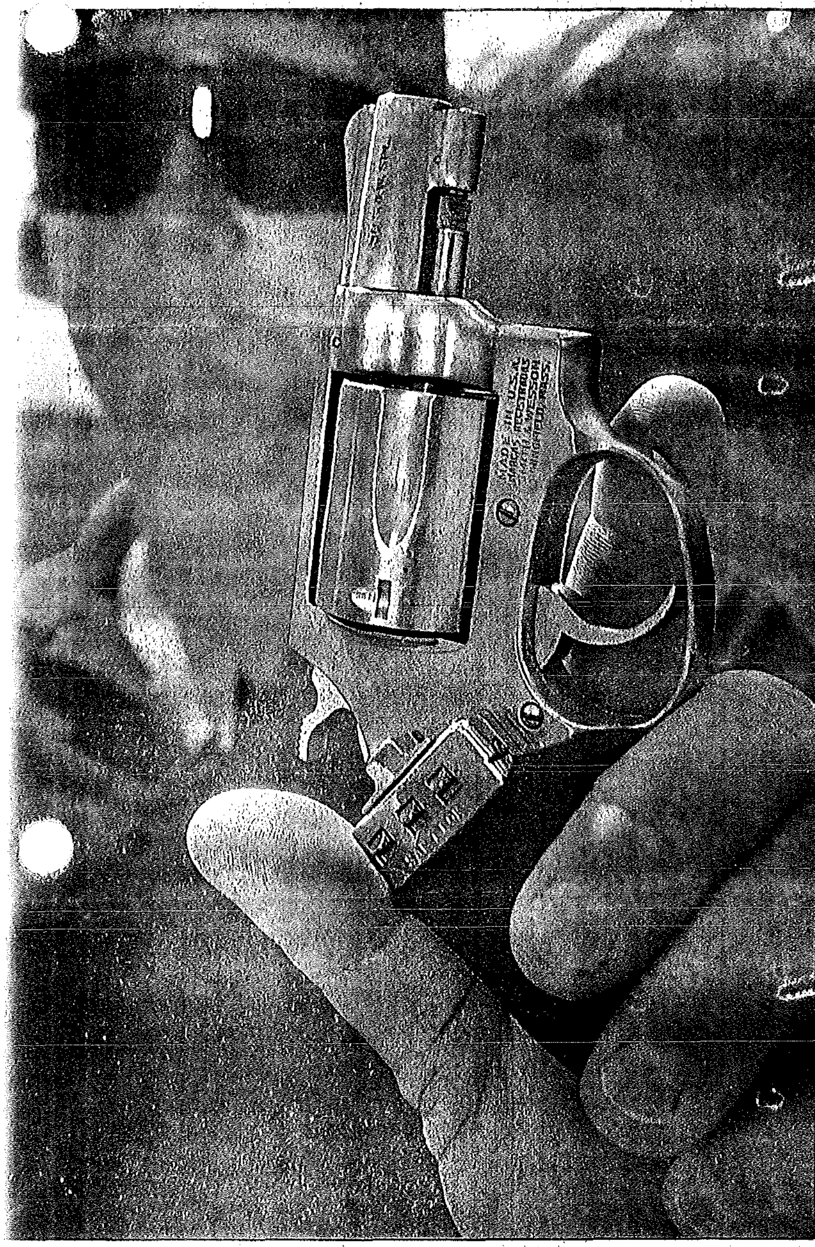

ROBERT BURKE/Tribune photo

“If you don't know how to get the thing unlocked, it's safe. And it doesn't at all affect the firing of the weapon.”

— Sgt. Bobby Jackson, range master Hillsborough County Sheriff's Office

By PAULO LIMA
Tribune Staff Writer

TAMPA — In a typical week, nine children will die from accidental shootings in America.

In 1994, a boon year for gun sales, companies made more than 2½ million handguns in this country and nearly a million more were imported. Many were sold to honest citizens hoping to shore up their defenses against criminals.

Yet those who choose to bring guns into their homes face a potentially deadly dilemma: How do you protect possessions and loved ones while keeping the weapons away from curious youngsters.

Frank Brooks thinks he has devised a way to do both.

The 61-year-old West Palm Beach businessman is the inventor of a product called Saf-T-Lok, a combination lock mounted into the grip of a pistol to prevent the gun from firing unless the holder punches in the correct code.

A series of three ratchets allow the owner to click the right combination in a matter of seconds with a few flicks of the thumb. And because no numbers appear on the lock, there is less chance of an unwanted party stumbling onto the right combination.

“I look at firearms as an insurance policy,” Brooks said. “Being the father of four grown children, I thought I was done having to worry about my kids getting hurt with guns. Then along came the grandchildren.”

Brooks, who runs an answering service on Florida's east coast, said he got the idea for the lock in 1989 while driving home from work one day. He glanced over at his briefcase, secured with a three-digit combination lock, and decided to get started.

After seven years and hundreds of conversations with gun experts, he finally has begun producing the steel contraptions he believes can make a handgun “child-proof.”

While looking for a company to market his product, he met Bob Gilbert, president of RGB Computer & Video, a West Palm Beach company that sells video editing systems. Gilbert was shopping for a new product following a weak 1995 for RGB in which it did $354,000 in sales.

The marriage became official when Saf-T-Lok merged with RGB in February and the first locks were already being produced in March.

The lock's tiny metal components are produced by Dynacast, a die-casting company in Spartansburg, S.C. The pieces are then assembled in an Orlando factory owned by Dayron, a division of Tampa-based D.S.E. Inc. The company, which specializes in mechanical assembly, has four plants and 190 employees statewide, said Steve Vallari, vice president of finance.

Brooks also pitches his lock as a theft deterrent. Once it's installed, it can be removed only by someone who knows the combination.

“It would kind of tough for a thief to take a gun to the pawn shop, because no pawn shop owner would be stupid enough to buy a gun that doesn't work,” Brooks said.

Saf-T-Lok is the latest in a line of gadgets aimed at lessening the danger of keeping guns

See INVENTOR, Page 8

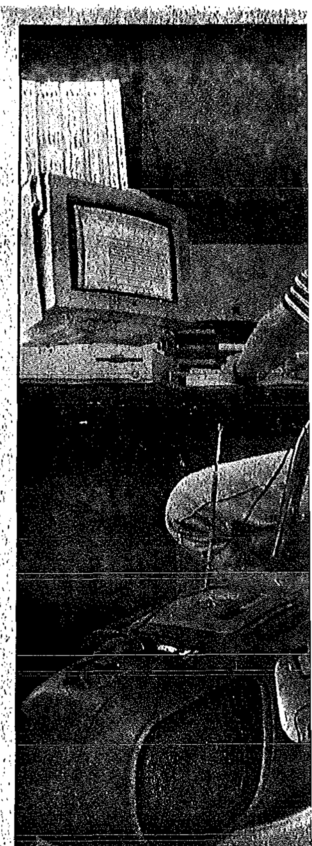

Mike Lear, a copy writer at adv... Inc. in Tampa, listens to music while he works at his computer

Office headpho... volume of work,

A Reuters Report

NEW YORK — Listening to your favorite music on your personal stereo headset may “dramatically” increase your productivity at work, a new study suggests.

It might also blot out unwanted office chatter or harsh noises from the factory floor, reduce fatigue and make you feel more relaxed.

The downside, new research indicates, is that “headset users may have difficulty hearing alarms, verbal warnings or instructions, and those who listen to music at high levels may expe-

Company exec fired for alleged sexual harassment, emb

An Associated Press Report

Stock	Close	Chg.
Astra	44⅛	+⅝

WESTBORO, Mass. — The chief executive of the pharmaceutical company Astra USA was fired after being accused of replacing older women with young beauties, pressuring female employees to have sex and embezzling $2 million.

AB of Sweden, Astra USA's parent, announced Wednesday that it had ousted Bildman, head of U.S. operations, after investigators confirmed misconduct and found evidence of embezzlement. Astra also fired a second executive, and two others resigned.

The company is the creator of Prilosec, an ulcer medicine that is the world's second-best selling drug.

“This is the end of an unfortunate and distasteful chapter in the history of Astra USA,” said C.G. Johansson, an Astra AB vice president who headed the investigation. “Our company has been appalled and disappointed with what we have discovered.”

But Astra board member Lars Ramqvist was quoted in the July-August edition of the Swedish monthly magazine Maanadens Affaerer as saying: “Of course it's not good with sex scandals, but in the U.S. this has helped us get out Astra's name without having to pay expensive advertising fees.”

Bildman's attorney, Roderick MacLeish, said his client is a victim of “cowardly and disloyal actions by the Swedish parent company” and “scurrilous and untrue allegations brought by disgruntled former employees.”

Johansson said there was evidence that Bildman had embezzled about $2 million for personal expenses, including vacations and renovations to three houses.

The company's investigating committee also found evidence of what it called “inappropriate behavior” by Bildman and other executives at company functions. Astra AB did not elaborate.

However, a federal lawsuit filed by six former employees last month alleged that Astra executives created “an organized pattern of sexual harassment ... in order to satisfy their personal desires.”

The lawsuit also alleged that within a year after Bildman's arrival at Astra, female staffers over 40, or those married with children, began to be replaced by “stunningly attractive” single young women.

According to the complaint, two senior vice presidents, Edward Aarons and George

Roadman ... cants bas... with the ... one at th...

Roadm... and sales... sion, was... stitutiona... company...

Astra ... fire Bildr... Anders L... who Joha... eties but ... signed.

more efficient in terms of costs per GHz as well.

Elliott says the transistors could be in production in a few years, if the cash can be raised to build a fabrication plant. The Defence Research Agency is proscribed from manufacturing, so Elliott is actively seeking a partner to commercialize the devices.

He says that in principle, an existing GaAs foundry could be converted to work with InSb. He expects such a venture to begin with discrete devices for use in applications such as low-noise front-end receivers for satellite receivers, mobile telephones, or wireless local-area network transceivers. Small analog integrated circuits for millimeter microwave applications or for more advanced mobile telephones will become practical in the medium term. In the longer term, he has high expectations that the devices will find their way into very-low-power computing applications. "The technology should fit well into the digital market because as a low-energy switching device, it has extreme potential for very-fast, very-low-voltage logic circuits and a huge potential for computing," says Elliott.

In the meantime, infrared emitters and detectors made from both InSb and HgCdTe are closer to commercialization. Negotiations are underway with a consortium of sensor instrumentation specialists led by Edinburgh Sensors Ltd., Livingstone, Scotland, to set up a pilot production line and to make prototype gas-detector instruments.

The plan is to make a range of integrated emitters and detectors that can be used to sense the presence of automobile exhaust gases such as carbon monoxide and nitrous oxide. Terry Christmas, managing director of Edinburgh Sensors, says that each gas has a unique absorption band that will block infrared radiation at specific wavelengths. By measuring the reduction in power of an infrared beam at the appropriate frequency as it is reflected through a measurement chamber, the presence of a particular gas can be registered and the gas identified.

Elliott says that for this application, InSb can operate at wavelengths of 3 µm to 6 µm, while HgCdTe takes over up to 12 µm. "Our devices are the first to work at these wavelengths without the need for cooling," he claims.

To date, the team has made LEDs that run at wavelengths to 10 µm without cooling. Outputs are limited to about 15 mW/cm^2. Recently, the group made its first InSb laser diode. It must be cooled to about 90K, but Elliott is convinced that it can be improved to run at room temperature. It works at 5.1 µm.

For more information contact Elliott at the Novel Devices Section, Defence Research Agency, St. Andrews Rd., Great Malvern, Worcestershire, WR14 3PS United Kingdom. Telephone: +44 (0)1684 894820. E-mail tashley@taz.dra.hmg.gb.

PETER FLETCHER

PROTOTYPE PERSONAL-AREA NETWORK MAKES POSSIBLE INTRA-BODY COMMMUNICATIONS VIA PICOAMPERE SIGNALS

Did you ever think you'd be exchanging electronic business cards just by shaking hands? Sounds like a science-fiction ploy, doesn't it? Well, it's not. A development from IBM's Almaden Research Center, San Jose, Calif., may allow "wearable" electronic devices to exchange data by capactively coupling modulated picoamp currents through the body. Research sponsored by Hewlett-Packard and the Festo Didactic Corp., and conducted at the Physics and Media Group of the MIT Media Lab, helped develop the emerging technology of a "personal area network." If successful, cellular phones, PDAs, and pagers will be just some of the devices capable of seamlessly exchanging data through an invisible human interface.

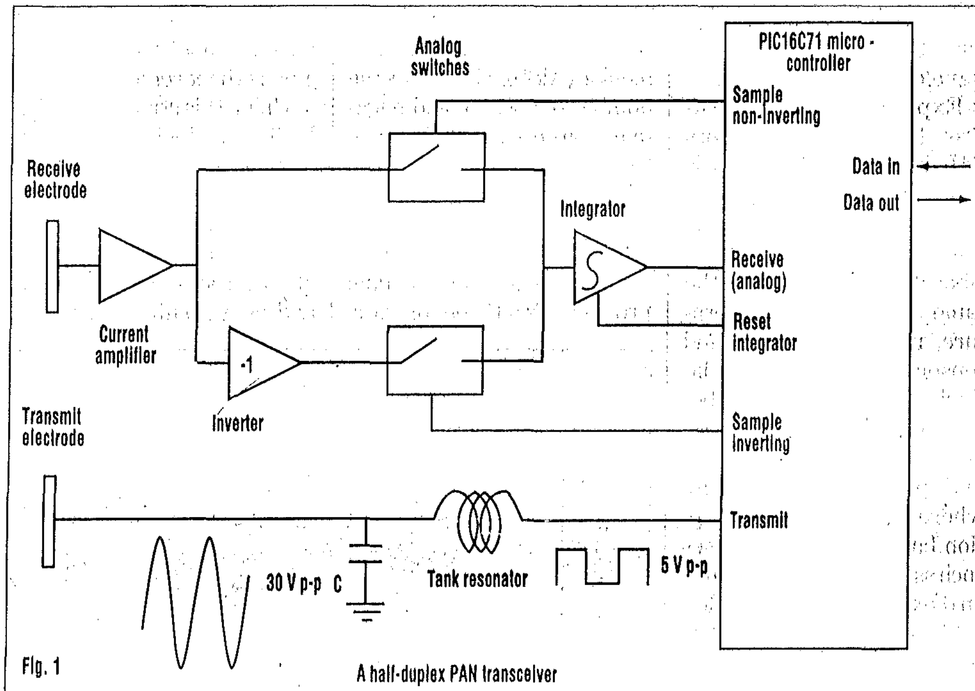

Fig. 1 A half-duplex PAN transceiver

According to the research, which was presented at the Fourth Annual Wireless Symposium, Feb. 12-16, at the Santa Clara Convention Center, Santa Clara, Calif. (sponsored by *Electronic Design's* sister publication *Microwaves & RF Magazine*) networking wearable devices reduces I/O redundancies and allows new conveniences and services. A low-frequency carrier (under 1 MHz) is used so no energy is propagated, minimizing remote eavesdropping and interference. The presentation was made by IBM's Thomas G. Zimmerman in a paper entitled "Personal-area networks (PANs): Near-field intra-body communication."

Cellular phones and laptop computers have neen liberating technologies; they've freed people typically confined to offices, and provided mobile workers instant access to customers, vendors, and databases. Nevertheless, their inability to exchange data limited their usefulness. A mobile computer user should not have to carry a cell phone *and* a cellular LAN; phone numbers retrieved from a PDA should not have to be manually typed into a cell phone; a message watch should not have to be programmed by four micro-switches when a full-sized QWERTY keyboard is nearby. Networking these devices would alleviate these inconveniences and allow for new features—a watch is too small to contain a multimedia computer, but is large enough to contain a microphone, display, and camera. An I/O-rich watch could be networked to a fast, powerful computer located in a waist pack or pocket.

In the IBM development, PAN devices communicate by electrostatically coupling picoamp currents through the body. The PAN uses the salty, blood-filled body as a "wet wire" to conduct the modulated currents. The body internally has a resistance of about 200 Ω from head to toe. Therefore, a low-frequency carrier (100 kHz to 1 MHz) is used to capacitively couple the direct (resistive) contact with the skin.

Near-field coupling is superior to infrared and far-field methods for PAN applications. Infrared coupling requires line-of-sight, which is not practical for devices located inside wallets, purses, and pockets. Far-field (radio) propagation falls off with distance squared (isotropic transmitter), while near-field propagation falls off with distance cubed, making near-field coupling less susceptible to eavesdropping and interference. Far-field transmission is subject to regulations and licensing that vary from country to country. Near-field communication avoids these complications. The PAN prototype, which is slightly larger and thicker than a credit card, has a field strength of 350 pV/m at 300 m, 86 dB below the allowable field strength specified by the FCC.

Near-field communication may be more energy efficient than far-field because power consumption generally increases with frequency. Any increase in the carrier frequency above that required to contain the information represents wasted energy. The PAN prototype operates at 330 kHz and 30 V with 10 pF of electrode capacitance, and consumes 1.5 mW to charge and discharge the electrode capacitance. A majority of this energy is conserved (recycled) by using a resonant LC tank circuit.

Near-field communication lends itself to greater integration than far-field does because the carrier can be generated directly by an inexpensive microcontroller. In fact, the PAN demonstration transceiver uses an inexpensive Microchip Technology PIC16C71 microcontroller that costs just $3.50 each in large quantities *(Fig. 1)*.

As envisioned by the paper's author, a PAN transmitter communicating with a PAN receiver uses the Earth's ground as a return path for the signal *(Fig. 2)*. The Earth and the human body have a pair of transmitting and receiving electrodes, each, labeled t_e, r_e, t_b, and r_b, respectively. These electrodes can be placed in various locations on the body by incorporating them into head-mounted displays, shoes, watches, credit cards, etc.

Shirt-pocket devices can serve as ID badges. Wrist watches are a natural location for a display, microphone, camera, and speak-er. Waist pouches can carry a PDA, cellular phone, keypad, or other large devices. PAN medical sensors can provide EKG, blood-pressure, and respiratory-rate monitoring. Pants pockets are a natural location for wallet-based devices. Shoe inserts can be self-powered, capturing energy from walking, and provide a data link to remote PAN devices located in the environment, such as workstations and floor transponders that detect the location and identity of people.

The PAN transmitter capacitively couples a modulated picoamp displacement current through the human body to the receiver. The return path is provided by the "Earth ground," which includes all conductors and dielectrics in close proximity to the PAN devices. The Earth ground needs to be electrically isolated from the body to prevent shorting of the communication circuit. In one experiment, standing barefoot reduced communication between wrist-mounted devices 12 dB.

The PAN transmitter and receiver can be modeled as an oscillator and a differential amplifier, respectively *(Fig. 3)*. The basic principle of a PAN communication channel is to break the impedance symmetry among the transmitter electrodes t_b and t_e, and the receiver electrodes r_b and r_e. The intra-electrode impedance of the devices are ignored since the oscillator is a load on an ideal voltage source and the differential amplifier is modeled as an open circuit. The four remaining impedances are labeled A, B, C, and D.

The circuit is rearranged to show that PAN-device communication works by breaking the impedance symmetry between the four electrodes. The circuit is a Wheatstone bridge where any imbalance of the relationship A/B = C/D causes a potential across the receiver. Because the ratios must be exactly equal to null the circuit, and body-based PAN devices are constantly

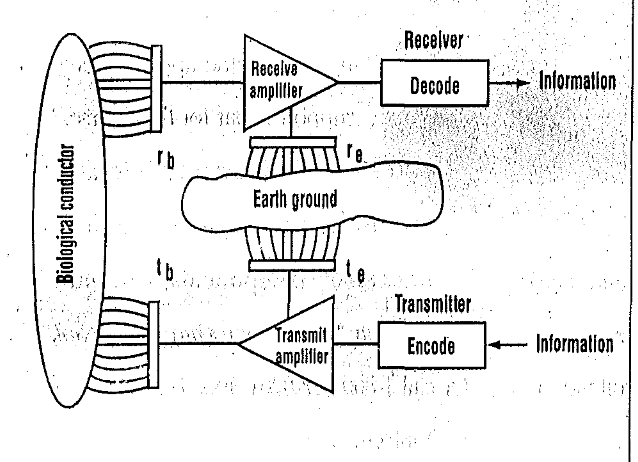

Fig. 2 PAN communications are achieved by modulating an electric field which capacitively couples to the human body.

... Fast Eth-
...r for the
Company
much of
...ne from
...lems up-

...way
...t is
...atures.
...net con-
...e Magic
...ated by
...ard Co.
...mption
the net-
...ely turn
need to
so net-
...ad soft-

...p mode
...eeping
active.
the PC
...ger ac-
...r said.

...of design problem with ASICs may not involve architectural flaws, subtle timing problems or arcane signal-integrity issues. It is that a signal comes out of the device with the wrong polarity or at the wrong time. That leads to a little halo of logic chips or PALs around the ASIC to patch up the interface problems that surfaced at board-integration time.

Unfortunately, the logic chips tend to be big, power-hungry, and largely underutilized. It is a shame to lay a 22V10 PAL on the board because you need a couple of NAND gates.

Step backward

Texas Instruments Inc. is offering an alternative. In a massive step backward for integration, the company is selling single gates in five-pin small-outline transistor (SOT) packages.

That gives the engineer a single gate in a roughly 3-mm x 5-mm package for patching ... logic family. Initial offerings will include two-input NAND, AND, OR and XOR gates, buffered and unbuffered inverters and a Schmitt-trigger inverter. The devices carry SN74AHCT1G nomenclature for TTL I/O or SN74AHC1G nomenclature for CMOS I/O.

Available now, the parts cost $0.28 each in 3,000-unit lots.

Call (800) 477-8924, ext. 4500

Reader Service No. 405

Chip uses encryption for security

San Jose, Calif. — A new eight-pin small-outline chip from Exel Microelectronics Inc. promises a new level of security for a variety of intruder-repelling situations—from foreign accessories plugged into electronic equipment to burglars trying to enter hotel rooms.

Essentially, the XL107 is a 32-bit encryption coprocessor. It is designed to be used in a challenge-response technique. For instance, when you plug the keycard into your hotel-room door, a microcontroller in the door would challenge the 107 via a three-wire interface. When the 107 senses power on the Vcc and ground pins of the three-wire port, it resets and sends an acknowledgment.

Random string

The host would then send the challenge: a randomly generated 32-bit string. The 107 would encrypt the string using its proprietary non-linear algorithm and a stored key. The encrypted response goes back over the three-wire interface, where the host can compare it to the expected result. Most likely, the host calculates the expected result by consulting its own 107 chip.

The 107 has room in E^2PROM for four 64-bit keys. The part draws its 1-mA typical operating current from the three-wire interface, which may operate any between 3 V and 6 V (Vcc). The chip is available now in an eight-pin PDIP or SOIC at 94 and 97 cents each, respectively, in lots of 1,000. Bare dice are also available.

Call (800) 853-5886

Reader Service No. 406

channel. Why? Because ... invisible: Hardware vendors and resellers will woo you with ads for network solutions, part of which will be the latest and greatest document-management/groupware/communications systems.

SURPRISE: MICROSOFT HAD IT FIRST

Microsoft not only saw the initial writing on the wall, it made the first specific move to tell corporate consumers that

number of ... packages you need to buy. And smaller ... as Commerce Corp., OneSource, and OpenText are close behind, seeing an opportunity to bring to market a holistic mix of data-mining features, intranet applications, and computer-telephony development tools.

This trend means that document management (including workflow management with versioning, tracking, and

million Notes users, ... intranets and the Internet and rem...

The direct channel is definitely a buyer... it comes to corporate software—for all the functionality that network hardware can sustain, for little more than the price of that hardware alone. ▼

Cash In Your Chips

Smart Cards to Put Digital Dollars in Consumer Wallets

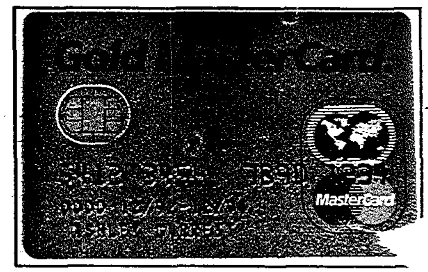

If a consortium organized by Visa, MasterCard, and their member banks gets its way, using an automated teller machine (ATM) to get cash may become passé. Instead, over the next two years, the financial companies hope to promote the mainstream commercial use of smart cards.

Smart cards, tried in pilot programs around the world in recent years, are ATM cards with built-in silicon chips capable of storing a digital reserve of up to $100 cash, along with other financial and personal data.

"There's only so much information you can store on [a conventional card's] magnetic stripe—with ATM cards, you're limited to certain financial transactions," explains Citibank spokesperson Shelley Wolfe, adding that a consumer could use the same smart card to arrange a ticketless airline flight and buy merchandise from a vending machine.

"The past two years have seen unprecedented partnering in a smart-card infrastructure," says Phoebe Simpson, a financial analyst with the market-research firm Jupiter Communications. Two U.S. projects of note are a Citibank/Chase Manhattan trial on Manhattan's Upper West Side and a Visa-sponsored trial at the Summer Olympics. "The Olympics is a significant project because it pulls in so many players," she says. "The merchants involved are large ones with franchises across the country."

Two kinds of smart cards will circulate. Disposable cards will be thrown away when emptied, while rechargeable or reloadable cards will likely involve adding a chip to existing ATM and credit cards. For the near future, smart cards will be usable at participating stores, and in retrofitted ATM machines and vending machines. After that, says MasterCard International representative Nancy Elders, wireless and PC Card-based card readers and chargers are a possibility.

Like cash, smart cards are weak on security. Though a personal identification number will protect data stored on the chip, losing a smart card will be like losing cash.

"Just because it's on a plastic card doesn't mean it's more advanced," Simpson says. "It's still money."

—David A. Harvey

Frequency-domain DSP: an enabling technology

MICHAEL E FLEMING, BUTTERFLY DSP INC

Most of today's DSP µPs, which are offspring of standard µPs, operate in the time domain. However, frequency-domain operation provides benefits for a whole spectrum of applications.

Ever-increasing levels of microchip integration have brought on major shifts in the electronics industry. The shift from discrete transistor amplifiers to operational amplifiers created a spectrum of practically perfect signal buffers and conditioners. The shift from discrete random logic to field-programmable logic increased the capability of the typical logic board many times over.

With the advent of multimillion-transistor ICs and complete systems on silicon, now is the time to shift real-time DSP from the current time-domain solutions to frequency-domain solutions. In the frequency domain, signal processing takes new dimensions of affordable, intelligent signal and image processing.

Time vs frequency domain

The vast majority of time-domain signal processing has an equivalent solution in the frequency domain. This inherent duality gives rise to a set of operations in the frequency domain, such as digital filtering and correlation. These operations surpass their time-domain equivalents in resolution and processing rates and enable utilization of past and present information and patterns.

If you look at music on an oscilloscope in the time domain, what you see is chaotic (**Figure 1a**). You can't tell what the music is doing from one moment to the next without the aid of your ear, which is doing its own sort of processing for pattern recognition. However, if you transform the music signal to the frequency domain, bins of discrete frequencies represent each frame of data (**Figure 1b**).

The frequency bins exhibit a smooth vertical change in amplitude as the music changes in tone and energy. These changes contain the information, or beauty, of the music. If the energy exists in all of the bins and changes rapidly, then the energy is probably noise. If the energy exists in only a few bins and does not change much, then this energy is a constant tone or single note that is very recognizable by its position in the frequency domain. This simple transformation, from the time-domain representation of a signal to the frequency domain, is extremely powerful. What was incoherent is now coher-

FIGURE 1

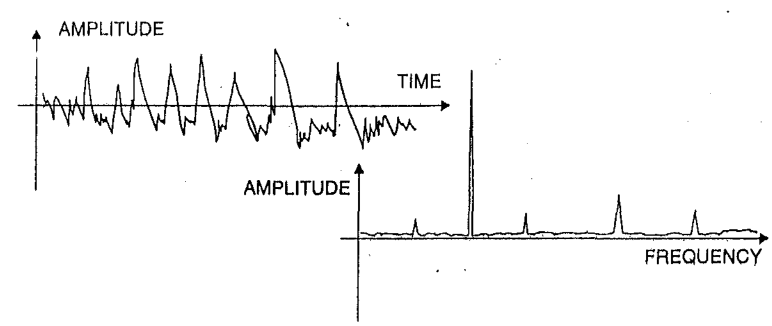

A time-domain view of music looks chaotic (a). In the frequency-domain, however, you can discern distinct frequency bins, the amplitude of which depends on the tone and energy of the music (b).

TECHNOLOGY NEWSLETTER

MCM-Substrate Technology Said To Boost Performance

Qualifications have been completed for a new multichip-module (MCM) substrate technology based on copper and benzocyclobutene (BCB). The technology was developed by MicroModule Systems (MMS), Cupertino, Calif., in partnership with the Dow Chemical Co., Midland, Mich. Dow is the maker of the BCB thin-film dielectric material, which is marketed under the name Cyclotene. The qualification vehicle for the technology was MMS's TwinStar dual-Pentium-processor module, designed for desktop multiprocessing applications. BCB is a photosensitive dielectric material that enables MMS to eliminate several process steps and to build multilayer thin-film substrates with 20% lower costs than the company's standard polyimide-based process. BCB has a dielectric constant of 2.65, which enables faster signal propagation when compared with similar structures built using polyimide (dielectric constant of 3.5), co-fired ceramic (dielectric constant of 9.5), or pc-board material (dielectric constant of 4.7). A typical implementation of BCB in MMS's D-series thin-film substrates features 10-µm line widths, dielectric thicknesses ranging from 3 to 10 µm, and interlayer connections (vias) running 20 µm in diameter. In contrast, typical pc-board traces are 5 mils wide (127 µm) on a 250-µm pitch. For more information, contact MMS' Howard Green at (408) 864-5986 or Dow's customer-service center at (800) 441-4369. *DM*

Air/Hydrogen Power Source Is Renewable And Clean

Electricity created from hydrogen and air may soon be powering cars, portable electronic devices, and lawn mowers. The quiet, inexpensive, and renewable power will be generated by fuel cells using low-cost materials. The technology was developed and patented by DAIS Corp., Troy, N.Y., an incubator company of Rensselaer Polytechnic Institute, Troy. The DAIS fuel cells rely on a membrane-electrode assembly (MEA) comprised of an ion-conducting membrane sandwiched between an anode and cathode, says Timothy Tangredi, DAIS's executive vice president. The cells generate electricity through a controlled reaction between hydrogen and air. The gases are separated by the company's proton-exchange membrane, which permits only positively charged hydrogen ions to cross to the oxygen side and form water. The resulting chemical reaction releases energy that can be put to work.

According to Tangredi, the company's MEA program is shifting from research to product development, and the company anticipates marketing a 100-W unit by the end of the year. Pricing is expected to be around $500. For more information on DAIS's fuel-cell technology, call Timothy Tangredi at (813) 942-8353. *DM*

FeRAM Development Opens Door To Electronic Money

A novel ferroelectric IC card has resulted in a product suited for use as electronic money and related applications. The integrated circuit, jointly developed by Matsushita Electronics Corp. and Motorola's Indala Corp., both of San Jose, Calif., introduces a ferroelectric memory (FeRAM) technology that overcomes the difficulties of limited-access cycles and low-access speeds that challenged conventional IC card technology. FeRAM offers a memory retention of at least 10 years without battery backup. With a capacity of 256 kbits, it can handle more than 10 billion cycles and a read-write cycle time of 7.8 kbits/s.

The card employs a ferroelectric material called Y-1, which is a layered Perovskite structure using a super lattice theory. The theory came from researchers at Colorado University, Boulder, Colo., and engineers at Symetrix Corp., Colorado Springs, Colo. Products will be released by Indala in the fall using the Matsushita chips. The companies envision a future with electronic cash accompanied by electronic financial transaction-processing applications. *RN*

Partnership Finds Uses For Microjet Printing

A method for microsoldering contact leads for integrated circuits soon may help improve productivity and reduce generation of hazardous industrial wastes. Developed by MicroFab Technologies, Plano, Texas, with co-funding from NIST's Advanced Technology Program, the technology applies the basic approach used in inkjet printing to produce tiny solder drops as small as 40 µm across or about half the width of a human hair. The solder drops provide the electrically conducting leads needed to attach semiconductor "chips" to circuit boards. This new technology, incorporating a programmable

Keeloq XL106 Rolling Code Encoder

Brief description

The XL106 is a rolling code encoder for secure remote control systems using IR, microwave or RF transmitters. It includes authentication capability for token-based systems and coprocessor capability for remote control decoders and authentication system controllers.

The XL106 encoder can be used with the Keeloq series decoders, and are pin compatible with the Keeloq XL105 in most applications.

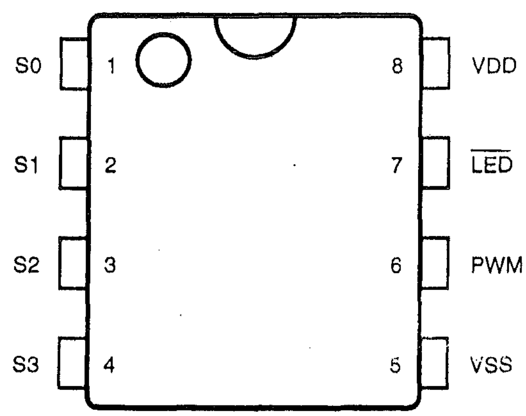

Pin Configuration

Typical applications

- Burglar alarm systems
- Remote control units
- Central locking systems
- Gate and garage door openers
- Access control systems
- Vehicle immobilizers
- Electronic door locks
- Identity tokens
- Tagging

Features

- Automatic power down
- Small 8 pin SOIC (DIP available)
- Simple programming interface
- Combined button activation
- Low voltage protection on EEPROM
- Selectable duty cycle reduction
- User EEPROM storage
- Over 1.8×10^{19} possible keys
- Low external component count:
  - On-chip 1024 bit EEPROM
  - EEPROM error correction
  - On-chip oscillator
  - On-chip oscillator timing components
  - Complete on-chip reset circuit
  - Current limiting on LED output
  - Internally debounced inputs
  - Inputs internally pulled low
  - No DIP switches required

All keys and code combinations are reprogrammable but keys are fully protected against attempts to gain access to them.

Key / Reader Technology

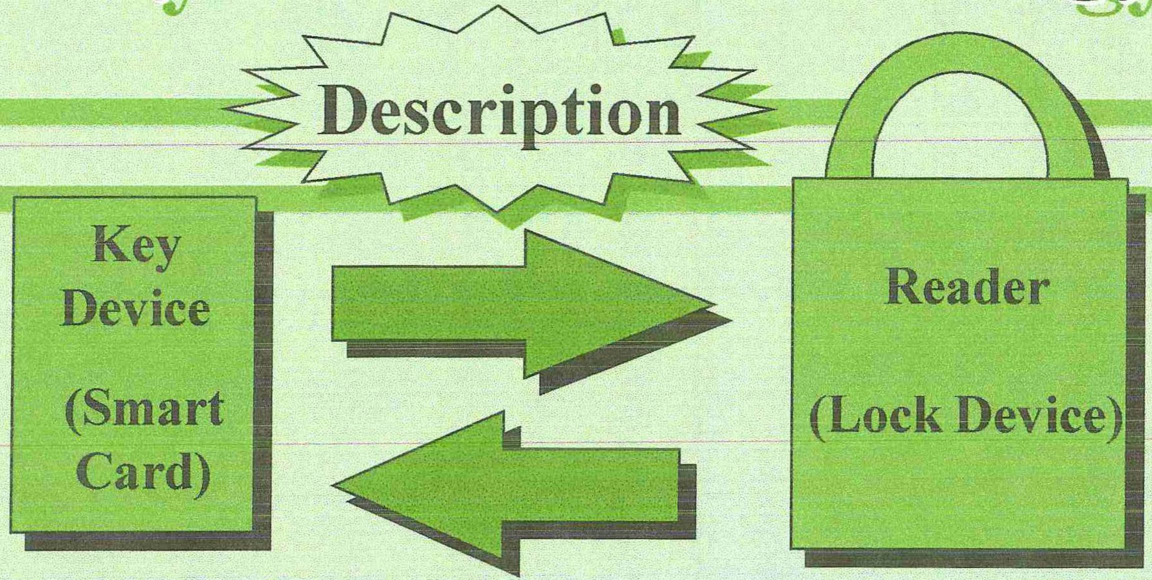

❶ **Proximity Operation**
- *Key* needs only to be 'close' to *Reader*
- Robust to geometrical orientation

❷ **Hardware Characteristics**
- No slots - no exposed electronics
- No electrical contacts - no magnetic strips
- *Key* requires no stored power (*i.e.* no batteries)

❸ **Software Capabilities**
- Key programmable by lock
- All programmable abilities of other smart cards

❹ **Reader Architecture Potentials**
- Reader surface may be
  - Flat
  - Disguised with plastic or other cover
- Reader may be isolated from environment
  - Weather
  - Vandalism

Key / Reader Technology

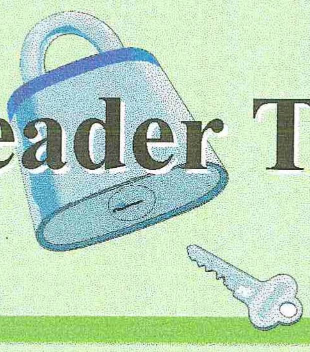

❺ Key can be configured as

- A credit card
- A key fob
- A ring

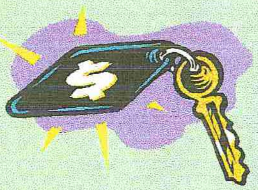

❻ Applications

- Smart Cards
  - Credit & debit cards
  - Medical & personal data storage
- Programmable hotel locks

  See April 12, 1996 *Wall Street Journal* article.
  Our technology solves the problems.
- Weapons security
  - Weapon will not fire unless ring is worn

Current Status

- Technology
  - ❖ Patent Filed
  - ❖ Experimental Verification
  - ❖ Needed
    - Development
    - Prototype
    - Packaging
- Needs
  - ❖ Development
    - Business Foundation
      - Business Plan
      - Management
    - Capitalization
    - Marketing
  - ❖ Business Leadership
    - Product Development
    - Licensing

Hotel-Room `Key' Cards Foil Prowlers - and Guests

By Jon Bigness
04/12/96
The Wall Street Journal

Hotels' electronic-lock systems are designed to foil would-be intruders. They do that -- and often they do more: They stymie guests trying to get in their own rooms and can even imprison those already inside.

Blame the problems on mechanical breakdown, faulty installation, failed batteries or desk-clerk error. But whatever the cause, the thousands of travelers forced to fiddle with malfunctioning locks are often vocal on the subject. "It's the most irritating thing in the world," says Nola Murphy, an aerobicsinstructor from Washington who was locked out of her room at.the Sheraton Manhattan Hotel in New York because the "key" card didn't work. (A spokeswoman for the Sheraton Manhattan says key-card malfunctioning "doesn't seem to be a big problem for us," adding, "It's got to be one of those rare situations.")

Marc Pazienza, a Washington lawyer, had a lock-out experience at the Omni Waterside Hotel in Norfolk, Va., because of a defective key card; he says he was kept from entering his room for more than half an hour. "You have so much more to be concerned about other than something with the hotel going wrong," he laments. (The hotel hasn't received any complaints about key cards, says Michelle Cheffer, assistant to the general manager.)

The precise failure rate isn't known. But Chicago-based EMG Associates Inc., which sells and services electronic locks, can attest that it is high. Last year, EMG sold about 5,000 electronic locks -- and repaired about 5,500. "Defects are prevalent," says Joshua Alper, president of EMG.

Manufacturers don't deny it. "All lock companies have problems," says Phil Wilder, director of marketing for Computerized Security Systems Inc. in Costa Mesa, Calif., one of the largest makers of electronic-lock systems.

One problem: Quality is getting lost in the rush to meet demand. In only a few years, electronic locks have been installed in a third of the nation's 3.2 million hotel rooms, and the pace is quickening because hotels feel the security advantages outweigh inconveniences.

The Holiday Inn, Howard Johnson's and Comfort Inn chains, among others, recently ordered their franchisees to ditch key-in-knob locks in favor of electronic systems, which cost about $250 a room. To fill orders, "companies are pushing locks out the doors and doing repairs regularly," says Mr. Alper.

Even functioning electronic locks can be confusing, because there are 30 different varieties coming from a dozen or so manufacturers. Arriving at the door, the traveler must determine whether to swipe or insert the card, have the arrow facing up or down or whether the card should be left in the lock while turning the handle. Then, if nothing happens, the problem is often a dead battery in the door lock.

Although most systems feature signals such as blinking lights that warn of low voltage, hotels routinely fail to replace batteries until they die, leaving guests locked in or out of rooms. Hotel executives such as Tom Daly, director of safety and security for Hilton Hotels Corp., play down that inconvenience to guests. "It's really only a matter of minutes" to get a battery changed, says Mr. Daly, whose company required all its hotels to upgrade to electronic locks three years ago.

THE CHARGE TRANSFER SENSOR

A New Class of Sensor Can Make Ordinary Objects Prox Sensitive Using Spread Spectrum Signals

It is not often that an old, simple lesson from freshman physics can be fashioned into a new type of sensor, yet it would appear that this is exactly what has occurred. Seemingly overlooked for decades, the elementary principle that the transferrance of charge from one capacitance to another conserves the charge has now led to a unique new class of proximity sensor with some interesting capabilities. The method lends itself extremely well to implementation with a microcomputer core and only a modest amount of external circuitry. At the same time, it can do several things that existing capacitance sensors are for all practical purposes incapable of; one of them is making many ordinary objects of almost arbitrary size proximity sensitive. More amazingly is an ability to analyze material characteristics such as moisture content or internal structure.

This new sensor has been dubbed the charge transfer, or 'QT' sensor. As a kickoff application, QT is now being applied to make common, everyday faucets automatic, without the need for infrared beams, wall plates, or special adaptors: the installer just clips a wire to a common faucet from underneath, and the entire spout becomes prox sensitive. Water splashes around the spout do not impact its operation.

THE BASIC PRINCIPLE

It is well known that a capacitance holding a charge, when connected to an uncharged second capacitor will transfer a portion of its charge to the second capacitor without a net loss of charge; put another way, electrons cannot be destroyed, they can only be transferred. This fact is merely a result of the principle of the conservation of matter; absent a leakage or a subatomic reaction, total free electron count cannot be altered. Energy of course is lost as heat during the transfer, but this is a different issue; the resistance of the switches and wiring serve to generate this heat, but do not affect the conservation of charge, no matter how large the resistance may be.

If the second capacitor is vastly larger than the first, the result will be a transfer of essentially *all* charge to the second capacitor, resulting in a voltage on the second capacitor that is directly proportional to the charge. This results from the basic charge transfer equation:

$$1)\quad V_s = V_r \times \frac{C_x}{C_x + C_s}\ .$$

where Vr is the charging voltage, Cx is the unknown capacitance, Cs is the second (known) capacitance, and Vs is the resulting voltage across Cs. Given the special case where Cs >> Cx, equation (1) simplifies to:

$$2)\quad V_s = V_r \times \frac{C_x}{C_s}$$

Rearranging the equation slightly gives the expression:

$$3)\quad C_x = C_s \times \frac{V_s}{V_r}\ .$$

Quite simply, it is possible to determine unknown capacitance Cx through the means of a known voltage Vr and a known capacitor Cs, as long as you have switches to make the charge transfer (figure 1). In operation, S3 is held closed briefly to make sure Cs is discharged. S1 then closes momentarily to charge Cx to voltage Vr. Then, with both S3 and S1 open, S2 closes briefly to transfer the charge from Cx to Cs; S2 can then reopen. The voltage Vs now gives a direct indication of the value of Cx. At first glance, most design engineers might think that Vs would be so small as to be unreadable, especially when attempting to determine sub-picofarad capacitances. Perhaps this line of reasoning is why the effect has been ignored for so long. But think again: in any sensing system, the *only* determinates of useful sensitivity are noise, drift, and if applicable ADC performance. Amplifiers can do all the scaling necessary to present a useful range of voltage to an ADC for processing by a micro; noise can be averaged out, and drift depends on the stability of the circuit elements and the sophistication of a compensating algorithm.

In fact, it turns out that with modern opamps and ADC's, it is fairly easy to get differential resolutions to 0.01 picofarads even with 'bulk' load capacitances that range from zero to 1000 picofarads *with the same sensor*. Using MOSFETs as switches gives a very repeatable, smooth, and stable response over a wide range of Cx. Averaging is easy to accomplish; in fact, it almost comes for free: simply by repeating the switch closure cycle repeatedly without closing S3, a voltage will build on

Cs with each charge/transfer cycle of Cx. In fact, Cs actually does a perfect boxcar average on the samples, weighting each sample identically until Vs is read. It also turns out that because the system contains no active-gain components (MOSFETs used as switches are employed as zero-gain resistive switching elements) there is only negligible front end noise. Of course, what noise there is gets fed to Cs, which acts to average the noise. Noise that does occur to any significance comes primarily from external induced sources, and if the switching is done quickly the time duration in which externals fields can have an effect is minimized. Contrast this with conventional capacitance sensors which modulate the sense element essentially 100% of the time; such sensors are inherently exposed to all manner of RF and e-field interference on a continuous basis.

QT CAN MAKE COMMON OBJECTS PROX SENSITIVE

The ability to range over many decades of load capacitance gives the QT sensor another unique advantage: you can connect the sensor to many common metal-bearing items, so long as they are not grounded, thereby making them prox sensitive. With only a modest amount of software intelligence, the sensor can adapt to the 'intrinsic' capacitive load and thereafter look only for small changes. For example, you can clip the sensor to a long metal strip under a carpet, and make a burglar alarm or machine safety sensor. Or, the exact same sensor can be clipped to a dime-sized piece of foil behind a plastic panel to make a touch control pad. Non-metallic objects can be made prox sensitive through the addition of a wire or some metalization, perhaps internally; the capacitance effect of course will flow through any dielectric to make all or a portion of the insulating object prox sensitive. Existing capacitance sensor designs are extremely limited in their ability to automatically adapt to a wide range of objects or plate size, and have serious problems dealing with large values of 'background' capacitance loading.

Because the QT sensor can measure capacitance in only one pulse or at most a short burst of pulses, then rest with a long 'dead' time, the spectral characteristic of the output appears spread. In fact, this is one form of spread spectrum signal. Conventional capacitance sensors usually use sine or square waves on a near continuous basis, which can cause cross interference and generate radio frequency interference. The QT sensor in contrast can operate with sparse, even randomized pulse spacings. In the real world this means that neighboring QT sensors do not need to be tuned to different 'frequencies' as many other sensors must. It also means higher pulse levels may be used without fear of violating government emissions standards, while resulting in more robust detection and range.

MOISTURE SUPPRESSION AND DETECTION

As an important side effect, the QT sensor can do something no other capacitance sensor can do: it can heavily suppress the effects of moisture in direct contact with the sensed object. To do this requires only that S1 and S2 be switched fast (see sidebar); doing this prevents parasitic conductances through water from charging and discharging and thus contributing to the sensed charge.

An example of a moisture suppressing product is an automatic faucet sensor, soon to be released. As shown in figure 3, a spout with a water splash at its base would be nearly impossible to properly make prox sensitive with any other capacitive method. The wild swings in conductivity from such water films drives other sensors crazy. A QT sensor on the other hand will barely respond to it, while remaining able to sense either hand proximity or touch. Furthermore, by using a dual width charge/transfer cycle, it can 'reach through' the water stream to sense the presence of a hand while water is on, thus allowing water to stay on even if the hand is lowered greatly in the stream. Using a wide pulse during times when water is on does in fact cause water films to be sensed as well, however the response from a hand has been found to be many times larger than these water film induced signals.

The ability to selectively sense or ignore moisture can be turned around to create an interesting type of sensor that will actually determine the internal properties of an object. For example, a fruit or vegetable ripeness meter can be constructed that capacitively examines the fruit at several pulsewidths. The response of the fruit at these pulsewidths is usable to give an indication of ripeness, since the fruits' response at various frequencies depends on moisture content and ionic cell permeability. The frequency response of a fruit also translates into a similar response with pulse width in the time domain. Other materials can similarly be analyzed: for example, grain level in a bin *and* its moisture can be determined simultaneously with one bare stainless steel rod connected to a QT sensor and some analysis software.

INCREASING RANGE WITH CHARGE NULLING

To extend range further and increase linearity, the concept of field nulling, patented by the author in 1989 can be applied. This method 'knocks back' or nulls the voltage Vs to near zero. While

S2 is closed, a charge Qz is simultaneously subtracted from Cs ; Qz comes from another capacitor, Cz (figure 4). Its voltage, Vz, is impressed upon it from a voltage source which may be a DAC under the control of an algorithm. With sucessive cycles, Vz can be adjusted so as to create a null on Cs. Not only does this improve linearity, it also enables a tremendously larger load capacity. The reason equation 2 can be linear is because Cs >> Cx, and as a result Vs << Vr. Nulling allows the designer to use smaller values of Cs while still keeping Vs << Vr.

As figure 4 shows, a second switch labelled S4 is introduced which provides the 'knock back' or nulling pulse. While figure 4 cannot be pulsed more than once prior to a reading, a simple variation permits bursts of many sense pulses with simultaneous null pulses to keep Vs from rising too high. Such a version, implemented with MOSFETs, is shown in figure 5. Such a circuit is extremely stable and repeatable, and can handle several thousands of picofarads of load capacitance while being able to sense variations well under 0.1pF. Although MOSFETs are not ideal switch elements, they come close. VMOS, DMOS, HEXFET, and similar devices have excellent switching speed, low resistance, and negligible noise, all of which contribute to overall performance. The only disadvantage of such devices is their flair for injecting charge into both Cx and Cs, which affects linearity and offset (but does so repeatably and can therefore be compensated by an algorithm).

In contrast, capacitance bridge circuits must create a null using a tunable capacitance. Varactor diodes are extremely nonlinear for this purpose, and great pains must be taken to linearize the result if absolute linearity is important. The only remaining alternatives are mechanically tuned capacitors or a switched capacitor array, both of which are fairly inconvenient. As a result, few bridge based circuits have been built that are able to automatically adapt to a wide load range. The QT method however can use a controlled voltage to achieve the same end, using a simple DAC or analog feedback loop. This contrast in complexity alone is quite striking; the other QT advantages such as RFI immunity, moisture suppression, and spread spectrum emissions characteristics add frosting to the cake.

PROPER CONNECTIONS REQUIRED

Because the QT sensor is capable of pulsing an object in a few tens of nanoseconds, the quality of the connection to the object and to the ground reference is of critical importance. Although it can always be slowed down, some of the more interesting results are obtained with short, fast pulses.

Unfortunately, wires do not always behave as ideal wires at these pulse widths. Under the influence of fast rise and fall times and a large Cx load, signal lead connections will ring or appear to resonate, while ground connections will have 'bounce' voltages on them. Larger guage wires will often resolve these issues by reducing lead inductance, but in many extreme cases this will not be enough. In such instances series resistance must be added to dampen ringing, and wires will need to be shortened to an absolute minimum. These matters are usually not an issue with small objects having low values of capacitance and that are nearby.

That being said, the QT sensor is fully able to sense remote objects through a coaxial cable, even of small guage like RG-174/U. Because the sensor can handle large capacitive loads with ease, the capacitance of the cable has no discernable effect on operation. For example, common single-shield 93 ohm coax can typically be run for over 20 meters before a 1,000pF capable QT sensor runs out of steam. The best any other sensor type can offer is short range operation with expensive, bulky, tough-to-terminate double shielded cable.

A SIMPLE, INEXPENSIVE SAMPLE CIRCUIT

A simple microprocessor based circuit that performs QT sensing is shown in figure 6. A Microchip PIC16C622 or comparable processor is directly connected via P1 to the sense object. This connection provides the Cx 'charge' pulse. A MOSFET S2 controlled by the micro subsequently transfers charge from Cx into Cs. This cycle may be repeated many times if desired, so long as Vs does not climb above about 0.4 volts. Then, line P6 is raised, and Vs starts to ramp up. The micro simultaneously starts an internal digital timer. At some point Vs equals an internal comparator reference voltage as measured via line P3, and a timer reading is taken. This reading is complemented and offset to form a measure of Cx. If needed, Cz1 and/or Cz2 are pulsed down via lines P4 and P5 at some point between sense pulses to provide nulling; in this manner load range can increase nearly four-fold.

While this circuit is not terribly linear, for set-point type applications it provides a very stable, repeatable measurement with a differential resolution to 0.05pF per bit over a 500pF load range. With a little more sophistication, for example by adding an amplifier and a 'real' ADC, range and linearity can be dramatically improved.

A FIRST APPLICATION - AUTOMATIC FAUCETS

The first QT product to be released will be the QProx™ faucet sensor. This product makes almost any ordinary faucet automatic, and should prove to be a boon to homeowners, hospitals, extended care facilities, restaurants, and airports. Unlike standard infrared products, the unit allows temperature mixing control either by use of the faucet's own valves (which are not disabled), or by recognizing simple fingertouch taps to the spout. For example, two quick taps will change temperature, while two long ones can make water flow 'hold on' to fill the basin or a pot. It runs on ordinary alkaline batteries for several years, and makes use of special magnetically latching solenoid valves which do not defeat the existing faucet valves. A version of this sensor will also be available for general evaluation purposes.

Numerous other applications are also envisioned. Along with material handling and safety uses, medical, lighting controls, touch pads, and material composition analysis are all being explored. Using a simple principle of physics, QT sensing will bring high reliability proximity detection to applications previously considered impossible, using circuitry that is much simpler and less expensive than current methods. Enabling technology will be in the form of integrated circuits or licensing arrangements.

About the Author

Harald Philipp earned his BSEE from Michigan Technological University, and is a lifetime honorary member of The Society of Photo-Optical Instrumentation Engineers (SPIE). He holds 12 patents in the fields of electro-optics, signal acquisition, controls, and sensor design, and currently has 4 other patents pending including an additional patent for the QT sensing method. He is a consulting engineer, designing sensors and systems for human detection related to safety and access controls, including for the disabled. Previously he was a senior design engineer for Tektronix Inc. of Beaverton, Oregon.

For more information:

Hal Philipp
email: hphil@NetBox.com